

AD-A035 071

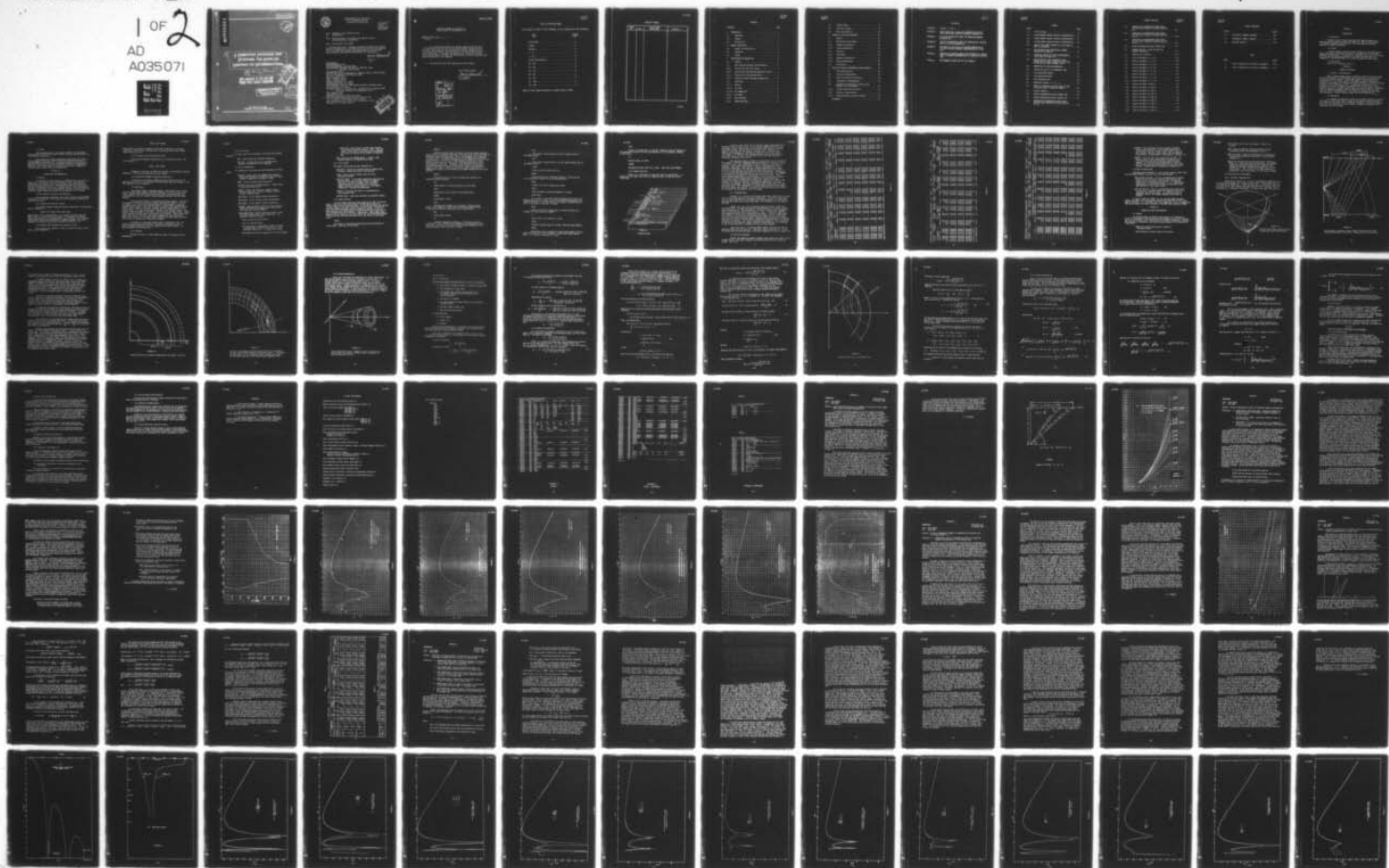
NAVAL SEA SYSTEMS COMMAND WASHINGTON D C  
A COMPUTER PROGRAM FOR STUDYING THE DOPPLER CONTENT OF REVERBER--ETC(U)  
1976 P MARSH  
NAVSEA-OD-52258

F/G 17/1

UNCLASSIFIED

NL

1 OF 2  
AD  
A035071



ADA 035071

20  
B.S.

A COMPUTER PROGRAM FOR  
STUDYING THE DOPPLER  
CONTENT OF REVERBERATION,

10 Philip Marsh

COPY AVAILABLE TO DDC DOES NOT  
PERMIT FULLY LEGIBLE PRODUCTION

DDC  
JAN 18 1976  
RECEIVED

**DISTRIBUTION STATEMENT A**  
Approved for public release;  
Distribution Unlimited

11 1976  
12 182

Published by Direction  
Commander, Naval Sea System Command

391 34  
68



DEPARTMENT OF THE NAVY  
NAVAL UNDERSEA CENTER  
SAN DIEGO, CALIFORNIA 92132

IN REPLY REFER TO:  
4514/HGP:1b  
735086  
Ser 451-1118  
2 Dec 1976

From: Commander, Naval Undersea Center  
To: Distribution

Subj: Computer Program for Studying the Doppler Content  
of Reverberation; forwarding of

Encl: (1) One copy of OD 52258

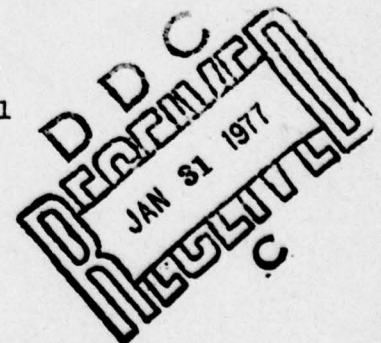
1. Ordnance Data 52258, A Computer Program for Studying the Doppler Content of Reverberation, was developed using Torpedo Mk 46 characteristics and approved by Engineering Change Proposal 46-2/NUC/2122. This document is forwarded to distribution for information.

*m. o. Heinrich*

M. O. HEINRICH  
By direction

Distribution:

COMOPTEVFORLANT w/encl  
DEPCOMOPTEVFORPAC, San Diego w/encl  
NAVSEASYSOMHQ (SEA-662D, SEA-662D-21, SEA-03B) w/encl  
(SEA-0342) w/3 cys encl  
ONR (ONR-466) w/encl  
PROJGR ASWS (PM-4), Washington D.C. (ASW-13, ASW-14, ASW-54) w/encl  
National Oceanographic Data Center w/encl  
NELC, San Diego w/encl  
NSRDC, Annapolis w/encl  
NSRDC, Carderock w/encl  
OCEANAV, Washington D.C. w/encl  
NAVSURFWPCEN, White Oak w/encl  
NAVPOSTGRADSCOL (Library, Tech Reports Section), Monterey w/encl  
NRL, Washington D.C. w/encl  
NAVTRPSTA (Quality Evaluation Lab., Technical Lab.), Keyport w/encl  
(Director, Research and Engineering) w/encl  
NUSC, Newport w/encl  
NUSC NLONLAB w/encl  
NAVWPNCEN, China Lake (Code 753) w/encl  
→ Defense Documentation Center (TISIA-1) w/20 cys encl  
APL, University of Washington, Seattle w/encl  
ARL, Pennsylvania State University, Pennsylvania w/encl  
Honeywell Inc., Seattle w/encl



A COMPUTER PROGRAM FOR STUDYING THE  
DOPPLER CONTENT OF REVERBERATION (U)

NAVORD Ordnance Data \_\_\_\_\_  
A Computer . . . . .

1. This publication documents the computer program called DOP which is a mathematical tool used in the study of the doppler content of reverberation. The program has been used primarily with the characteristics of the Torpedo MK 46, however, the characteristics of other acoustic systems can be substituted. The program was authored by Mr. Philip Marsh of the Naval Undersea Center, San Diego, and any questions relating to interpretations should be addressed to his attention.

2. This publication does not supersede any other document.

Naval Undersea Center

*M. O. Heinrich*

M. O. Heinrich  
By Direction.

ACCESSION FOR		
NTIS	Write Section	<input checked="" type="checkbox"/>
DDC	Draft Section	<input type="checkbox"/>
UNANNOUNCED		<input type="checkbox"/>
JUSTIFICATION	<i>Per ltr.</i>	
	<i>on file.</i>	
BY		
DISTRIBUTION/AVAILABILITY CODES		
Dist.	AVAIL. and/or SPECIAL	
<i>A</i>		

LISTS OF EFFECTIVE PAGES

Total number of pages in this document is 111, consisting of the following:

Sheet No.	#Change No.
Title Sheet. . . . .	0
A page . . . . .	0
Flyleaf. . . . .	0
i - iv . . . . .	0
1 - 32 . . . . .	0
Initial Distribution . . . . .	0
A1 - A3. . . . .	0
B1 - B4. . . . .	0
C1 - C11 . . . . .	0
D1 - D4. . . . .	0
E1 - E5. . . . .	0
F1 - F39 . . . . .	0
G1 - G70 . . . . .	0

#Zero in this column indicates an original page or sheet.

## RECORD OF CHANGES

CHANGE NO.	DATE	TITLE OR BRIEF DESCRIPTION	ENTERED BY

Flyleaf

CONTENTS

Paragraph	Sheet
1. INTRODUCTION. . . . .	1
1.1 Background . . . . .	1
1.2 Purpose. . . . .	1
1.3 Publications . . . . .	1
2. GENERAL DESCRIPTION . . . . .	1
2.1 Doppler in Reverberation . . . . .	1
2.2 Boundaries . . . . .	1
2.3 Volume . . . . .	2
3. INSTRUCTIONS FOR RUNNING DOP. . . . .	2
3.1 General. . . . .	2
3.2 User Supplied Functions and Subroutines. . . . .	2
3.2.1 Function OXL (Off-axis Losses) . . . . .	2
3.2.2 Function RRF (Reverberation Rejection Filter). . . . .	2
3.2.3 Function TVG (Time Variable Gain). . . . .	3
3.2.4 Subroutine SPRCMP (Spreading Computation). . . . .	3
3.3 Input Data . . . . .	3
3.3.1 Options. . . . .	3
3.3.1.1 For Input. . . . .	4
3.3.1.2 For Computation. . . . .	4
3.3.1.3 For Output . . . . .	5
3.3.2 Data Variables . . . . .	5
3.3.3 Sample Data Deck . . . . .	8

3.4	Program Output . . . . .	9
3.5	Ancillary Programs . . . . .	9
3.6	Other Considerations . . . . .	13
4.	THEORETICAL BASIS AND PROCEDURE . . . . .	13
4.1	General. . . . .	13
4.2	Description of the Models. . . . .	14
4.2.1	Boundary Reverberation . . . . .	14
4.2.2	Volume Reverberation . . . . .	19
4.3	Equations. . . . .	20
4.3.1	Preliminary. . . . .	20
4.3.2	Boundary Reverberation . . . . .	21
4.3.3	Volume Reverberation . . . . .	26
4.4	Verification . . . . .	29
5.	AREAS FOR POSSIBLE IMPROVEMENTS AND REFINEMENTS . . . . .	29
5.1	Volume Reverberation . . . . .	29
5.2	Multi-path Reverberation . . . . .	30
5.3	Vehicle Translation During Ping. . . . .	30
5.4	"Spreading" of Reverberation . . . . .	30
5.5	Preferential Orientation of Vehicle with Respect to the Environment . . . . .	30
5.5.1	Current and/or Wind Direction. . . . .	31
5.5.2	Sloping or Broken Bottom . . . . .	31
5.5.3	Three-dimensional Velocity Profiles. . . . .	31
	REFERENCES. . . . .	32

APPENDICES

- APPENDIX A      FIGURES 1, 2 AND 3
- APPENDIX B      ERROR FROM USING  $10 \log_{10} \tau$  AS A MEASURE OF EFFECTIVE  
                    TRAIN LENGTH WHEN COMPUTING BOUNDARY REVERBERATION
- APPENDIX C      REVIEW OF MATHEMATICAL MODEL FOR COMPUTING BOUNDARY  
                    REVERBERATION
- APPENDIX D      REVIEW OF MATHEMATICAL MODEL FOR COMPUTING THE EXPECTED  
                    LEVEL OF VOLUME REVERBERATION
- APPENDIX E      ASSESSMENT OF THE EFFECT OF PLATFORM TRANSLATION ON  
                    THE AREA RETURNING BOUNDARY REVERBERATION AT A GIVEN  
                    TIME
- APPENDIX F      COMPARISON OF COMPUTER MODELS FOR OBTAINING THE EXPECTED  
                    LEVEL OF BOUNDARY REVERBERATION AS A FUNCTION OF ELAPSED  
                    TIME
- APPENDIX G      DOP PROGRAM LISTINGS FOR THE TEST PROBLEM.

FIGURES

FIGURE		Sheet
3-1	A DOP Data Deck . . . . .	8
3-2	Program 800003--Doppler Content of Reverberation. .	10
3-3	Program 800003--Doppler Content of Reverberation. .	11
3-4	Program 800003--Doppler Content of Reverberation. .	12
4-1	LOCUS OF RAYS FROM A SOURCE AT $d_0$ AT AN ANGLE $\theta_0$ FROM THE HORIZONTAL . . . . .	14
4-2	TWO DIFFERENT PATHS INSONIFYING A COMMON PORTION OF THE SURFACE. . . . .	15
4-3	INSONIFIED PORTION OF SURFACE CORRESPONDING TO RAY PATHS IN FIGURE 4-6. . . . .	17
4-4	REGION BROKEN UP INTO INCREMENTAL AREAS, BOUNDED ON TWO SIDES BY EQUAL-TIME LINES AND ON TWO SIDES BY EQUAL-FREQUENCY LINES . . . . .	18
4-5	COMPUTATION OF VOLUME REVERBERATION . . . . .	19
4-6	FINDING THE VALUE OF AN INCREMENTAL AREA. . . . .	24
A-1	TEST-PROBLEM/DOP-SONARS . . . . .	A-1
A-2	TEST-PROBLEM/DOP-RAYSRT . . . . .	A-5
A-3	TEST-PROBLEM/DOP-DOP. . . . .	A-5
B-1	METHOD FOR FINDING $\tau^* = X_2 - X_1$ . . . . .	B-3
B-2	ERROR AS A FUNCTION OF INITIAL ANGLE OF PATH TO TRAILING EDGE OF INSONIFIED ANNULUS. . . . .	B-4
C-1	VELOCITY PROFILES . . . . .	C-5
C-2	SURFACE REVERBERATION VERSUS ELAPSED TIME . . . . .	C-6
C-3	SURFACE REVERBERATION VERSUS ELAPSED TIME . . . . .	C-7
C-4	COMPARISON OF REVERBERATION LEVELS AFTER SHIFTING CURVE OBTAINED BY REGULAR EQUATION BY $\Delta t/2$ . . . . .	C-8

C-5	COMPARISON OF REVERBERATION LEVELS AFTER SHIFTING CURVE OBTAINED BY REGULAR EQUATION $\Delta T/2$ . . . . .	C-9
C-6	COMPARISON OF REVERBERATION LEVELS AFTER SHIFTING CURVE OBTAINED BY REGULAR EQUATION BY $\Delta t/2$ . . . . .	C-10
C-7	COMPARISON OF REVERBERATION LEVELS AFTER SHIFTING CURVE OBTAINED BY REGULAR EQUATION BY $\Delta t/2$ . . . . .	C-11
D-1	VOLUME REVERBERATION VERSUS ELAPSED TIME. . . . .	D-4
F-1	COMBINED VERTICAL - PLANE PATTERNS FOR TRANSMIT AND RECEIVE. . . . .	F-11
F-2	SOUND-VELOCITY PROFILES . . . . .	F-12
F-3	RESULTS FOR MODELS I, II, III . . . . .	F-13
F-4	RESULTS FOR MODELS I, II, III . . . . .	F-14
F-5	RESULTS FOR MODELS I, II, III . . . . .	F-15
F-6	RESULTS FOR MODELS I, II, III . . . . .	F-16
F-7	RESULTS FOR MODELS I, II, III . . . . .	F-17
F-8	RESULTS FOR MODELS I, II, III . . . . .	F-18
F-9	RESULTS FOR MODELS I, II, III . . . . .	F-19
F-10	RESULTS FOR MODELS I, II, III . . . . .	F-20
F-11	RESULTS FOR MODELS II AND IV. . . . .	F-21
F-12	RESULTS FOR MODELS III AND IV . . . . .	F-22
F-13	RESULTS FOR MODELS III AND IV . . . . .	F-23
F-14	RESULTS FOR MODELS III AND IV . . . . .	F-24
F-15	RESULTF FOR MODELS III AND IV . . . . .	F-25
F-16	RESULTS FOR MODELS III AND IV . . . . .	F-28
F-17	RESULTS FOR MODELS III AND IV . . . . .	F-31
F-18	RESULTS FOR MODELS III AND IV . . . . .	F-34
F-19	RESULTS FOR MODELS III AND IV . . . . .	F-37

FIGURES CONTINUES

FIGURES		SHEET
G-1	HORIZONTAL, NARROW, STRAIGHT. . . . .	G-2
G-2	HORIZONTAL, BROAD, STRAIGHT . . . . .	G-3
G-3	HORIZONT RECEIVE. . . . .	G-4

TABLE

TABLE		SHEET
I	Errors Computed with Ellipse as Standard. . .	E-5
II	Errors Computed with Ellipse as Standard. . .	E-5

## SECTION I

## INTRODUCTION

## 1.1 Background

Torpedoes are the prime conventional antisubmarine weapons and they use acoustic systems to detect the submarine. Some of these systems use frequency dependent characteristics of the returned echo from the submarine to enhance performance.

## 1.2 Purpose

A digital computer program has been developed at the Naval Undersea Center (NUC) which facilitates the analysis of systems that use frequency dependent characteristics. The program is called DOP and is used in conjunction with two other NUC developed programs called SONAR and RAYSRT which are documented in references 1 and 2. This report documents the DOP program.

## 1.3 Publications

See list of references, page 32.

## SECTION II

## GENERAL DESCRIPTION

## 2.1 Doppler in Reverberation

When a single-frequency pulse is emitted from an active sonar system on a moving platform, the reverberation seen by the system is spread due in large part to doppler effects. Program DOP computes the spectrum of such reverberation in a refractive medium. The doppler content is computed as a function of the speed of the sonar platform and (optionally) of circular turning or motion of the scatterers, or both. In addition, the spectrum of the original pulse can be included as a spreading effect, since even a "single-frequency" pulse has a harmonic content due to its finite duration. The energy level is computed in frequency bands of specified width at specified times relative to the transmitted pulse. Four values are computed for each band/time combination: surface, bottom, volume, and total reverberation.

## 2.2 Boundaries

For boundary reverberation (surface or horizontal bottom), increments are summed in random phase from all areas of the boundary returning energy in a given band at a given time. Scattering strength is a function of grazing angle, and all combinations of paths (direct, refracted, reflected) to the scattering areas are included.

### 2.3 Volume

Volume reverberation is, at present, computed in an unbounded uniform medium, summing contributions from all volumes returning energy in a given band at a given time.

Both boundary and volume computations consider two-way losses in the environment and average transmit and receive beam-pattern losses to each incremental scattering unit. In addition, optional filtering can be applied to each band and TVG (Time Varied Gain) action can be applied at each time. Also, total energy in all bands at each time is computed for surface, bottom, volume, and total reverberation.

## SECTION III

### INSTRUCTIONS FOR RUNNING DOP

#### 3.1 General

The program is written primarily in FORTRAN IV for execution on a UNIVAC 1110. The program is not self-contained in that there are some functions and subroutines that must be supplied by the user to match the particular system being studied. (The program has been exercised here at NUC with the characteristics of the Torpedo MK 46 Mod 1 and an experimental torpedo.) A description of these user supplied routines, the input data, and ancillary programs necessary or useful to the execution of DOP follows.

#### 3.2 User Supplied Functions and Subroutines

For any specific application, one or more of the following FORTRAN functions will be required. Since they are vehicle dependent, they must be supplied by the user.

##### 3.2.1 Function OXL (Off-axis Losses)

This routine computes transducer pattern attenuation in any direction. The call sequence is:

VALUE = OXL (IFLAG, COSA, COSB, COSC)

where IFLAG is 0 for receive pattern, 1 for transmit and COSA, COSB, and COSC are the X, Y, and Z direction cosines in the direction of interest. Other values necessary for the computation, e.g. transducer type, frequency, sound velocity, etc. may be supplied via a COMMON statement. The value returned is a fraction of the on-axis intensity, from 0.0 to 1.0.

##### 3.2.2 Function RRF (Reverberation Rejection Filter)

This routine will interpose a filter to modify the energy in each band. The call sequence is:

$$\text{VALUE} = \text{RRF} (\text{FREQ})$$

where FREQ is the center frequency of the band in question. The value returned is the fraction of energy which is passed by the filter in that band, from 0.0 to 1.0.

### 3.2.3 Function TVG (Time Variable Gain)

This routine computes receiver gain as a function of time. The call sequence is:

$$\text{GAIN} = \text{TVGF} (\text{TIME})$$

Examples of OXL, RRF, and TVGF are provided in the program listings, Appendix G. These are unrelated to any real system.

### 3.2.4 Subroutine SPRCMP (Spreading Computation)

In addition to the above, SPRCMP may be provided by the user to generate one or more of the spreading function tables when the program is run. The subroutine has no arguments.

## 3.3 Input Data

Input data to DOP is from two sources: the output file of sorted ray data from programs SONAR and RAYSRT (references 1 & 2) and input data cards. Besides the sorted ray data returned from insonified portions of the boundaries, the file contains eleven parameters passed from the SONAR program.

The card input format is free-form with blanks ignored. Variables are punched in fields of arbitrary length, separated by commas. Data may be integer, real (including a decimal point) or alpha-numeric (appearing between single quotes). Note that no check is made for the appropriateness of any piece of data to any name. Neither names nor numbers may be split between cards. All data cards appear literally in the printed output. Two kinds of data may appear on the cards: option fields and data fields. Option fields contain only the name of the option to be invoked. These options may modify the form or content of input data, computation, and output data. Data fields consist of a variable name followed by an equal sign and one or more values, as appropriate, separated by commas.

For option or data names longer than six characters, only the first six characters are interpreted. Additional characters may be used to improve readability, but are ignored by the input routine. All data variables are initially zero.

### 3.3.1 Options

Options for DOP are listed below for input, for output, and for computation.

### 3.3.1.1 For Input

For input, there are two options, which have the following meanings:

- GO - Stop reading data and begin computation.
- NO TAPE - No input data file is provided and no boundary reverberation will be computed.

### 3.3.1.2 For Computation

For computation, the options and their meanings are listed below:

- CENTER - Doppler bands are computed such that the transmitted frequency is centered in one of the bands instead of appearing at the edge of a band.
- END - Stop all program activity and exit.
- FILTER (Used only with SPREAD option ) - Apply filter to the spread output data.
- KNOTS - Compute the intensity in bands of equal apparent range rate or "knots of doppler" instead of equal frequency range.
- NO BOTTOM - Do not compute bottom reverberation.
- NO SURFACE - Do not compute surface reverberation.
- NO VOLUME - Do not compute volume reverberation.
- SPREAD - Apply spreading function to output data and change the format of the output data listing. (See note under data variable BSPRED.)
- TIME COMPUTATION - Compute additional values of time for which reverberation is to be determined. The additional values of time are:
  - Ping interval (See PING below.)
  - $1/2 \Delta t$  (See DELT below.)
  - For every path or combination of paths to surface or bottom whose earliest arrival time is  $t$ , the additional values are:  $t$ ,  $t+1/2\Delta t$ , and  $t-1/2\Delta t$ .
  - Seventeen fixed values ranging from .01 to 2.0 seconds.

- Additional values every 1/2 second from 2 seconds to the value of the PING interval, NOTE: The total number of time entries read from cards and computed as a result of the use of this option is limited to 400.

- TVG (used only with SPREAD option) - Apply a time-varying function to the spread output data.

### 3.3.1.3 For Output

For output, the options and their meanings are:

- NO PRINT - Suppress the printed output of doppler data. Printing of input data cards is not affected.
- PLOT - Write a tape of doppler data for use by subsequent programs.
- RELATIVE BANDS - If the KNOTS computation option has not been specified, print the band limits in kilohertz relative to the source frequency; with the KNOTS computation option, print band limits in knots of doppler relative to vehicle speed; i.e. zero doppler (unspread) is returned from dead ahead.
- TOTALS - Print only the totals of reverberation at each requested time.
- (PRINT EVERY - Under Data Variables also modifies output.)

### 3.3.2 Data Variables

In the following listing of data variables for DOP, an asterisk (which is NOT part of the name) denotes variables whose values are normally taken from the input data tape. If the same variables are supplied on cards, however, the data from the cards would be used. It should be noted that some values which could be changed are implicit in the ray data supplied by the SONAR program and that changing these values by card would be meaningless and misleading. Examples are: source depth (D0), sound velocity of medium at the source depth (C0) and bottom depth (DBTM). (Please note that the second character of C0, D0, and F0 is the numeral zero.)

#### ALPHC\*

The product of attenuation coefficient and sound velocity at source depth. Units are dB per second.

## BSPRED

Spreading function table for bottom. Since the bottom scatterers would usually be considered stationary, this table would usually represent the spectrum of the transmitted pulse. NOTE: The appearance in the data deck of BSPRED, SSPRED, or VSPRED makes the use of the SPREAD option redundant and unnecessary. Each table is entered as half a symmetrical table of an odd number of entries. First value is the proportion of energy in a band remaining after spreading. Next value is the proportion spread to the two neighboring bands, etc. Therefore, twice the total of all values entered should equal one plus the first value. Each of the tables has a maximum of 150 values. Failure to include all three tables with the SPREAD option causes a call to SPRCMP in an attempt to generate the missing table(s).

## BWIDTH

Band width in hertz or knots as appropriate, based on the computation option selected.

## CO\*

Sound velocity in yards per second at source depth.

## DATE\*

Alpha-numeric date, maximum of two machine words.

## DBTTM\*

Bottom depth in feet.

## DELT

Effective pulse length,  $\Delta t$ , in seconds. Effective pulse length is the length of a square pulse with the same energy content as the pulse of interest, which may not be a square pulse.

## DO\*

Source depth in feet.

## FO

Transmit frequency in kilohertz. If no value is supplied, 1 kilohertz is used. Although this parameter is not supplied from the input tape, it is implicit in the ray data from the attenuation values (and the spreading loss correction, if used).

IDC\*

Alpha-numeric identification as on the "constant card" of the SONAR program.

IDV\*

Alpha-numeric identification as on the "semi-variable card" of the SONAR program.

LOGMV\*

Volume scattering coefficient, dB.

NBEAM

Coded description of transducer patterns, if more than one can be generated; intended for use by subroutine OXL.

OMEGA

Platform turn rate in degrees per second.

PING\*

Interval between successive transmits in seconds.

PRINT EVERY

For a value n, print only every nth doppler band at each time. Bands to be printed are chosen so as to include the band containing the transmit frequency as its lower bound or its center, if CENTER option is used. If no value is supplied, 1 is used.

PULSE

Coded description of pulse shape, if several options exist. Intended for use by subroutine SPRCMP.

S\*

Source level in dB relative to 1 yard.

SSPRED

Spreading function table for surface. (See note under BSPRED.)

THTMAX

Approximate value in degrees of largest angle (between velocity vector and sound rays) to be considered in computing unspread doppler bands. If no value is supplied, 90 is used.

OD 52258

**TIME**

Values of elapsed time, in seconds, (measured from the midpoint of the transmitted pulse) at which reverberation is to be computed. Maximum of 400 values.

**VS**

Vehicle speed, in knots.

**VSPRED**

Spreading function table for volume. (See note under BSPRED).

**3.3.3 Sample Data Deck**

Figure 3-1 illustrates an input card deck for program DOP. It assumes that at least four files (or complete sets) of data are on the input tape.

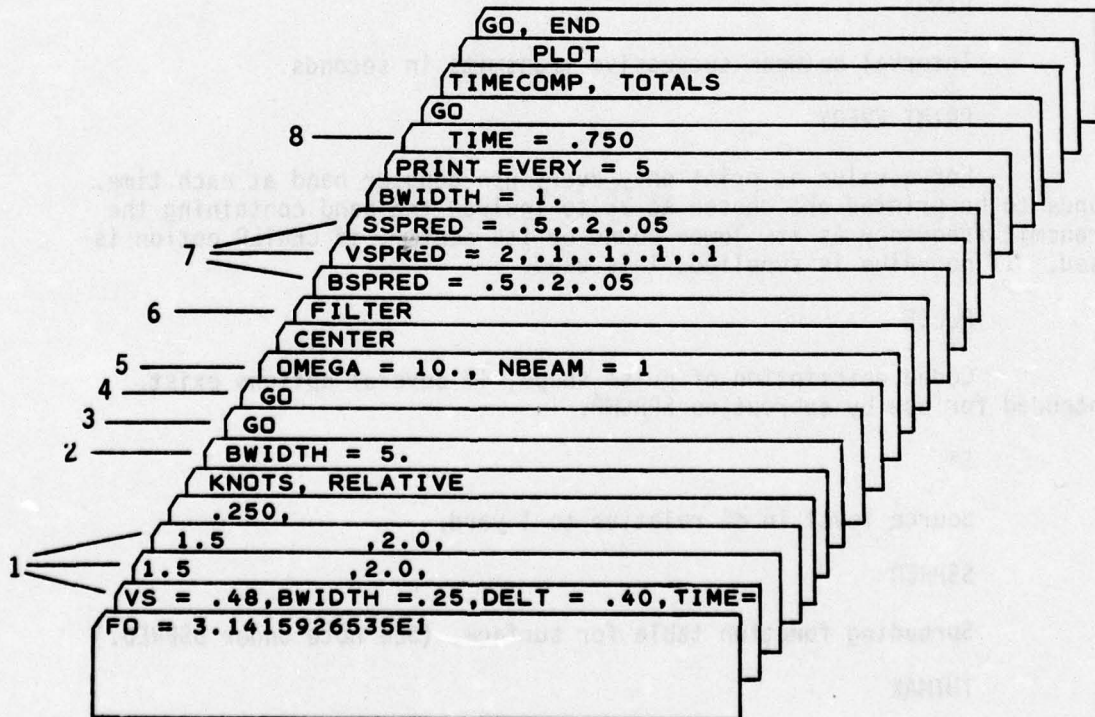


FIGURE 3-1

A DOP DATA DECK

In such a case, each file on the input tape (corresponding to different "semi-variable" cards in the original SONAR program deck) is processed in turn. Options and data variables from cards are retained until over written from the tape or from new cards. (Please note, however, that options once invoked or turned "on" can not be turned "off" again.) In general, the program proceeds until an END option is read from a card, or until the last data file on the tape has been processed, whichever occurs first.

The indicated cards in Figure 3-1 illustrate certain features of the program. Cards at 1 exemplify the continuation of a string of values on several cards. Also, note that of the six values of time, two are repeated. The program sorts values of time in ascending order and eliminates duplicates. The card at 2 redefines band width as 5. knots although it had been set to .25 knots on the second card of the deck. Card at 3 marks the end of card data for file 1 on the tape. The card at 4 indicates that all the same data is to be used for File 2. At 5 NBEAM is used because the hypothetical torpedo has two transmit beams. Some sonar problems might never use this feature. At 6 invocation of FILTER will cause a call to require RRF to modify the level of each band. Without this option, no RRF would be required. Similarly, if one of the variables at 7 was not supplied, a subroutine SPRCMP would have been called by the program. The card at 8 replaces all of the values of TIME previously read. Note throughout, the free, even arbitrary use of blanks which, we repeat, are ignored. Also note that values used on these cards are arbitrary and unrelated to any real system.

### 3.4 Program Output

Figures 3-2, 3-3, and 3-4 illustrate the output from Files 1, 3, and 4 of an input tape used with the sample input deck. In addition, the input deck, up to the GO option, or between successive GO options, is listed on a separate page before each output data page. No illustration of this page is provided.

Figures 3-2, 3-3, and 3-4 show the three principal formats for the output data. The pages are mostly self-explanatory. One point, however, should be mentioned. The appearance of .00 dB in a column seems ambiguous, since it may mean zero dB or zero energy (- dB). In practice, however, this ambiguity should rarely present any difficulty. The truly empty bands will always lie at the top or the bottom of a column of data. Unless the first or last nonvoid band has exactly zero dB, which can usually be determined from the band and column totals, leading and trailing zeros in a column represent zero energy. This form of printout was chosen in lieu of printing an arbitrary large negative number, because it made the page less cluttered. It has to date presented no problems to users of the program.

Three data decks, to programs SONAR, RAYSRT, and DOP were used to generate Figures 3-2, 3-3 and 3-4. These are listed in Appendix A. It will be noticed that the DOP data deck is not quite identical to that in Figure 3-1.

### 3.5 Ancillary Programs

Besides the SONAR and RAYSRT programs which produce the input file of sorted ray data, two other programs exist which may be of help to the user of DOP. These are:

PROGRAM 80003 -- DOPPLER CONTENT OF REVERBERATION																					
WAVELENGTH		C.O. YDS./SEC.		F.O. KMZ.		D.O. FT.		S. DB.		XI. DEG.		OMEGA, DEG./SEC.		P.I., SEC.		DEL. T, SEC.		D. BTM., FT.			
45.00		1625.41		31.4159		750.0000		100.00		-2.000		.000		2.00000		.0400		4000.0000			
FREQUENCY BAND		TIME = .250000000		TIME = 1.500000000		TIME = 2.000000000		TIME = 2.000000000		TIME = 2.000000000		TIME = 2.000000000		TIME = 2.000000000		TIME = 2.000000000		TIME = 2.000000000			
FROM-	KILOHERTZ	SURFACE	BOTTOM	VOLUME	TOTAL	SURFACE	BOTTOM	VOLUME	TOTAL	SURFACE	BOTTOM	VOLUME	TOTAL	SURFACE	BOTTOM	VOLUME	TOTAL	SURFACE	BOTTOM	VOLUME	TOTAL
32.4109	32.4059	.00	.00	-23.28	-23.28	.00	.00	-51.15	-51.15	.00	.00	-58.56	-58.56	.00	.00	-61.91	-61.91	.00	.00	-64.91	-64.91
32.4059	32.4009	.00	.00	-26.63	-26.63	.00	.00	-54.50	-54.50	.00	.00	-60.33	-60.33	.00	.00	-63.12	-63.12	.00	.00	-66.75	-66.75
32.4009	32.3959	.00	.00	-29.63	-29.63	.00	.00	-60.33	-60.33	.00	.00	-63.12	-63.12	.00	.00	-66.75	-66.75	.00	.00	-70.54	-70.54
32.3959	32.3909	.00	.00	-32.47	-32.47	.00	.00	-63.12	-63.12	.00	.00	-66.75	-66.75	.00	.00	-70.54	-70.54	.00	.00	-73.34	-73.34
32.3909	32.3859	.00	.00	-35.26	-35.26	.00	.00	-66.75	-66.75	.00	.00	-70.54	-70.54	.00	.00	-73.34	-73.34	.00	.00	-76.19	-76.19
32.3859	32.3809	.00	.00	-38.06	-38.06	.00	.00	-68.78	-68.78	.00	.00	-73.34	-73.34	.00	.00	-76.19	-76.19	.00	.00	-79.15	-79.15
32.3809	32.3759	.00	.00	-40.91	-40.91	.00	.00	-71.73	-71.73	.00	.00	-76.19	-76.19	.00	.00	-79.15	-79.15	.00	.00	-82.23	-82.23
32.3759	32.3709	.00	.00	-43.87	-43.87	.00	.00	-74.82	-74.82	.00	.00	-78.08	-78.08	.00	.00	-81.57	-81.57	.00	.00	-84.49	-84.49
32.3709	32.3659	.00	.00	-46.95	-46.95	.00	.00	-77.60	-77.60	.00	.00	-81.57	-81.57	.00	.00	-84.49	-84.49	.00	.00	-87.56	-87.56
32.3659	32.3609	.00	.00	-50.21	-50.21	.00	.00	-80.71	-80.71	.00	.00	-84.49	-84.49	.00	.00	-87.56	-87.56	.00	.00	-90.71	-90.71
32.3609	32.3559	.00	.00	-53.71	-53.71	.00	.00	-84.49	-84.49	.00	.00	-87.56	-87.56	.00	.00	-90.71	-90.71	.00	.00	-93.17	-93.17
32.3559	32.3509	.00	.00	-57.50	-57.50	.00	.00	-87.61	-87.61	.00	.00	-90.71	-90.71	.00	.00	-93.17	-93.17	.00	.00	-95.92	-95.92
32.3509	32.3459	.00	.00	-61.70	-61.70	.00	.00	-91.17	-91.17	.00	.00	-93.17	-93.17	.00	.00	-95.92	-95.92	.00	.00	-96.88	-96.88
32.3459	32.3409	.00	.00	-66.47	-66.47	.00	.00	-93.17	-93.17	.00	.00	-95.92	-95.92	.00	.00	-98.88	-98.88	.00	.00	-101.75	-101.75
32.3409	32.3359	.00	.00	-72.05	-72.05	.00	.00	-95.92	-95.92	.00	.00	-98.88	-98.88	.00	.00	-101.75	-101.75	.00	.00	-102.59	-102.59
32.3359	32.3309	.00	.00	-77.12	-77.12	.00	.00	-98.88	-98.88	.00	.00	-101.75	-101.75	.00	.00	-102.59	-102.59	.00	.00	-102.59	-102.59
32.3309	32.3259	.00	.00	-82.58	-82.58	.00	.00	-101.75	-101.75	.00	.00	-102.59	-102.59	.00	.00	-102.59	-102.59	.00	.00	-102.59	-102.59
32.3259	32.3209	.00	.00	-87.61	-87.61	.00	.00	-102.59	-102.59	.00	.00	-102.59	-102.59	.00	.00	-102.59	-102.59	.00	.00	-102.59	-102.59
32.3209	32.3159	.00	.00	-91.17	-91.17	.00	.00	-102.59	-102.59	.00	.00	-102.59	-102.59	.00	.00	-102.59	-102.59	.00	.00	-102.59	-102.59
32.3159	32.3109	.00	.00	-95.92	-95.92	.00	.00	-102.59	-102.59	.00	.00	-102.59	-102.59	.00	.00	-102.59	-102.59	.00	.00	-102.59	-102.59
32.3109	32.3059	.00	.00	-101.75	-101.75	.00	.00	-102.59	-102.59	.00	.00	-102.59	-102.59	.00	.00	-102.59	-102.59	.00	.00	-102.59	-102.59
32.3059	32.3009	.00	.00	-106.04	-106.04	.00	.00	-102.59	-102.59	.00	.00	-102.59	-102.59	.00	.00	-102.59	-102.59	.00	.00	-102.59	-102.59
32.3009	32.2959	.00	.00	-106.04	-106.04	.00	.00	-102.59	-102.59	.00	.00	-102.59	-102.59	.00	.00	-102.59	-102.59	.00	.00	-102.59	-102.59
32.2959	32.2909	.00	.00	-106.04	-106.04	.00	.00	-102.59	-102.59	.00	.00	-102.59	-102.59	.00	.00	-102.59	-102.59	.00	.00	-102.59	-102.59
32.2909	32.2859	.00	.00	-106.04	-106.04	.00	.00	-102.59	-102.59	.00	.00	-102.59	-102.59	.00	.00	-102.59	-102.59	.00	.00	-102.59	-102.59
32.2859	32.2809	.00	.00	-106.04	-106.04	.00	.00	-102.59	-102.59	.00	.00	-102.59	-102.59	.00	.00	-102.59	-102.59	.00	.00	-102.59	-102.59
32.2809	32.2759	.00	.00	-106.04	-106.04	.00	.00	-102.59	-102.59	.00	.00	-102.59	-102.59	.00	.00	-102.59	-102.59	.00	.00	-102.59	-102.59
32.2759	32.2709	.00	.00	-106.04	-106.04	.00	.00	-102.59	-102.59	.00	.00	-102.59	-102.59	.00	.00	-102.59	-102.59	.00	.00	-102.59	-102.59
TOTAL REVERBERATION		.00	.00	-20.39	-20.39	.00	.00	-48.25	-48.25	.00	.00	-55.67	-55.67	.00	.00	-55.67	-55.67	.00	.00	-55.67	-55.67

Figure 3-2

PROGRAM 800003 -- DOPPLER CONTENT OF REVERBERATION										IDV	DOPL 2	DATE	07/23/76	PAGE	1 OF 1		
V.S. KTS.		C.O. VDS./SEC.		F.O. KHZ.		D.O. FT.		S. DB.		XI, DEG.		P.I., SEC.		DEL. 1, SEC.		D. BTM., FT.	
45.00		1636.70		31.4759		500.0000		100.00		-2.000		2.0000		.0400		4000.0000	
DOPPLER BAND, KNOTS		PURE TONE		TIME = .75000000		TIME = .75000000		TIME = .75000000		TIME = .75000000		TIME = .75000000		TIME = .75000000		TIME = .75000000	
FROM-	TO-	SURFACE	BOTTOM	VOLUME	TOTAL	SURFACE	BOTTOM	VOLUME	TOTAL	SURFACE	BOTTOM	VOLUME	TOTAL	SURFACE	BOTTOM	VOLUME	TOTAL
5.5000	4.5000	.00	.00	.00	.00	.00	.00	.00	.00	.00	.00	.00	.00	.00	.00	.00	.00
5.000	5.5000	.00	.00	.00	.00	.00	.00	.00	.00	.00	.00	.00	.00	.00	.00	.00	.00
4.5000	5.0000	-57.17	.00	-58.75	-54.88	-55.55	.00	-48.43	-47.66	-95.55	.00	-88.43	-87.66	-104.09	.00	-101.20	-101.20
9.5000	10.5000	-65.89	.00	-66.94	-63.37	-64.33	.00	-64.09	-61.20	-104.33	.00	-104.09	-101.20	-115.29	.00	-112.90	-112.90
14.5000	15.5000	-78.55	.00	-77.50	-74.98	-76.63	.00	-75.29	-72.90	-116.63	.00	-115.29	-112.90	-126.62	.00	-124.15	-124.15
19.5000	20.5000	-77.96	.00	-76.78	-74.32	-78.17	.00	-77.32	-74.72	-118.17	.00	-117.32	-114.72	-129.33	.00	-126.66	-126.66
24.5000	25.5000	-84.81	.00	-84.25	-81.51	-84.10	.00	-82.40	-80.15	-124.10	.00	-122.40	-120.15	-134.34	.00	-132.63	-132.63
29.5000	30.5000	-92.36	.00	-90.03	-88.03	-91.32	.00	-88.41	-86.62	-131.32	.00	-128.41	-126.62	-147.22	.00	-144.89	-144.89
34.5000	35.5000	-89.16	.00	-86.00	-84.29	-89.33	.00	-86.47	-84.66	-129.33	.00	-126.47	-124.66	-152.51	.00	-149.89	-149.89
39.5000	40.5000	-89.64	.00	-86.61	-84.86	-89.75	.00	-86.80	-85.02	-129.75	.00	-126.80	-125.02	-155.18	.00	-152.65	-152.65
44.5000	45.5000	-95.58	.00	-89.87	-88.83	-94.34	.00	-89.63	-88.37	-134.34	.00	-129.63	-128.37	-161.67	.00	-159.13	-159.13
49.5000	50.5000	-101.06	.00	-95.29	-94.27	-100.71	.00	-94.49	-93.56	-139.36	.00	-135.71	-134.29	-171.01	.00	-168.53	-168.53
54.5000	55.5000	-108.88	.00	-103.38	-102.30	-108.06	.00	-101.57	-100.69	-147.22	.00	-142.89	-141.89	-182.90	.00	-179.95	-179.95
59.5000	60.5000	-120.76	.00	-116.18	-114.88	-118.63	.00	-111.71	-110.91	-152.56	.00	-147.22	-146.22	-195.01	.00	-192.05	-192.05
64.5000	65.5000	-124.05	.00	-121.79	-120.40	-125.89	.00	-121.65	-120.26	-158.61	.00	-153.01	-152.01	-204.09	.00	-201.20	-201.20
69.5000	70.5000	-128.01	.00	-123.87	-122.45	-128.07	.00	-123.93	-122.51	-159.84	.00	-155.18	-154.18	-214.89	.00	-211.95	-211.95
74.5000	75.5000	-137.85	.00	-135.01	-133.19	-136.21	.00	-131.04	-129.89	-161.67	.00	-157.32	-156.32	-226.66	.00	-223.72	-223.72
79.5000	80.5000	-142.21	.00	-138.86	-137.21	-142.28	.00	-139.74	-137.82	-164.89	.00	-160.13	-159.13	-238.55	.00	-235.65	-235.65
84.5000	85.5000	-145.60	.00	-146.01	-142.79	-145.36	.00	-143.19	-141.13	-168.53	.00	-162.05	-161.05	-250.44	.00	-247.54	-247.54
89.5000	90.5000	.00	.00	-150.08	-150.08	-161.67	.00	-152.72	-152.20	-171.01	.00	-162.05	-161.05	-262.33	.00	-259.43	-259.43
94.5000	95.5000	.00	.00	.00	.00	.00	.00	.00	.00	.00	.00	.00	.00	.00	.00	.00	.00
TOTAL REVERBERATION		-45.36	.00	-38.46	-37.65	-45.36	.00	-38.46	-37.65	-85.35	.00	-78.66	-77.66	-95.36	.00	-94.66	-94.66

FIGURE 3-3

PROGRAM 800003 -- DOPPLER CONTENT OF REVERBERATION										DATE	07/23/76	PAGE	1 OF 1
V-S, KTS.	C-O, VDS./SEC.	F-O, KMZ.	D-O, FT.	S, DB.	SI, DEG.	OMEGA, DEG./SEC.	P-I., SEC.	DEL. T, SEC.	D. BTM., FT.				
45.00	1679.30	31.4159	275.0000	100.00	-2.000	10.000	2.0000	.0400	4000.0000				
TOTAL REVERBERATION FROM 101 BANDS, EACH OF 1.000 KNOIS BANDWIDTH													
PURE TONE													
TIME	SURFACE	BOTTOM	VOLUME	TOTAL	SURFACE	BOTTOM	VOLUME	TOTAL	SURFACE	BOTTOM	VOLUME	TOTAL	SPREAD WITH FILTER AND TVG
0.20000000	.00	.00	1.13	1.13	.00	.00	1.13	1.13	.00	.00	.00	.00	-48.48
0.50000000	.00	.00	-8.34	-8.34	.00	.00	-8.34	-8.34	.00	.00	.00	.00	-57.44
0.81818396	.00	.00	-13.89	-13.89	.00	.00	-13.89	-13.89	.00	.00	.00	.00	-62.41
1.00000000	-15.98	.00	-14.99	-12.45	-15.98	.00	-14.99	-12.45	-53.74	.00	.00	.00	-63.36
1.0818396	-15.90	.00	-15.83	-12.85	-15.90	.00	-15.83	-12.85	-53.59	.00	.00	.00	-64.08
1.2918395	-15.80	.00	-17.45	-13.54	-15.80	.00	-17.45	-13.54	-53.32	.00	.00	.00	-65.45
2.00000000	-26.71	.00	-21.74	-20.54	-26.71	.00	-21.74	-20.54	-73.82	.00	.00	.00	-67.72
3.00000000	-31.57	.00	-25.90	-24.86	-31.57	.00	-25.90	-24.86	-77.82	.00	.00	.00	-72.18
4.00000000	-25.75	.00	-29.00	-24.07	-25.75	.00	-29.00	-24.07	-71.28	.00	.00	.00	-74.52
5.00000000	-24.94	.00	-31.53	-24.08	-24.94	.00	-31.53	-24.08	-69.82	.00	.00	.00	-76.60
6.00000000	-25.87	.00	-33.69	-25.20	-25.87	.00	-33.69	-25.20	-70.19	.00	.00	.00	-77.99
7.00000000	-27.37	.00	-35.59	-26.76	-27.37	.00	-35.59	-26.76	-71.19	.00	.00	.00	-79.40
7.50000000	-28.58	.00	-36.47	-27.92	-28.58	.00	-36.47	-27.92	-72.17	.00	.00	.00	-80.05
8.00000000	-29.42	.00	-37.31	-28.77	-29.42	.00	-37.31	-28.77	-72.80	.00	.00	.00	-80.67
9.00000000	-32.61	.00	-38.88	-31.69	-32.61	.00	-38.88	-31.69	-75.57	.00	.00	.00	-81.83
1.00000000	-35.24	.00	-40.33	-34.07	-35.24	.00	-40.33	-34.07	-77.84	.00	.00	.00	-82.92
1.20000000	-39.67	.00	-42.98	-38.01	-39.67	.00	-42.98	-38.01	-81.61	.00	.00	.00	-84.91
1.40000001	-44.11	.00	-45.39	-41.69	-44.11	.00	-45.39	-41.69	-85.47	.00	.00	.00	-86.75
1.50918451	-45.20	.00	-46.63	-42.85	-45.20	.00	-46.63	-42.85	-86.29	.00	.00	.00	-87.71
1.52918451	-45.50	-68.71	-46.86	-43.10	-45.50	-68.71	-46.86	-43.10	-86.53	-98.67	.00	.00	-87.88
1.54918450	-46.21	-65.83	-47.08	-43.59	-46.21	-65.83	-47.08	-43.59	-87.20	-96.52	.00	.00	-88.06
1.59999999	-48.27	-67.81	-47.65	-44.91	-48.27	-67.81	-47.65	-44.91	-89.13	-101.25	.00	.00	-88.50
1.61836843	-48.82	-68.88	-47.85	-45.28	-48.82	-68.88	-47.85	-45.28	-89.64	-102.51	.00	.00	-88.66
1.63836843	-49.37	-70.16	-48.08	-45.65	-49.37	-70.16	-48.08	-45.65	-90.14	-103.70	.00	.00	-88.84
1.65836842	-49.86	-71.44	-48.30	-45.99	-49.86	-71.44	-48.30	-45.99	-90.58	-104.75	.00	.00	-89.01
1.7275235	-51.28	-73.47	-49.09	-47.03	-51.28	-73.47	-49.09	-47.03	-91.85	-107.38	.00	.00	-89.65
1.7475235	-51.64	-72.28	-49.32	-47.30	-51.64	-72.28	-49.32	-47.30	-92.16	-106.16	.00	.00	-89.83
1.7675235	-51.95	-71.42	-49.55	-47.56	-51.95	-71.42	-49.55	-47.56	-92.43	-105.37	.00	.00	-90.02
1.80000000	-52.43	-71.13	-49.93	-47.97	-52.43	-71.13	-49.93	-47.97	-92.84	-106.34	.00	.00	-90.33
2.00000000	-54.96	-70.84	-52.26	-50.35	-54.96	-70.84	-52.26	-50.35	-94.96	-109.21	.00	.00	-92.25

FIGURE 3-4

- DENFSP - This program may be used to prepare spreading function tables for DOP. It will combine (convolve) a spectrum and a density function and/or convert a spectrum into a density function. Print, punch, and plot options are available. Program DENSFP is documented in reference (3).
- SRNBT4 - This uses the 'plot' output tape from DOP. The program prints or plots reverberation in doppler bands. It can translate the data into broader bands than were computed. It can also plot selected bands vs. time, and plot or punch cards for enabling level for use by the SONAR program. Program SRNBT4 is documented in reference (3).

### 3.6 Other Considerations

Although standard FORTRAN IV is the primary language of DOP, there are two UNIVAC FORTRAN V features which have been employed:

- The INCLUDE Statement - This is a convenient way of adding blocks of cards to several routines, insuring that such blocks will be identical in each routine. For compilers without this or an analogous feature, it is a comparatively simple matter to duplicate the blocks of cards and to add them physically in the proper places.
- The FLD Function - This is a bit-manipulating function which is used only in subroutine INPUT for assembling individual characters into variable names. For compilers without a comparable feature, an assembly-language routine must be written.

As used in subroutine INPUT, the two constants NWORD and NCHAR contain the number of bits per machine word and the number of bits per alpha-numeric character. For the UNIVAC 1110, these numbers are 36 and 6 respectively. They can be changed via a data statement in the BLOCK DATA subroutine, INBLK.

## SECTION IV

### THEORETICAL BASIS AND PROCEDURE

#### 4.1 General

The thinking which led through various models of reverberation to the one implemented in DOP has been covered extensively in earlier informal works by A.B. Poynter. Five of these works are included as Appendices B through F. The conventions, assumptions, and simplifications employed in the program are listed below:

- Both the surface and bottom are treated as horizontal planes.
- The platform's velocity vector is horizontal.

- The medium varies only with depth. There is no current.
- All times are measured from the midpoint of the transmitted pulse (see Appendices C and D).
- No allowance is made for differences in transmit and receive paths caused by translation of the platform (Appendix E).
- When the transmit and receive paths are of different types, e.g. one direct and one reflected, the boundary scattering strength between paths is taken as the average of the back scattering strengths for the two single paths. This is one of the least defensible assumptions, and investigation in this area is needed.

#### 4.2 Description of the Models

##### 4.2.1 Boundary Reverberation

Refer now to Figure 4-1. A ray is considered as emanating from a source at some depth,  $d_0$ , located on the Z axis. Since sound velocity is a function of depth only, a ray lies entirely in a vertical plane, and the locus of all rays leaving the source at an initial angle  $\theta_0$  from the horizontal is a surface of revolution.

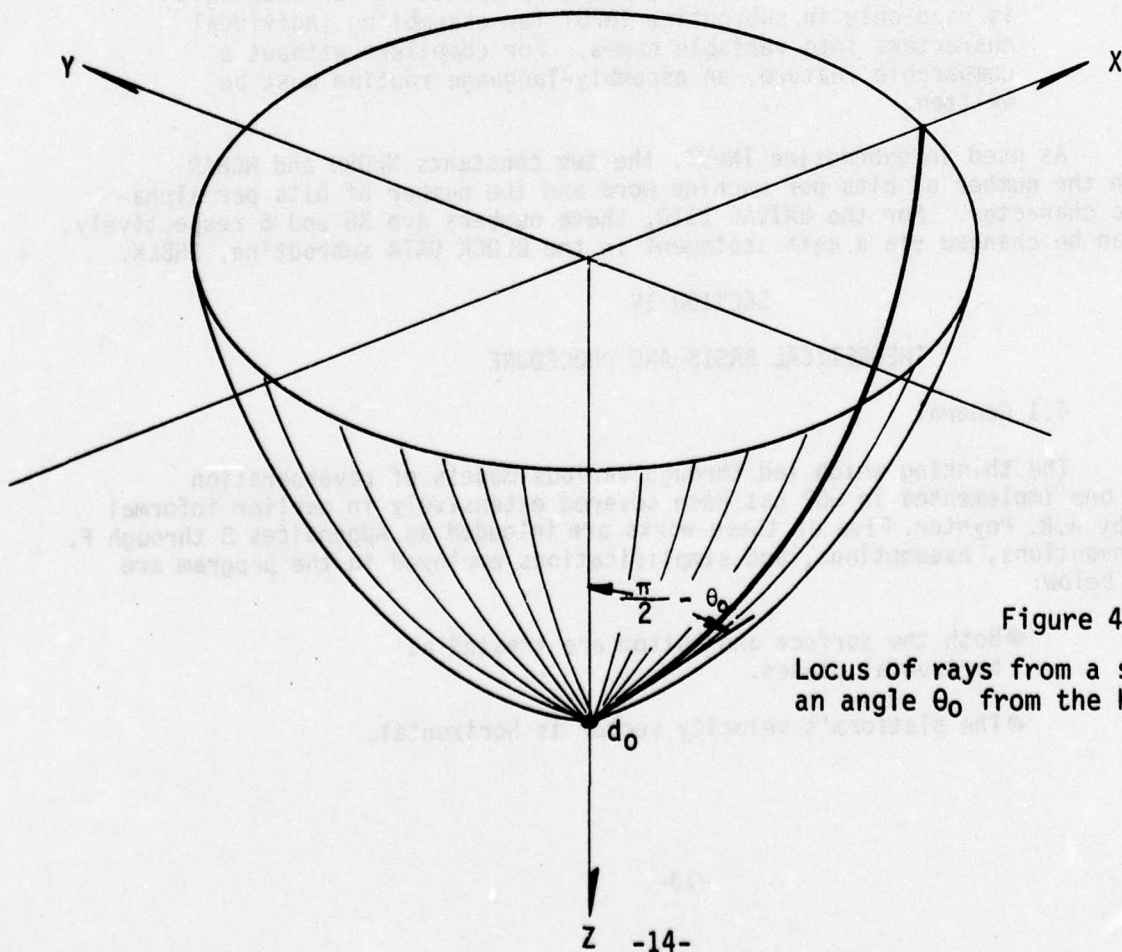


Figure 4-1

Locus of rays from a source at  $d_0$  at an angle  $\theta_0$  from the horizontal.

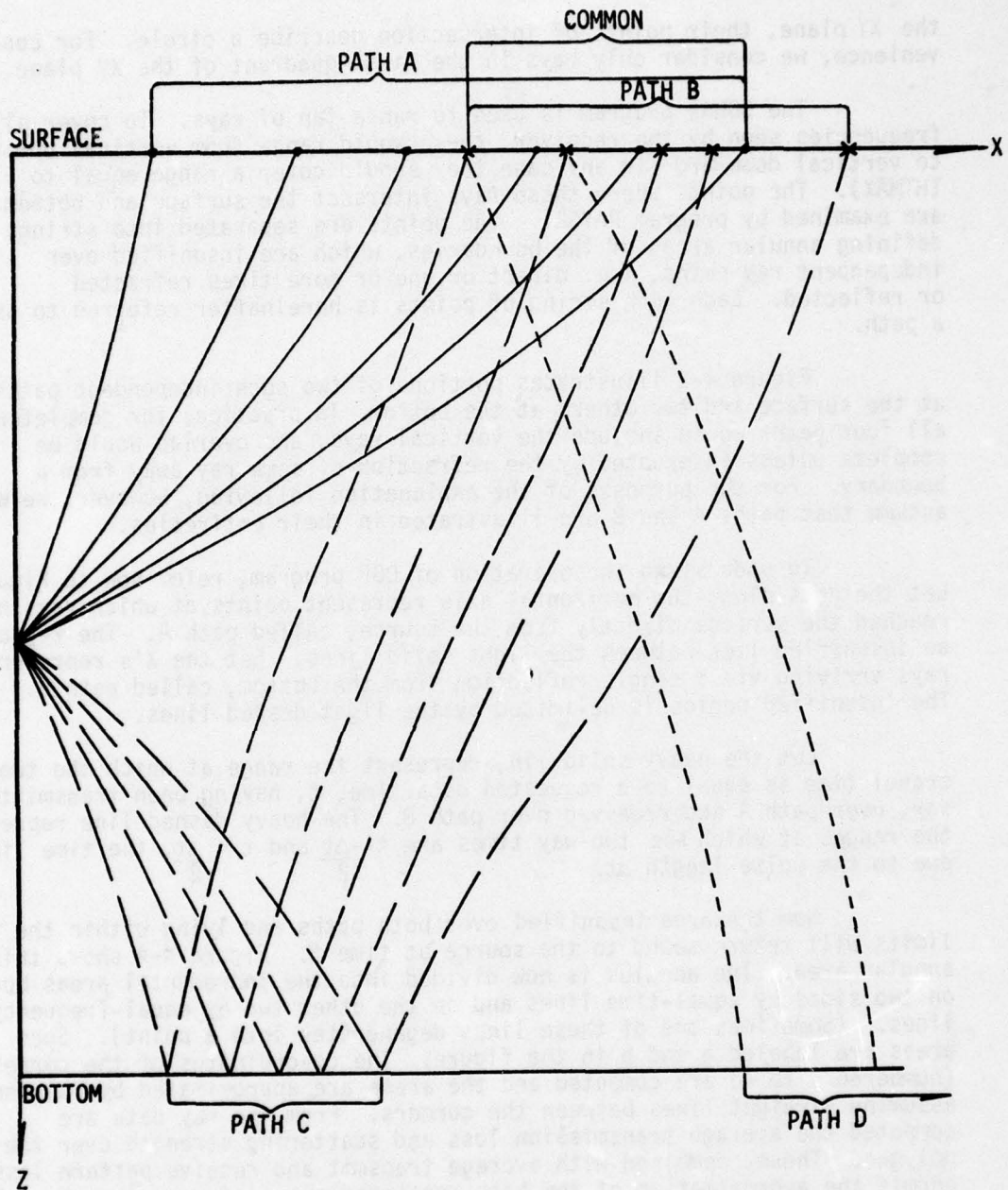


FIGURE 4-2

Two different ray-bundles, called "paths" (direct path and singly bottom-reflected path) insonifying a common portion of the surface.

the XY plane, their points of intersection describe a circle. For convenience, we consider only rays in the first quadrant of the XY plane.

The SONAR program is used to run a fan of rays. To cover all frequencies seen by the receiver, these would range from vertical upward to vertical downward (In any case they should cover a range equal to  $\pm$  THMAX). The points where these rays intersect the surface and bottom are examined by program RAYSRT. The points are separated into strings defining annular areas of the boundaries, which are insonified over independent ray paths, i.e. direct or one or more times refracted or reflected. Each such string of points is hereinafter referred to as a path.

Figure 4-2 illustrates portions of two such independent paths at the surface and two others at the bottom. In practice, for completeness, all four paths would include the vertical rays, and overlap would be complete unless interrupted by the refraction of some ray away from a boundary. For the purposes of the explanation following, however, we will assume that paths A and B are illustrated in their entireties.

To understand the operation of DOP program, refer now to Figure 4-3. Let the dots along the horizontal axis represent points at which rays have reached the surface directly from the source, called path A. The region so insonified lies between the light solid lines. Let the X's represent rays arriving via a single reflection from the bottom, called path B. The insonified region is delimited by the light dashed lines.

Let the heavy solid line represent the range at which the two-way travel time is equal to a requested data time,  $t$ , having been transmitted, say, over path A and received over path B. The heavy dashed line represents the ranges at which the two-way times are  $t - \frac{\Delta t}{2}$  and  $t + \frac{\Delta t}{2}$ , the time limits due to the pulse length  $\Delta t$ .

Now the area insonified over both paths and lying within the time limits will return sound to the source at time  $t$ . Figure 4-4 shows this annular area. The annulus is now divided into the incremental areas bounded on two sides by equal-time lines and on the other two by equal-frequency lines. (Sometimes one of these lines degenerates into a point). Such areas are labeled a and b in the figure. The co-ordinates of the corners (numbered 1 to 4) are computed and the areas are approximated by polygons, assuming straight lines between the corners. From the ray data are computed the average transmission loss and scattering strength over the polygon. These, combined with average transmit and receive pattern losses, permit the approximation of the back-scattered energy from each area. These contributions, expressed in intensities, are summed in random phase within the requested time and band limits.

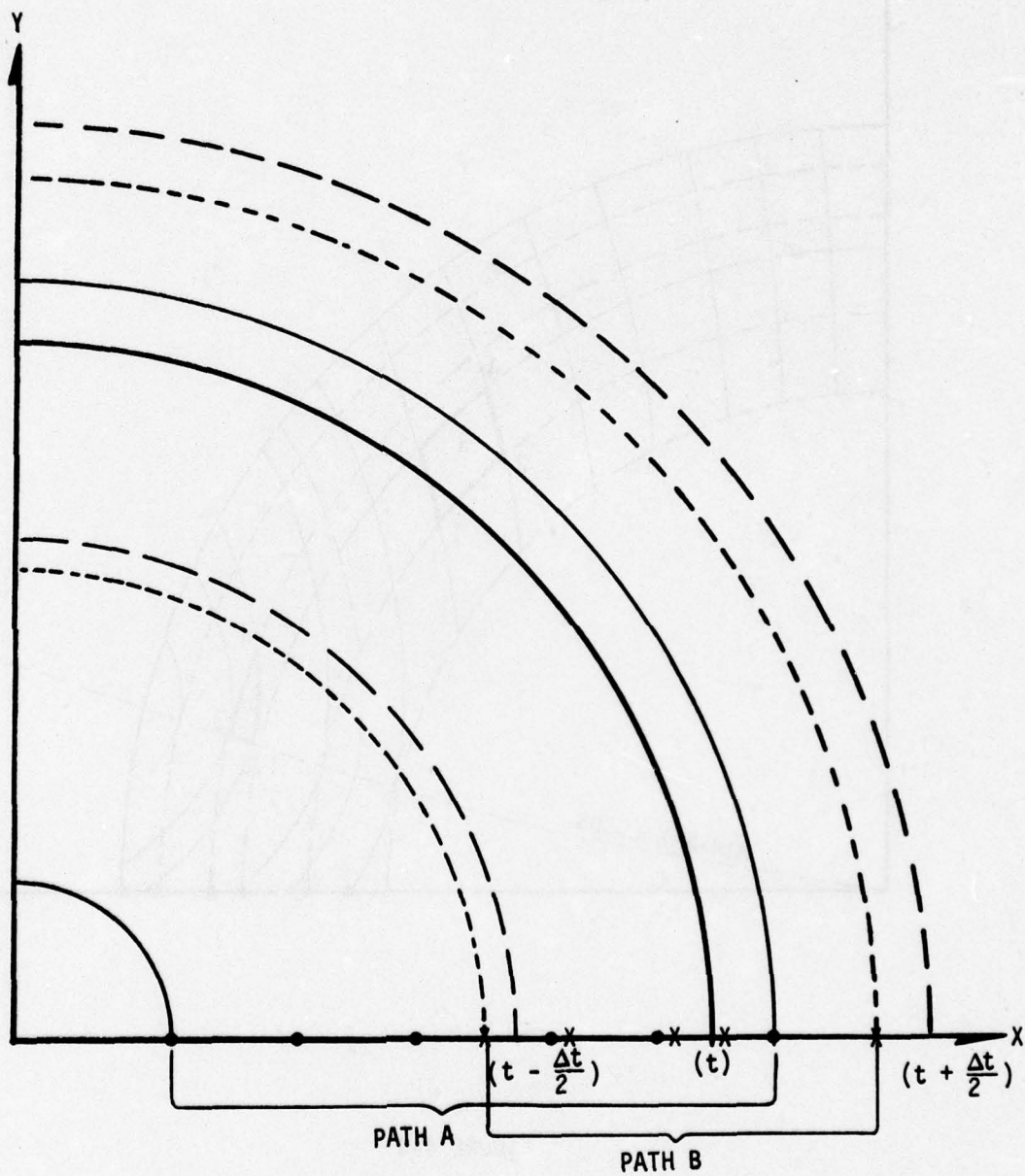


FIGURE 4-3

Insonified portion of surface corresponding to ray paths in Figure 6.

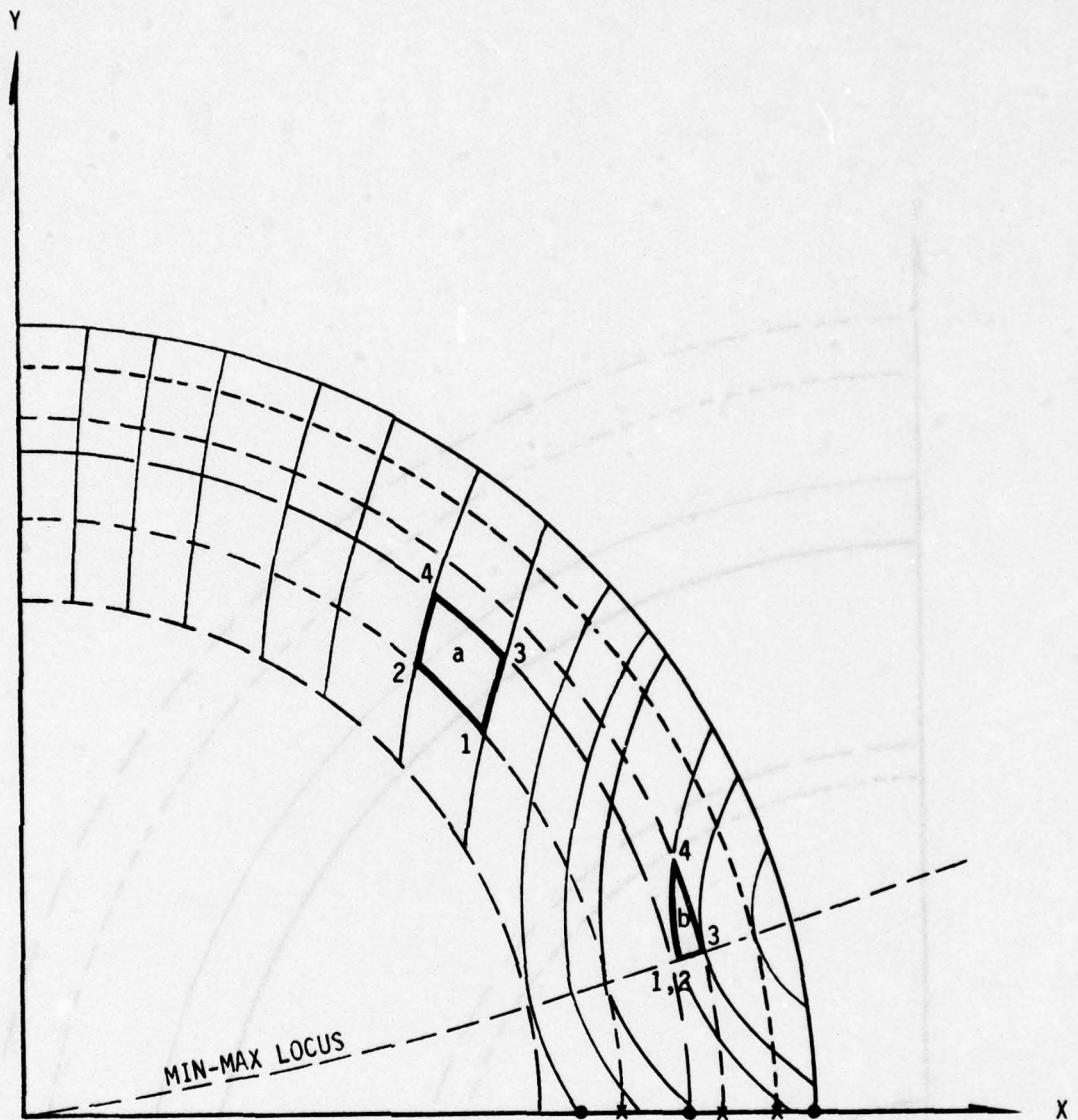


FIGURE 4-4

The part of the common insonified region which also lies between the time limits returns energy to the source at time  $t$ . This region has been broken up into incremental areas, bounded on two sides by equal-time lines and on two sides by equal-frequency lines.

### 4.2.2 Volume Reverberation

Figure 4-5 illustrates the computation of volume reverberation. For the straight-running case, the return in a band at a given time,  $t$ , is from the frustum of a hollow cone with spherical bases. The cone is divided radially about its face forming small areas, and the pattern losses to each area are combined to yield an average pattern loss for the iso-frequency volume. Volume reverberation is computed using this pattern loss, average two way transmission losses, volume of the hollow frustum, and volume scattering coefficient. In the turning case the insonified volume is not a cone, and the transmit and receive directions are different. However, the basic procedure is the same as for the non-turning case.

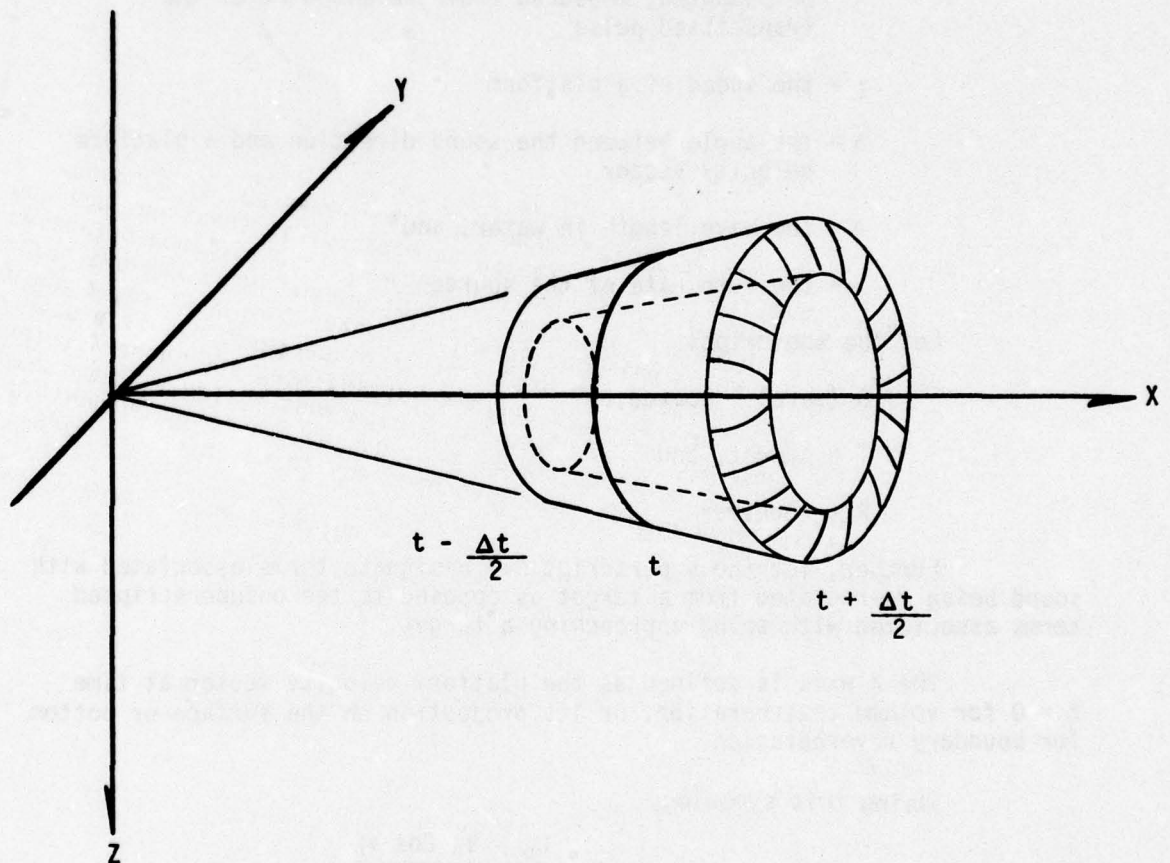


FIGURE 4-5

Volume insonified at time  $t$  between two equal-frequency cones and two equal-time spheres. Pattern losses are measured to each area marked on the end.

4.3 Equations

4.3.1 Preliminary

The following symbols and definitions are used in this section:

C = the velocity of sound in water, a function of water depth

f = the frequency of a sound wave

t = the elapsed time at which reverberation is to be computed, measured from the midpoint of the transmitted pulse

V = the speed of a platform

Y = the angle between the sound direction and a platform velocity vector

λ = the wave length in water, and

ω = the turn rate of the source

Let the subscripts

0 (zero) = source,

T = target, and

R = receiver

Further, let the superscript "\*" designate terms associated with sound being re-radiated from a target as opposed to the unsuperscripted terms associated with sound approaching a target.

The X axis is defined as the platform velocity vector at time t = 0 for volume reverberation, or its projection on the surface or bottom for boundary reverberation.

Using this symbology

$$\lambda_0 = \frac{C_0 - V_0 \cos \gamma_0}{f_0}$$

Approaching a target

$$\lambda_T = \frac{C_T}{C_0} \lambda_0 = \frac{C_T (C_0 - V_0 \cos \gamma_0)}{C_0 f_0}$$

The frequency observed by a receiver on the target, and that re-radiated into the water will be

$$f_T = \frac{C_T - V_T \cos \gamma_T}{\lambda_T} = f_0 \frac{C_0 (C_T - V_T \cos \gamma_T)}{C_T (C_0 - V_0 \cos \gamma_0)}$$

The wave length of re-radiated sound is

$$\lambda_T^* = \frac{C_T^* - V_T \cos \gamma_T^*}{f_T} = \frac{C_T (C_0 - V_0 \cos \gamma_0) (C_T^* - V_T \cos \gamma_T^*)}{f_0 C_0 (C_T - V_T \cos \gamma_T)}$$

approaching the receiver,

$$\lambda_R = \frac{C_R}{C_T^*} \lambda_T^* = \frac{C_R C_T (C_0 - V_0 \cos \gamma_0) (C_T^* - V_T \cos \gamma_T^*)}{f_0 C_0 C_T^* (C_T - V_T \cos \gamma_T)}$$

and the frequency seen by the receiver is

$$f_R = \frac{C_R - V_R \cos \gamma_R}{\lambda_R} = f_0 \frac{C_0 C_T^* (C_T - V_T \cos \gamma_T) (C_R - V_R \cos \gamma_R)}{C_R C_T (C_0 - V_0 \cos \gamma_0) (C_T^* - V_T \cos \gamma_T^*)}$$

Simplifying, in the vicinity of the target,  $C_T^* = C_T$ , and considering reverberation as being from motionless scatterers (their motion is handled statistically as "spreading" in the returned sound)  $V_T = 0$ . Also, we are interested only in the monostatic case (source and receiver at the same point), so  $C_R = C_0$  and  $V_R = V_0$ . Applying these identities we have

$$f_R = f_0 \frac{C_0 - V_0 \cos \gamma_R}{C_0 - V_0 \cos \gamma_0} \quad (1)$$

#### 4.3.2 Boundary Reverberation

For calculations of boundary reverberation, we will resolve the angle  $\gamma$  into its spherical components, the horizontal angle  $\phi$  and the vertical angle,  $\theta$ . The equation now becomes

$$f_R = \frac{C_0 - V_0 \cos \theta_R \cos \phi_R}{C_0 - V_0 \cos \theta_0 \cos \phi_0}$$

Since  $C$  is a function of depth only, the transmitted and received rays are in the same vertical plane. For the straight-running case,  $\phi_R = \pi + \phi_0$  but in general  $\phi_R = \pi + \phi_0 - \omega t$ . Finally, then, the frequency of reverberation received from a point on a boundary,

$$f_R = f_0 \frac{C_0 + V_0 \cos \theta_R \cos (\phi_0 - \omega t)}{C_0 - V_0 \cos \theta_0 \cos \phi_0} \quad (2)$$

Refer again to Figure 4-4. In order to be certain that all incremental areas are assigned to the correct frequency bands, it is important to know what iso-frequency line is tangent to an iso-time line. This is equivalent to finding the maximum or minimum frequency occurring at a given time. It is clear from Figure 4-4 that all the variables of equation (2) except  $\phi_0$  have been given fixed values. Therefore, we find at what azimuth angle received frequency is a maximum or minimum. Differentiating equation (2),

$$\frac{df_R}{d\phi_0} = -f_0 \frac{V_0 \cos \theta_R \sin(\phi_0 - \omega t)}{C_0 - V_0 \cos \theta_0 \cos \phi_0}$$

$$-f_0 \frac{C_0 + V_0 \cos \theta_R \cos(\phi_0 - \omega t)}{(C_0 - V_0 \cos \theta_0 \cos \phi_0)^2} V_0 \cos \theta_0 \sin \phi_0 = 0$$

Clearing fractions and rearranging terms,

$$V_0^2 \cos \theta_0 \cos \theta_R [\sin \phi_0 \cos(\phi_0 - \omega t) - \cos \phi_0 \sin(\phi_0 - \omega t)]$$

$$+ C_0 V_0 [\cos \theta_R \sin(\phi_0 - \omega t) + \cos \theta_0 \sin \phi_0] = 0$$

Reducing the first term and expanding the second term using the sin (a-b) identity,

$$V_0^2 \cos \theta_0 \cos \theta_R \sin \omega t$$

$$+ C_0 V_0 (\cos \theta_R \sin \phi_0 \cos \omega t - \cos \theta_R \cos \phi_0 \sin \omega t + \cos \theta_0 \sin \phi_0) = 0$$

Again rearranging terms

$$(\cos \theta_R \cos \omega t + \cos \theta_0) \sin \phi_0 - \cos \theta_R \sin \omega t \cos \phi_0$$

$$+ \frac{V_0}{C_0} \cos \theta_0 \cos \theta_R \sin \omega t = 0$$

Substituting

$$a = \cos \theta_R \cos \omega t + \cos \theta_0$$

$$b = \cos \theta_R \sin \omega t$$

$$c = \frac{V_0}{C_0} \cos \theta_0 \cos \theta_R \sin \omega t$$

we have

$$a \sin \phi_0 - b \cos \phi_0 + c = 0$$

Squaring and substituting for  $\sin^2 \phi_0$  we arrive at the quadratic

$$(a^2 + b^2) \cos^2 \phi_0 - 2bc \cos \phi_0 + c^2 - a^2 = 0$$

Set into the quadratic formula and simplified, this becomes finally

$$\cos \phi_0 = \frac{bc \pm a \sqrt{a^2 + b^2 - c^2}}{a^2 + b^2} \quad (4)$$

To understand the significance of the sign of the radical, consider that when  $\omega = 0$ ,  $\sin \omega t = 0$ , and  $\cos \phi_0 = \pm 1$ . That is, the locus of the points of tangency between iso-time and iso-frequency lines (the min-max locus) is the X axis. Also, in this case the iso-frequency line for  $f = f_0$  is the Y axis, with greater frequencies to the right, lesser frequencies to the left. Thus it is seen that the positive and negative signs define  $\phi_0$  for frequency maximum and minima, respectively.

We will now find the co-ordinates of the corners of the insonified polygon labeled 1, 2, 4, 3 in Figure 4-6. At time  $t$  and frequency  $f$ , from equation (2),

$$f_R C_0 - f_R V_0 \cos \theta_0 \cos \phi_0 = f_0 C_0 + f_0 V_0 \cos \theta_R \cos (\phi_0 - \omega t) \quad , \text{ or}$$

$$f_0 \cos \theta_R \cos (\phi_0 - \omega t) + f_R \cos \theta_0 \cos \phi_0 - \frac{f_R C_0 - f_0 C_0}{V_0} = 0 \quad , \text{ or}$$

$$f_0 \cos \theta_R (\cos \omega t \cos \phi_0 + \sin \omega t \sin \phi_0) + f_R \cos \theta_0 \cos \phi_0 - \frac{C_0}{V_0} (f_R - f_0) = 0 \quad , \text{ or}$$

$$(f_0 \cos \theta_R \cos \omega t + f_R \cos \theta_0) \cos \phi_0 + (f_0 \cos \theta_R \sin \omega t) \sin \phi_0 - \frac{C_0}{V_0} (f_R - f_0) = 0$$

Setting

$$a = f_0 \cos \theta_R \cos \omega t + f_R \cos \theta_0 \quad ,$$

$$b = f_0 \cos \theta_R \sin \omega t \quad , \text{ and}$$

$$c = \frac{C_0}{V_0} (f_R - f_0) \quad ,$$

we have

$$a \cos \phi_0 + b \sin \phi_0 - c = 0$$

Squaring and substituting for  $\sin^2 \phi_0$  as previously, we obtain the quadratic

$$(a^2 + b^2) \cos^2 \phi_0 - 2ac \cos \phi_0 + c^2 - b^2 = 0,$$

and by quadratic formula

$$\cos \phi_0 = \frac{ac \pm b \sqrt{a^2 + b^2 - c^2}}{a^2 + b^2}$$

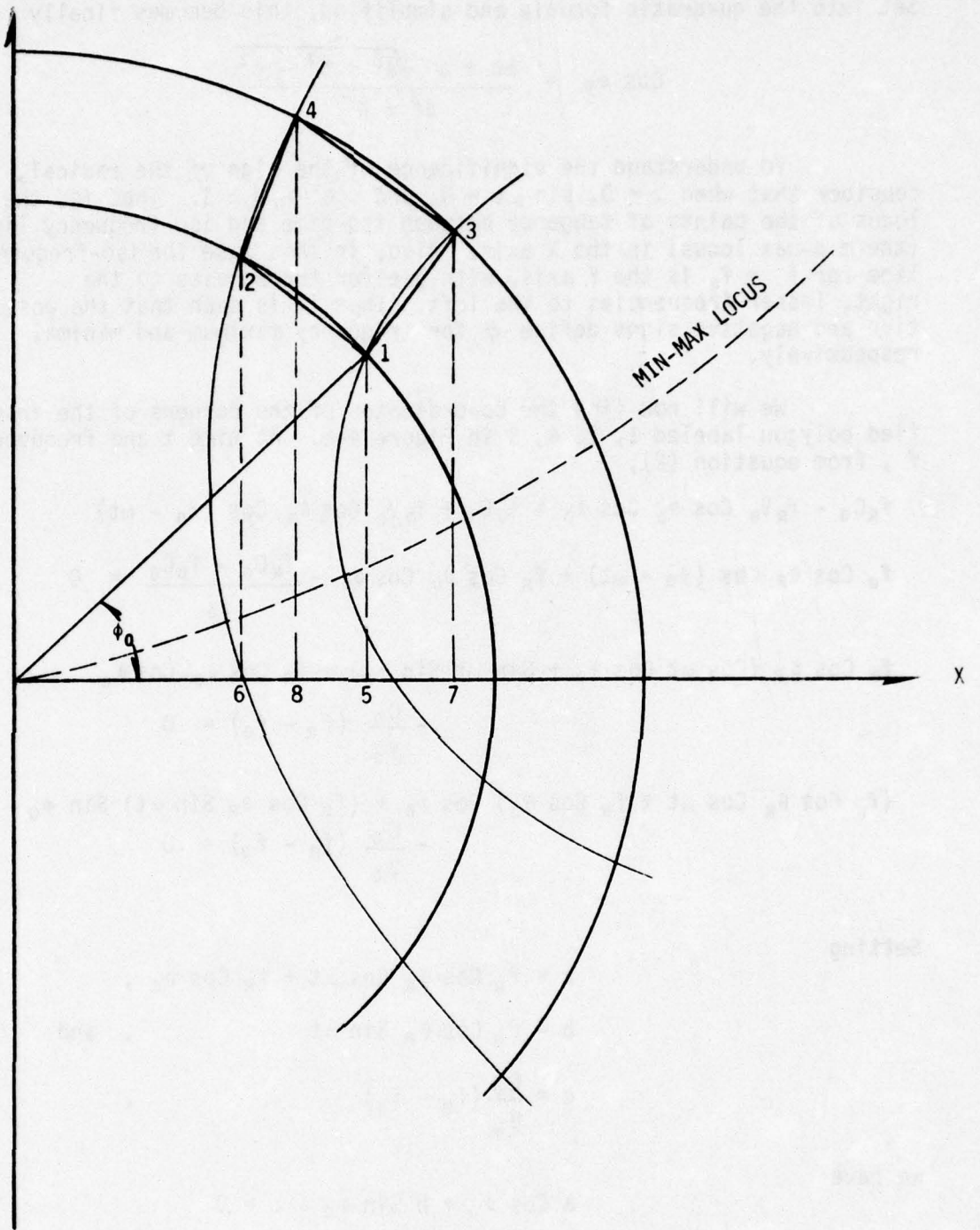


FIGURE 4-6

Finding the value of an incremental area.

Similarly it can be shown that

$$\sin \phi_0 = \frac{bc \mp a \sqrt{a^2 + b^2 - c^2}}{a^2 + b^2}$$

opposite polarity of the radicals being required by the  $\sin^2 \phi + \cos^2 \phi = 1$  identity.

Now from Figure 4-6, it is seen that for point 1

$$\cos \phi_0 = \frac{X_1}{X_t} \quad \text{and} \quad \sin \phi_0 = \frac{Y_1}{X_t}$$

where  $x_t$  is the  $x$  value associated with time  $t$ , i.e.  $x_t$  is the radius of the iso-time circle. Therefore for point 1

$$\begin{aligned} X_1 &= X_t \frac{ac \pm b \sqrt{a^2 + b^2 - c^2}}{a^2 + b^2} \quad \text{and} \\ Y_1 &= X_t \frac{bc \mp a \sqrt{a^2 + b^2 - c^2}}{a^2 + b^2} \end{aligned} \quad (5)$$

From considering the geometry when  $\omega = 0$ , it can be seen that the upper signs are used for insonified polygons which are clockwise of the min-max locus when  $f_R > f_0$ , counter clockwise of the locus when  $f_R < f_0$ , and conversely for the lower signs.

The area of the polygon in Figure 4-6 is clearly the sum of trapezoids 2, 4, 8, 6 and 4, 3, 7, 8 less the sum of 2, 1, 5, 6 and 1, 3, 7, 5. That is,

$$\begin{aligned} A &= \frac{1}{2}(X_4 - X_2)(Y_4 + Y_2) + \frac{1}{2}(X_3 - X_4)(Y_3 + Y_4) \\ &\quad - \frac{1}{2}(X_1 - X_2)(Y_1 + Y_2) - \frac{1}{2}(X_3 - X_1)(Y_3 + Y_1) \quad \text{or} \end{aligned}$$

$$\begin{aligned} A &= \frac{1}{2}(X_4 Y_4 + X_4 Y_2 - X_2 Y_4 - X_2 Y_2 + X_3 Y_3 + X_3 Y_4 - X_4 Y_3 - X_4 Y_4 \\ &\quad - X_1 Y_1 - X_1 Y_2 + X_2 Y_1 + X_2 Y_2 - X_3 Y_3 - X_3 Y_1 + X_1 Y_3 + X_1 Y_1) \end{aligned}$$

Consolidating, we arrive at the computational form used in the program:

$$A = \left| \frac{1}{2} [(X_4 Y_2 + X_3 Y_4 + X_2 Y_1 + X_1 Y_3) - (X_2 Y_4 + X_4 Y_3 + X_1 Y_2 + X_3 Y_1)] \right| \quad (6)$$

The taking of absolute value avoids negative areas in some quadrants.

Equation 6 is quite general and computes correct areas even for triangles.

## 4.3.3 Volume Reverberation

Now in the straight-running case, as has been mentioned before, the iso-frequency surface is a cone. In the turning case, this surface becomes quite complex, even discontinuous for certain combinations of frequency and turn angle. We will now derive a method of expressing the volume within an iso-frequency surface in the general case.

To begin with, equation (2) is equally applicable to volume reverberation. However, in the simplified model, using a uniform unbounded medium, the transmit and receive paths will necessarily be the same for the straight running case. In any case,  $\theta_R$  will equal  $\theta_0$ . Thus the equation becomes

$$f_R = f_0 \frac{C_0 + V_0 \cos \theta_0 \cos (\phi_0 - \omega t)}{C_0 - V_0 \cos \theta_0 \cos \phi_0}$$

clearing the fraction and rearranging terms

$$\cos \theta_0 [f_0 \cos (\phi_0 - \omega t) + f_R \cos \phi_0] = \frac{C_0}{V_0} (f_R - f_0)$$

Substituting

$$\cos (\phi_0 - \omega t) = \cos \phi_0 \cos \omega t + \sin \phi_0 \sin \omega t,$$

$$\cos \phi_0 = \frac{X}{\sqrt{X^2 + Y^2}},$$

$$\sin \phi_0 = \frac{Y}{\sqrt{X^2 + Y^2}}, \text{ and}$$

$$\cos \theta_0 = \frac{\sqrt{X^2 + Y^2}}{\sqrt{X^2 + Y^2 + Z^2}}, \text{ we obtain}$$

$$\frac{\sqrt{X^2 + Y^2}}{\sqrt{X^2 + Y^2 + Z^2}} \left[ f_0 \left( \frac{X}{\sqrt{X^2 + Y^2}} \cos \omega t + \frac{Y}{\sqrt{X^2 + Y^2}} \sin \omega t \right) + f_R \frac{X}{\sqrt{X^2 + Y^2}} \right] = \frac{C_0}{V_0} (f_R - f_0)$$

$$\text{or } f_0 (X \cos \omega t + Y \sin \omega t) + f_R X = \frac{C_0}{V_0} (f_R - f_0) \sqrt{X^2 + Y^2 + Z^2}$$

$$\text{or } X(f_0 \cos \omega t + f_R) + Y(f_0 \sin \omega t) = \frac{C_0}{V_0} (f_R - f_0) \sqrt{X^2 + Y^2 + Z^2} \quad (7)$$

Equation (7) describes the iso-frequency surface in cartesian coordinates.

For simplicity let us substitute

$$a = f_0 \cos \omega t + f_R \quad ,$$

$$b = f_0 \sin \omega t \quad , \text{ and}$$

$$c = \frac{C_0}{V_0} (f_R - f_0) \quad , \text{ yielding}$$

$$aX + bY = c \sqrt{X^2 + Y^2 + Z^2} \quad (8)$$

By rotating axes through some angle  $\delta$ , the Y term of the above equation can be eliminated. Using the superscript "prime" to denote measurements in a rotated system and the transformations

$$X' = X \cos \delta + Y \sin \delta \quad \text{and}$$

$$Y' = Y \cos \delta - X \sin \delta \quad ,$$

it can be seen that to eliminate the Y term in the left half of equation (8),  $\delta$  must be chosen such that

$$a \sin \delta + b \cos \delta = 0 \quad , \text{ or}$$

$$a^2 \sin^2 \delta = b^2 \cos^2 \delta \quad , \text{ or}$$

$$\sin^2 \delta = \frac{b^2}{a^2 + b^2} \quad \text{and} \quad \cos^2 \delta = \frac{a^2}{a^2 + b^2} \quad , \text{ or}$$

$$\sin \delta = \frac{-b}{\sqrt{a^2 + b^2}} \quad \text{and} \quad \cos \delta = \frac{a}{\sqrt{a^2 + b^2}}$$

applying this to equation (8) we have

$$\frac{a^2 X'}{\sqrt{a^2 + b^2}} - \frac{ab Y'}{\sqrt{a^2 + b^2}} + \frac{ab Y'}{\sqrt{a^2 + b^2}} + \frac{b^2 X'}{\sqrt{a^2 + b^2}} = c \sqrt{(X')^2 + (Y')^2 + Z^2} \quad , \text{ or}$$

$$\frac{a^2 + b^2}{\sqrt{a^2 + b^2}} X' = c \sqrt{(X')^2 + (Y')^2 + Z^2} \quad , \text{ or}$$

$$\frac{X'}{\sqrt{(X')^2 + (Y')^2 + Z^2}} = \frac{c}{\sqrt{a^2 + b^2}}$$

Resubstituting,

$$\frac{X'}{\sqrt{(X')^2 + (Y')^2 + Z^2}} = \frac{\frac{C_0}{V_0} (f_R - f_0)}{\sqrt{f_0^2 \cos^2 \omega t + f_R^2 + f_0^2 \sin^2 \omega t}}, \text{ or}$$

$$\frac{X'}{\sqrt{(X')^2 + (Y')^2 + Z^2}} = \frac{\frac{C_0}{V_0} (f_R - f_0)}{\sqrt{f_0^2 + f_R^2 + 2f_R f_0 \cos \omega t}}$$

remembering that  $\sqrt{(X')^2 + (Y')^2 + Z^2} = C_0 t$ , the distance that the sound has traveled in time  $t$ .

But the left hand member of this equation is  $\cos \gamma'$ , the  $X'$  direction cosine. For a particular set of values of the parameters in the right-hand member of the equation,  $\cos \gamma'$ , and hence  $\gamma'$  are constant. Thus it can be seen that for each time,  $t$ , the intersection of the iso-frequency surface of frequency  $f_R$  and the sphere of radius  $C_0 t$  is a circle centered on the  $X'$  axis, which is at angle  $\delta$  from the  $X$  axis. This circle defines a spherical segment.

Let us define our differential of the volume enclosed by an iso-frequency surface as the area of this segment times the differential of range or

$$dv = A dr$$

Now the area of a segment with thickness of  $h$  of a sphere of radius  $r$  is

$$A = 2\pi r h \quad \text{where}$$

$$h = r - r \cos \gamma$$

Therefore

$$A = 2\pi r^2 (1 - \cos \gamma) \quad , \text{ and}$$

$$dv = 2\pi r^2 (1 - \cos \gamma) dr$$

Substituting for  $r$ ,  $dr$ , and  $\cos \gamma$  we have

$$dv = 2\pi C_0^3 t^2 \left[ 1 - \frac{\frac{C_0}{V_0} (f_R - f_0)}{\sqrt{f_0^2 + f_R^2 + 2f_R f_0 \cos \omega t}} \right] dt$$

The volume returning energy from within the iso-frequency surface at time  $t$  will be

$$V = 2\pi C_0^3 \int_{t - \frac{\Delta t}{2}}^{t + \frac{\Delta t}{2}} t^2 \left[ 1 - \frac{\frac{C_0}{V_0} (f_R - f_0)}{\sqrt{f_0^2 + f_R^2 + 2f_R f_0 \cos \omega t}} \right] dt \quad (9)$$

The integral in equation (9) has no analytic solution, but is evaluated digitally. The volume returning energy within any band, obviously, would be the difference between two such integrals at the two values of  $f_R$  representing the band limits.

#### 4.4 Verification

Appendix F gives the results of an extensive comparison between various models for computing the boundary reverberation. This compares results only for straight-running cases. In addition, comparisons were made in 1973 with an independent model developed by Dr. J. H. Slaton of the Naval Undersea Center for a limited number of turning cases. These revealed several difficulties in the turning case which have been corrected. Agreement was very good, considering the difference in mathematical approach.

For the straight-running case, comparisons of volume reverberation with the method described in reference 1 have been excellent. This was expected because of the similarity in assumptions in the two very simplified models.

### SECTION V

#### AREAS FOR POSSIBLE IMPROVEMENTS AND REFINEMENTS

##### 5.1 Volume Reverberation

The simulation of volume reverberation includes two gross simplifications; the medium is homogeneous, and it is unbounded. Thus, several known features of particular environments cannot be realistically approximated. In particular, returns from scattering layers, returns from regions of greater or lesser focusing, e.g. caustics, and returns over multiple paths are ignored. Still it is hoped that the model can supply numbers of the right order of magnitude in some useful cases.

Almost from the beginning, the three-dimensional analogue of the boundary calculations was recognized as more realistic. A preliminary study was made in 1967 by M.M. Jacoby of NUC, which outlined the geometric problems of computing incremental volumes. Although precise formulae have still not been developed, the problems seem mainly those of bookkeeping; that is, of ensuring that the entire insonified volume is accounted for. The calculations would also be very costly in computer time.

Implementations of this model: tedious and time-consuming to write and check-out, but require only re-writing of one DOP subroutine, plus the changes in SONAR mentioned in 5.2.

### 5.2 Multi-path Reverberation

The current model approximates the ray-path losses when transmit and receive paths are not the same. The approximation is simply the average of the two-way losses over each single path. Now the transmitted and reflected rays have different spreading loss even over the same (reciprocal) path. The difference is small, however, rarely amounting to so much as 0.2 dB.

Another discrepancy is in the implicit averaging of the scattering strengths. The tacit assumption (not to be dignified as an approximation) is that scattering strength from one path into another is the average of the back scattering strengths for the two paths. In the absence of a good theoretical or empirical alternative, this assumption was allowed to stand. There is a need for a single expression of scattering strength in all directions from an incident ray.

Incorporating such an expression in DOP would require that scattering strength be removed from total losses passed by program SONAR.

Assesment of these changes: given the scattering expression, the latter change would be an easy matter; the former would not be much more difficult.

### 5.3 Vehicle Translation During Ping

Appendix E discusses the consequences of using the same ray-path for transmit and receive, ignoring the translation of the vehicle. This change is of secondary importance, but should probably be included for completeness if the changes in 5.2 were implemented. It would be easy under these circumstances.

### 5.4 "Spreading" of Reverberation

There are theoretical reasons to believe that doppler shifts caused by motions of scatterers, particularly at the surface, are a function of grazing angle. No such provision is made in this model. Incorporation of this feature would require a fundamental change in the handling of boundary "spreading" and probably minor changes in SONAR and RAYSRT.

Difficulty of these changes: moderately lengthy, but not complicated.

### 5.5 Preferential Orientation of Vehicle with Respect to the Environment.

Real environments are non-uniform in every direction, not merely in depth as currently modeled.

The following three additions to the model would take account of some non-uniformities. All would come under the heading of major revisions. In addition, it is clear that, conditions being different at all points and times in the environment, a single ping cycle would no longer give a general description of reverberation. The changes would, however, make possible the calculation of ranges of values that might be expected.

### 5.5.1 Current and/or Wind Direction

Only DOP would need revision. Doppler content due to both vehicle motion and scatterer motion is affected.

### 5.5.2 Sloping or Broken Bottom

The SONAR program can compute rays reflected from any bottom made of plane segments which reflect rays in the vertical plane of incidence. Such bottom segments must be perpendicular to the plane containing the rays, and such bottoms are of limited usefulness in modeling real environments.

Spreading losses and directions of reflections can be computed for rays striking any analytically describable bottom. However a properly general treatment would require considerable changes not only in SONAR and DOP, but also in RAYSRT. These changes would seem of little value without also the ones in 5.5.3.

### 5.5.3 Three-dimensional Velocity Profiles

The use of velocity profiles varying in two or three dimensions requires completely new SONAR, RAYSRT and DOP programs; no mere adaptation would suffice. While ray tracing programs already exist and could be adapted, the running times would be increased by an order of magnitude, at least.

REFERENCES

1 - Naval Undersea Center. Digital Computer Programs for Analyzing Acoustic Search Performance in Refractive Waters, by Philip Marsh and A. B. Poynter, Pasadena, California, NUC, DEC 1969 (NUC TP 164, Vols. 1 & 2).

2 - NUC TP 164 Vol. 3 prepared by H. C. Bertucelli of Bendix Corporation updating Vols. 1 & 2.

3 - The Bendix Corporation. Plotting Program SRNBT4 and Density Spreading Program DENFSP, by H. C. Bertucelli, re programs of A. B. Poynter, North Hollywood, California, OCT 1975 (Bendix SR 75.58).

## INITIAL DISTRIBUTION

Operational Test and Evaluation Force (1)  
Deputy, Operational Test and Evaluation Force, Pacific (1)  
Naval Sea Systems Command (SEA-662D) (1)  
  (SEA-662D-21) (1)  
  (SEA-03B) (1)  
  (SEA-0342) (3)  
Office of Naval Research (ONR-466) (1)  
Anti-Submarine Warfare Systems Project (PM-4) (ASW-13) (1)  
  (ASW-14) (1)  
  (ASW-54) (1)  
National Oceanographic Data Center (1)  
Naval Electronics Laboratory Center, San Diego (1)  
Naval Ship Research and Development Center  
    Annapolis Division (1)  
    Carderock Division (1)  
Naval Oceanographic Office (1)  
Naval Surface Weapons Center, White Oak (1)  
Naval Postgraduate School, Monterey (Library, Technical Reports Section) (1)  
Naval Research Laboratory (1)  
Naval Torpedo Station, Keyport  
    Quality Evaluation Laboratory, Technical Library (1)  
    Director, Research and Engineering (1)  
Naval Underwater Systems Center, Newport (1)  
Naval Underwater Systems Center, New London (1)  
Naval Weapons Center, China Lake (Code 753) (1)  
Defense Documentation Center (TISIA-1) (20)  
Applied Physics Laboratory, University of Washington, Seattle (1)  
Applied Research Laboratory, Pennsylvania State University (1)  
Honeywell, Inc., Hopkins (1)  
Honeywell, Inc., Seattle (1)  
Bendix, Sylmar (1)

Naval Undersea Center

- Code 14
- 252
- 3044
- 307
- 35021
- 353
- 35302
- 3542
- 3543
- 3573 (3)
- 401
- 4532
- 4534 (2)
- 6565

BELT, JL A. TEST-PROBLEM/DOP-SONARS									
ELTOT7 RL1870 07/23-12:45:39-(1,0)									
000001	000	1REVERB	16.	2.	1800.	-31.4159	-60.	15.	
000002	000	2							
000003	000	36.	7.	8.	9.				
000004	000	4-90.	1.5	0.	-31.4	-90.	9.	0.	0.
000005	000	4-82.	-1.5	10.	-25.7	0.	9.	8.	19.8
000006	000	4-77.	-5.	20.	-22.3	0.		10.	22.9
000007	000	4-68.	-16.5	30.	-19.6			12.	25.3
000008	000	4-60.	-24.	40.	-17.2			14.	27.1
000009	000	4-53.	-28.	50.	-14.9			16.	28.3
000010	000	4-48.	-30.	60.	-12.9			18.	29.3
000011	000	4-40.	-32.	70.	-11.1			20.	30.1
000012	000	4-30.	-34.	80.	-9.2			25.	31.4
000013	000	4-9.	-37.	90.	-7.6			30.	32.
000014	000	40.	-43.	90.				40.	31.6
000015	000	40.						50.	27.4
000016	000	0						90.	22.8
000017	000	31.	2.	3.	5.				
000018	000	4 -180.	0.	0.	0.	0.	0.	0.	0.
000019	000	0 180.	0.	10.	0.	200.	0.	200.	0.
000020	000	3 4.	10.						
000021	000	4 0.	0.	0.	4000.				
000022	000	0 10.	0.	9000.	4000.				
000023	000	11.	12.						
000024	000	50.		2820421.4		-0.27303767		69.502715	3.70
000025	000	525.							
000026	000	550.							
000027	000	5100.							
000028	000	5150.							
000029	000	5180.							
000030	000	5190.							
000031	000	5200.							3.70
000032	000	5205.							
000033	000	5208.50815		2820421.4		-0.27303767		69.502715	
000034	000	5215.							
000035	000	5225.							
000036	000	5235.							
000037	000	5245.							
000038	000	5250.00149		2820409.3		-0.29729444		70.631276	3.71
000039	000	5265.							
000040	000	5280.							
000041	000	5284.68723		2819915.8		-0.3610.669		94.893745	
000042	000	5284.85							
000043	000	5285.00194		1840654.5		0.18280822		1473.2444	3.72
000044	000	5320.							
000045	000	5350.							4.31
000046	000	5380.							
000047	000	5403.							4.78
000048	000	5430.							
000049	000	5450.00484		-1364724.5		0.021384351		-8236.7312	5.15
000050	000	5470.							
000051	000	5491.16777		2680549.1		0.11.65644		164.15731	
000052	000	5492.00578		4796782.1		-0.064514513		-3334.0923	5.50
000053	000	5520.							
000054	000	5550.							5.68
000055	000	5570.							

APPENDIX A  
FIGURE 1

000056	000	5600.00860	4201878.8	-0.06859745	-2713.1275	5.80
000057	000	5630.				
000058	000	5655.968408	2643857.5	8233.5634	218.67190	
000059	000	5656.01029	3669419.3	-0.00065898565	-24043.178	6.00
000060	000	5680.				
000061	000	5700.				6.02
000062	000	5720.				
000063	000	5750.01344	2640912.4	0.33833872	284.05826	
000064	000	5765.				
000065	000	5783.34800	2641521.0	-1.1518146	254.37530	
000066	000	5792.				
000067	000	5800.01529	2627055.9	0.037415208	643.14143	6.08
000068	000	5850.				
000069	000	5900.				6.12
000070	000	5950.				
000071	000	51000.				6.18
000072	000	51100.				
000073	000	51250.				
000074	000	51312.0411	2629880.5	0.11624671	503.65531	6.32
000075	000	51400.				
000076	000	51510.9659	2629880.5	0.11624671	503.65531	
000077	000	51537.3904	2629909.7	-0.49887228	514.51595	
000078	000	51543.5479	2629909.7	-0.49887228	514.51595	
000079	000	51650.0650	2618522.7	0.0839802	760.02509	6.41
000080	000	51900.				
000081	000	51968.				6.58
000082	000	52280.0753	2618522.7	0.0839802	760.02509	
000083	000	52297.				6.71
000084	000	52400.				
000085	000	52500.1493	2622869.3	-0.031541745	1029.0237	6.72
000086	000	52790.8537	2621947.8	0.22082943	918.17354	
000087	000	52936.2060	2670552.4	-0.011193266	2234.7444	6.79
000088	000	53500.				6.77
000089	000	53904.				6.76
000090	000	54000.				6.77
000091	000	6DOPLER 750.	119. 17.	-2. 2.9		020040
000092	000	7-90.	90. 1.			
000093	000	7	MAXN			
000094	000	7	MAXP			
000095	000	7	DEPTHN			
000096	000	7	DEPTHP			
000097	000	+				
000098	000	6DOPL 2 500.	119. 17.	+2. 2.9		020040
000099	000	GLIST				
000100	000	6DOPL 3 275.	119. 17.	-2. 2.9		020040
000101	000	+				
000102	000	GLIST				
000103	000	,				

END ELT.

APPENDIX A  
FIGURE 1 (CONTINUED)

FIGURE 2

```

@      ELT,IL  A-TEST-PROBLEM/DOP-RAYSRT
ELT077 RL1870 09/24-14:39:18-(1,0)
000001      000      PLOT
000002      000      0.      4000.
000003      000      +
000004      000      0.      4000.
000005      000      +
000006      000      0.      4000.
000007      000      +
END ELT.
    
```

FIGURE 3

```

@      ELT,IL  A-TEST-PROBLEM/DOP-DOP
ELT077 RL1870 07/23-12:45:50-(1,0)
000001      000      FO = 3.1715926535 E1
000002      000      VS= 45., BWIDTH = .25, DELT = .040, TIME =
000003      000      1.5      ,2.0
000004      000      1.5      ,2.0
000005      000      .250
000006      000      TMTMAX = 30.
000007      000      BWIDTH = 5.
000008      000      GO
000009      000      TMTMAX = 180.
000010      000      KNOTS,RELATIVE
000011      000      OMEGA = 10., NBEAM = 1
000012      000      CENTER
000013      000      FILTER
000014      000      VSPRED=.2,.1,.1,.1,.1
000015      000      SSPRED = .5,.125,.0625,.03125,.015625,.015625
000016      000      BSPRED=.5,.2,.05
000017      000      BWIDTH = 1.
000018      000      PRINT EVERY = 5
000019      000      TIME = .750
000020      000      GO
000021      000      TIMECOMP, TOTALS
000022      000      TVG
000023      000      PLOT
000024      000      GO
000025      000      GO, END
END ELT.
    
```

## APPENDIX B

## MEMORANDUM

P80203/ABP:pas  
18 January 1965From: Code P80203  
To: Code P802Subject: Error from Using  $10 \log_{10} \tau$  as a Measure of Effective Train Length When Computing Boundary Reverberation.

In mathematical models commonly in use for computing boundary reverberation levels in dB, a factor of  $10 \log_{10} \tau$  is added to account for the fact that an insonified annulus of finite width returns energy to the transducer at the same instant of time. In this context  $\tau$  is taken to be  $V(\Delta t)/2$  where  $V$  is the velocity of sound and  $\Delta t$  is the ping length in seconds. It is rather obvious that  $\tau$  is an accurate measure of annulus width only when the transmission path is essentially horizontal. Since analyses are contemplated for applications in which long pings and steep paths are involved, it seemed desirable to investigate the magnitude of errors which might accrue.

Some simple calculations were made after the fashion indicated in Figure 1, assuming an isotropic medium ( $V = 5000$  ft/sec). Starting with a source depth and an initial ray angle relative to the horizontal, the slant range ( $R_1$ ) to surface intercept was computed along with the horizontal range ( $X_1$ ) to this point and the two-way travel time. If time is measured from the end of transmission, this two-way travel time ( $2t_1$ ) would identify the instant when the trailing edge of the wave train will return energy from point  $P_1$ . At this same instant the leading edge of the wave train will be returning energy from point ( $P_2$ ) for which the horizontal range ( $X_2$ ) can be found on the basis of a slant range ( $R_2$ ) consistent with a two-way travel time of  $2t_2 = 2t_1 + \Delta t$ . The width of the insonified annulus is  $\tau^* = X_2 - X_1$ . A measure of the dB error involved by using  $\tau$  instead of  $\tau^*$  is given by  $10 \log_{10} \frac{\tau^*}{\tau}$ .

Such calculations were carried out over a range of values for  $Q_1$  of  $20^\circ$  through  $80^\circ$  for combinations of conditions that can be obtained from source depths of 500, 1000, 2000, and 5000 feet, and ping lengths of .040, .100, and .250 seconds. The results are plotted in Figure 2. The error as plotted is the number of dB that should be added to values computed when  $10 \log \tau$  is used. It appears that the error from this source is negligible when the significant paths are less than  $20^\circ$  from the horizontal as is the case for the directional systems we have previously analyzed in circular search. Even when a refractive environment is considered, the uncertainty in using an average velocity in computing  $\tau$  should not increase the error appreciably. As expected, the inaccuracy mounts rapidly with increasing path angles above  $20^\circ$  and with increasing source depth. However, the decrease in error as the ping length becomes longer was not anticipated. This trend occurs because in the ratio  $\frac{\tau^*}{\tau}$  the numerator increases less rapidly than does the denominator with increasing ping length.

If the annulus width itself were the only potential source of error, it would be possible to devise a correction procedure. Unfortunately, the contribution of each unit width of the insonified area to the reverberation level is not necessarily the same since the transmission and vertical pattern losses may vary substantially for the different paths involved. Nor in general can a total error be computed by summing the independent errors for each of the factors handled separately. A method for assessing the composite error will be presented in a subsequent memorandum.

A. B. POYNTER

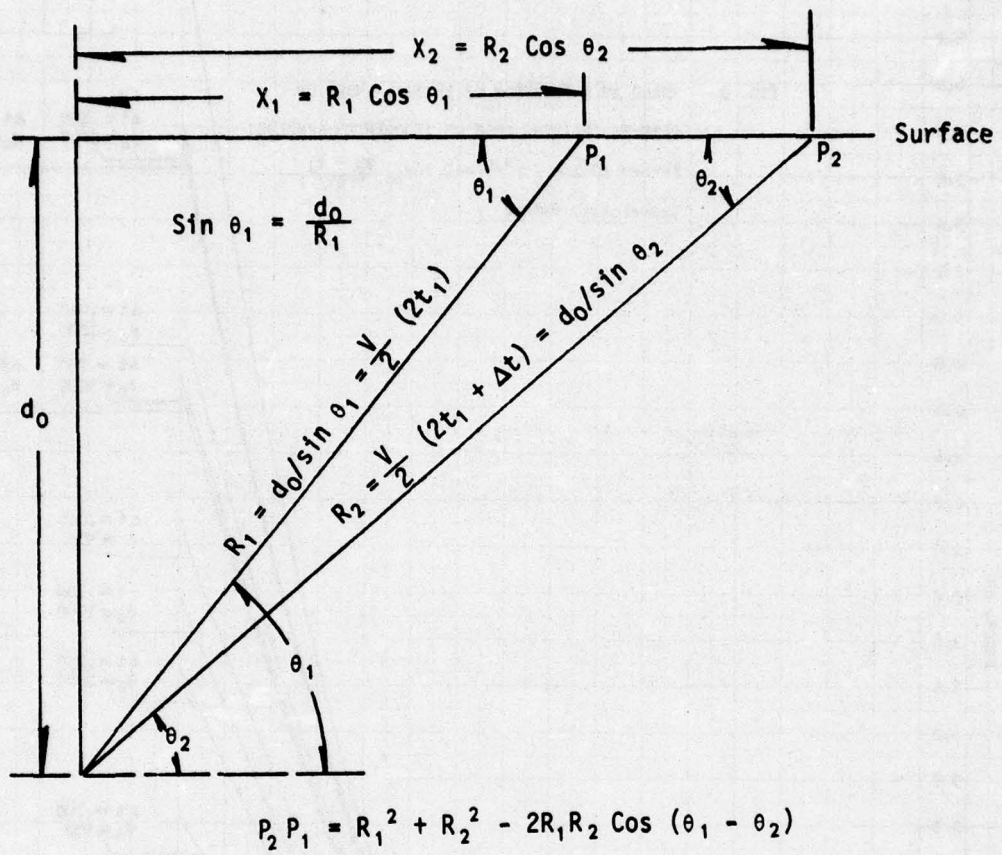


FIGURE 1

Method for finding  $\tau^* = X_2 - X_1$

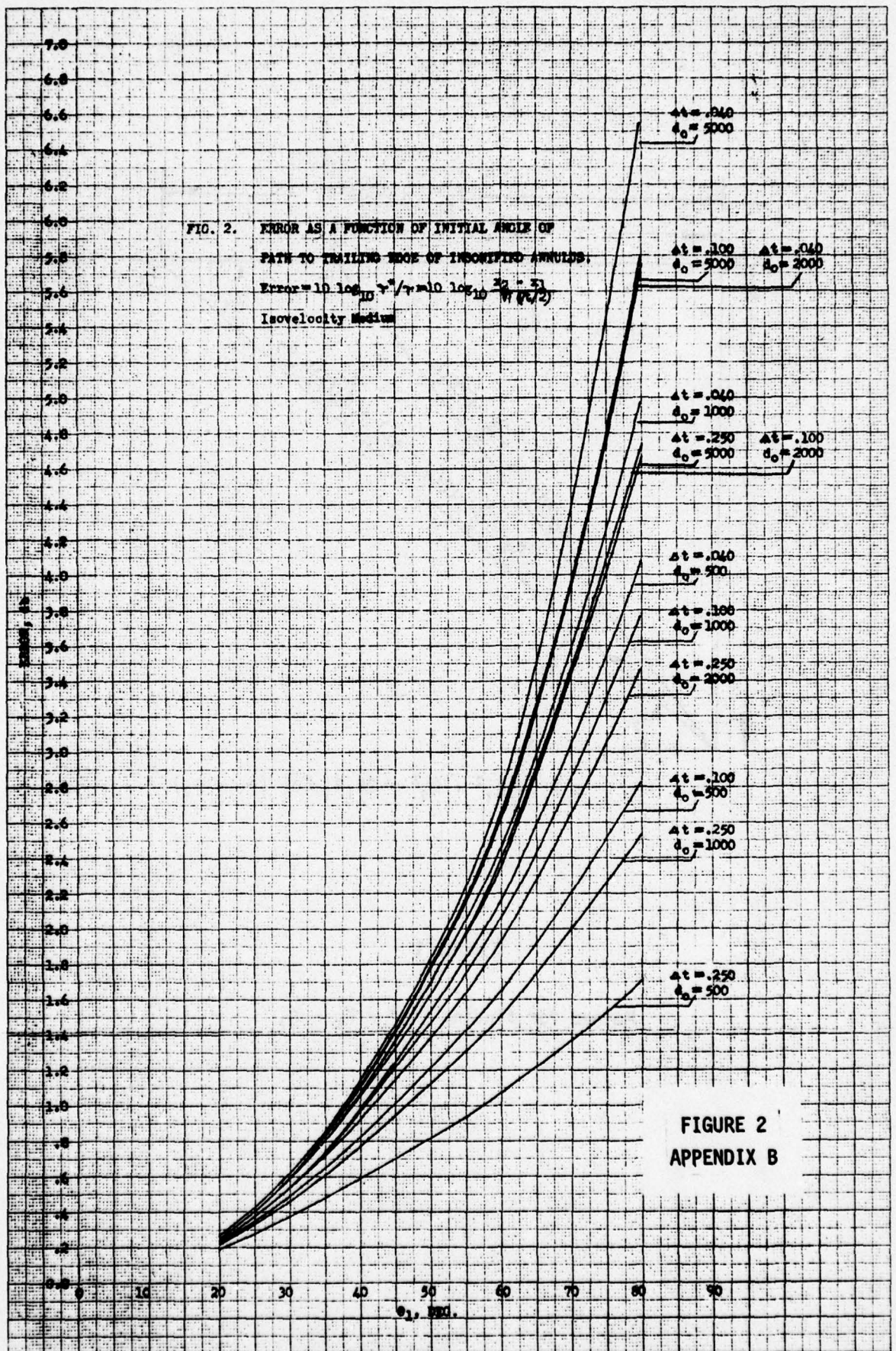


FIGURE 2  
APPENDIX B

Fig. 2.

## APPENDIX C

## MEMORANDUM

P80203/ABP:pas  
20 January 1965From: Code P80203  
To: Code P802

Subject: Review of Mathematical Model for Computing Boundary Reverberation.

- References:
- A. NAVORD Report 5606 (NOTS 1818) - Analytical Methods for Predicting Acoustic Performance of Homing Torpedoes in Circular Search.
  - B. TPR 246 (NOTS TP 2498) - Analytical Studies of Sonar in Refractive Water.
  - C. P80203 Memo, "Error from Using  $10 \log_{10} \tau$  as a Measure of Effective Train Length when Computing Boundary Reverberation," of 18 January 1965.

In the analytical work, it is necessary to develop mathematical models of the phenomenon to be studied so that quantitative results can be computed. These models are seldom exact, either because the process is not completely understood or because of a desire to avoid complexities which do not materially affect the results. The models may be adequate for the purpose originally intended, but it is dangerous to extend their use to new situations without reassessing their adequacy. The surface and bottom reverberation equations used in our computer programs are cases in point. The equations in general use are those given in References A and B.

For boundary reverberation a ray is traced to the surface (or bottom) and the expected reverberation level at the time in the ping cycle corresponding to the two-way travel time is computed, using: the transmission loss over this path; vertical pattern losses based on the initial ray angle, and a scattering coefficient per unit area based on the grazing angle at which the ray strikes the surface. Since the annular ring on the surface which returns energy at the time in question is unlikely to be unit distance wide, an additional term ( $10 \log_{10} \tau$ ) is added ( $\tau = \text{half the train length} = V(\Delta t)/2$  where  $V$  is the velocity of sound and  $\Delta t$  is the ping duration in seconds). The equation was formulated in the context of fairly shallow systems using relatively short pings and highly directional transducers oriented to emphasize horizontal coverage. For such systems the equation could be expected to yield acceptable accuracy. Future applications may involve one or more of the following:

- Long ping lengths for correlation detection
- Broad vertical patterns to provide greater depth coverage
- Steep paths (deep source or bottom bounce)

In preparation for such work it seems advisable to re-examine the mathematical model to ascertain whether or not it is still satisfactory.

In Reference C it was shown that  $10 \log_{10} \tau$  may not adequately account for the linear extent of the insonified area of the boundary which returns energy at the same instant of time. Moreover, when this annulus has considerable width, as is the case for the longer pings, the contribution of various parts of the insonified area to the total energy return may be substantially different because of variations in transmission loss, pattern loss, and even in the scattering coefficient for the different paths involved. To better account for these things and to provide a reference for assessing the accuracy of the model now in use, modifications were made in the computational procedures.

The key to the method is the temporary assumption that  $10 \log_{10} \tau = 0$ . This is equivalent to saying that a ping length is chosen so that the insonified annulus at the boundary is 1-yard wide. This is consistent with the way in which the scattering coefficient is given as a function of grazing angle, and, over such a distance, no change in transmission or pattern loss need be considered. Otherwise, the desired sets of environmental conditions and equipment parameters are used. A whole family of rays are run from the selected source depth to the surface, and reverberation levels are computed as before. However, instead of plotting reverberation level versus two-way travel time as is usual, both reverberation and travel time are plotted against the horizontal range at which each ray strikes the surface. If the beginning of transmission is taken as zero time, any selected time ( $2t_i$ ) on the two-way time curve will identify the horizontal range at the surface from which the leading edge of the wave train is returning reverberation. It follows that  $2t_i - \Delta t$  identifies the range from which the trailing edge is returning energy at the same instant. Integrating the reverberation curve between these two limits should give the actual reverberation level quite accurately. It should be noted that the values in the one-yard increments must be converted from dB to intensity before summing and then reconverted. Reasonable accuracy can be achieved with much less work by using average values for range increments several yards wide and multiplying each average value by the number of yards in the increment before summing.

After sufficient points have been determined in this manner, the values of reverberation can be replotted against elapsed time to yield the type of presentation generally desired. To obtain comparable results from the original model, one can rerun the computer program using the appropriate value for  $10 \log_{10} \tau$  as determined by the ping length of the transmission. It is more efficient, however, to return to the working curves and add  $10 \log_{10} \tau$  to the values of the reverberation curve for  $\tau = 1$  at the range determined by the travel time curve at the elapsed times for which data are desired.

Surface reverberation levels were computed by the two methods using parameters for the Torpedo MK 46 Mod 0 in circular search. Attenuation by the RRF was not considered. The source depth was assumed to be 750 feet. The velocity profile for the environment is shown in Figure 1A. The new computer program which permits use of a continuous gradient profile was used. The comparative results for a 40-ms ping are shown in Figure 2. The vertical patterns, of course, dominate the shape of the curves at times less than one second. The integration procedure would normally be expected to lower the peaks and fill in the troughs as well as to shift them slightly. The fact that the peaks in this case are lower for the curve obtained via the old

model suggests that the  $10 \log \tau$  correction is insufficient, particularly at the shorter times which would be identified with steeper paths. It might be kept in mind that the curve obtained by means of the original equation has the same shape as would the  $10 \log \tau = 0$  curve. The initial ray angles associated with a few points on this curve are shown as a matter of interest.

Figure 3 shows the comparative reverberation levels that would obtain if a ping length of 250-ms were used. It is clear that one must be very careful in computing reverberation levels when long pings are used; the two curves are substantially different. The integrated curve was not determined at times less than .55 seconds because before that time all of the ping has not reached the surface.

For both ping lengths, the curves would match more closely if the curves obtained by means of the original model were advanced in time by one-half the ping length. This follows since the computed ray path would then, in effect, intercept the surface near the middle of the insonified area and the transmission loss, vertical pattern loss, and scattering coefficient would be more representative of the area as a whole than is the case when the ray falls at one end of the insonified area. Figures 4 and 5 compare the results when this subterfuge is used for the .040 and .250 ping lengths, respectively.

As a further check, additional calculations were made for a non-turning vehicle at 500 feet in an environment characterized by velocity Profile B shown in Figure 1. Our old computer program based on linear-gradient layers was used in this instance. Other parameters were unchanged. The results are similar to those from the first set of calculations. Figure 6 compares the 40-ms ping data from the integrated method with that from the original model after the latter had been advanced in time by half the ping length.

Figure 7 presents similar data for the 250-ms ping. Part A, on the left shows the results out to 1.4 seconds. Calculations for this case were carried out to about 7.5 seconds, and the curves (after translation) remain in close agreement until about 6.7 seconds. For this elapsed time the paths involved are from rays that start out below the horizontal and are refracted back toward the surface by the positive velocity gradients which characterize this environment below 170 feet. The ray having a two-way travel time of 6.705 seconds and subsequent ones having slightly steeper initial angles, reverse at depths where the velocity gradient becomes less positive. This results in an abrupt increase in transmission loss and a resulting drop in reverberation level as indicated in Figure 7B (recall that the curve based on the original model has been advanced by 0.125 seconds.) In the vicinity of such anomalies the integrated method offers the only approach for computing expected values of boundary reverberation levels with reasonable accuracy.

Some general observations appear warranted:

- Within the limits imposed by the input data, accurate expected levels of surface reverberation as a function of elapsed time can be computed by means of ray tracing

programs by summing the contributions of 1-yard increments of the insonified annulus which contribute at the same instant.

- At present, this can be accomplished manually, but it may be possible to program the computer to this end.
- The present mathematical model can yield results which are reasonably accurate over the elapsed time interval during which the sound paths are such that  $10 \log_{10} \tau$  is a good measure of the width of the insonified annulus and the change in transmission loss, pattern losses, etc. over this annulus is not appreciable.
- The accuracy attainable and/or the time interval over which a given accuracy can be maintained will be increased if, in effect, the elapsed time is measured from the middle of the transmittal ping. If time is measured from the beginning of transmission the computed two-way travel time to the surface for each ray should be increased by  $\Delta t/2$  to obtain the time consistent with the computed reverberation level.
- Even if the technique in the above paragraph is used, errors may become substantial when:
  - The paths are very steep so that  $10 \log_{10} \tau$  is not a good measure of annulus width;
  - The insonified annulus is wide enough to encompass a spread of paths through the minor lobes of the transducer;
  - In the vicinity of transmission loss anomalies (either substantial focusing or defocusing)

The above observations should also apply to bottom reverberation, except that additional complications may arise if the bottom is irregular.

A. B. POYNTER

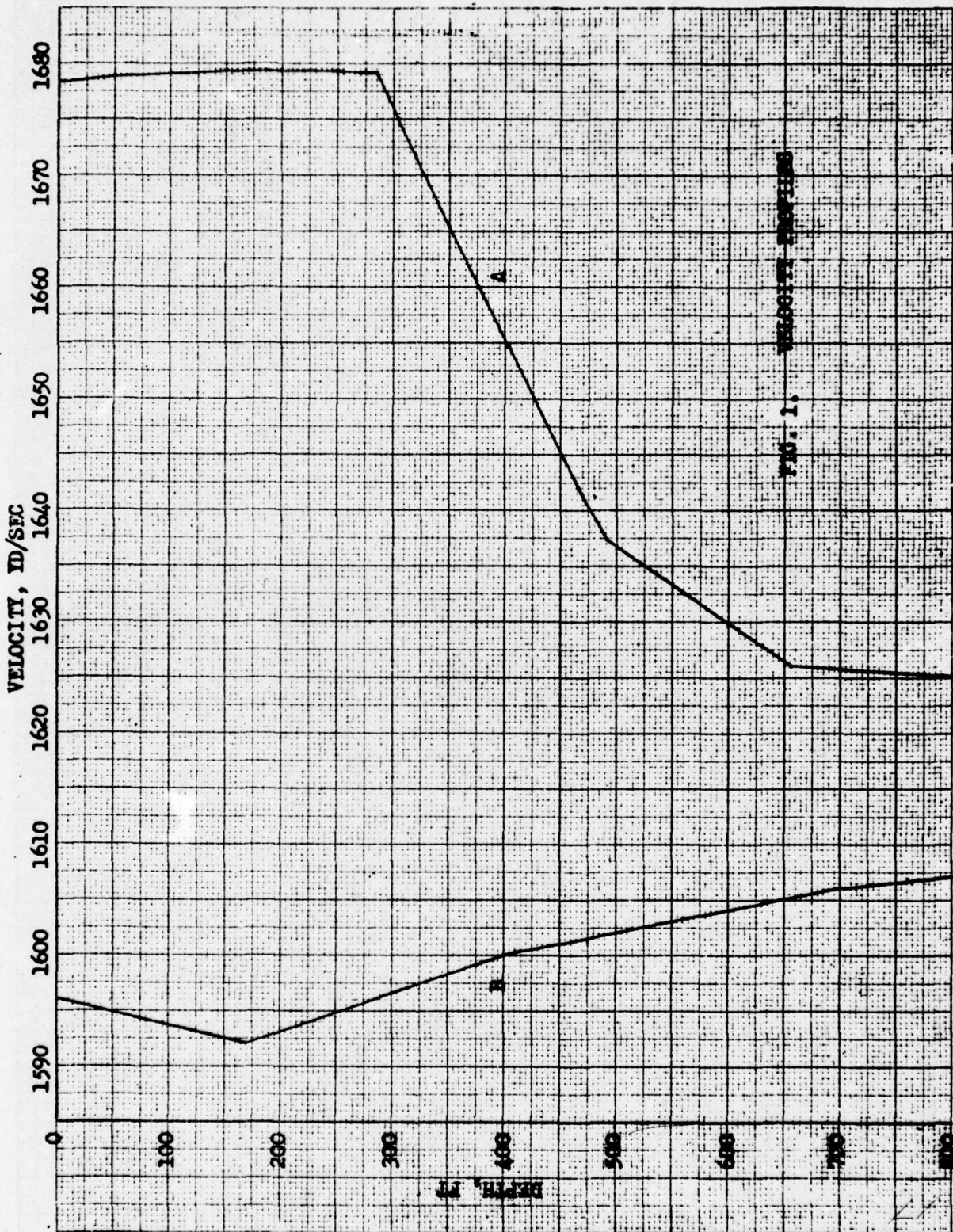


FIG. 1. VELOCITY PROFILE

Fig. 1.

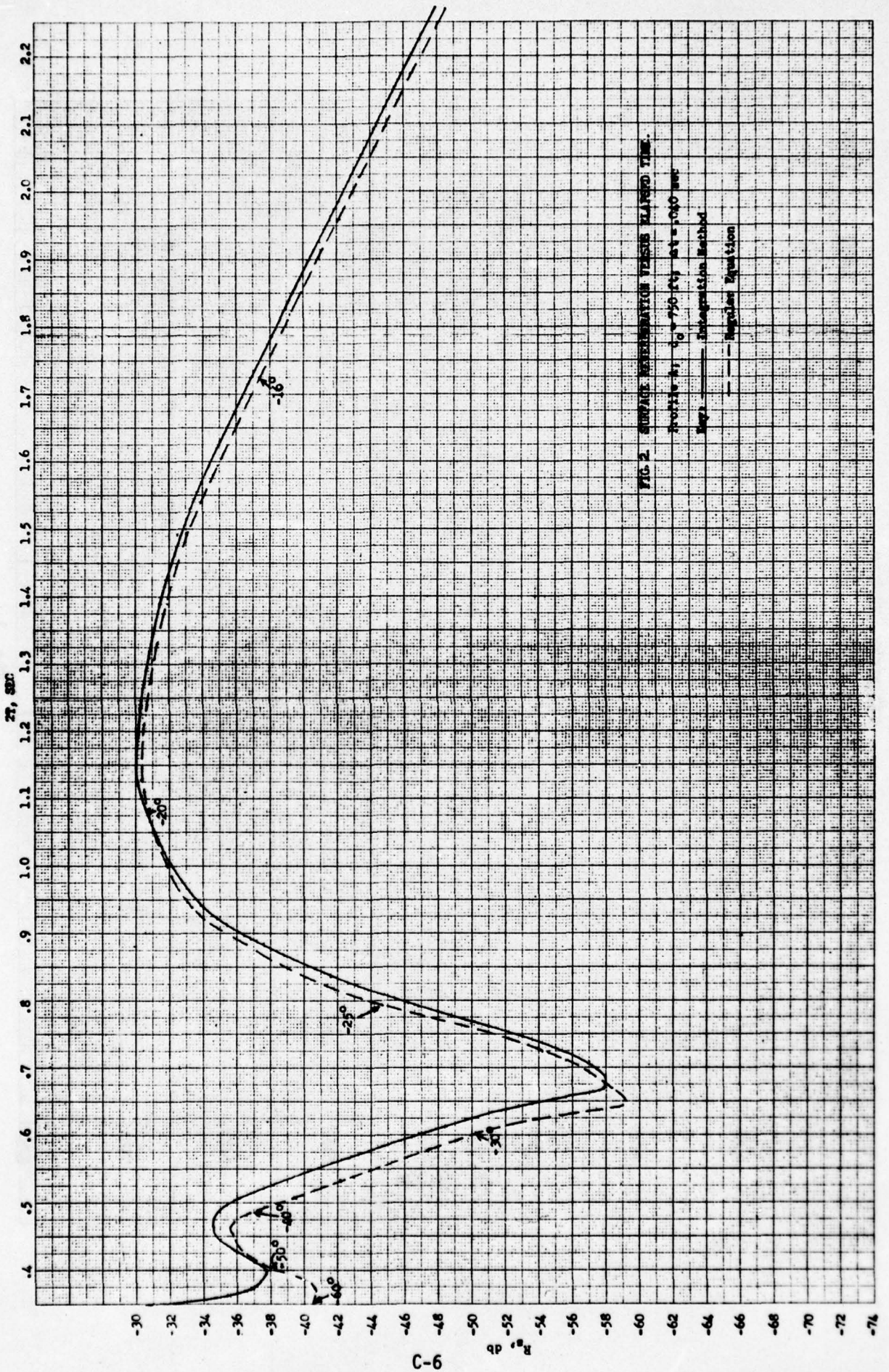


FIG. 2 SURGE ELEVATION VERSUS ELAPSED TIME.

Profile at  $t_0 = 750$  ft) at  $t = 0.010$  sec

Legs: — Integration Method

--- Regular Equation

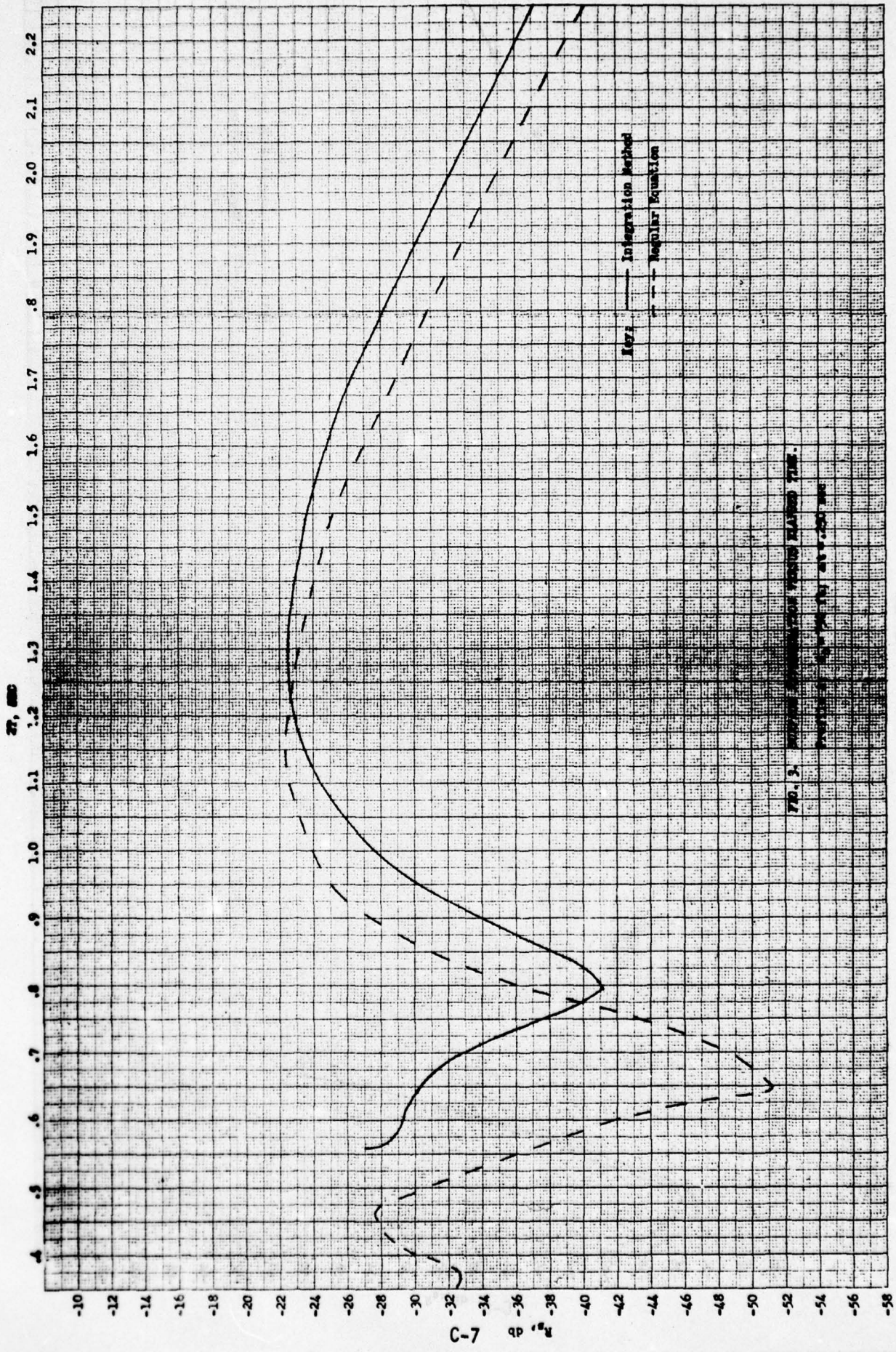


FIG. 3. PREDICTED VIBRATION RESPONSE SPECTRA. TIME  
 CONSTANT = 0.001 SEC. AT 1000 Hz.

C-7

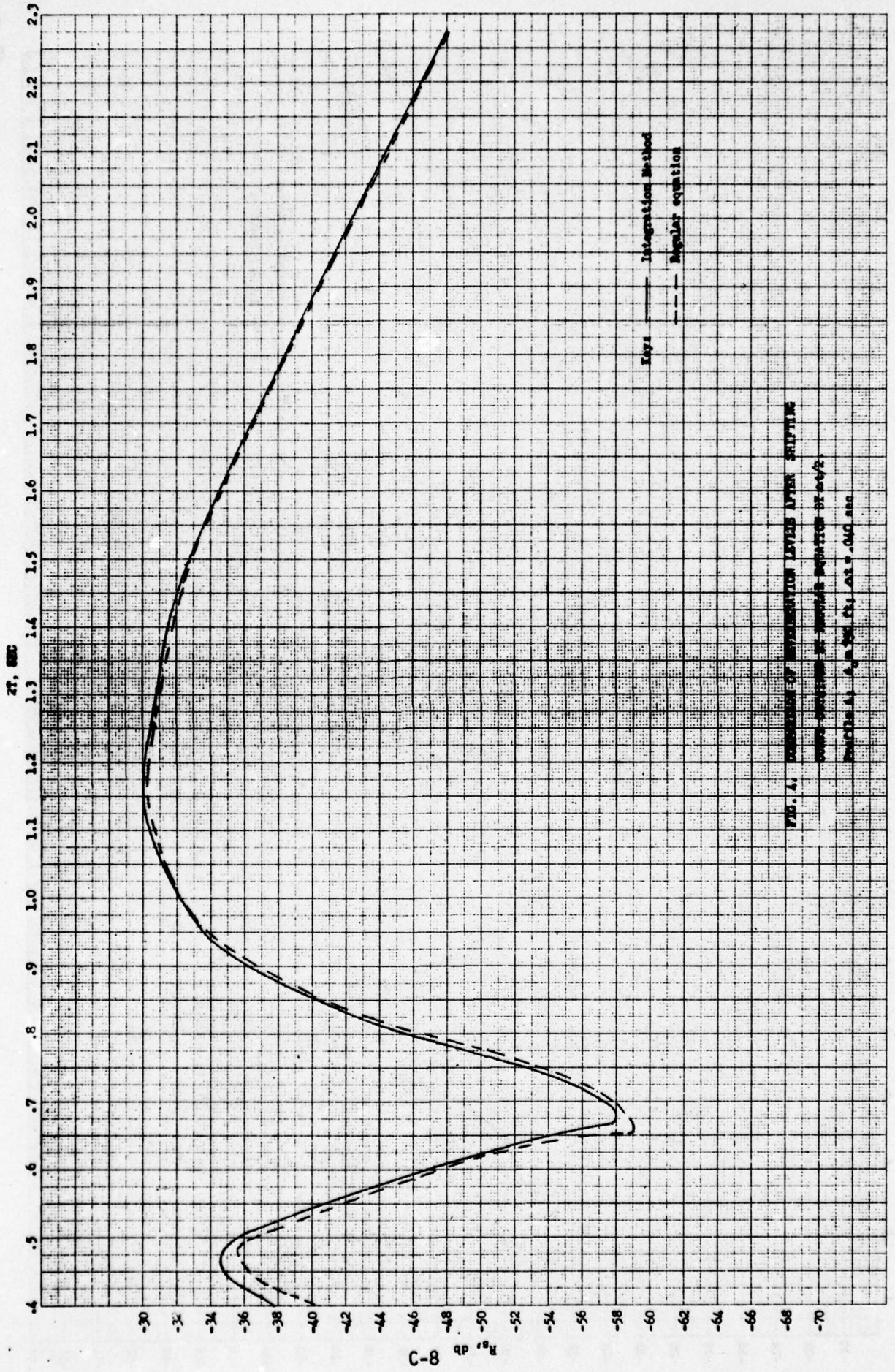


FIG. 1. COMPARISON OF INTEGRATION LEVELS AFTER SHIFTING  
SOME LEVELS BY PERIODS EQUAL TO  $0.5T$ .  
Scale: A,  $A = 0.5$ ; B,  $B = 0.5$ ; C,  $C = 0.5$ .

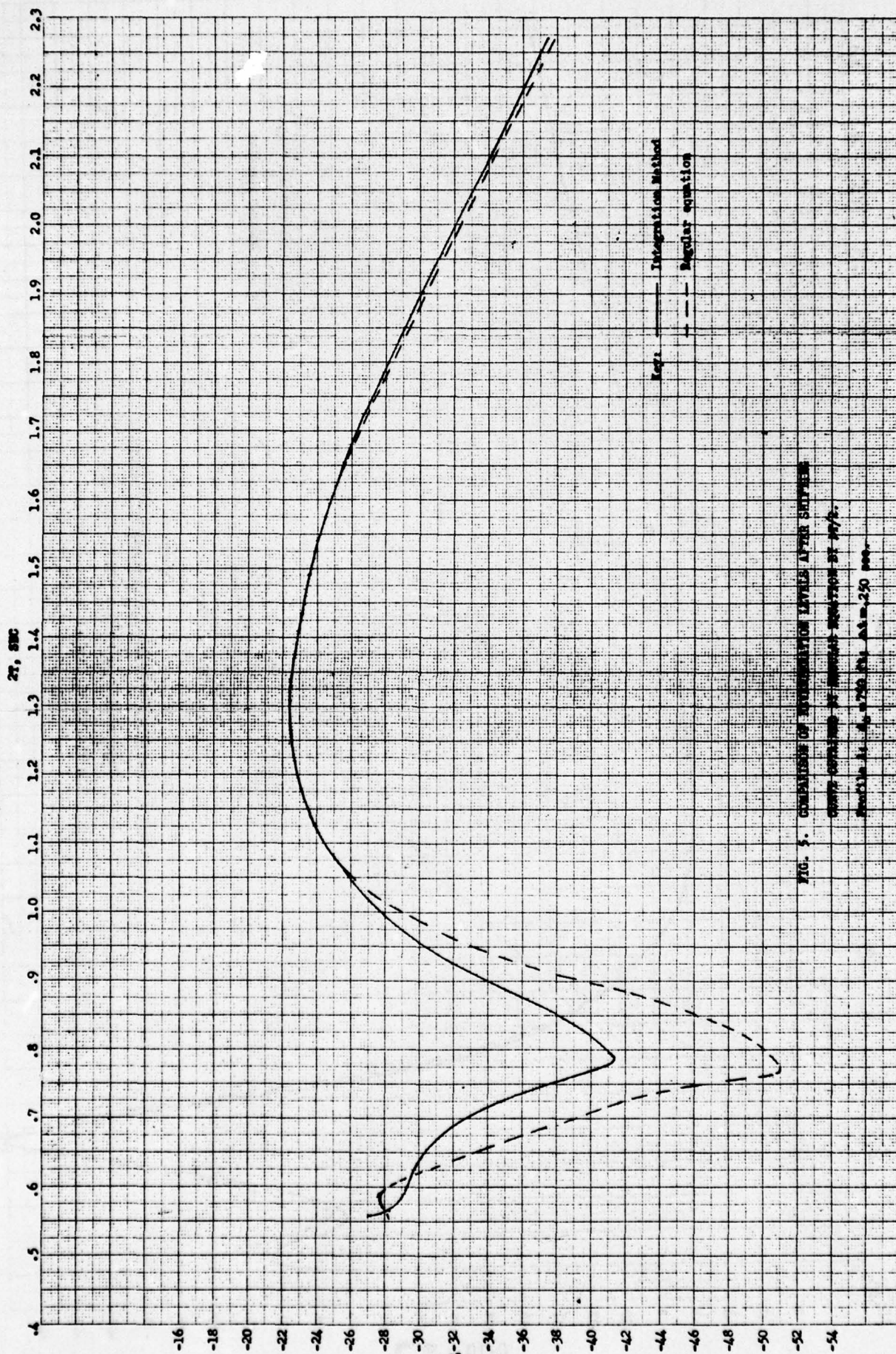


FIG. 5. COMPARISON OF INTEGRATION LEVELS AFTER SHIPPER

CHART CONTAINS 32 INSTANT READINGS OF 100%.

SCALE IS 0.1750 (10) ΔΔ = 250 sec.

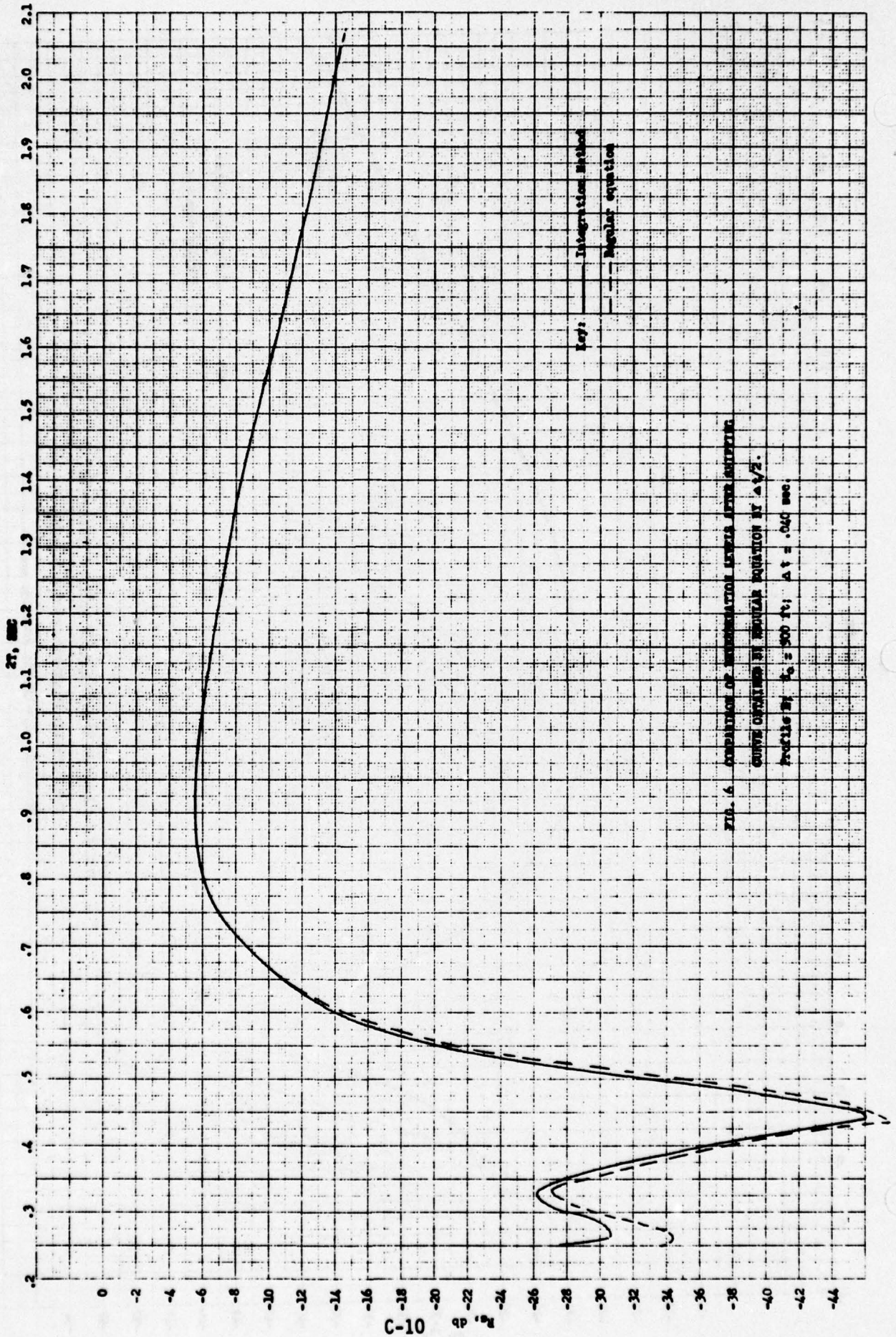


FIG. 4. COMPARISON OF INTEGRATION RESULTS AFTER SPLITTING CURVE OBTAINED BY REGULAR EQUATION BY  $\Delta t/2$ . Profile by  $v_0 = 500$  ft;  $\Delta t = .040$  sec.

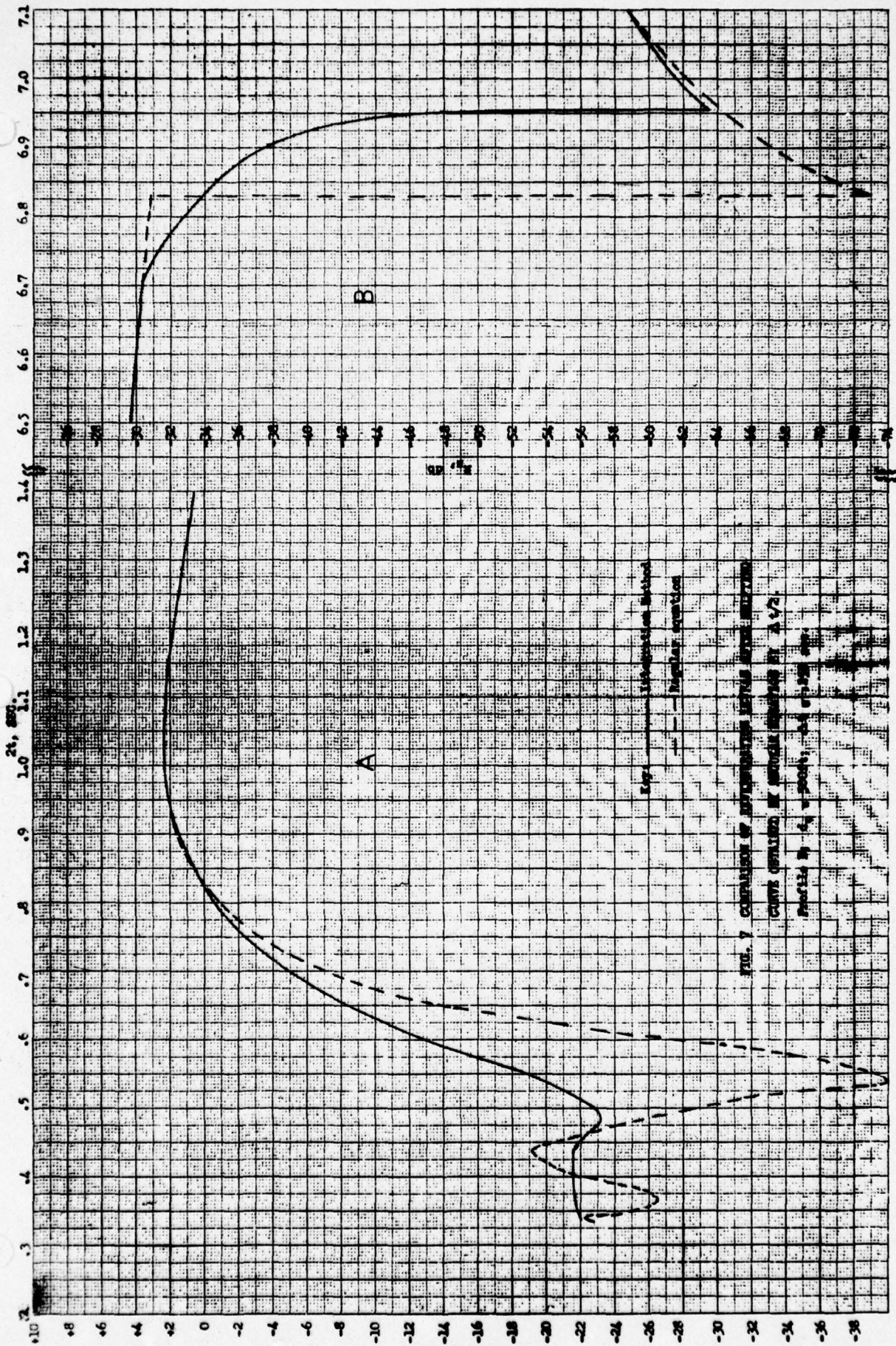


FIG. 7 COMPARISON OF INTEGRATION METHOD WITH METHOD  
 CURVE OBTAINED BY METHOD DESCRIBED BY A/2  
 PARTIAL BY  $\Delta t = 0.001$ ,  $\Delta t = 0.001$  sec.

## APPENDIX D

## MEMORANDUM

P80203/ABP:pas  
25 January 1965From: Code P80203  
To: Code P802Subject: Review of Mathematical Model for Computing the Expected Level  
of Volume Reverberation.Reference: A. P80203 Memo "Review of Mathematical Model for Computing  
Boundary Reverberation," of 20 January 1965.

Reference A discussed the problems associated with the mathematical model for computing boundary reverberation. It was pointed out that the model currently in use in our computer programs generally gives reasonable accuracy over a large portion of the ping cycle provided time is measured from the middle of the transmittal ping. The errors may still be appreciable over the time intervals during which the paths to the surface are quite steep and involve transmission through the minor lobe structure of the transducer, and/or exhibit anomalous transmission loss. A method is delineated by which errors can be reduced by summing the contributions from narrow increments of the insonified annulus.

The model currently in use for calculating volume reverberation in dB again involves the addition of a factor  $10 \log_{10} \tau = 10 \log V (\Delta t/2)$  to account for the lateral extent of the insonified region which returns energy to the transducer at the same instant of time. ( $V$  is the velocity of sound and  $\Delta t$  is the ping duration in seconds.) Since for volume reverberation the insonified region is a spherical shell, the lateral extent is measured radially. Thus  $10 \log_{10} \tau$  is a reasonably accurate measure of the thickness of this shell providing the value chosen for  $V$  is a good average value for the environment being considered. Since in general the velocity is not constant throughout the volume of interest, there are resulting errors. However, the percentage variation in velocity is so slight that the errors from this source can be expected to be less than 0.2 dB, an insignificant amount in view of our inaccurate knowledge of the scattering coefficients which obtain.

A somewhat more significant error can result from the variation in transmission loss over the shell width, particularly for long pings. To obtain a measure of the inaccuracy, calculations of volume reverberation were made for two postulated ping lengths in an environment with an average velocity taken to be 1660 yd/sec. The levels computed with values of  $10 \log_{10} \tau$  appropriate for the selected ping lengths were compared with those obtained by a modification of the integration method described in Reference A with  $10 \log_{10} \tau$  set at zero. The levels were plotted as functions of elapsed time measured from the beginning of the transmission. The  $10 \log_{10} \tau = 0$  curve can be integrated over the ping length in seconds except that the resulting intensity is multiplied by a factor of 0.83 before reconvertng to dB to account for the fact that one millisecond is equivalent to an 0.83-yard shell thickness when  $V$  has the value previously selected.

The results for ping lengths of 0.040 and 0.250 seconds are shown in Figure 1. As was the case for boundary reverberation, the corresponding curves from the two methods would be in much better agreement if the one for the integrated method were shifted back in time by half the ping length. This is equivalent to measuring elapsed time from the middle of the transmission. When this is done, there is still a residual error at the very short times due to the fact that the spreading loss at short ranges is changing rapidly. The integration method accounts for the fact that the latter portion of the ping is contributing a considerably greater portion of energy to the reverberation level. The errors for short pings do not seem large enough to justify the additional work of using the integration method.

Our analyses in the past have involved systems with ping lengths of .040 seconds or shorter. The elapsed time for both interference and echo levels was taken to be the two-way travel time for the paths being computed. For the short pings this is roughly equivalent to measuring time from the transmission mid-point. Consequently, the results of the analysis can be considered valid insofar as the factors discussed here are concerned.

There is, however, a basic weakness in our volume reverberation model which may be really serious, especially if performance analyses of long-range systems are attempted. Moreover, there is no means at hand for ascertaining what errors might be involved. This situation arises because the present model for volume reverberation is based on the assumption of an insonified shell over expanding in time in an infinite, uniform medium. It is well known that an ocean is neither infinite in extent nor uniform in its acoustic properties. From whatever transducer position the sound paths will, at one time or another, intercept the surface or bottom, and variation in the physical properties of the water results in differences in transmission loss depending on which path is considered. Furthermore, the volume scattering coefficient in general is not constant over any sizable volume of water, and is often observed to be a rather strong function of depth and time of day (deep scattering layer migration). To further complicate the situation, the paths in various directions are weighted in accordance with the three-dimensional transducer patterns.

The difficulty of realistically delineating the distribution of acoustic properties over a large volume coupled with the even greater difficulty of integrating the return from the entire spherical shell has no doubt led to the common use of the simplified model. Its use can be rationalized as follows. While it is true that the transmission loss to various portions of the insonified shell may be substantially different due to refraction, the integration process will average out such effects. Similarly the variation in scattering coefficient will average out in the integration so that selection of a constant value consistent with the volume being considered should suffice. When the insonified spherical shell is truncated by a boundary, energy aside from the backscattered as boundary reverberation or lost in the reflection mechanism will be returned to the water to insonify volume scatterers. If one can assume that boundary losses are offset by the multiple paths that are set up, the truncating of the sphere can be ignored.

There is little doubt that in a qualitative sense these trends can be expected. There is no available evidence, however, that they quantitatively balance out within acceptable limits. Faith that they will do so deteriorates further when one considers that directional transducer patterns may weight the return from anomalous regions so that their contribution is grossly out of proportion to their share of the total volume. The depth and orientation of the transducer as well as the patterns themselves can be significant factors. For example, if there is a pronounced deep scattering layer, the behavior of the volume reverberation level with elapsed time can be expected to be quite different when a transducer is oriented vertically than when it is oriented horizontally.

One can also argue that the need for a more complex and realistic model for estimating volume reverberation is not great on the basis that most systems have TVG thresholds which protect them against volume reverberation at short range, boundary reverberation is likely to exceed volume reverberation at intermediate ranges, and noise will be the dominant interference at long ranges. While this reasoning may be valid for many (if not most) situations analyzed to date, there is no assurance that it will always hold. Volume scattering coefficients above average when coupled with long pings may raise this type of interference to new prominence in some important situations. The point is, no one can be sure that the simple model is adequate in new applications unless there is a comprehensive model available with which to compare results. Efforts by able mathematical physicists to develop a more realistic approach to the problem of estimating volume reverberation should be solicited. A companion problem of great difficulty is the development of a practical method for estimating the doppler spectrum of both boundary and volume reverberation. Such information is needed for assessing performance of systems which employ doppler discrimination.

In the meantime, the best that one can do is to continue using the present method, taking care that the elapsed time is measured from the middle of the transmitted ping and then adjusted, if desired, to the same time base used in computing boundary reverberation and echo level. It is clear that the expected values of both the echo level and threshold must be figured on the same time base for valid results. It is worth noting that for elongated echoes (long pings or other reasons) the applicable threshold level may vary appreciably depending on which portion of the echo leads to the detection.

A. B. POYNTER

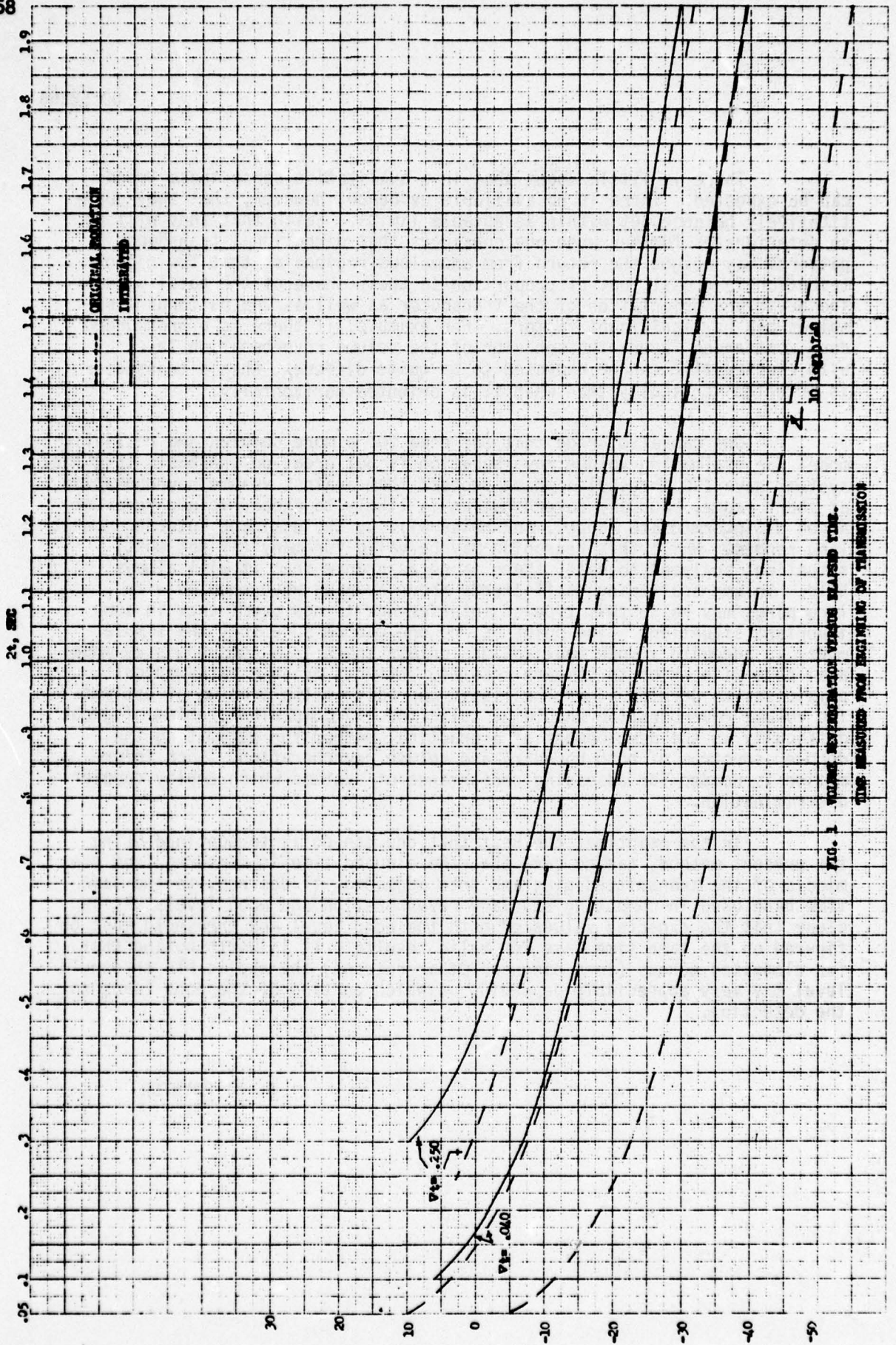


FIG. 1. RANGE EXTENSION VERSUS ELAPSED TIME.  
TIME MEASURED FROM BEGINNING OF TRANSMISSION

## APPENDIX E

## MEMORANDUM

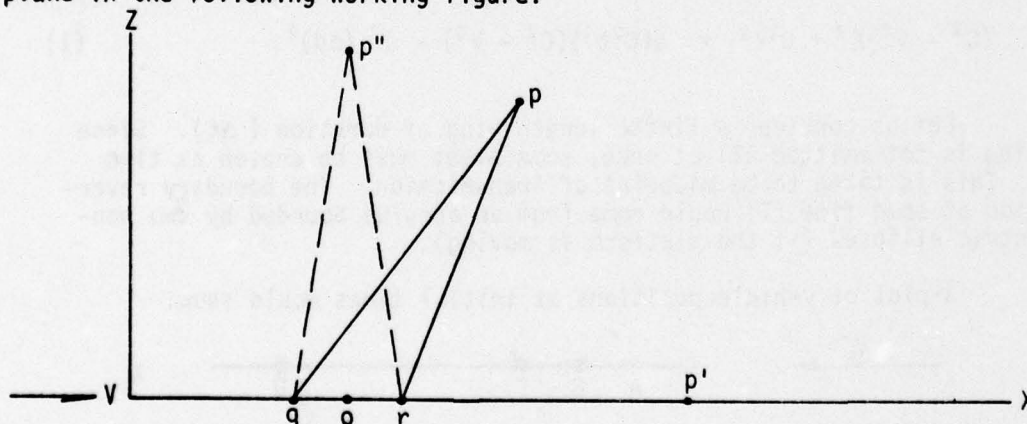
P80203/ABP:slh  
24 November 1965From: Code P80203  
To: Code P802

Subject: Assessment of the Effect of Platform Translation on the Area Returning Boundary Reverberation at a Given Time.

Math models for computing expected levels of reverberation nearly always include the concept that the return at any given time comes from scatterers contained in a sphere-like shell. The outer and inner surfaces are determined by the sound velocity multiplied by one-way travel times (equal to one-half the elapsed time in the ping cycle) plus and minus one-fourth of the ping duration. This concept fits volume reverberation at least for times less than that required for the expanding shell to be truncated by the surface or bottom. The area returning boundary reverberation is considered to be bounded by the traces of the shell boundaries on the surface or bottom. These traces will be concentric circles if the shell is truly spherical.

The approach is clearly realistic if the transducer is stationary and the sound velocity is a function only of depth. It is desirable to have some quantitative indication of the error introduced if the transducer is mounted on a moving platform. For practical cases it can be assumed that the velocity of the platform will be small in comparison with the sound velocity.

Assume that the platform is moving at a constant velocity ( $V$ ) directed horizontally along the  $X$ -axis in an oceanographic coordinate system. The  $X$ -axis is taken to be at platform depth. Since the velocity of sound in the whole ocean really varies over a range of only about 10% it is reasonable to assume, as a first approximation in determining range, that the sound velocity ( $C$ ) is a constant in a limited volume of water. Consider the  $X$ - $Z$  plane in the following working figure:



Let  $q$  be the position of the platform at transmission of a particular part of the ping and  $r$  be the platform position when return is received from a point ( $p$ ) after some elapsed ( $t$ ). We know that the distance traveled over  $qpr = tC = qp'r = qp''r$ . The locus of all  $p$  in this plane is an ellipse with foci at  $q$  and  $r$ . If the origin is placed half-way between  $q$  and  $r$ , the equation of the ellipse is  $x^2/a^2 + z^2/b^2 = 1$ .

When the point is on the X-axis (at p'), z = 0 and a = op' = Ct/2. It is also known that qo = or = Vt/2. When the point is at p'', X = 0, and qp'' = p''r = Ct/2. Therefore,

$$b = \sqrt{(Ct/2)^2 - (Vt/2)^2} = (t/2) \sqrt{C^2 - V^2}$$

The distance from either focus to the origin should be:

$$\sqrt{C^2 t^2/4 - (C^2 t^2/4 - V^2 t^2/4)} = \sqrt{V^2 t^2/4} = Vt/2$$

which checks with what was known directly from the movement of the platform.

The equation of this ellipse is 
$$\frac{X^2}{C^2 t^2/4} + \frac{Z^2}{t^2/4(C^2 - V^2)} = 1$$

The eccentricity of such an ellipse is  $e = \sqrt{(a^2 - b^2)}/a^2 = V/C$ . Now C is of the order of 5000 ft/sec while a V of 15 knots is approximately 25 ft/sec. In this case  $e = 25/5000 = .005$ . For a 45-knot V, e would be three times larger or about .015. Therefore, circular assumption is not bad.

If excursions in the Y direction are allowed, the insonified area would be the surface of an ellipsoid

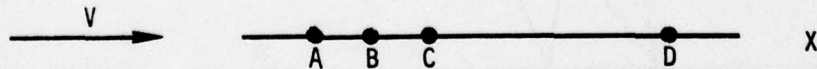
$$\frac{X^2}{C^2 t^2/4} + \frac{Y^2}{(t^2/4)(C^2 - V^2)} + \frac{Z^2}{(t^2/4)(C^2 - V^2)} = 1$$

The trace of this ellipsoid intersecting a horizontal plane (e.g. surface or bottom) would be an ellipse with the same eccentricity previously computed. The equation of such an ellipse may be found by substituting ( $\Delta d$ ), the depth differential between the platform and the boundary in question, for Z in the equation above. The new X - Y plane now coincides with the surface or bottom, and the equation for the ellipse can be expressed in the form

$$(C^2 - V^2)X^2 + C^2 Y^2 = \frac{1}{4}(C^2 t^2)(C^2 - V^2) - C^2 (\Delta d)^2. \tag{1}$$

Let us consider a finite length ping of duration ( $\Delta t$ ). Since the ping is not emitted all at once, some event must be chosen as time zero. This is taken to be midpoint of transmission. The boundary reverberation at some time (T) would come from an annulus bounded by two non-concentric ellipses (if the platform is moving).

A plot of vehicle positions at initial times would show:



where A is the position at transmission of the leading edge of ping; B is the position at  $t = 0$ ; C is the position at transmission of the trailing edge; and D is the position when reverberation is returned at time T. The distances A to C =  $(\Delta t)V$ ; A to D  $V(T + \Delta t/2)$ ; and C to D =  $V(T - \Delta t/2)$ . By alternately substituting  $T + \Delta t/2$  and  $T - \Delta t/2$  for the t in Eq. (1), one finds the equation for the two ellipses when the origin for each is half-way between their respective foci.

The origin of the ellipse stemming from the trailing edge of the ping will be located  $V(\Delta t/2)$  further along the X-axis than the one associated with the leading edge. Choosing an origin appropriate to the midpoint of the ping and substituting in Eq. (1), one obtains the following equations:

$$\text{Leading edge: } (C^2 - V^2) [X + V(\Delta t/4)]^2 + C^2 Y^2 = [C^2(T + \Delta t/2)^2/4](C^2 - V^2) - C^2(\Delta d)^2$$

$$\text{Trailing edge: } (C^2 - V^2) [X - V(\Delta t/4)]^2 + C^2 Y^2 = [C^2(T - t/2)^2/4](C^2 - V^2) - C^2(\Delta d)^2$$

When y is 0 and letting subscripts L and T designate the leading and trailing edges, respectively:

$$X_L = \pm \sqrt{(C^2/4)(T + \Delta t/2)^2 - C^2(\Delta d)^2/(C^2 - V^2)} - V(\Delta t/4)$$

$$X_T = \pm \sqrt{(C^2/4)(T - \Delta t/2)^2 - C^2(\Delta d)^2/(C^2 - V^2)} + V(\Delta t/4)$$

Using primes to differentiate between concepts, the similar equations for the concentric circle approximation with the origin at the same place (half-way between the midpoint of transmission and the point of reception) would be:

$$X'_L = \pm \sqrt{(C^2/4)(T + \Delta t/2)^2 - (\Delta d)^2}$$

$$\text{and } X'_T = \pm \sqrt{(C^2/4)(T - t/2)^2 - (\Delta d)^2}$$

It is clear that  $X_L < X'_L$  first, by the quantity  $V(\Delta t/4)$ , and then by the amount the evaluation of the square root term is reduced because  $(\Delta d)^2$  is multiplied by  $C^2/(C^2 - V^2)$  rather than by  $C^2$ . Now  $V(\Delta t/4)$  will be small in practical situations. For a platform velocity of 45 knots and at  $\Delta t$  of 0.25 seconds,  $V(\Delta t/4) < 5$  feet. The other term is more difficult to evaluate since it depends on so many factors. At  $V = 45$  knots,  $C^2/(C^2 - V^2)$  is the order of 1.00025. However, the extent to which this factor modifies  $X_L$  depends not only on  $\Delta d$ , but also on  $\Delta t$  and the value of  $T$  for which the evaluation is desired. At the times for which the evaluation is important, the first term under the square root will be much larger than the second, so the difference in  $X_L$  and  $X'_L$  will be small.

In the forward direction the differences in  $X_T$  and  $X'_T$  (when  $Y = 0$ ) is less than in the case of the leading edge since the correction for translating the origin from the center of the ellipse to the center of the circle changes sign. The two factors causing the difference tend to compensate rather than add. In the  $-X$  direction the opposite trend is seen and  $-X_T$  is affected more than  $-X_L$ .

Another interesting case to evaluate is the one where  $X = 0$ . In this case

$$Y_L = \pm \sqrt{(C^2/4)(T + \Delta t/2)^2 - (\Delta d)^2 - (V^2/4)(T + \Delta t/2)^2 - [(C^2 - V^2)/C^2](V \Delta t/4)^2}$$

$$Y_T = \pm \sqrt{(C^2/4)(T + \Delta t/2)^2 - (\Delta d)^2 - (V^2/4)(T - \Delta t/2)^2 + [(C^2 - V^2)/C^2] (V \Delta t/4)^2}$$

For the circular approximation

$$Y'_L = \pm \sqrt{(C^2/4)(T + \Delta t/2)^2 - (\Delta d)^2}$$

$$Y'_R = \pm \sqrt{(C^2/4)(T - \Delta t/2)^2 - (\Delta d)^2}$$

The difference between the corresponding Y and Y' expressions comes from the two additional terms under the square root in the equations for Y. As long as V remains very small in comparison with C, the Y values will not be materially smaller than the Y' values.

In a JP training assignment, Lee Sheldon numerically evaluated the error to be expected in a variety of cases by computing the X-axis intercepts of the ellipses and circle approximations, with the center of the circles taken as the origin. It is in this dimension that the errors are maximum. Vehicle speeds of 45 and 15 knots were assumed. Results are shown in Table 1 when the sound velocity is considered to be a constant 5,000 ft/sec and the ping duration is 0.25 sec. Three elapsed times were examined in combination with two depth differentials between vehicle and boundary. Table 2 shows some results obtained by using ray tracing data in a refracting medium.

On the basis of these data, it would appear that for vehicle speeds less than say 50 knots the circular approximation of the boundaries of the annulus returning reverberation at a given time introduces only very minor errors. These are certainly negligible in the light of other sources of error, such as in the determination of the scattering coefficients. The maximum error in X occurs to the rear of the vehicle where pattern discrimination generally is high.

Another study by Charles Williams, a summer employee, showed that, for vehicle speeds up to 50 knots, the difference between the initial path angles from the respective vehicle positions at transmission and reception of reverberation from selected points on the surface amounted to less than 1° for a wide variety of situations. The errors were largest when geometries and elapsed times were such that the effective paths were steep. Since, in computing boundary reverberation, the circular approximation uses what is essentially a median of these two angles for both transmission and reception in computing pattern losses, the circular assumption should provide an adequate model for most practical cases.

All of the above discussion assumes that the boundaries and vehicle velocity vector are horizontal. The situation is much more complicated when one or both of these conditions are not applicable. Work in this area is needed.

A. B. POYNTER

TABLE I  
 C = 5000 ft/sec;  $\Delta t = 0.25$  sec; Errors Computed with Ellipse as Standard

PARAMETERS			CIRCLES $\pm$ X-AXIS						ELLIPSES							
y ft/sec	d ft.	T sec.	$\pm$ X-AXIS			+ X-AXIS			- X-AXIS			% ERROR				
			$X_L$ yd.	$X_T$ yd.	$X_L$ yd.	$X_T$ yd.	$X_L$ yd.	$X_T$ yd.	$X_L$ yd.	$X_T$ yd.	$X_L$	$X_T$	$X_L$	$X_T$		
25.33 (15 kt)	250	0.250	301.18	62.50	300.53	63.02	301.68	61.97	301.68	61.97	+0.18	-0.83	301.68	61.97	-0.35	+1.69
		1.000	933.79	724.39	933.18	724.85	934.23	723.79	934.23	723.79	+0.07	-0.06	934.23	723.79	-0.11	+0.15
		10.000	8437.09	8228.74	8435.83	8228.56	8436.88	8227.50	8436.88	8227.50	+0.01	0.01	8436.88	8227.50	0.01	+0.01
76.0 (45 kt)	3000	1.425	817.56	416.67	816.94	417.12	817.99	416.07	817.99	416.07	+0.08	-0.11	817.99	416.07	-0.05	+0.25
		2.625	2061.97	1827.64	2061.25	1827.99	2062.30	1826.94	2062.30	1826.94	+0.03	-0.02	2062.30	1826.94	-0.02	+0.04
		10.000	8378.03	8168.18	8376.78	8167.99	8377.83	8166.94	8377.83	8166.94	+0.01	0.01	8377.83	8166.94	0.01	+0.02
76.0 (45 kt)	250	0.250	301.18	62.50	299.53	64.01	302.70	60.89	302.70	60.89	+0.55	-2.36	302.70	60.89	-0.50	+2.64
		1.000	933.79	724.39	931.99	725.80	935.16	722.64	935.16	722.64	+0.19	-0.19	935.16	722.64	-0.15	+0.24
		10.000	8437.09	8228.74	8433.55	8228.42	8436.72	8225.26	8436.72	8225.26	+0.04	0.01	8436.72	8225.26	0.01	+0.04
76.0 (45 kt)	3000	1.425	817.56	416.67	815.65	417.88	818.81	414.71	818.81	414.71	+0.23	-0.29	818.81	414.71	-0.15	+0.47
		2.625	2061.97	1827.64	2059.86	1828.74	2063.02	1825.57	2063.02	1825.57	+0.10	-0.12	2063.02	1825.57	-0.05	+0.11
		10.000	8378.03	8168.18	8374.49	8167.86	8377.66	8164.69	8377.66	8164.69	+0.04	0.01	8377.66	8164.69	0.01	+0.04

TABLE II  
 Refracting Medium;  $\Delta t = 0.25$  sec; Errors Computed with Ellipse as Standard

y ft/sec	d ft.	T sec.	$\pm$ X-AXIS			+ X-AXIS			- X-AXIS			% ERROR				
			$X_L$ yd.	$X_T$ yd.	$X_L$ yd.	$X_T$ yd.	$X_L$ yd.	$X_T$ yd.	$X_L$	$X_T$	$X_L$	$X_T$				
76.0 (45 kt)	3000	1.875	1307.0	1035.0	1305.0	1035.6	1308.1	1032.4	1308.1	1032.4	+0.15	-0.06	1308.1	1032.4	-0.08	+0.06
		2.625	2032.0	1799.0	2030.0	1800.1	2033.1	1796.9	2033.1	1796.9	+0.10	-0.06	2033.1	1796.9	-0.05	+0.12
		11.000	9118.5	8911.0	9116.9	8911.8	9120.1	8908.7	9120.1	8908.7	+0.02	.01	9120.1	8908.7	-0.02	+0.03

## APPENDIX F

## MEMORANDUM

P3502/ABP:dd  
 Reg No. P3502-136  
 15 April 1968

From: Code P35021  
 To: Code P3502

Subject: Comparison of Computer Models for Obtaining the Expected Level of Boundary Reverberation as a Function of Elapsed Time.

- References:
- A. NAVORD Conf Report 5606, "Analytical Methods for Predicting the Acoustic Performance of Homing Torpedoes in Circular Search" (NOTS 1818) of 26 July 1957.
  - B. NOTS P80203 memo, "Review of Mathematical Model for Computing Boundary Reverberation", of 20 January 1965.
  - C. NOTS P80203 memo, "Error from Using  $10 \log_{10} \tau$  as a measure of Effective Train Length when Computing Boundary Reverberation", of 18 January 1965.
  - D. NUWC P35021 memo, "Integration of Power under a Curve Plotted in Decibels", of 10 January 1968.
  - E. NAVORD Report 4962, "A Study of the Effects of Refraction on Reverberation (NOTS 1284) of 7 November 1955.
  - F. NOTS P80203 memo "Doppler Content of Boundary Reverberation Due to Vehicle Translation-Refractive Environment Case" of 21 December 1965.

Over the last few years various aspects of the problem of computing the expected level of boundary reverberation in a refractive medium have been re-examined. The purpose of this memorandum is to compare the results obtained from four models selected as being practical for computer application and to assess their relative accuracy. In general, the accuracy to be anticipated increases with the complexity. The study is made in terms of surface reverberation. In the case of a flat bottom, bottom reverberation is computed in an identical fashion.

Model I has been used since the inception of our first ray-tracing program and was based on Reference A. The form of the equation used in the program is

$$R_s = S - 2H + 10 \log_{10} m_s - J_s + 10 \log_{10} \tau + 10 \log_{10} \frac{x}{\cos \theta_0}$$

where

- $R_s$  is the expected level of surface reverberation at a given time
- $S$  is the on-axis source level in dB re one microbar at one yard
- $2H$  is the two-way transmission loss along the ray path

- $10 \log_{10} m_s$  is the surface scattering coefficient in dB as a function of grazing angle of the ray path at the surface
- $J_s$  is the boundary reverberation index of the transducer
- $10 \log_{10} \tau$  is the effective annulus width in dB
- $10 \log_{10} \frac{X}{\cos \theta_0}$  allows for the fact that horizontal spreading is compensated for in the outgoing direction by the fact that the whole annulus back-scatters toward the source. Here  $X$  is the horizontal range traversed by the ray to boundary intercept, and  $\theta_0$  is the ray angle at the source.

In this model  $10 \log_{10} \tau = \frac{V(\Delta t)}{2}$  where  $V$  is the nominal velocity of sound (1667 yd./sec.) and  $\Delta t$  is the ping duration in seconds.

It was shown in Reference B that the model produces the best results if the elapsed time  $T$  is considered to be measured from the midpoint of transmission so that, in effect,  $T = 2t$ , the two-way travel time of the ray being run. This ray then reaches the surface near the mid-range of the insonified annulus so that the associated value of transmission loss,  $J_s$ , and grazing angle are reasonable representative for the annulus as a whole.

Reference C showed that  $\tau$  was not a good measure of annulus width where steep paths are involved. Model II is a simple attempt to improve this situation. The only change from Model I is to compute

$$\tau = \frac{V_s}{2} \frac{t}{\cos \theta_s}$$

where  $V_s$  is the velocity at the surface and  $\theta_s$  is the grazing angle of the path at the surface. This is largely an intuitive "fix", and it is being tried here for the first time. Obviously, both models I and II get into trouble when  $T = 2t_{\theta_c} < 2t_{90^\circ} + \Delta t/2$  because the full ping is not insonifying the surface. In Model II a test was made to ascertain whether or not this criterion was being met. If not, it was assumed that the paths would be sufficiently steep to approximate straight lines. Since  $\tau$  would equal the horizontal range to surface intercept of the leading edge,

$$\tau \approx \frac{\bar{V}}{2} \left( 2t_{\theta_0} + \frac{\Delta t}{2} \right) \cos \theta_0.$$

$\bar{V}$  is the average velocity over these straight paths and can be found by dividing the source depth by the one-way travel time of the  $-90^\circ$  ray.

As pointed out in Reference B, the above models in some situations could be expected to give inaccurate results for long pings even if the annulus width were modeled adequately. Values of transmission loss, vertical pattern losses, and grazing angle found by tracing a ray to any single point in a wide annulus cannot be expected to represent those over the full annulus, particularly in regions where one or more of the parameters is varying rapidly. Moreover, at elapsed times sufficiently short so that all of the ping has not insonified the surface, the ray path for which the two-way

travel time is computed no longer reaches the surface near the mid-point of the annulus. These difficulties are overcome in the next model. Model III in this study follows the scheme delineated in Reference B and computes boundary reverberation levels as in Model I with  $10 \log$  set to zero. This is equivalent to a one-yard annulus width. From the data produced by the ray-tracing program, both the two-way travel time ( $2t$ ) and computed reverberation level ( $R_0$ ) are plotted as functions of the horizontal range ( $x$ ) to surface intercept as determined for each ray path. For each desired elapsed time ( $T$ ), which can be selected at will, the limits of the true annulus corresponding to  $\Delta t$  is found by evaluating  $x$  on the time curve for  $T - \frac{\Delta t}{2}$  and  $T + \frac{\Delta t}{2}$ .

The actual reverberation level at time  $T$  is then found by summing in random phase the contributions of each one-yard increment between the above limits as shown by the  $R$  curve. The summation was a hand operation in Reference B but it was computerized in this study in the manner delineated in Reference D.

These first three models all require a table input to account for the weighting effect of the horizontal patterns on the reverberation return. These data are combined with vertical pattern losses and a geometric correction for transducer pitch to give  $J_s$ , the boundary reverberation index of the transducer. NUWC computer program 819001 is available for generating the data for the table showing the average weighting effects of the horizontal patterns. For a non-turning transducer, this is a single value. The equations for evaluation  $J_s$  were developed in Reference E. Because of certain simplifications introduced in the concept, the accuracy of the results is suspect when the transducer axis is tilted considerably and/or when the steep sound paths are producing the reverberation at time  $T$ . The basic simplifications are the assumptions that pattern effects can be obtained when only the patterns in the cardinal planes are known and that the variables can be separated for integration.

Model IV uses a different approach. The concept was developed in Reference F for the purpose of computing the boundary reverberation returned in doppler bands when the doppler is introduced by own vehicle speed. Briefly, the insonified annulus is divided into incremental areas bounded on two sides by equal doppler lines and on the other two sides by equal travel-time circles. Rays are traced to the corners of these little areas yielding the coordinates of the corners in space so that the areas of each can be computed. Other ray data permit evaluation of the transmission loss, scattering strength, and the transmit and receive pattern losses needed to ascertain the back-scatter received from each incremental area. When these contributions are summed in random phase (expressed in intensities) for each doppler band, one gets the reverberation levels as might be observed by a system which processes signals in narrow frequency bands. The summation of contributions from all bands gives the total surface reverberation received. (The first three models yield only the total reverberation as might be observed in

These first three models all require a table input to account for the weighting effect of the horizontal patterns on the reverberation return. These data are combined with vertical pattern losses and a geometric correction for transducer pitch to give  $J_v$  the boundary condition for the transducer. An average value of  $J_v$  was used. Later this was changed to 35 dB down as noted in Figure 1. These data are useful in interpreting the reverberation levels which will be shown later. Transducer pitch angles of  $0^\circ$  and  $10^\circ$  were used. The same table of scattering coefficients versus grazing angle were used in Models I through III. These values were each reduced by  $10 \log_{10} 2\pi$  for Model IV so that they would reflect scattering strength as required in that model. Computations were made for all four models using each of two quite different sound-velocity profiles in order to see that the conclusions arrived at from comparing the results obtained from the four models were not prejudiced by some over-riding characteristic of the profile. The velocity profiles are shown in Figure 2. A transmit frequency of 20 kHz was chosen, and an appropriate table giving the attenuation losses as a function of depth was input with each profile. Ping durations of 40 and 250 milliseconds were considered. Model IV assumed a horizontally-directed, straight-running platform at a 40-kt. speed, and reverberation was computed in 1/4-kt. doppler bands. The vehicle speed is an artifact here since we are interested only in the total return. It was selected to insure sufficiently small area increments to yield good accuracy. Actually, the results can apply to a stationary system since speed is not considered in the other three models. A 120-dB source level was used in all cases. The transducer is assumed to be at a 1000-ft. depth.

It proved to be impracticable to show the results for all four models on a single graph because of the clutter. Consequently, for each combination of environment, ping length, and pitch angle, two figures will be used. The first will compare the data from Models I, II, and III. On the second graph the data from Model III will be repeated and compared with that from Model IV. This is a natural grouping for our purpose in that the first three models assume common values for  $J_v$ . Then by comparing the most accurate of these models with the doppler-band method, one should be able to obtain an idea of the accuracy with which we now evaluate  $J_v$ .

Figure 3 shows the surface reverberation levels computed in Environment A for a 40-ms ping and a  $0^\circ$  pitch angle. With the source at a 1000-ft. depth the middle of the ping has a two-way travel time to the surface of about 0.405 seconds via a vertical path ( $\theta_0 = -90^\circ$ ). The velocity profile is dominated by negative gradients and the  $-15^\circ$  ray is very nearly the last to reach the surface. The 3.8-sec. ping interval was selected with this in mind. The combined vertical patterns largely determine the peaks and valleys in the respective reverberation curves. Of course, the trailing off of the reverberation at times greater than about 1.7 seconds is caused by the transmission loss increasing more rapidly than the pattern losses are decreasing. In addition, the scattering coefficient tends to be smaller at the lower grazing angles. All three models tend to be in good agreement beyond about 1.05 seconds when the major lobes of the vertical patterns govern. The integrated method (Model III) tends to smooth out the narrow peaks and valleys generated by the other two models. It is undoubtedly the more accurate since it does not consider the particular values of pattern and transmission loss associated with a data point as being necessarily representative of the entire annulus returning reverberation at that elapsed time. The cosine correction to the annulus width used in Model II seems to yield good agreement with the integrated model over the broad minor lobe. (The surface velocity used in Model II is not significantly different than the nominal velocity used in the first model). However, it tends to drastically over-compensate on the other minor lobe as can be expected; the cosine is rapidly approaching zero as the path angle approaches  $-90^\circ$ .

The results for the 250-ms ping under otherwise similar conditions are presented in Figure 4. The curves for Models I and II have the same shape as in Figure 3; they are merely at a higher level because of the longer ping. The agreement between the three models is still good beyond about 1.2 seconds, but the importance of the integrated method when long pings are used is quite evident at shorter elapsed times. The results of its use are most striking in modeling the onset of boundary reverberation. The flat portion of Model III curve centered at about  $T = 0.35$  is due to the narrow lobe being fully covered by some portion of the effective train length while the rest is contributing negligible return. With the quarter-second ping the broad minor lobe dominates the return until such time that the contribution from the major lobe begins to build up.

Figure 5 shows the corresponding data for the 40 ms-ping in Environment A when the transducer is pitched up  $10^\circ$ . The gross effect is to make the peaks and valleys in the expected level of reverberation more narrow than was the case when the transducer was directed horizontally. This is to be expected since each path making a particular angle with the transducer axis is  $10^\circ$  steeper in the oceanographic coordinate system and returns reverberation at a shorter elapsed time. The difference in results for the three models are of the same order as were found for the horizontally-directed transducer.

Figure 6 shows the results under the same conditions as in the preceding paragraph except that the ping duration is increased to 250 ms. As anticipated, the integration method (Model III) gives a decidedly different curve than the other two models at times less than one second. This model permits development of the onset of the surface reverberation starting where

$$T > 2t_{90} - \frac{\Delta t}{2}$$

The flat portion starting at 0.3 seconds covers the time region where the narrow minor lobe alone is contributing a substantial return. The level then rises as the next lobe also contributes. The drop-off starting at about 0.52 seconds is caused by the narrow minor lobe dropping out of the picture. The next flat portion occurs when only the second lobe is contributing materially. The shape of the remaining portion of the curve is rather obvious.

The next group of figures (Figure 7-10, inclusive) compare the results from the same three models when Environment B applies. Note that the dB scale has been changed. The two-way travel time from 1000 feet to the surface via a vertical path is about 0.418 seconds. Surface reverberation is continuous thereafter to an elapsed time greater than the ping interval which was taken as 10 seconds. The path yielding this two-way travel time to the surface has an initial path angle of approximately  $+3.7^\circ$  with respect to the horizontal. At the scale plotted there is no discernible difference in the results from Models I, II, and III at elapsed times beyond 1.6 seconds. Therefore, only the first portion of the ping interval is shown in these figures.

For Environment B the coincidence of the three curves begins shortly after the major lobe of the patterns assume dominance. This occurs at an earlier time than in Environment A for a given pitch angle since refraction is such that a ray with a given initial angle will tend to reach the surface much sooner. Also, in the case of Environment B, the reverberation declines at a lower rate after the peak is reached so that the integrated curve does not begin to rise above the levels shown for the other two models later in the ping cycle as occurred to some degree in the case of the first environment.

At the shorter elapsed times, the differences in the three curves tend to be quite similar (for each of the four combinations of ping length and pitch angle) to those prevailing for the same combination when Environment A applied. Model III, the integration method, tends to smooth out the peaks and valleys as shown for the other two models, particularly when they are narrow with respect to the ping duration. This method also is better in modeling the onset of boundary reverberation. For the shorter ping, the annulus width correction applied in Model II appears to compensate adequately in the region of the broader minor lobe, but it tends to over-compensate when the paths become steep enough for  $\cos \theta_0$  to become very small. The introduction of a  $10^\circ$  up pitch produces about the same effect in both environments.

Now we turn to the interesting task of comparing the results of the integrated method with those of the doppler-band model. Figure 11 shows the data obtained in Environment A for a zero pitch angle and a pulse length of 40 ms. The larger scale again is used for clarity. Earlier, the hypothesis was advanced that agreement between data from the two models at the longer elapsed times (where flat paths obtain) would be a good indication that the doppler-band program (Model IV) was functioning as intended. The agreement is reasonably close over the region dominated by the major lobes of the patterns, but there remains a slight difference at 3.8 seconds. However, in this environment the path angles yielding this elapsed time is still over  $15^\circ$  off the transducer axis. As anticipated, some rather substantial differences are observed in the region dominated by the minor lobes of the patterns. Since there is little reason to suspect that Model IV is materially less accurate in this region than in any other, the evidence tends to substantiate fears that the current method for evaluating  $J_s$  is in error when large off-axis path-angles are involved. In this example (as in subsequent ones where the transducer is oriented horizontally) the differences in reverberation levels at the peaks are rather moderate (no more than 2 dB). The wide troughs are something else again. The higher minimums observed in Model IV results are believed due to the complexity of the minor lobe structure. For the results shown in Figure 11, all of the incremental areas contributing a return at an elapsed time of about one second are not subjected to maximum pattern loss. Of course, in practical applications the actual values in the valleys are not likely to be important since the interference level probably will be dominated by volume reverberation or noise at corresponding times.

Figure 12 shows comparable data when the ping duration is increased to 250 ms. The reverberation levels agree to about the same degree as for the shorter pulse over the peaks, and the differences in the valleys have been reduced. The narrow peaks and the valleys have been smoothed considerably.

Figures 13 and 14 compare the results from Models III and IV for ping lengths of 40 and 250 ms, respectively, when the transducer is pitched  $10^\circ$  up. Environment A still applies. The extent of the agreement between the respective curves is substantially the same as for the comparable cases when zero pitch was used except at the shortest times shown. It is felt that when path angles are involved which approach  $-90^\circ$  the geometric correction factor,

$$-10 \log_{10} [\cos (\theta_0 - \xi) / \cos \theta_0]$$

(where  $\xi$  is the transducer pitch angle)

in  $J_s$  over-compensates and makes the levels a few dB higher than they should be for Model III. At the longest times (where the initial path angles are approaching  $-15^\circ$ ) the angles with respect to the transducer axis are approaching  $-5^\circ$ . One might expect the two curves to coincide. The one for the integrated method is still a few tenths of a dB above the other one as it was for the zero pitch cases. This leads one to suspect that the  $\cos (\theta_0 - \xi) / \cos \theta_0$  correction is slightly over-compensating even at these angles.

Figures 15 through 18 compare data from Model III and IV for the various combinations of pulse lengths and pitch angles when Environment B applies. In all four figures the two curves come into coincidence near or before an elapsed time of about 1.9 seconds which, in Environment B, corresponds to an initial path angle of approximately -12 degrees. For zero pitch, Figure 15 and 16, the agreement persists to the 10-second ping interval which corresponds to a path angle of approximately +4 degrees. This is the most convincing evidence that Model IV is properly programmed since it is under these conditions that  $J_s$  should be most accurate.

For pitch angles of 10 degrees up, Figures 17 and 18, the near perfect coincidence begins near 1.7-sec. elapsed time, corresponding to a path angle of about -13.5 degrees. Note, however, that this corresponds to -3.5 degrees from the transducer axis. On the basis of path angle alone one might think that coincidence should occur earlier. It is suspected that the delay is caused by the  $\text{Cos}(\theta_0 - \xi)/\text{Cos} \theta_0$  term in  $J_s$  over-compensating for the pitch. The agreement persists to about an elapsed time of 7 seconds, at which time the reverberation level computed by means of the integration method begins to fall slightly below that computed by Model IV. At 7 seconds the initial path angle is about +0.6 degrees while the angle with respect to the transducer axis is approximately +10.6 degrees. It seems possible that the slight divergence from 7 to 10 seconds results from the  $\text{Cos}(\theta_0 - \xi)/\text{Cos} \theta_0$  correction to  $J_s$  tending to under-compensate at appreciable off-axis angles when the sign of the pitch angle is opposite that of the path angle. However, the evidence is by no means conclusive since the divergence does not increase consistently as the elapsed time approaches 10 seconds. The differences are so slight that they well may be due to errors in the numerical integration process in one or both models. Although data points are taken at relatively short intervals, they are still at finite intervals apart, and linear interpolation is used.

For the relatively short elapsed times (less than 1.5 sec.), the differences in results from the two models in Environment B are essentially the same as they were when Environment A was used with one exception. For both ping lengths with zero pitch, the minor lobe at minimum time for the integrated method (Model III) is a little over one dB lower than for the doppler method for Environment B computations. For Environment A the difference is about the same amount but in the opposite direction. This is attributed to the fact that we changed the constant pattern value assumed for the back portion of the pattern as was announced earlier. The transition was most severe when Environment A was used, and these results are considered to be unreliable. For the 10 degree up pitch, this portion of the vertical pattern does not come into play in Model III.

It was decided to make one further effort to clarify the effect of transducer pitch by computing a case involving a 40 degree up attitude. As other conditions it was decided that Environment B and a 40-ms ping would combine to produce the most useful results. Remaining parameters have the same values used throughout the study. Figure 19 compares the results produced by means of Models III and IV. The on-axis ray ( $\theta_0 = -40^\circ$ ) reaches the surface at  $T = .647593$  sec. At this pitch angle, at least in Model III, the major lobe of the pattern controls the reverberation

level over a relatively small portion of the total ping interval. The first minor lobe above the transducer axis controls the level of the peak following the onset of surface reverberation. The first minor lobe below the axis governs the reverberation level over the last 75% of the 10-sec. ping interval. It is difficult to visualize physically just how the patterns interact in Model IV.

In comparing the results from the two models, it is noted first that the two curves coincide only briefly at a time centered about  $T = 0.85$  sec. This corresponds to an initial path angle in the vertical plane of  $-29.1$  degrees or  $+10.9$  degrees with respect to the transducer axis. At times shorter than this the curves diverge with the integrated method giving the higher values. At about 0.43 sec. the separation is nearly 8 dB. At times greater than 0.85 seconds, the curves cross and there again is an increasing difference but with the integrated method yielding the lower values. The large difference in the vicinity of 1.9 seconds can be attributed to the fact that the null in the vertical plane patterns is not characteristic of the whole annulus which returns reverberation at times of this order. If this region is discounted, then the remainder of the ping cycle shows a very gradual increase in the difference between the two curves from about 1.7 dB at 2.5 sec. to 2.8 dB at 10 sec.

The above data would seem to support certain conclusions. In the first place, the doppler-band method (Model IV) is working properly. Although it is judged to be the most accurate way of computing the expected level of boundary reverberation, it increases the computing time by a factor of ten over that required by any of the other methods. Therefore, its general use as part of the ray tracing program is not recommended. It should be a separate program reserved for special cases. Even then it requires insertion of appropriate equations for the transducer patterns for obtaining pattern losses in any directions. Alternately, one could use a matrix of measured patterns in such a large number of planes that accurate results could be obtained by interpolation.

The other three models have in common the inaccuracy resulting from errors in computing values of the boundary reverberation index, for various geometries which obtain, as functions of transducer depth and elapsed time in the ping cycle. The evidence is that the errors inherent in the present method of computing  $J_s$  are small for path angles falling in the major lobe of the transducer when the pitch angle is not much greater than 10 degrees from the horizontal. For small pitch angles, the error in the first minor lobe may be tolerable in view of the usual uncertainty as to the proper values to assign for the scattering coefficient per unit area. Paths falling in the nulls between pattern lobes lead to values for  $J_s$  which are too high, but in general the boundary reverberation at corresponding times will be below other types of interference and is of no practical consequence. Model I, the method presently incorporated in our ray tracing program, also suffers from underestimating the width of the insonified annulus as the paths become steeper. Model II will improve this situation over a considerable range of path angles, but this improvement is unimportant relative to another source of error common to both models I and II. Here we refer to the assumption that values of  $J_s$  and transmission loss computed to a single point in the annulus are characteristic of the entire insonified area.

Except for very short pings, this assumption can introduce substantial errors when the rate of change of one or more of these parameters is large. On this basis it seems logical to adopt the integration method (Model III) as the regular routine in the ray tracing programs. Surprisingly enough, this can be accomplished without a significant increase in run time on the computer. With a suitable selection of rays, accurate modeling of the expected level of boundary reverberation should be achieved within the accuracy inherent in  $J_s$ . If an improved method of evaluating this factor is found, the benefits will automatically accrue in the reverberation computation.

Because of the other variables involved, it is difficult to pin down the actual errors in  $J_s$  by comparing the reverberation levels computed by means of Models III and IV. During the course of this study, a technique was envisioned whereby  $J_s$  could be investigated directly.

A. B. POYNTER

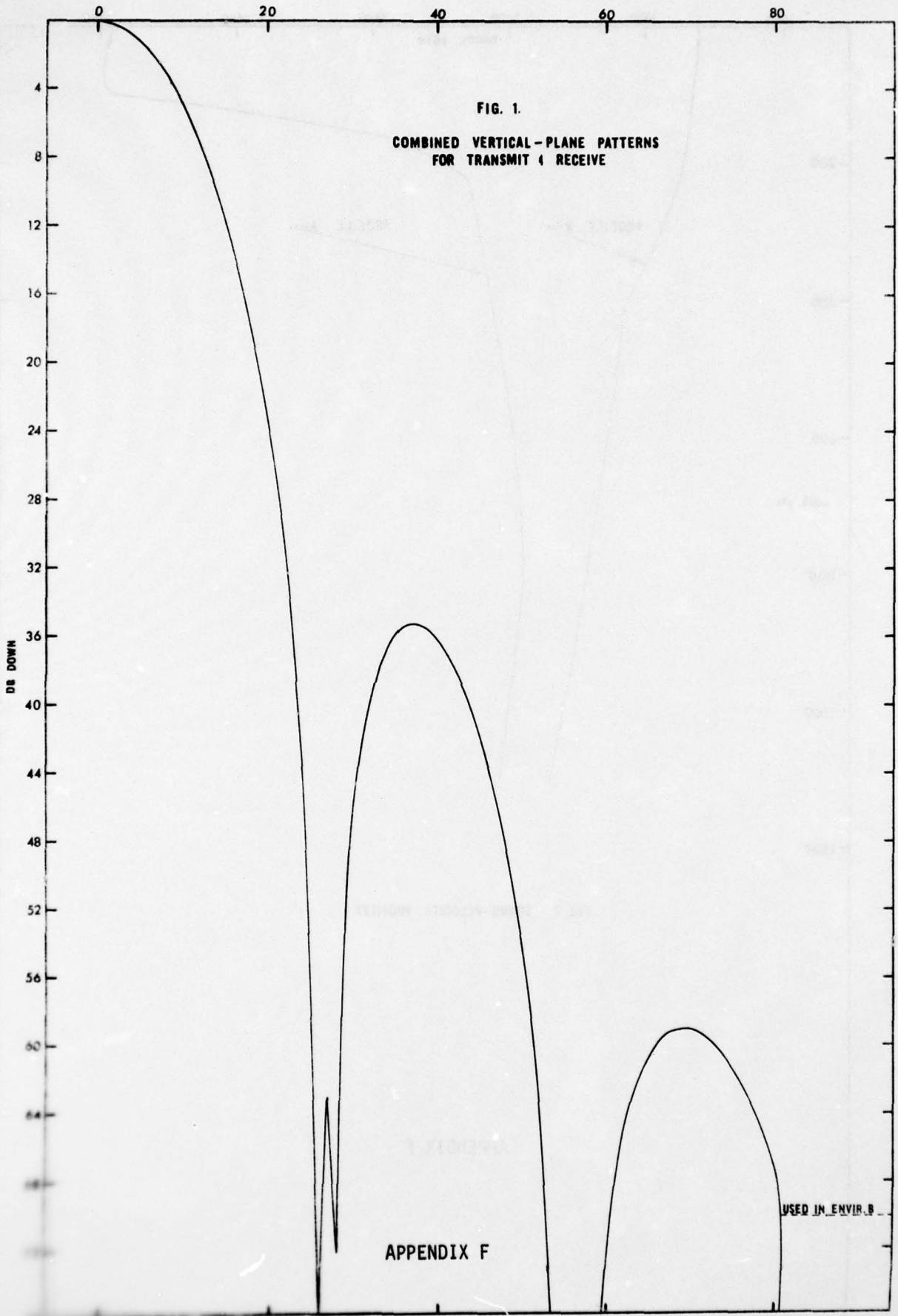


FIG. 1.  
COMBINED VERTICAL-PLANE PATTERNS  
FOR TRANSMIT & RECEIVE

APPENDIX F

USED IN ENVIR. B

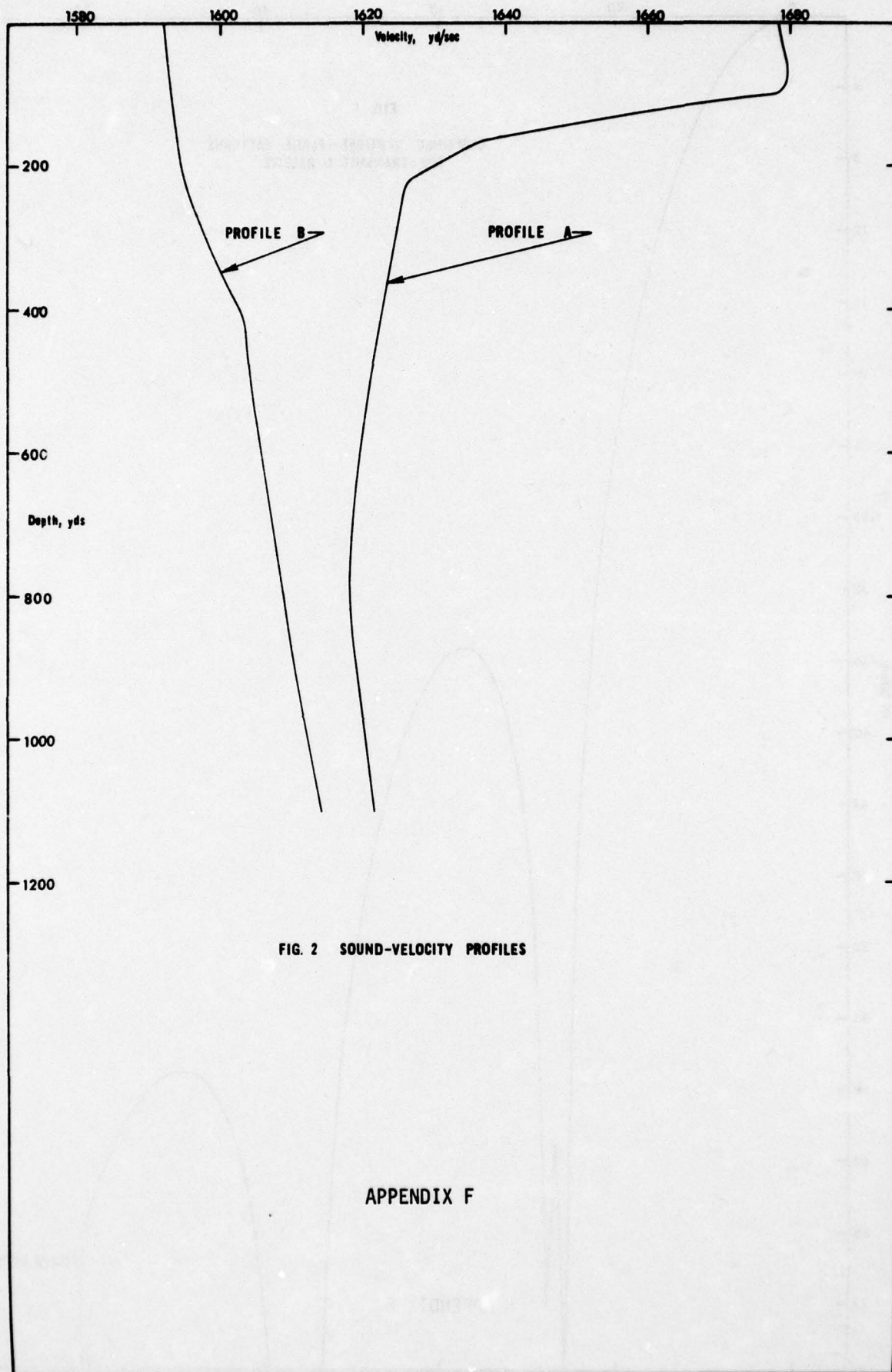


FIG. 2 SOUND-VELOCITY PROFILES

APPENDIX F

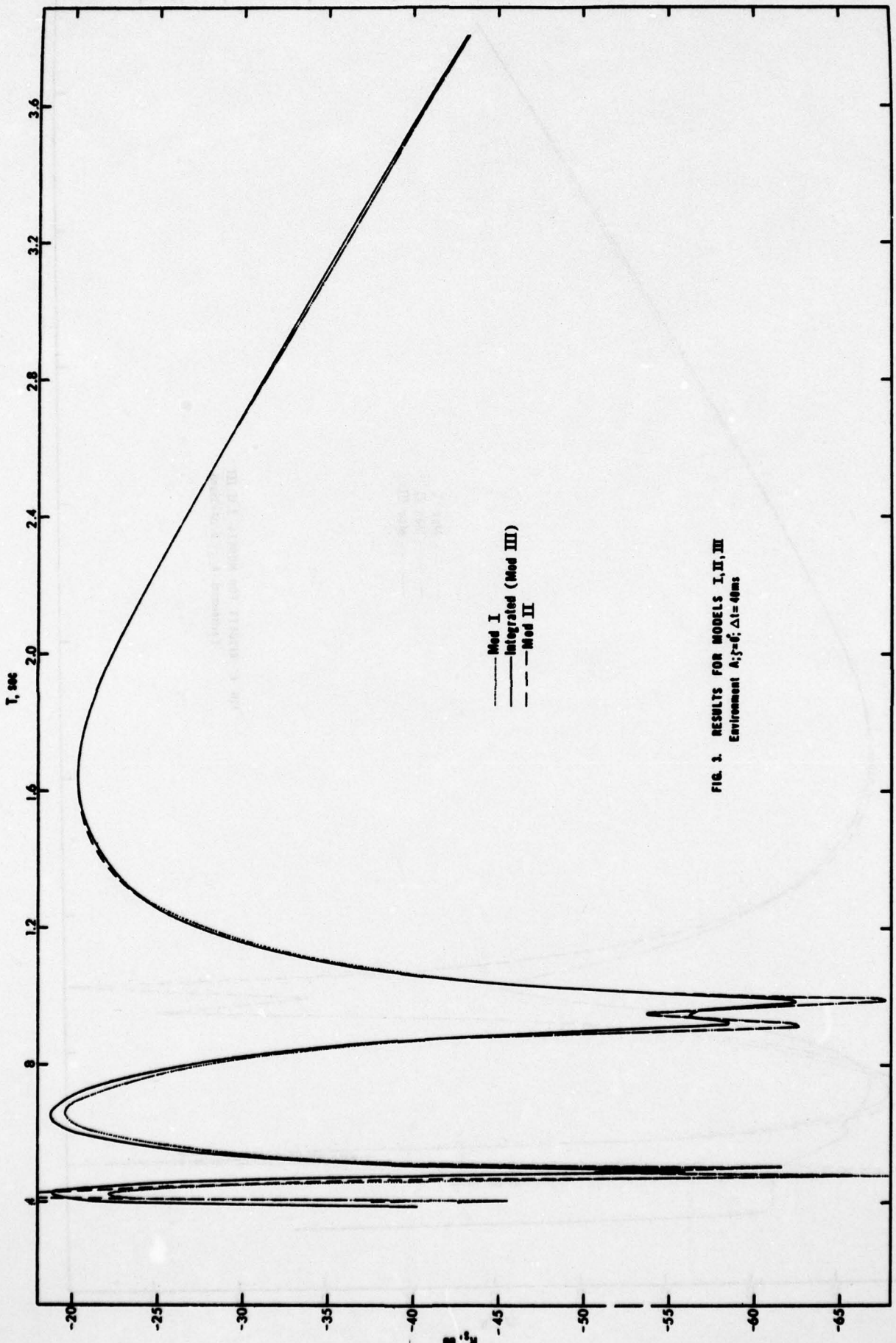


FIG. 1. RESULTS FOR MODELS I, II, III  
Environment  $A, \beta=6, \Delta t=40ms$

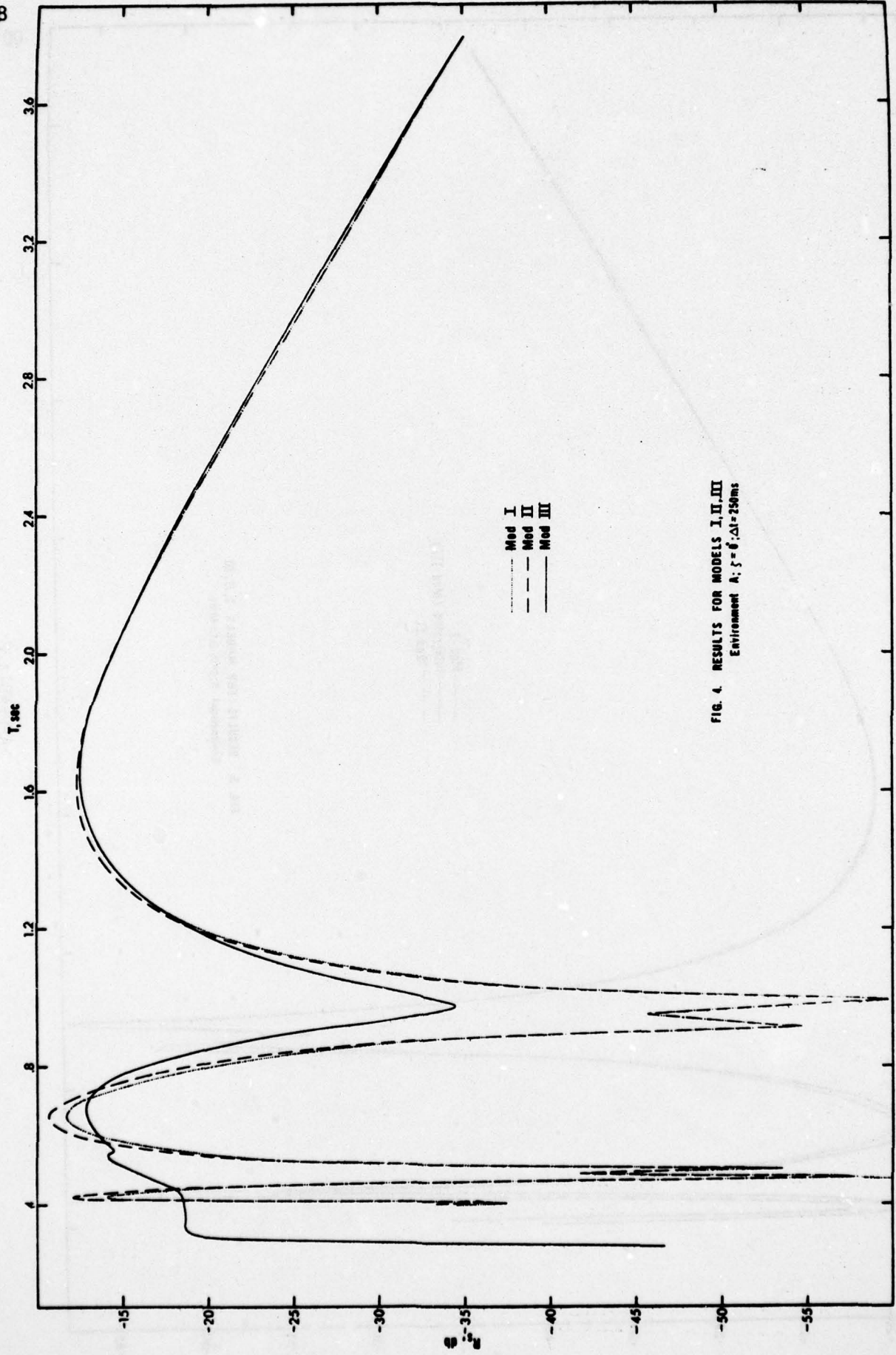


FIG. 4. RESULTS FOR MODELS I, II, III  
Environment A;  $\epsilon = 6^\circ$ ;  $\Delta t = 250ms$

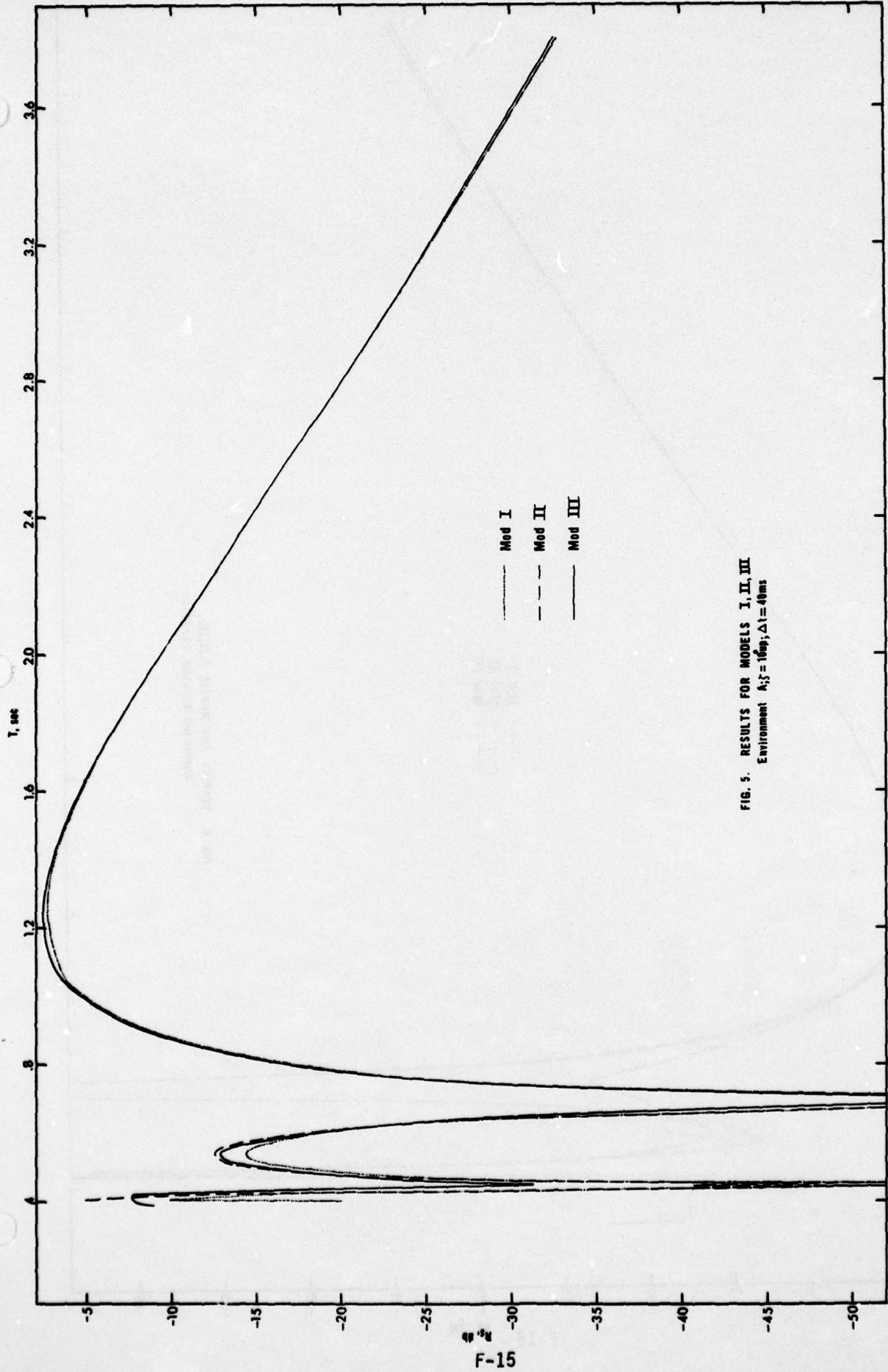


FIG. 5. RESULTS FOR MODELS I, II, III  
Environment  $A_1 S = 160g, \Delta t = 40ms$

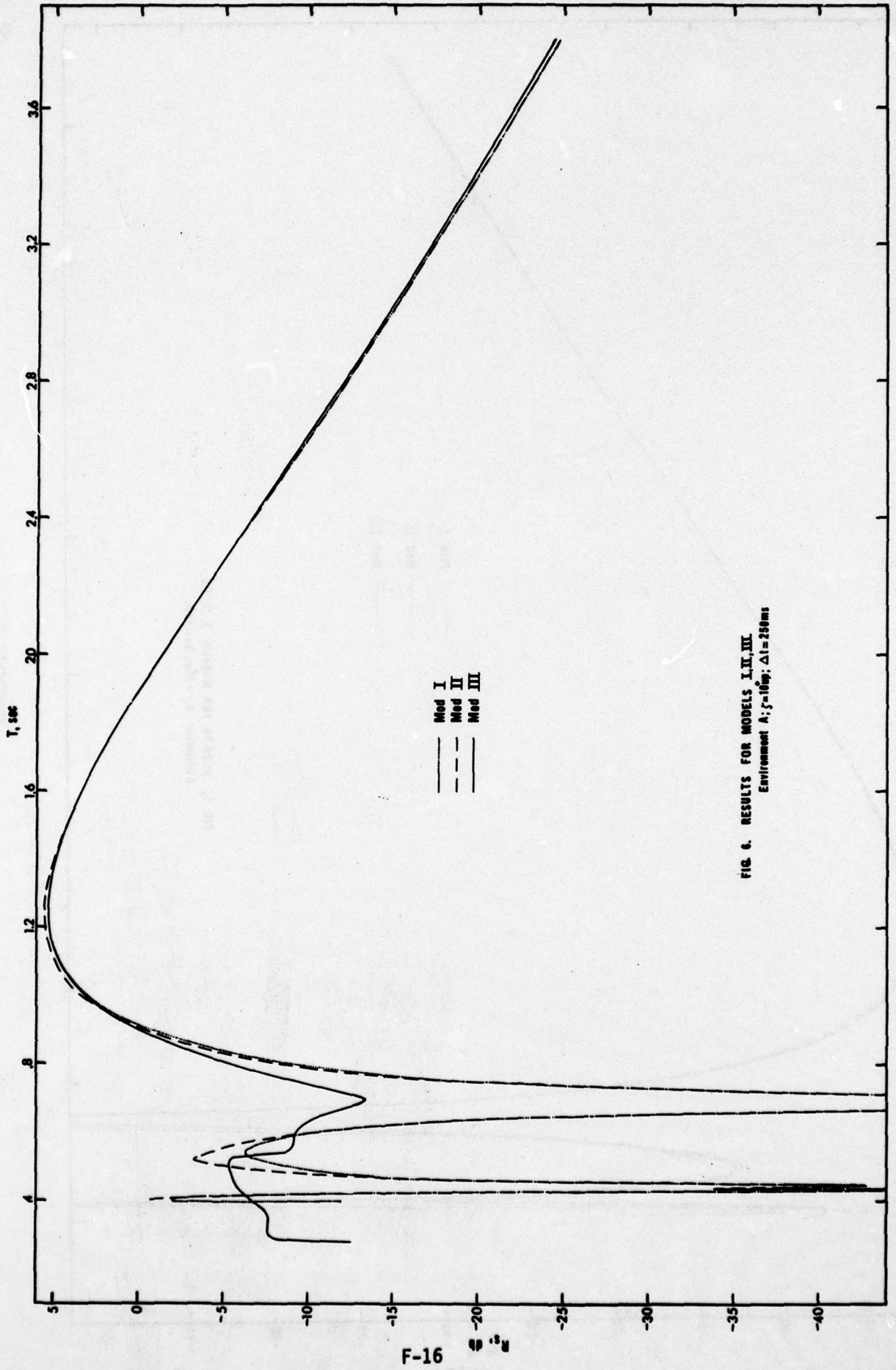


FIG. 6. RESULTS FOR MODELS I, II, III  
Environment A;  $\zeta = 10\%$ ;  $\Delta t = 250\text{ms}$

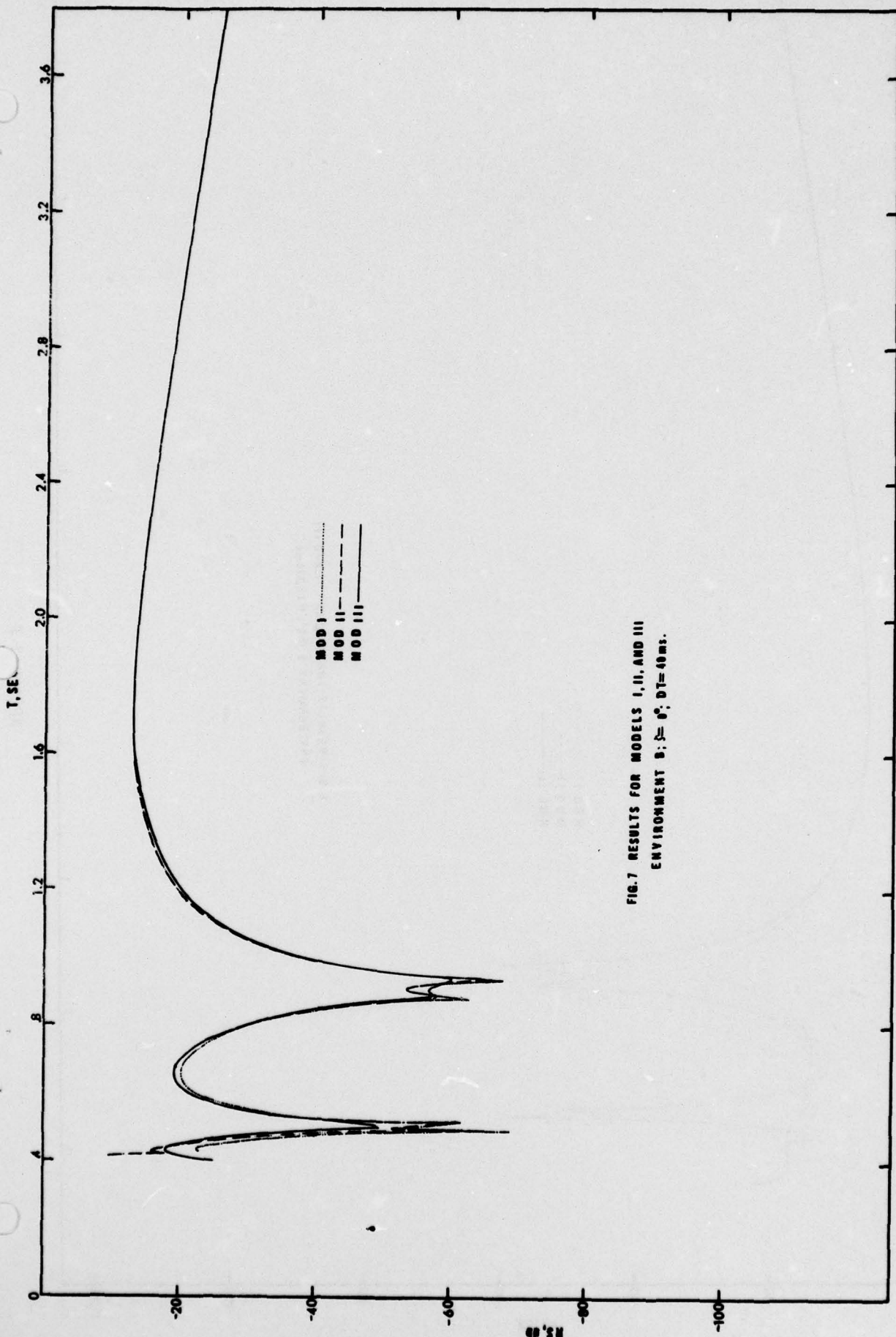


FIG. 7 RESULTS FOR MODELS I, II, AND III  
ENVIRONMENT B;  $\beta = 0^\circ$ ;  $\Delta T = 40$  ms.

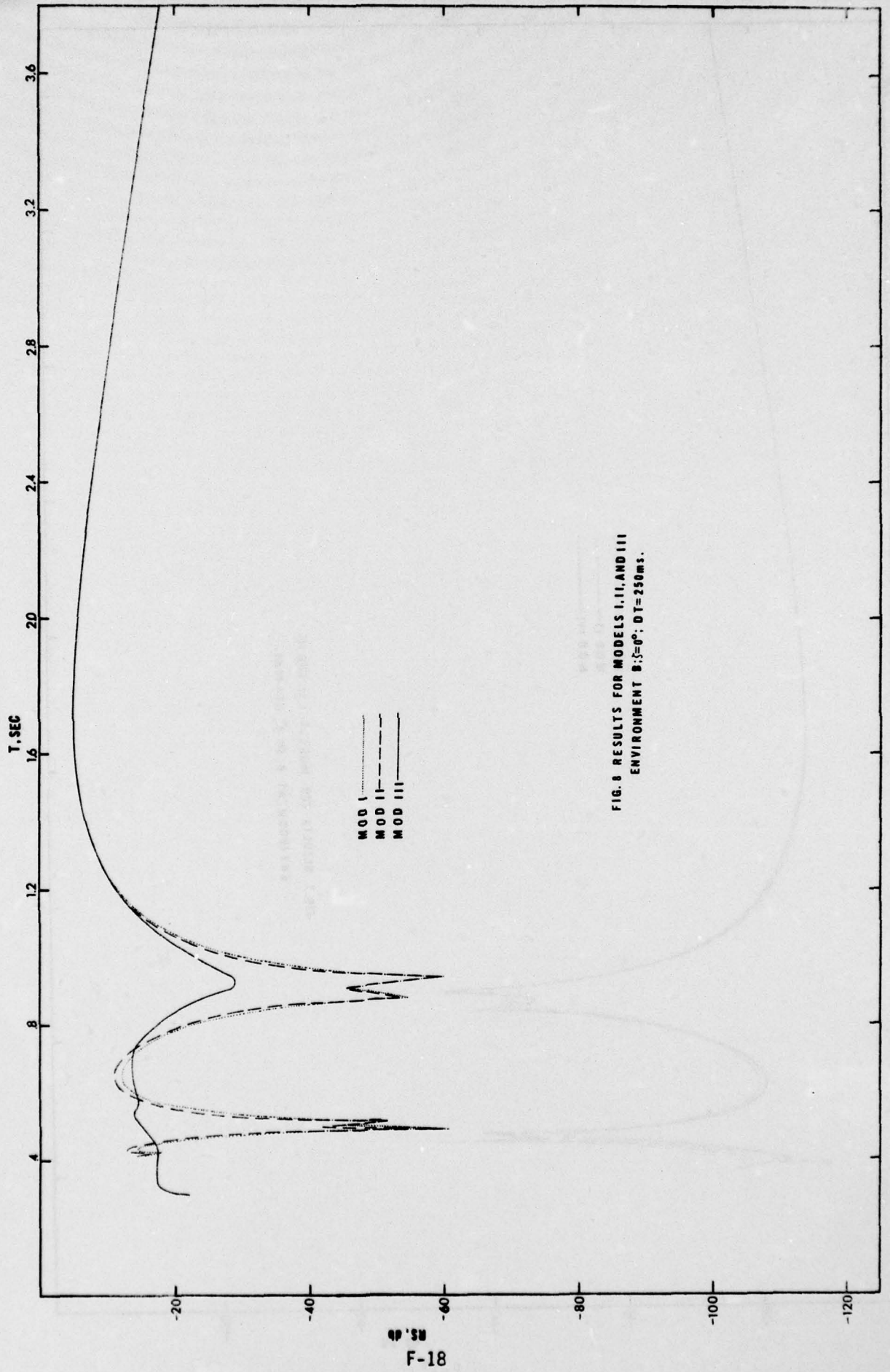


FIG. 8 RESULTS FOR MODELS I, II, AND III  
ENVIRONMENT B:  $\beta=0^\circ$ ;  $DT=250ms$ .

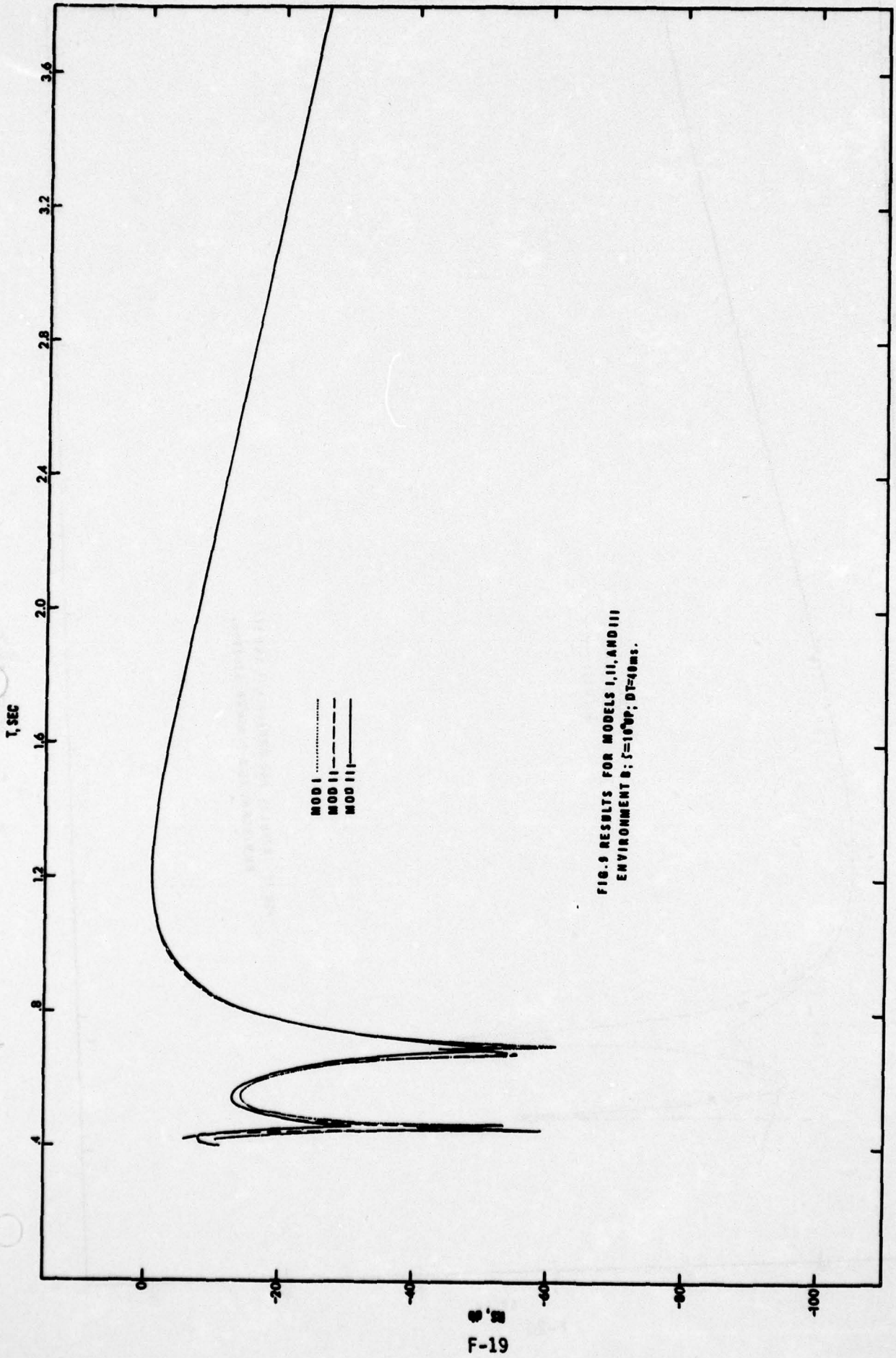


FIG. 9 RESULTS FOR MODELS I, II, AND III  
ENVIRONMENT B;  $\tau=10^6$ ;  $DT=40ms$ .

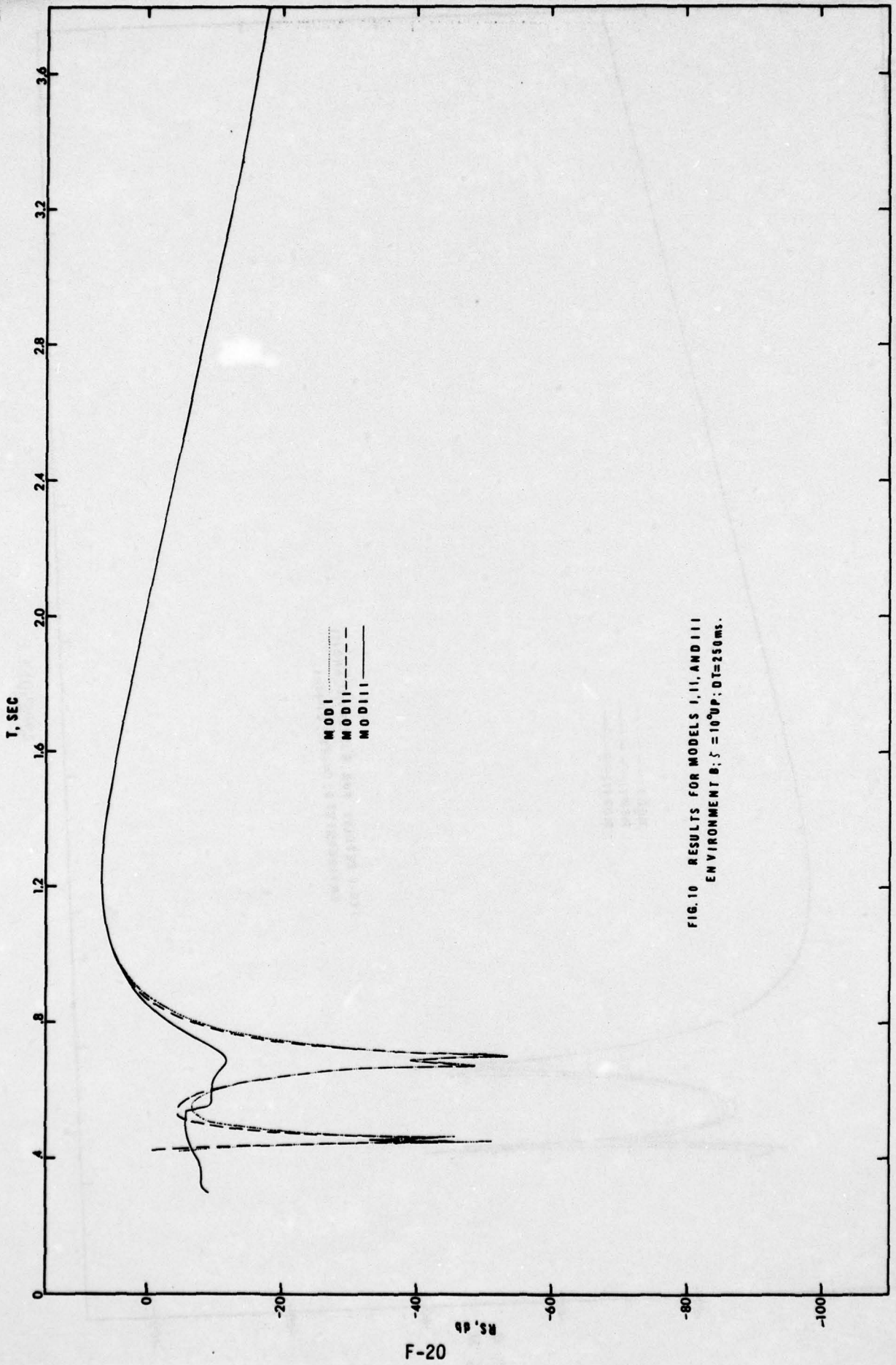


FIG. 10 RESULTS FOR MODELS I, II, AND III ENVIRONMENT B;  $\xi = 10^{\circ}$ UP; DT=250ms.

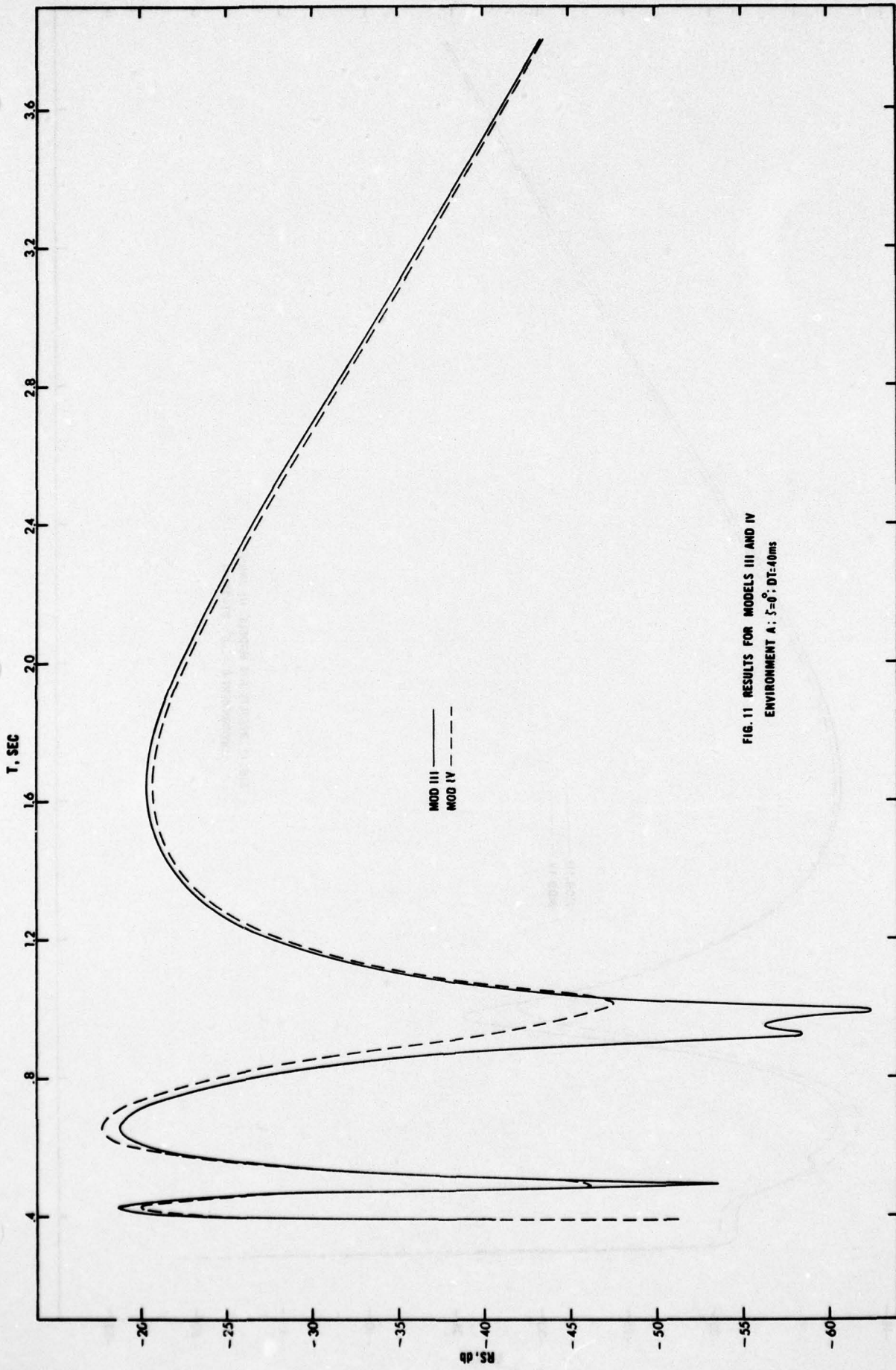


FIG. 11 RESULTS FOR MODELS III AND IV  
ENVIRONMENT A:  $\xi=0^\circ$ ; DT=40ms

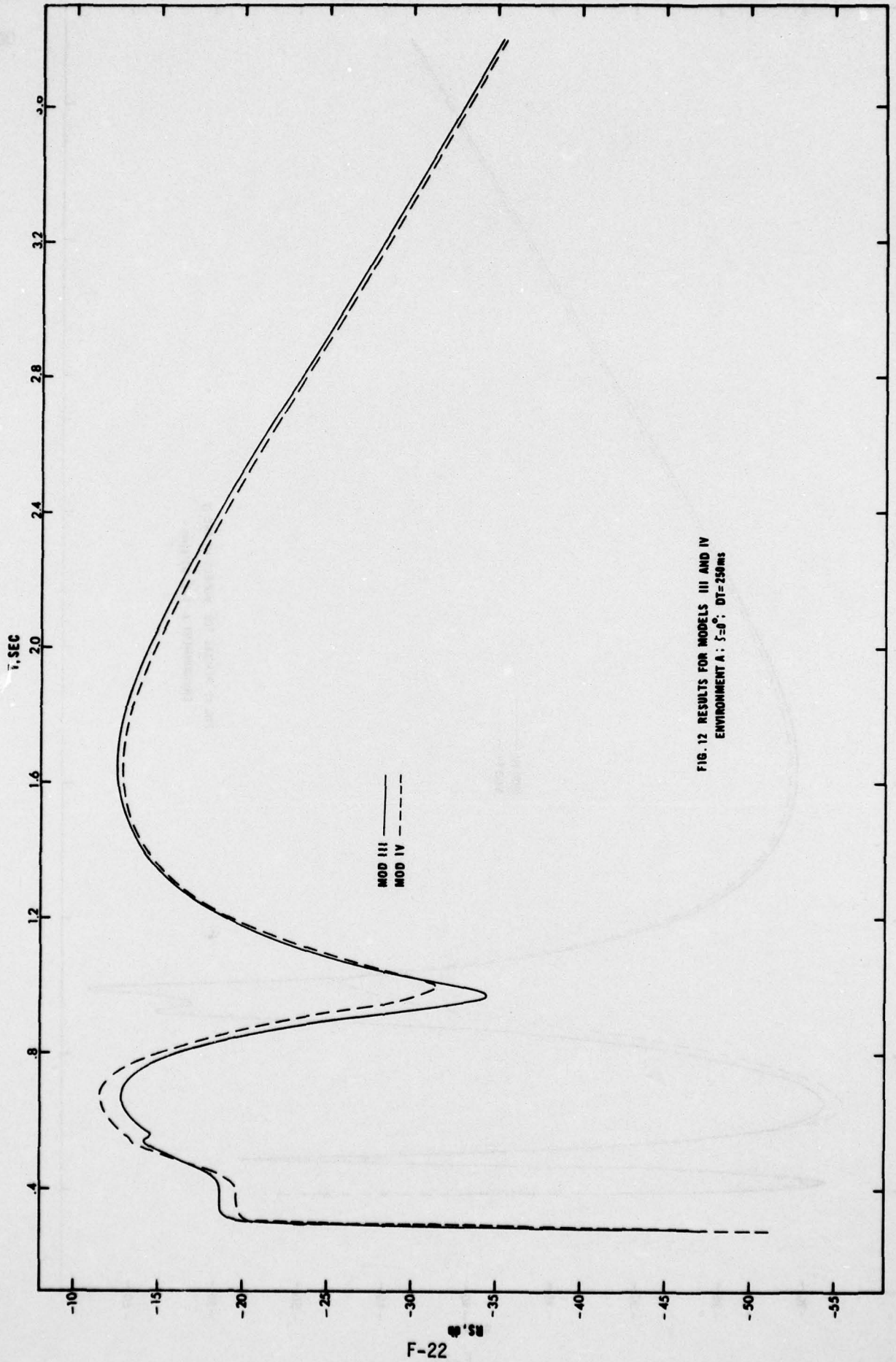


FIG. 12 RESULTS FOR MODELS III AND IV  
ENVIRONMENT A:  $\xi=0^\circ$ ;  $DT=250ms$

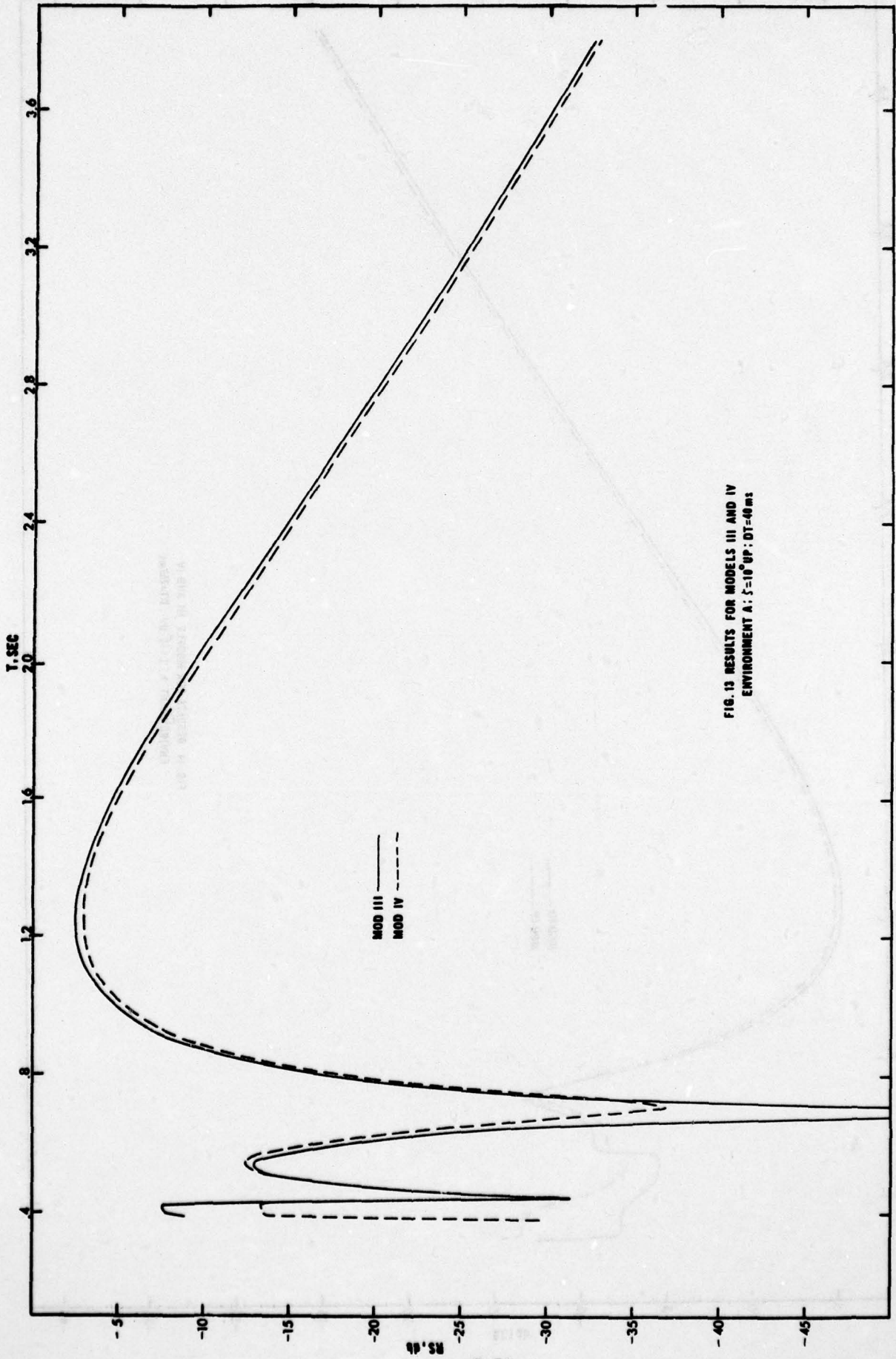


FIG. 13 RESULTS FOR MODELS III AND IV  
ENVIRONMENT A:  $\delta=10^\circ$  UP: DT=60ms

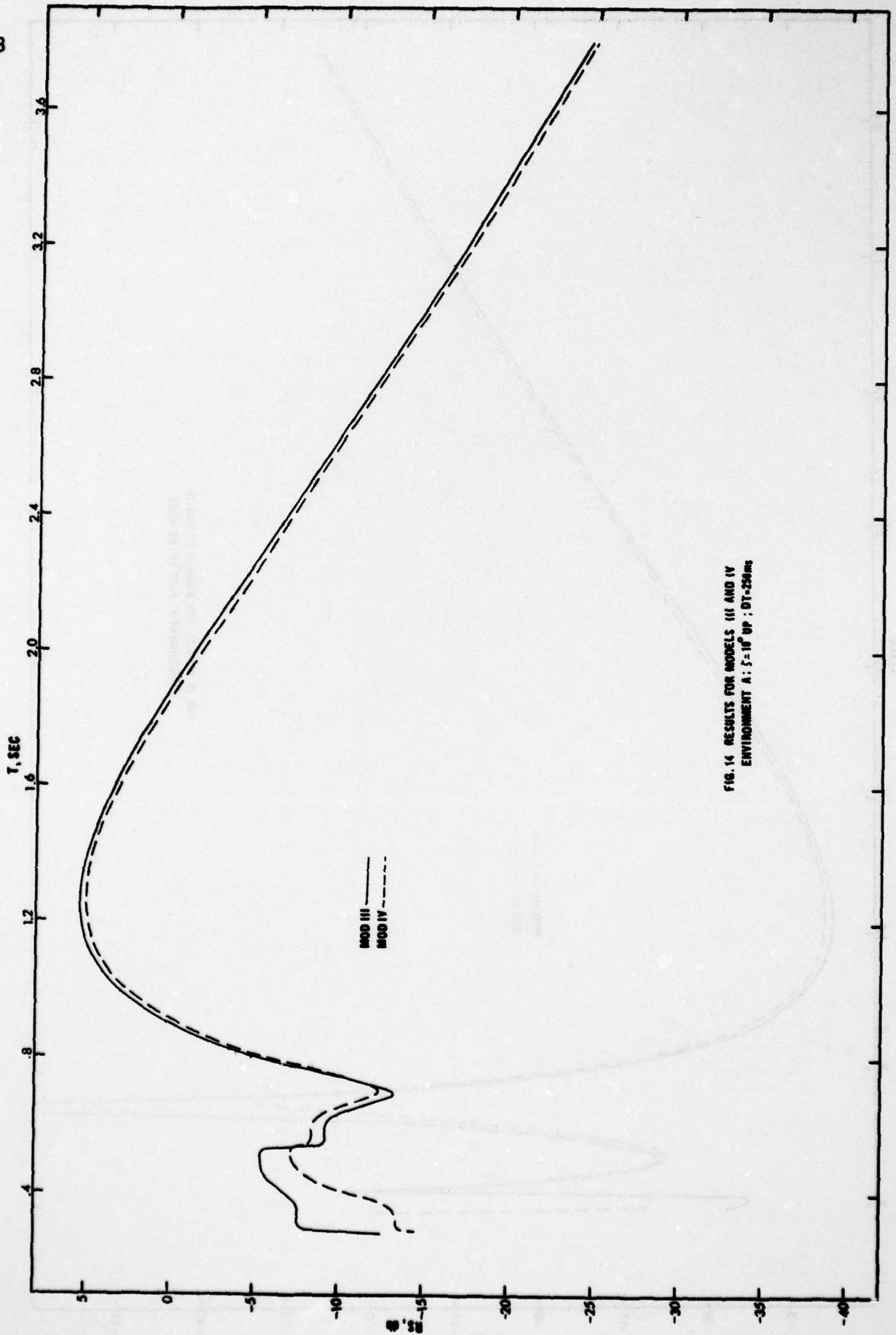


FIG. 14 RESULTS FOR MODELS III AND IV  
ENVIRONMENT A: 5-10° UP; DT-250ms

AD-A035 071

NAVAL SEA SYSTEMS COMMAND WASHINGTON D C  
A COMPUTER PROGRAM FOR STUDYING THE DOPPLER CONTENT OF REVERBER--ETC(U)  
1976 P MARSH

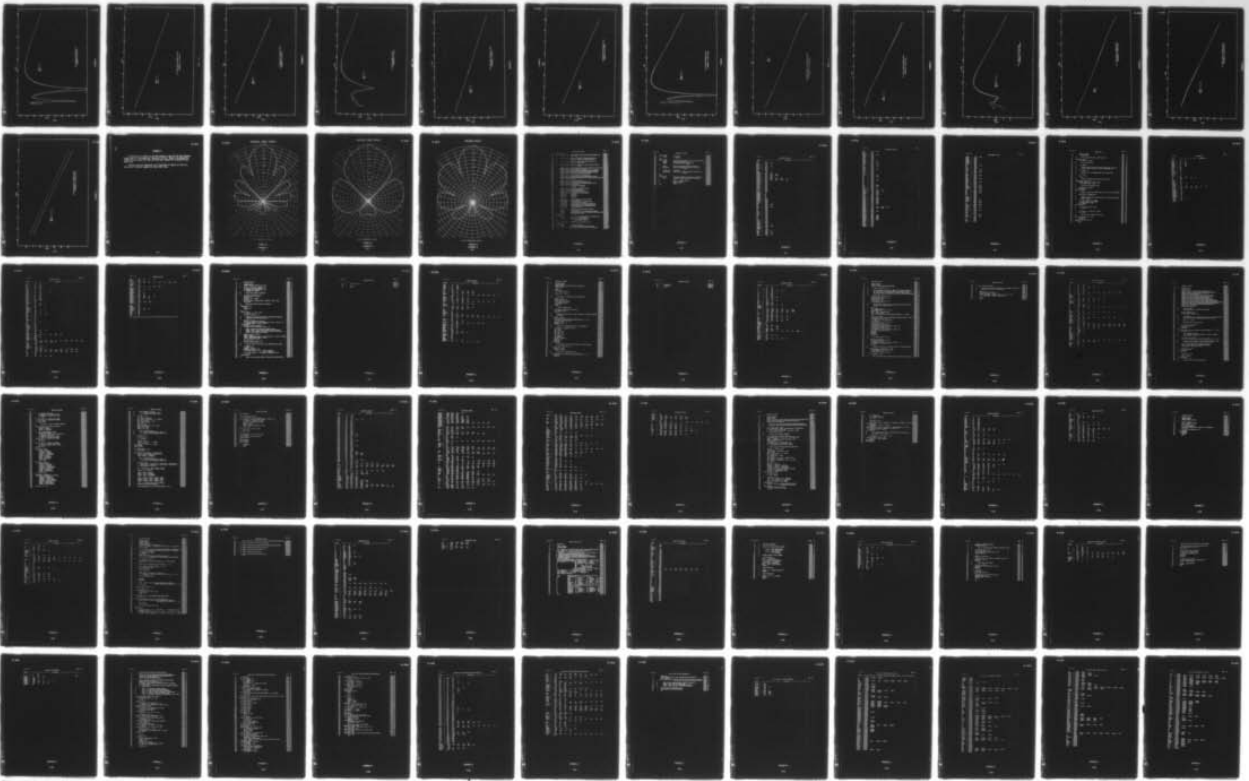
F/G 17/1

UNCLASSIFIED

NAVSEA-0D-52258

NL

2 OF 2  
AD  
A035071



END

DATE  
FILMED  
3 - 77

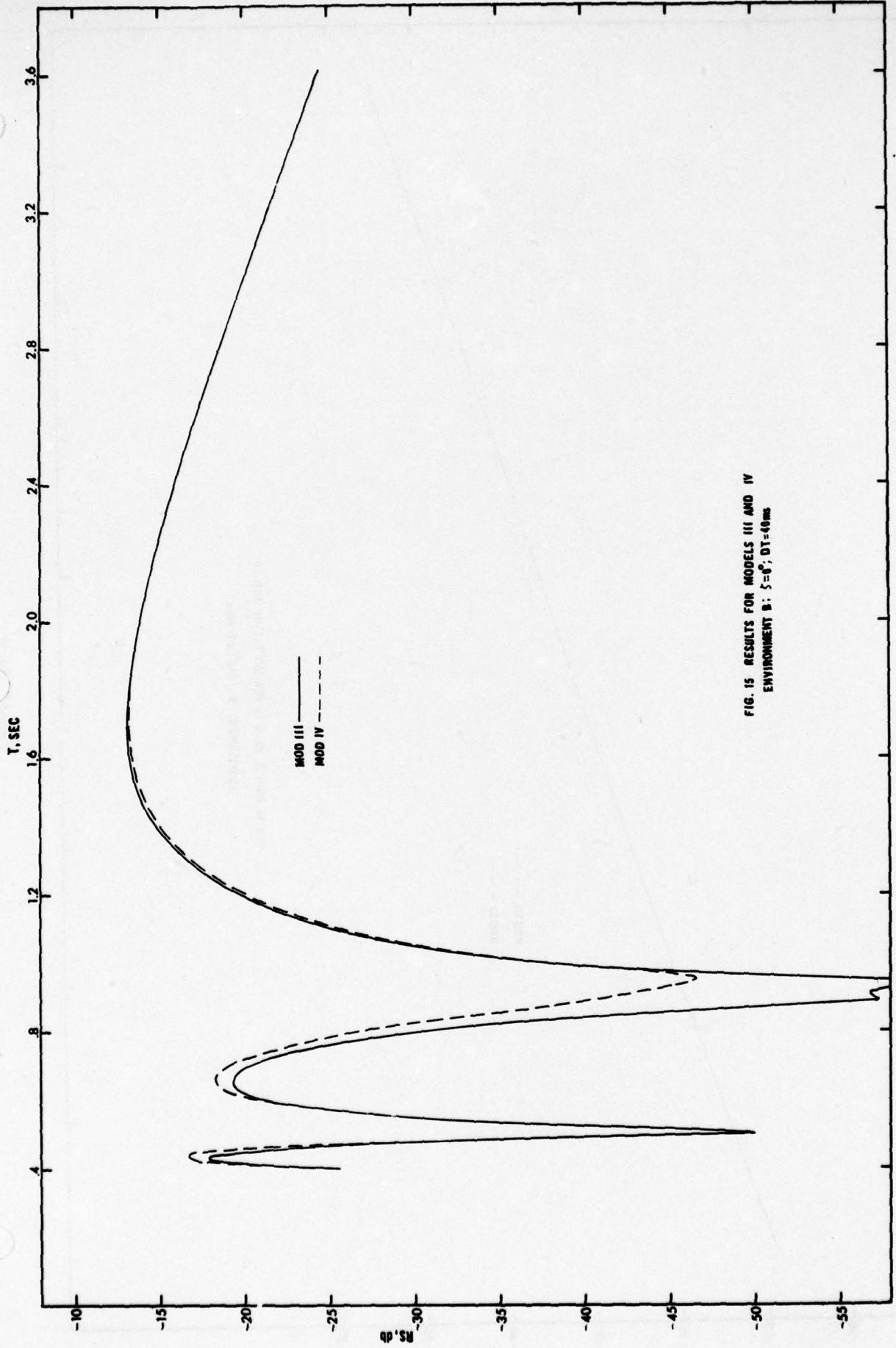


FIG. 15 RESULTS FOR MODELS III AND IV  
ENVIRONMENT B:  $S=6'$ ;  $DT=40ms$

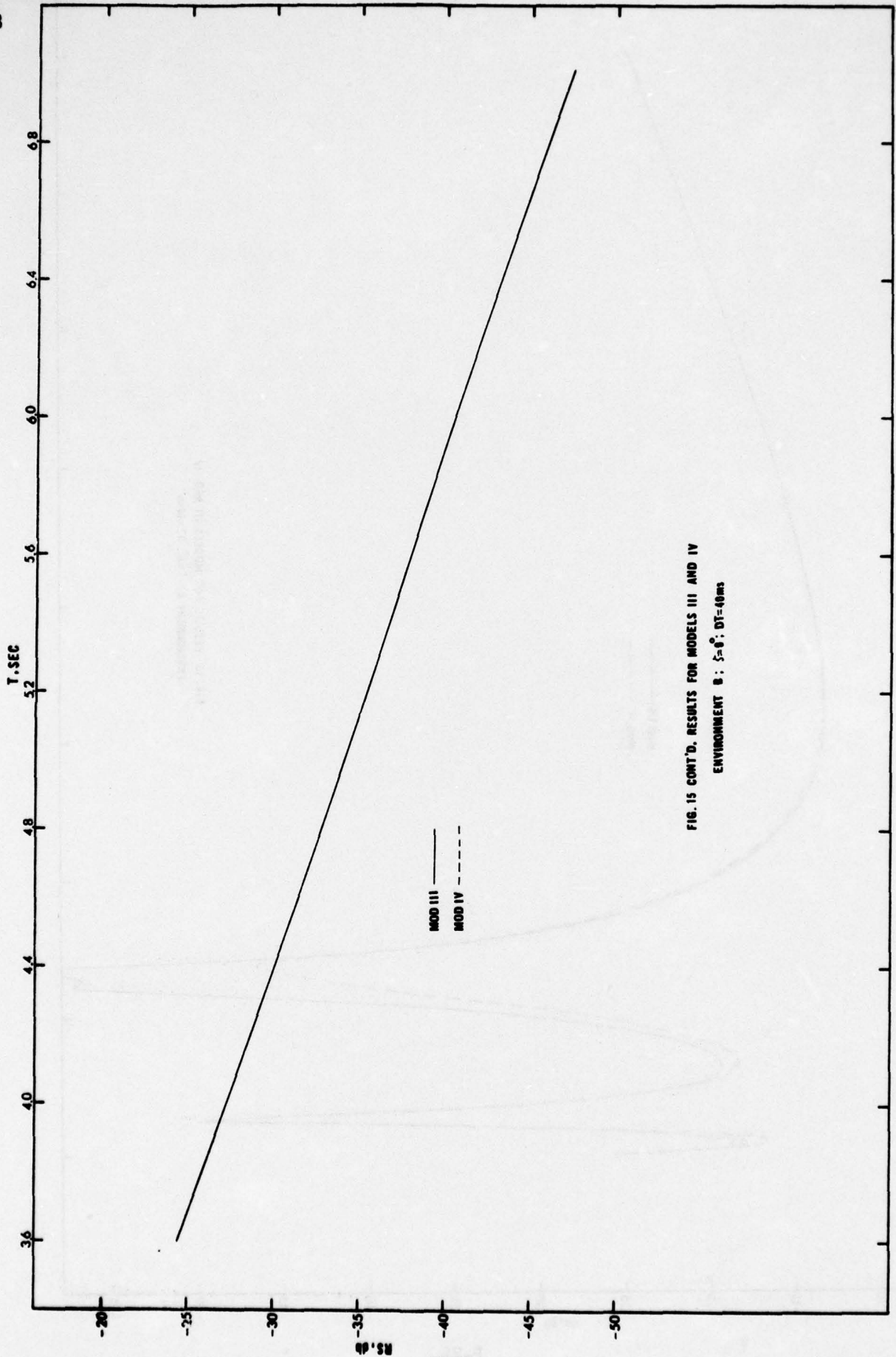


FIG. 15 CONT'D. RESULTS FOR MODELS III AND IV  
ENVIRONMENT B :  $S=0$ ;  $DT=40ms$

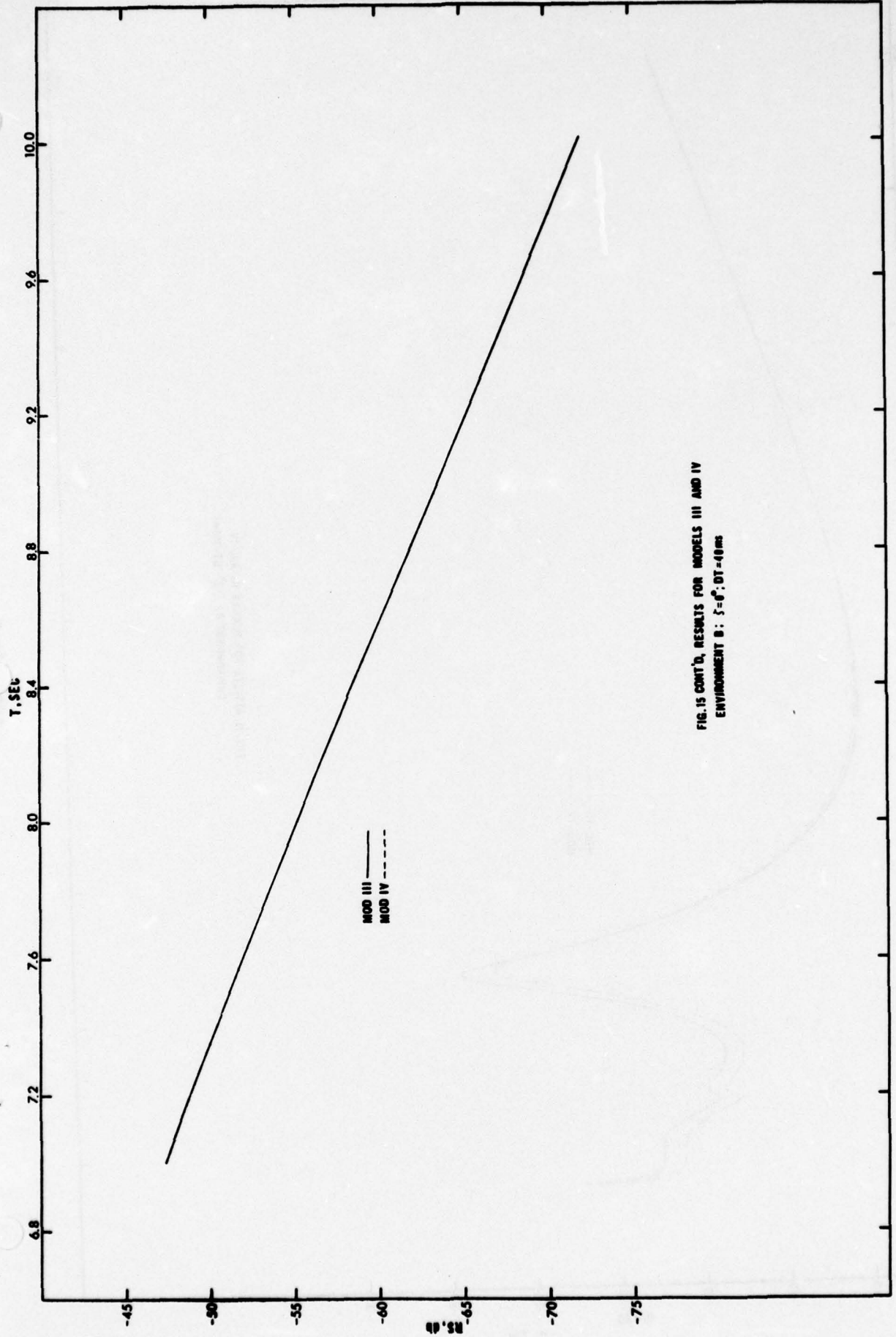


FIG. 15 CONT'D, RESULTS FOR MODELS III AND IV  
ENVIRONMENT B :  $\dot{\epsilon} = 6^\circ$ ; DT = 40ms

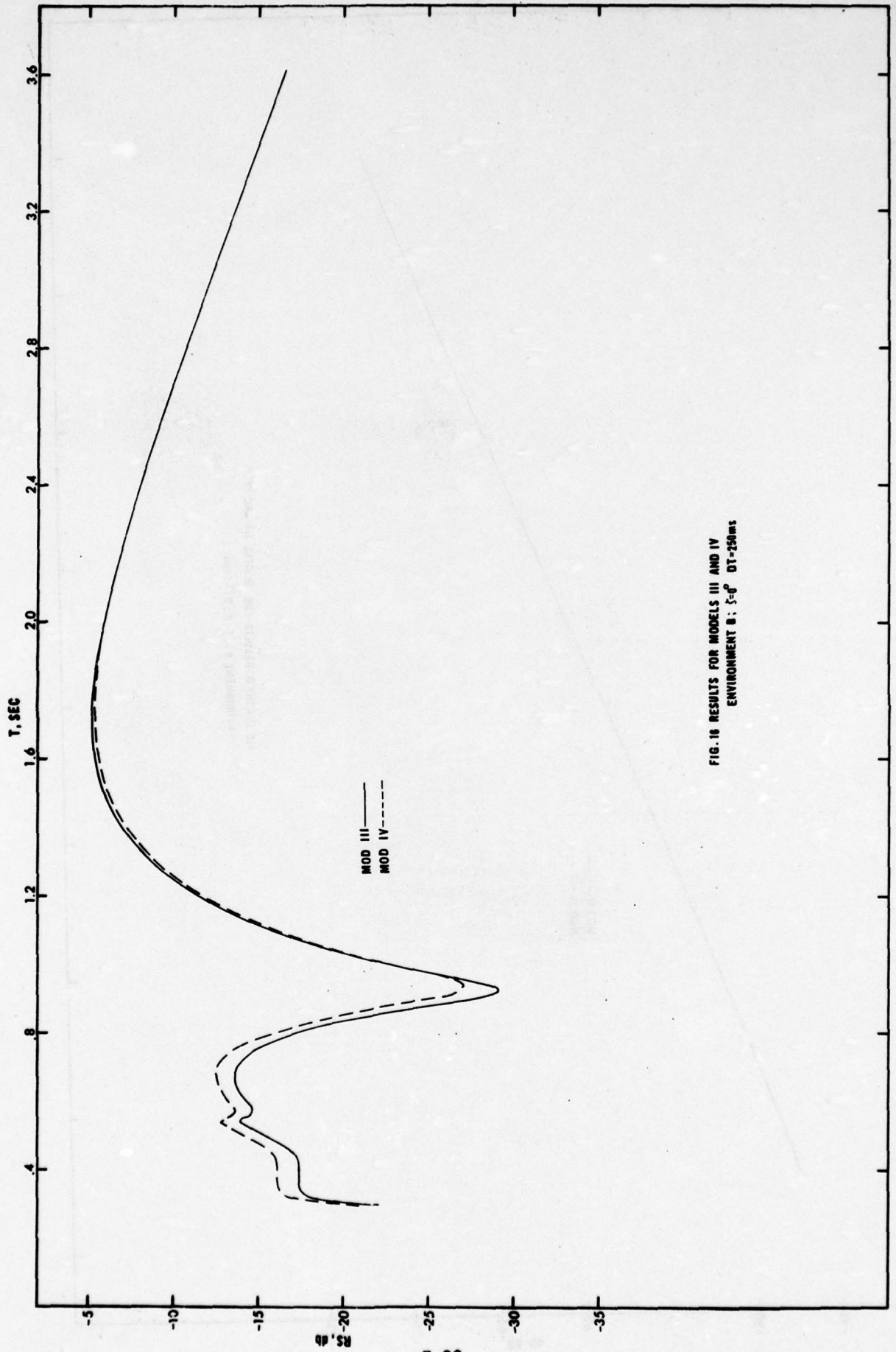


FIG. 16 RESULTS FOR MODELS III AND IV  
ENVIRONMENT B: 5-0° DT-250ms

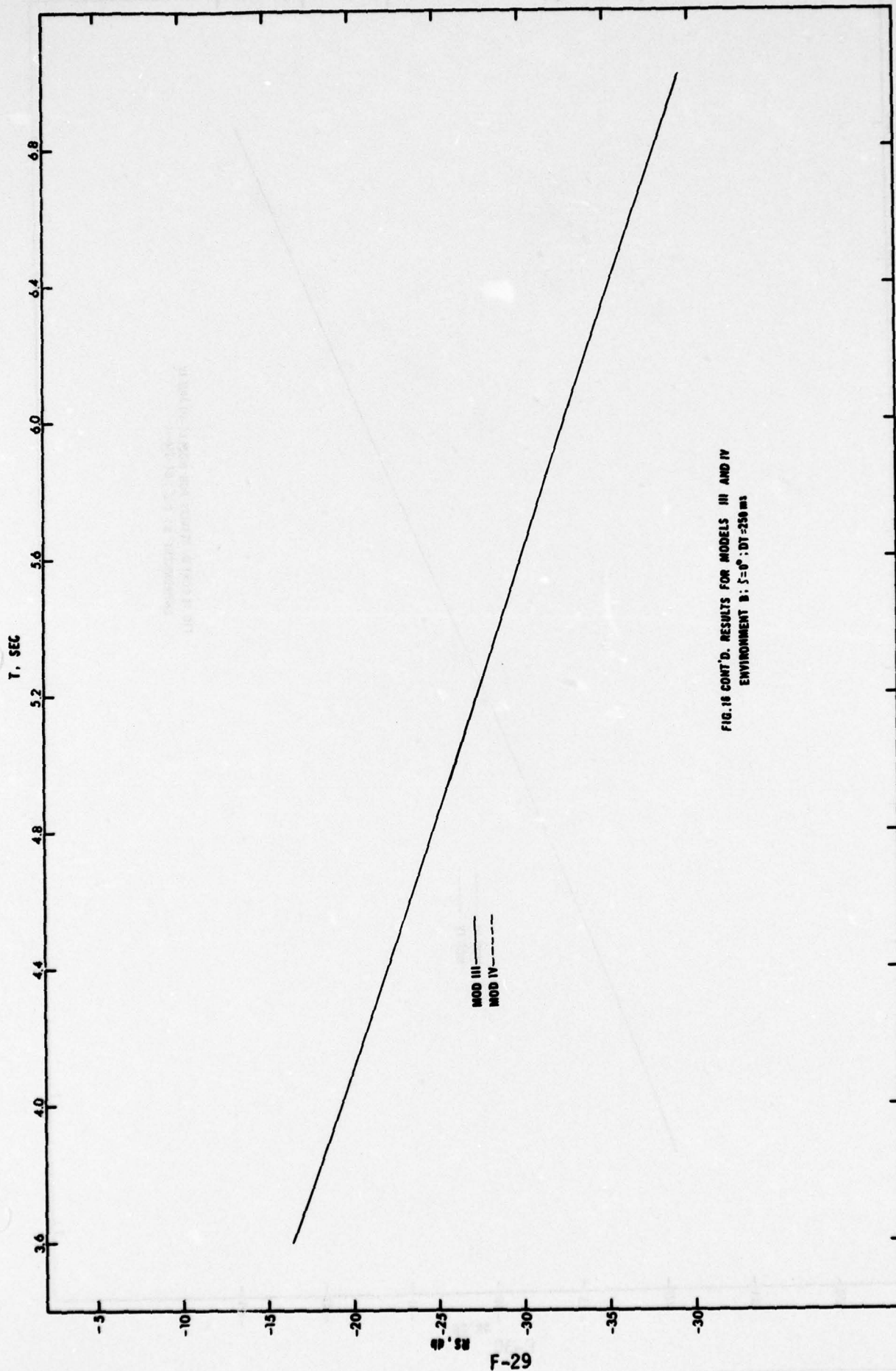


FIG. 16 CONT'D. RESULTS FOR MODELS III AND IV  
ENVIRONMENT B:  $\delta = 0^\circ$ ; DT = 250 ms

APPENDIX F

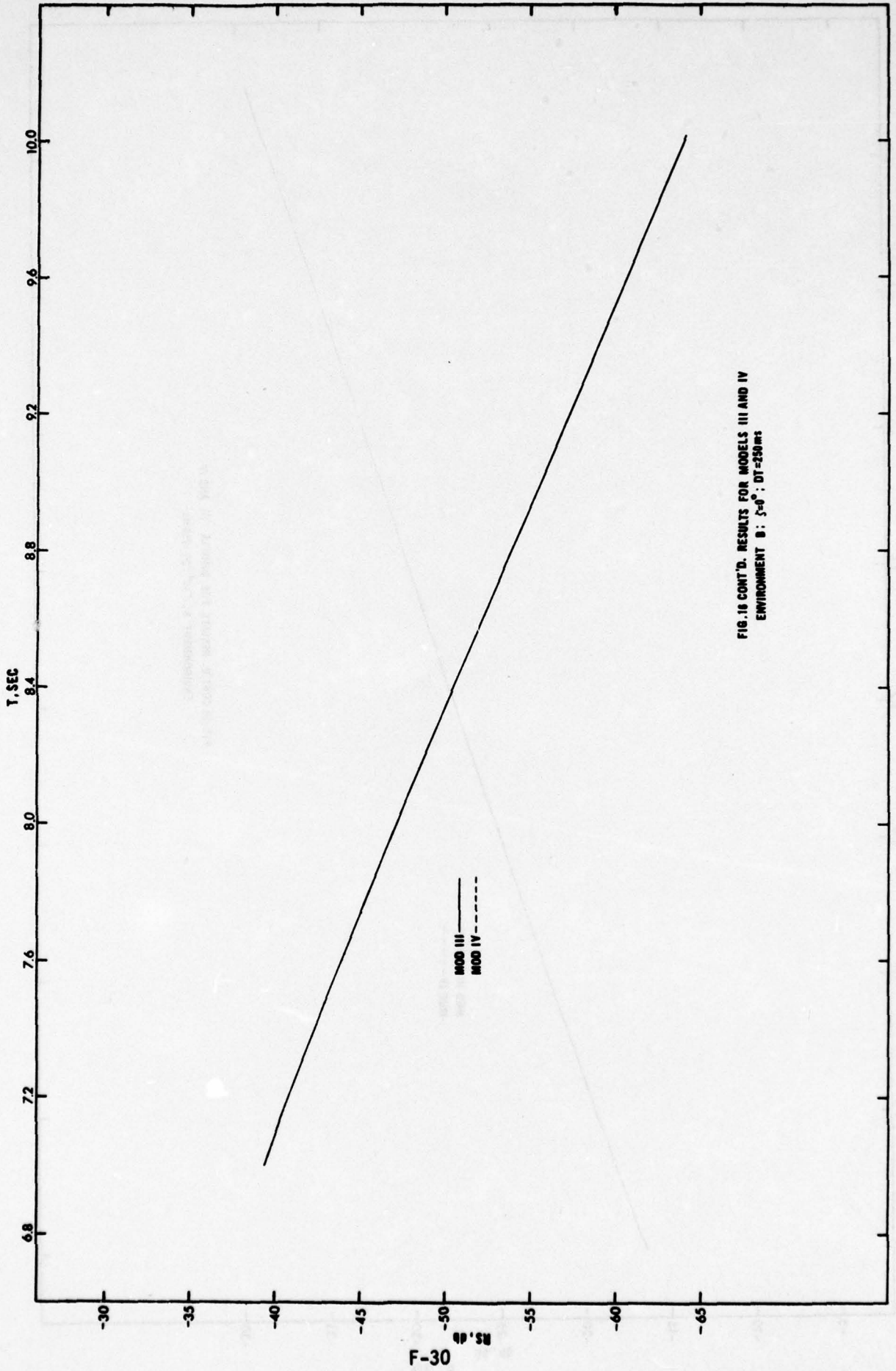


FIG. 16 CONT'D. RESULTS FOR MODELS III AND IV  
ENVIRONMENT B :  $\gamma=0^\circ$  ; DT=230ms

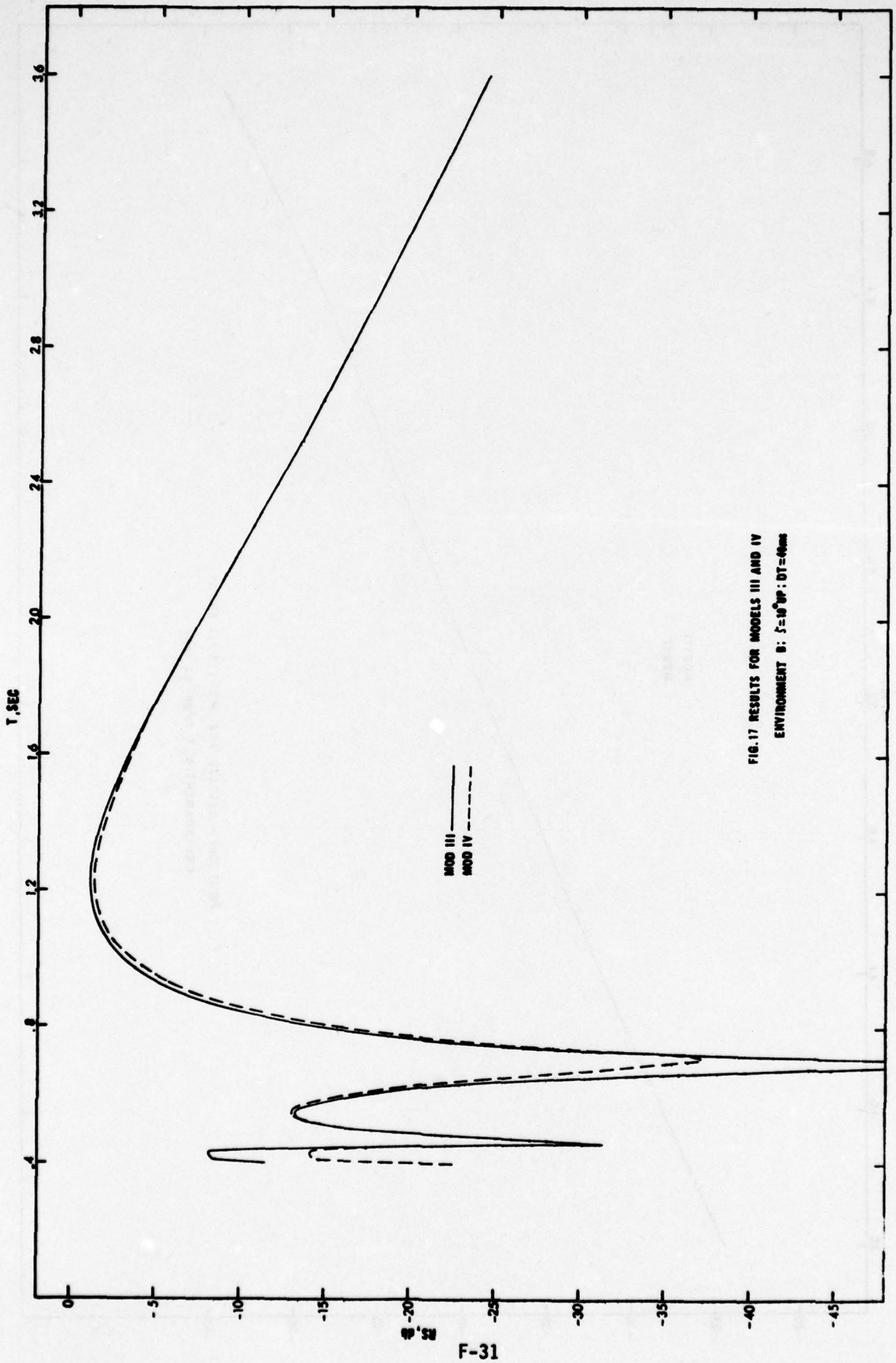


FIG. 17 RESULTS FOR MODELS III AND IV  
ENVIRONMENT B:  $\delta = 10^{\circ}$  UP; DT = 40ms

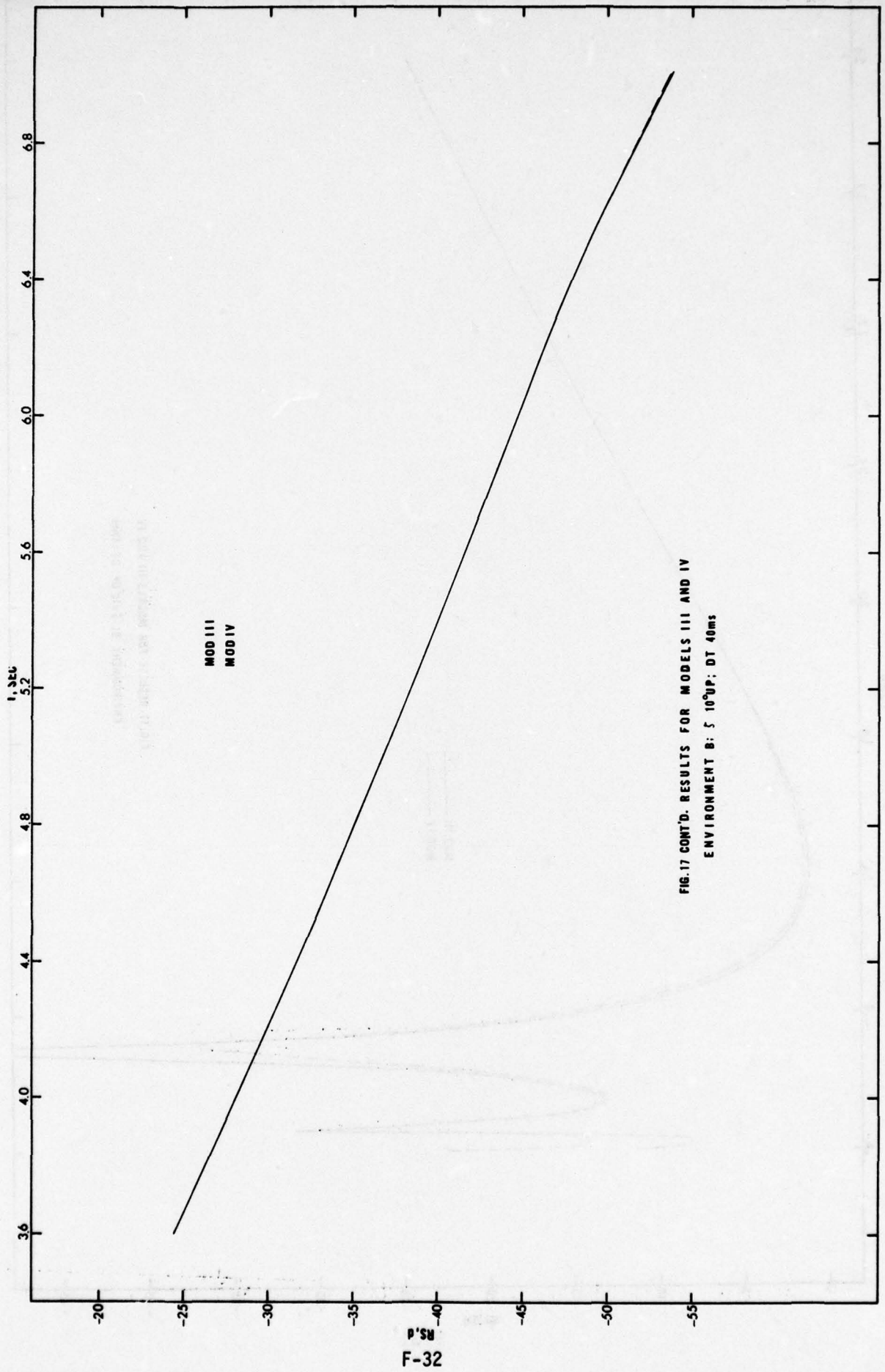


FIG. 17 CONT'D. RESULTS FOR MODELS III AND IV  
ENVIRONMENT B: 5 10°UP; DT 40ms

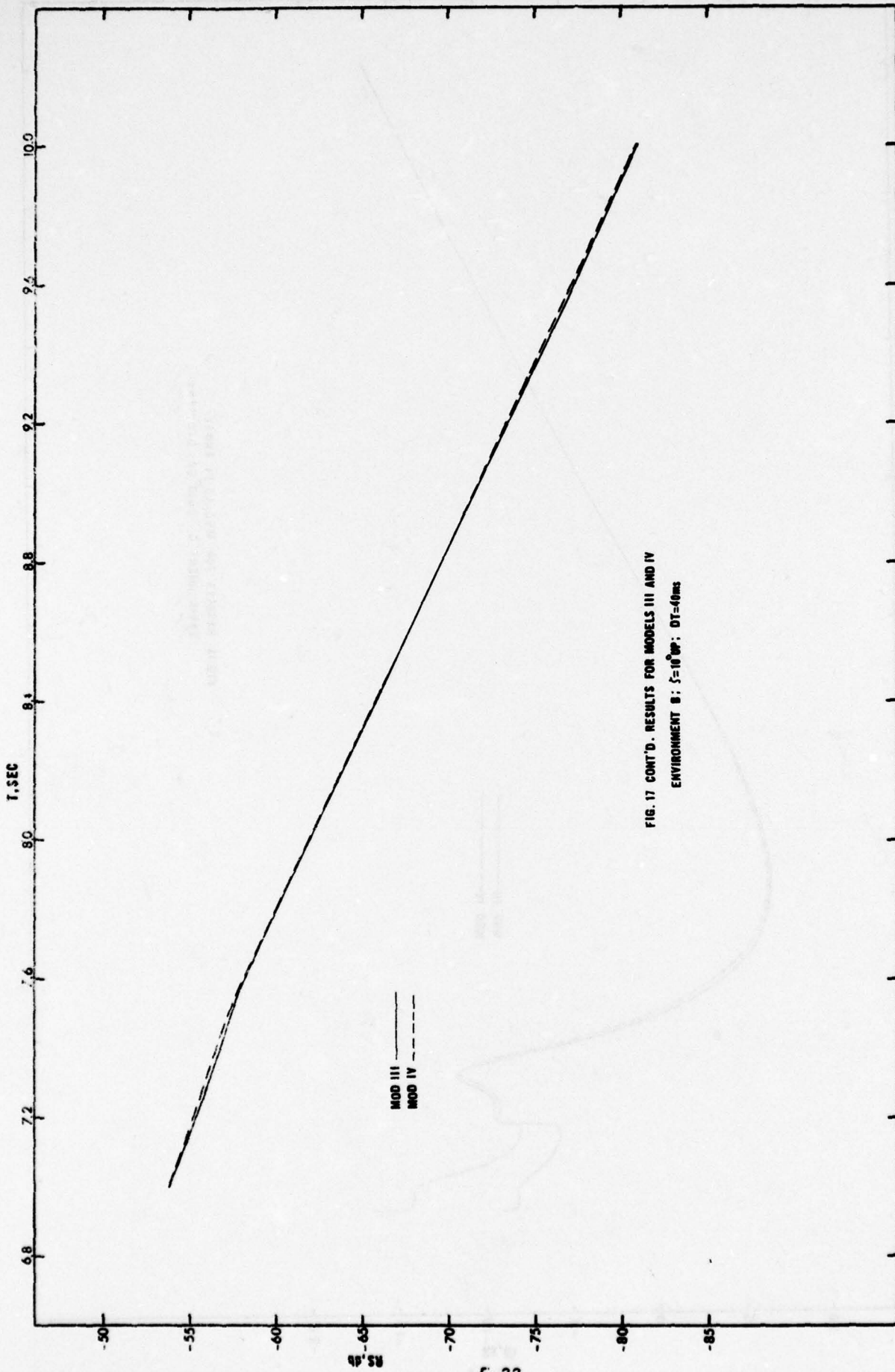


FIG. 17 CONT'D. RESULTS FOR MODELS III AND IV  
ENVIRONMENT B:  $S=10^6$  W; DT=40ms

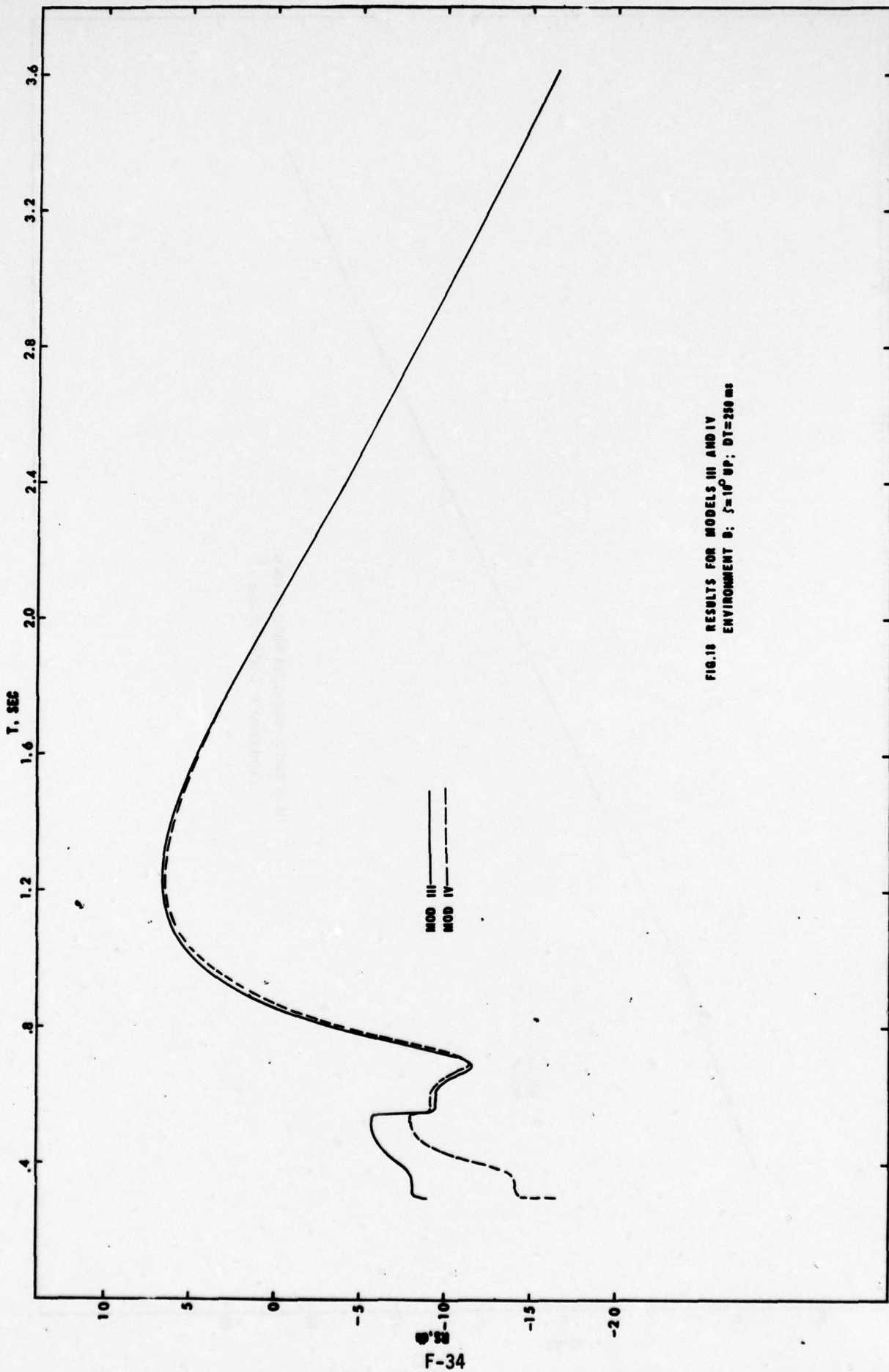


FIG. 10 RESULTS FOR MODELS III AND IV  
ENVIRONMENT B;  $\zeta=10^6$  GP; DT=200 MS

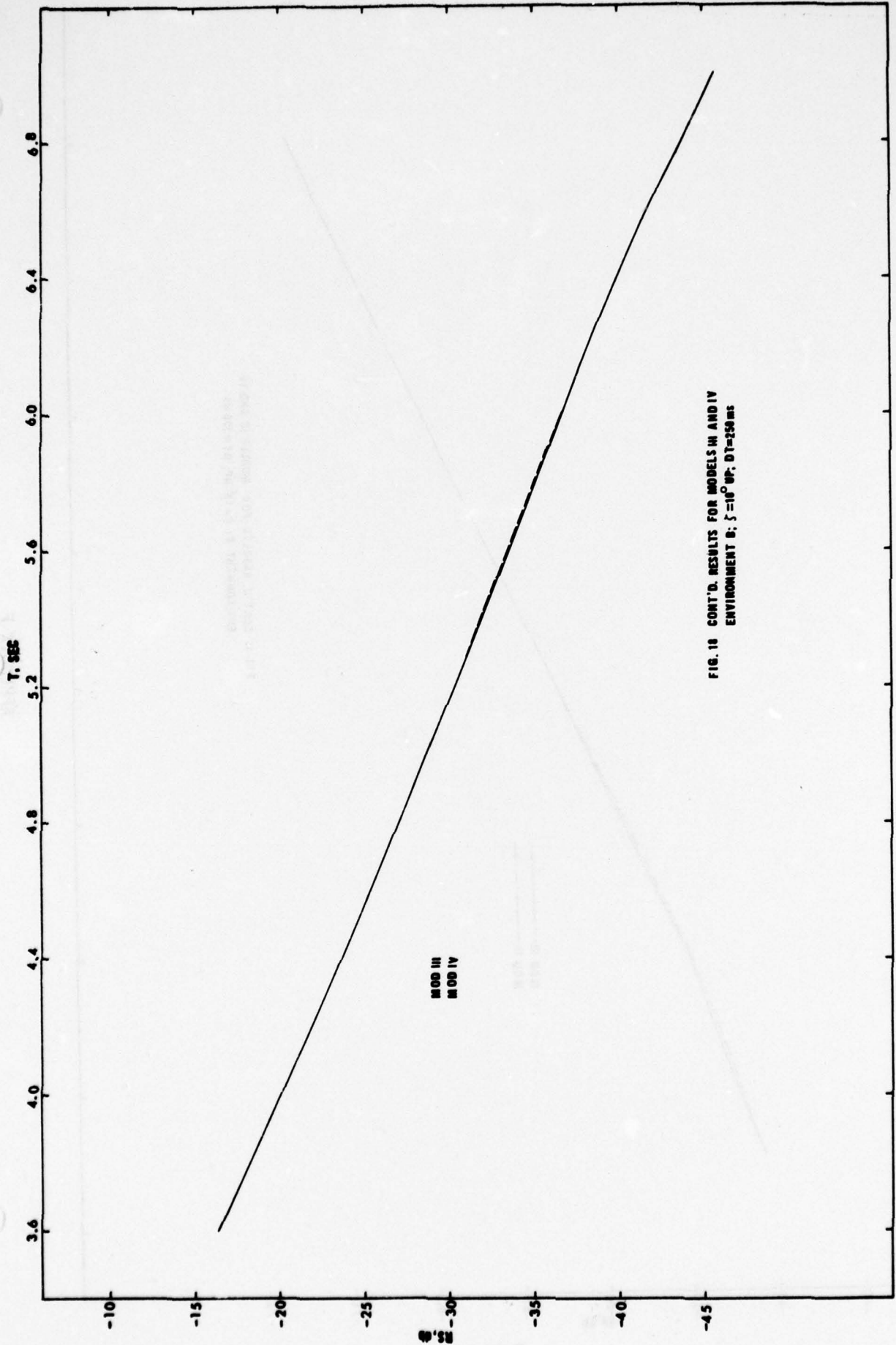


FIG. 18 CONT'D. RESULTS FOR MODELS III AND IV  
ENVIRONMENT B;  $\xi = 10^6$  WP; DT=550ms

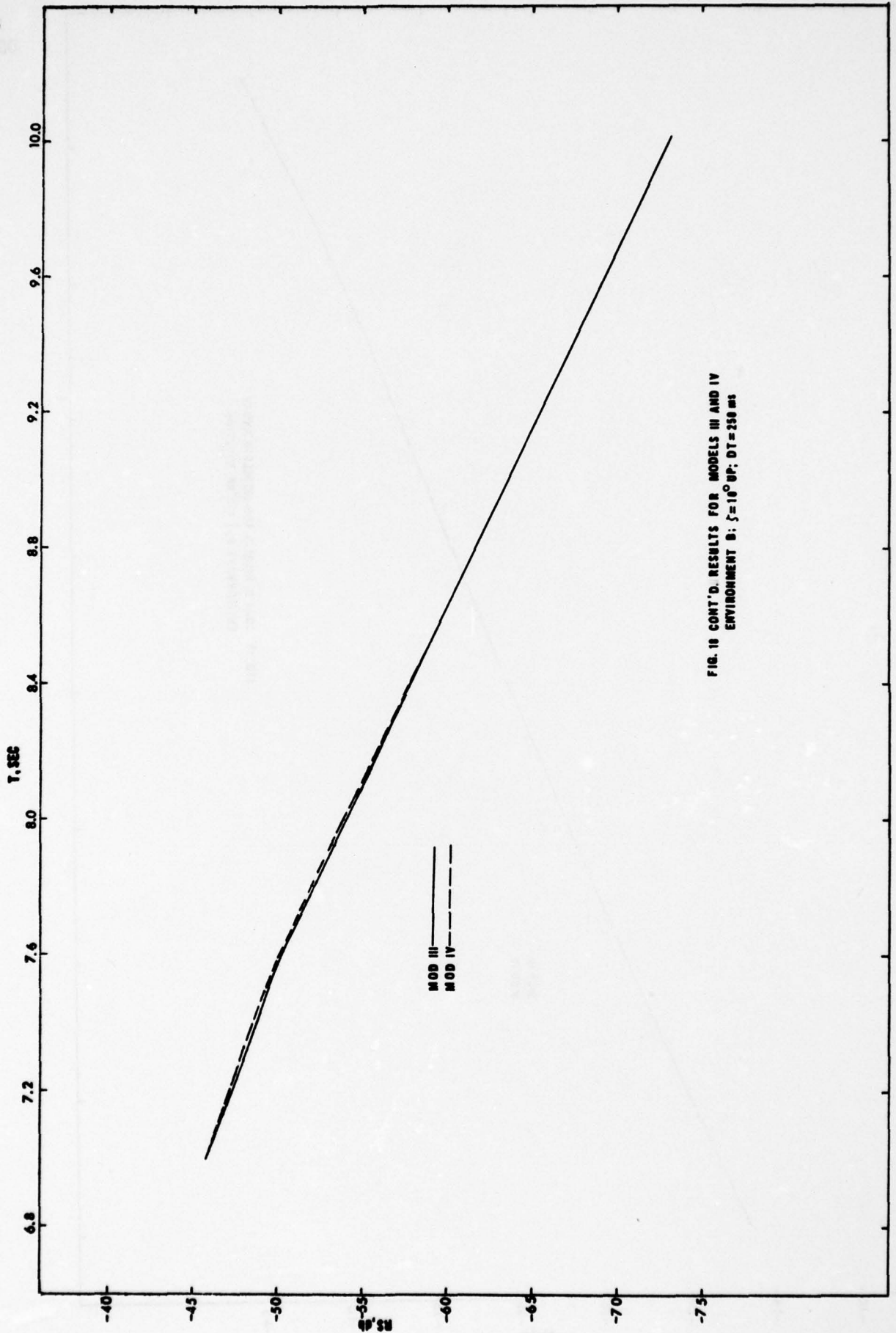


FIG. 18 CONT'D. RESULTS FOR MODELS III AND IV ENVIRONMENT B;  $\xi=10^{\circ}$  BP; DT=250 ms

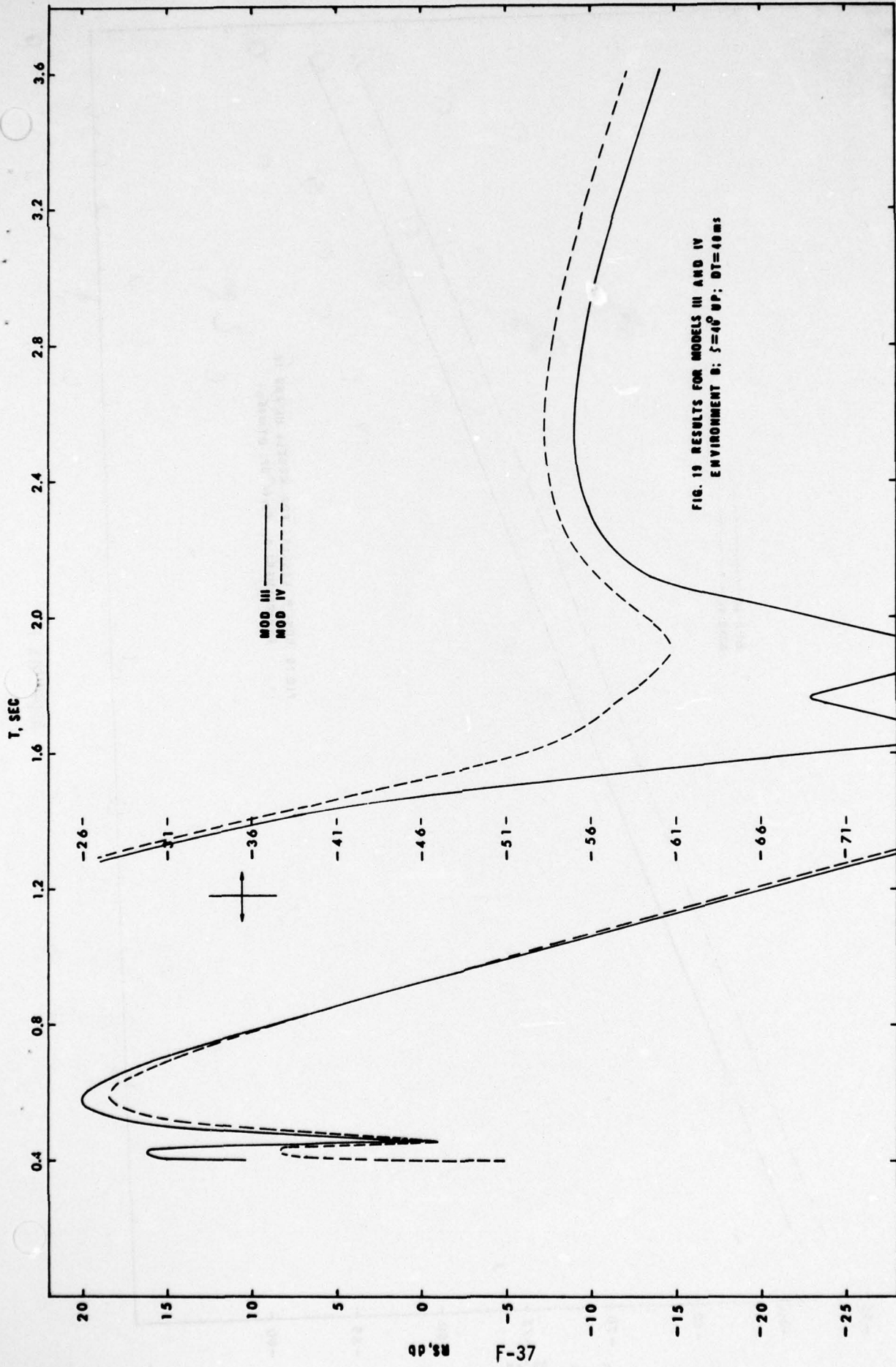


FIG. 19 RESULTS FOR MODELS III AND IV ENVIRONMENT B; S=40° UP; DT=40ms

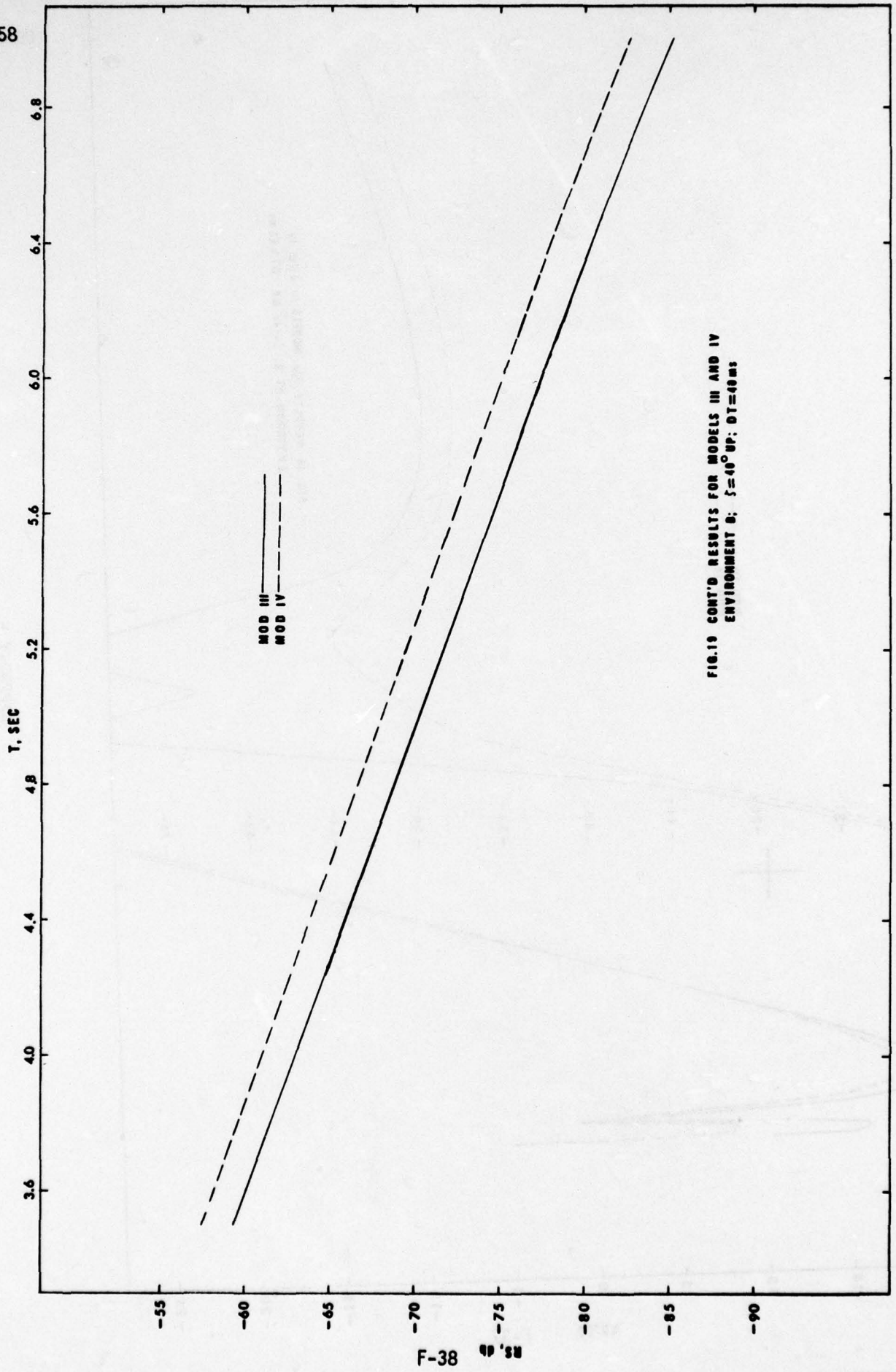


FIG. 19 CONT'D RESULTS FOR MODELS III AND IV  
ENVIRONMENT B;  $\xi=40^\circ$  UP;  $\Delta T=40$ ms

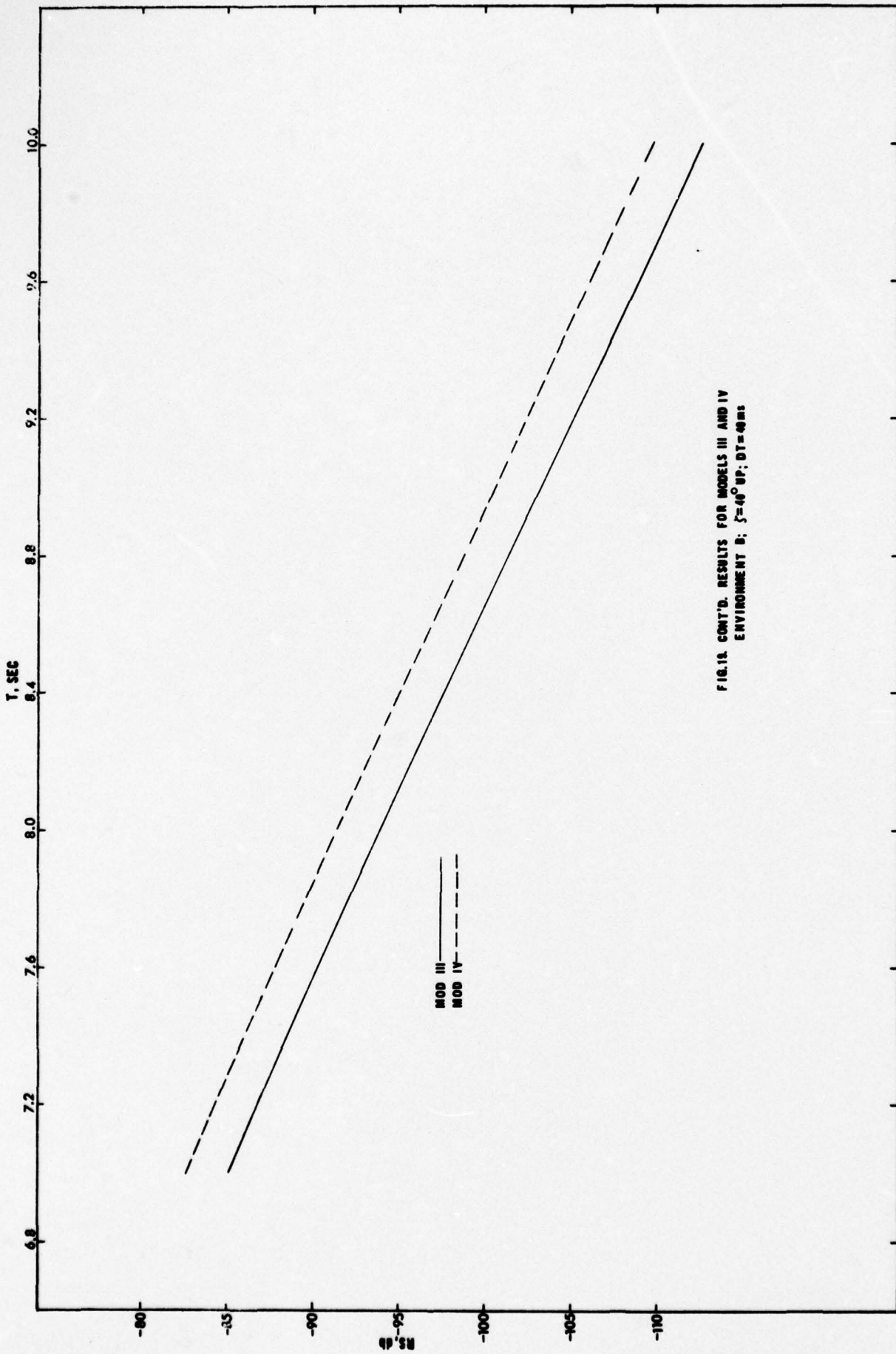


FIG. 1A. CONT'D. RESULTS FOR MODELS III AND IV  
ENVIRONMENT B;  $\zeta=40^\circ$  UP; DT=40ms

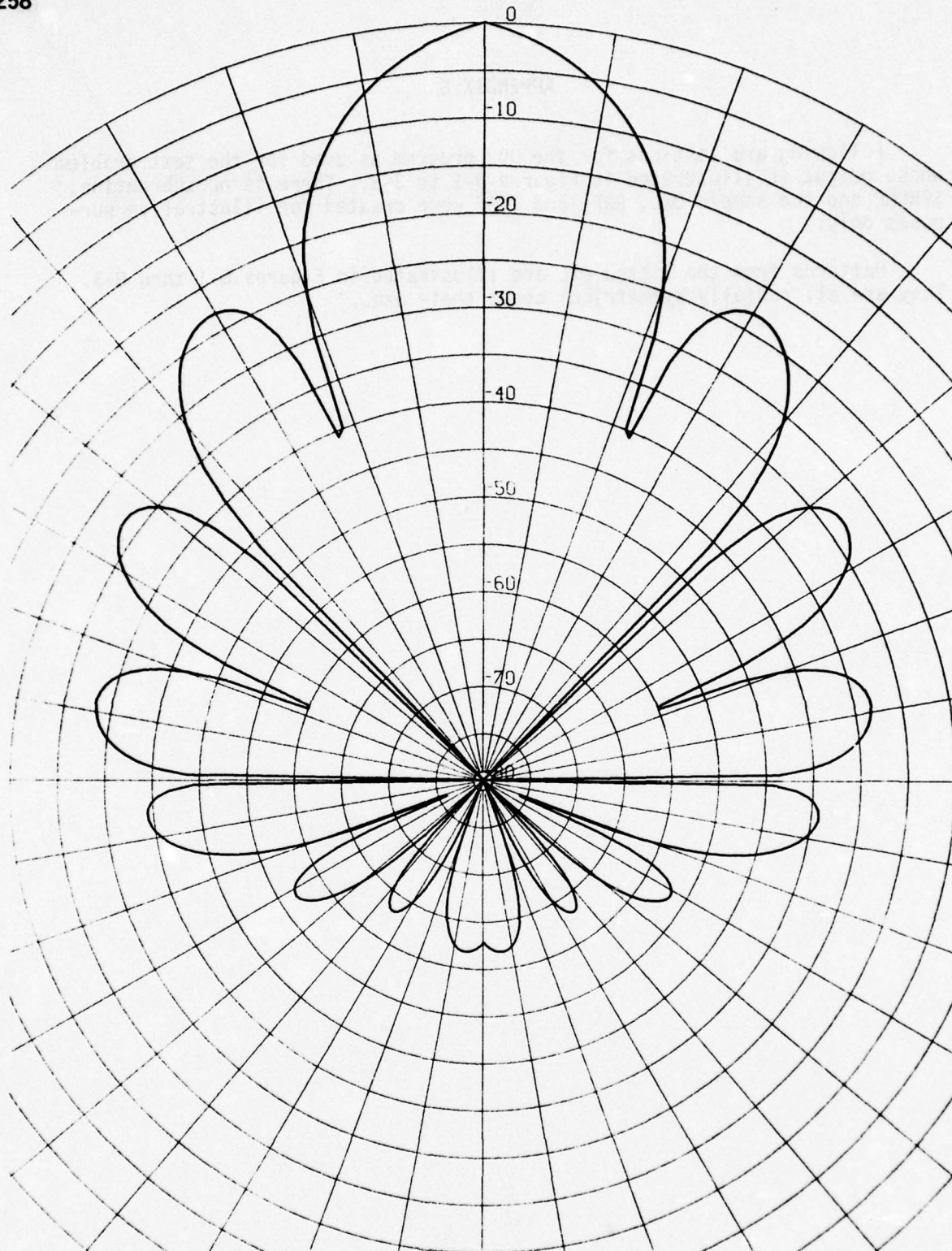
**APPENDIX G**

Following are listings for the DOP program as used for the test problem whose output is illustrated in Figures 3-1 to 3-3. There is no subroutine, SPRCMP and the sample OXL, RRF, and TVGF were created for illustrative purposes only.

Patterns from the listed OXL are illustrated in Figures G-1 thru G-3. They are all radially symmetrical about their axes.

OD 52258

HORIZONTAL, BROAD, STRAIGHT

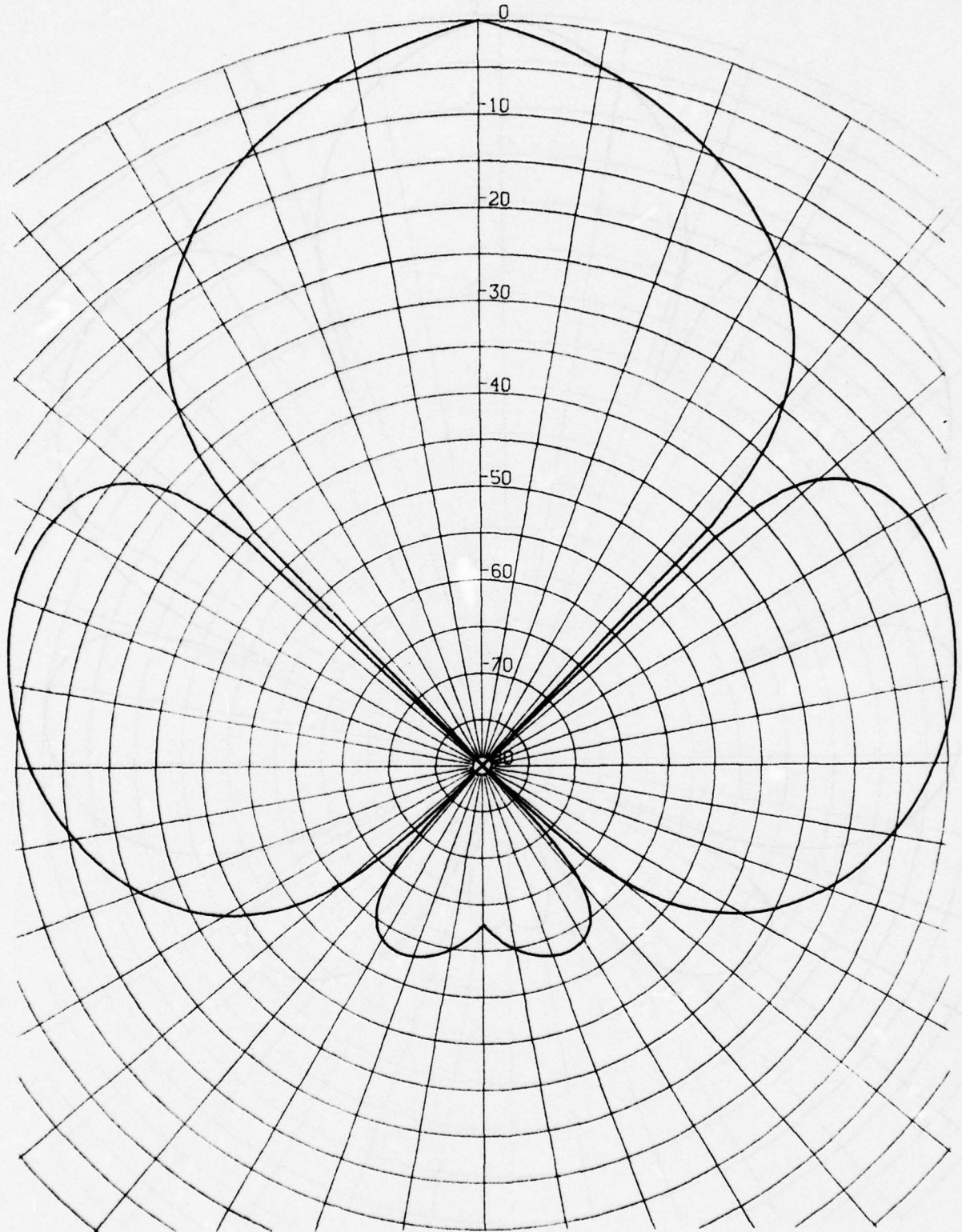


AXIAL COORDINATE PLANES

FIGURE G-2

APPENDIX G

G-2



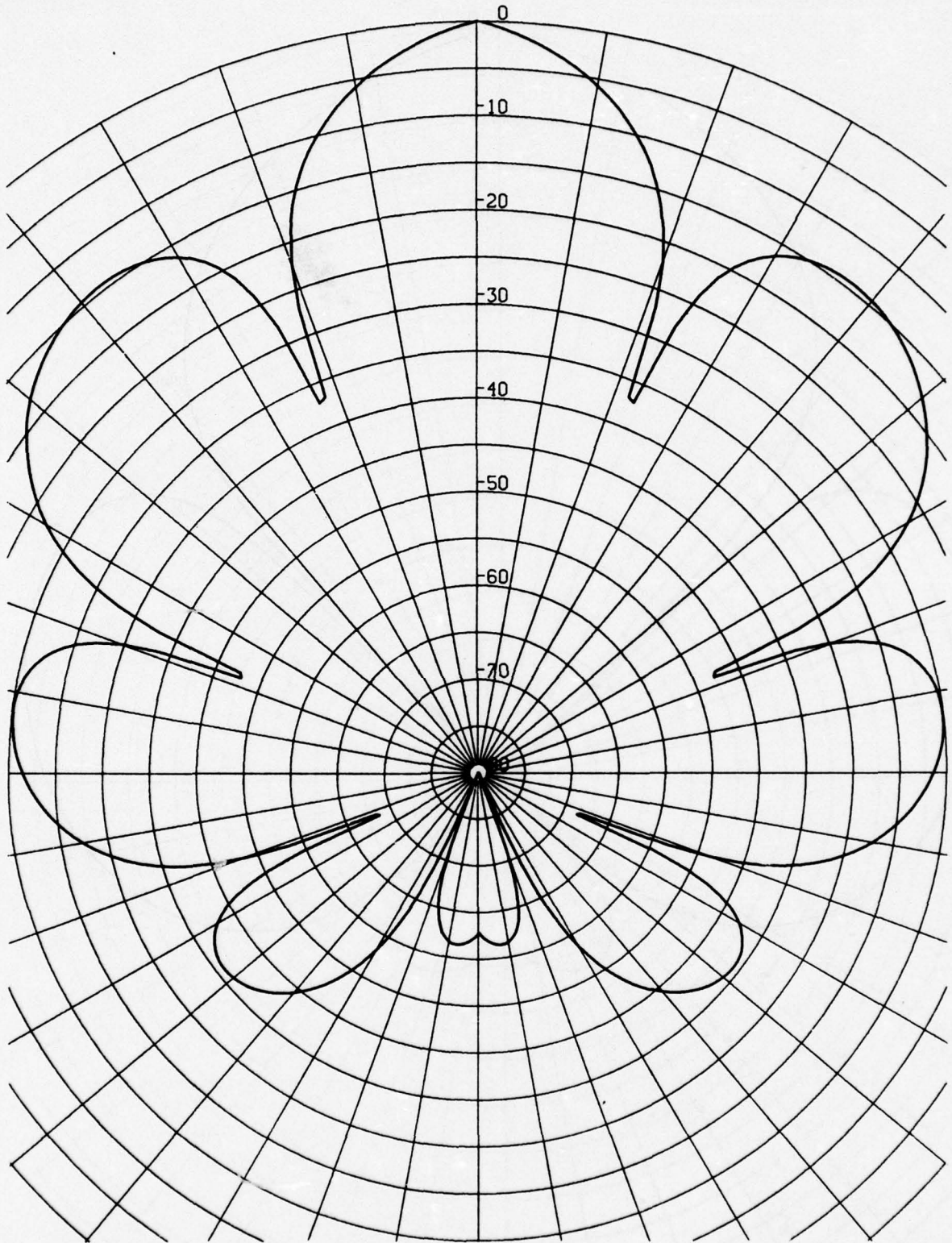
AXIAL COORDINATE PLANES

FIGURE G-2

APPENDIX G

G-3

HORIZONTAL RECEIVE



AXIAL COORDINATE PLANES

FIGURE G-1  
APPENDIX G  
G-4

PROCEDURES FOR DOP

```

1 DCOMM1 PROC
2 COMMON /CBAND/ LMBAND,LMBND1,NBAND,NBAND,MNBND,FNBAND,VPTRN
3 C 800 , 801
4 C
5 COMMON /CBAND/ BAND(801),RRFS(800),FGAN(800),BNDOUT(801)
6 C (LMBND1) ,(LMBAND) ,(LMBAND) ,(LMBND1)
7 C
8 COMMON /CCOUNT/ LARB,LMTRS,LKXS,LKXS2,NSURF,NBTH,KT,KTT
9 C 9612, 17 , 400, 800
10 C
11 COMMON /CFCNST/ TRS(6),FPT5,TRS2(4),F1,TRS3(4),F2,F4,F10,F20
12 C ( LMTRS )
13 C
14 COMMON /CFCNST/ FLOG10,INFNT,P123,PI,TWOPI,DEGRAD,SHIFT,VOKT,F1E3
15 COMMON /CFCNST/ LOG4PI,F1MIN,F3,F90,F180
16 COMMON /CFCNST/ MBAND(3),MUNIT(2),NSPRD(5),NSPRV(5),NFRON(2)
17 COMMON /CFCNST/ HEADS(4),HTOT1(4),HTOT2(3),HTOT3(3),HEB(9)
18 COMMON /CINDAT/ OMEGA,DELTA,CSKSI,SNKSI,KSID,DR,FCOVS,COKT
19 COMMON /CINDAT/ EXPS,FZSQ,FZ2,FCO3,BUINT,LOGRV1
20 C
21 COMMON /CINDEF/ NNAME,NARDAT(40,3),NARCNT(24)
22 COMMON /CINDEF/ CENTER,GO,END,FILTER,KTSBND,NOBTH,NOPRNT
23 COMMON /CINDEF/ NOSURF,NOTAPE,NOVOLN,PLOT,SPREAD,TIMCNP,TOTALS,TV6
24 COMMON /CINDEF/ RELBND
25 C
26 COMMON /CINPUT/ IDC,IDATE(2),IDV,DO
27 COMMON /CINPUT/ CO,ALPHC,PING,DRTH,LOGRV,S,KS1
28 COMMON /CINPUT/ VS,RWIDTH,DELTA2,FZRO,NBEAN,OMEGA0,THTRAX
29 COMMON /CINPUT/ PULSE,IPEVRY
30 COMMON /CINPUT/ TIME(400),SPRED(150,3)
31 C (LNTIM) (LNSPRD)
32 C
33 COMMON /CPRINT/ NTHIN,NTRAX,PAGE,NPAGE,NPSTR
34 COMMON /CSPRED/ NSPR1,NSPRH,NSPRH1
35 COMMON /CTAPE/ AR1,BR1,INPT,IPRT,IPLT
36 COMMON /CTBLKP/ DELIND,DELDEP,FACTOR,ITABLE
37 COMMON /CXCNST/ K0,K1,K2,K3,K5,K6,K8,K10,K40
38 DIMENSION
39 DIMENSION HOUTPT(14)
40 DIMENSION IDATA(1)
41 DIMENSION LFLAGS(16)
42 C
43 EQUIVALENCE (K0,FO,RECV),(K1,XMIT),(K3,LRNT)
44 EQUIVALENCE (NSURF,NBOUND)
45 EQUIVALENCE (IBLANK,HEADS(16)),(MUNIT,HOUTPT)
46 EQUIVALENCE (IFZRO,FZRO),(IDC,IDATA)
47 EQUIVALENCE (LNTIM,NARDAT(21,3)),(NTIME,NARCNT(21))
48 EQUIVALENCE (LNSPRD,NARDAT(22,3)),(LFLAGS,CENTER)
49 EQUIVALENCE (NSSPRD,NARCNT(22)),(NBSPRD,NARCNT(23))
50 EQUIVALENCE (NVSPRD,NARCNT(24))
51 C
52 REAL INFNT,KSID,KSID,LOGRV,LOG4PI,LOGRV1
53 INTEGER AR1,BR1,PAGE
54 LOGICAL CENTER,GO,END,FILTER,KTSBND,NOBTH,NOPRNT
55 LOGICAL NOSURF,NOTAPE,NOVOLN,PLOT,SPREAD,TIMCNP,TOTALS,TV6
56 LOGICAL RELBND,VPTRN,LFLAGS
57 END
58 DCOMM2 PROC
59 COMMON
60 C RVS(3,801),RVB(3,801),RVV(3,801),RVT(3,801)
61 DIMENSION ( LMNT,LMBND1 )
62 C REVERB(9612),RV(3,801,3)
63 C (LMRB),(LMNT,LMBND1,3)
64 EQUIVALENCE (REVERB(1),RVS(1,1),RV(1,1,1))
65 END
66 DCOMM3 PROC
67 COMMON
68 COMMON XMIN(400),TMIN(400)
69 C RRX(400),RBT(400),RBTM(400),RBH(400)
70 END ( LKXS = MAX. NO. OF RAYS SORTED BY "RAYSRT" )

```

APPENDIX G

I N D E X		PROCEDURES FOR DOP	PAGE 2
71	DCORN4	PROC	DCORRN71
72		COMMON	DCORRN72
73		C	DCORRN73
74		END	DCORRN74
75	DCORN5	PROC	DCORRN75
76		COMMON	DCORRN76
77		COMMON	DCORRN77
78		COMMON	DCORRN78
79		C	DCORRN79
80		C	DCORRN80
81		COMMON	DCORRN81
82		DIMENSION	DCORRN82
83		C	DCORRN83
84		C	DCORRN84
85		EQUIVALENCE	DCORRN85
86		EQUIVALENCE	DCORRN86
87		C	DCORRN87
88		C	DCORRN88
89		END	DCORRN89
90	DCORN6	PROC	DCORRN90
91		DATA	DCORRN91
92		DATA	DCORRN92
93		C	DCORRN93
94		C	DCORRN94
95		C	DCORRN95
96		C	DCORRN96
97		C	DCORRN97
98		END	DCORRN98

APPENDIX G

I N D E X

PROCEDURES FOR DOP

SYMBOL	-----	REFERENCES	-----
ALPHC	- 27CO		
AR1	- 35CO	53IN	
BAND	- 5CO		
BNDOUT	- 5CO		
BR1	- 35CO	53IN	
BNIDTH	- 28CO		
BNINT	- 19CO		
CD	- 27CO		
CCKT	- 18CO		
CBAND	- 2CL	5CL	
CCOUNT	- 8CL		
CENTER	- 22CO	48ER 54LG	
CFCNST	- 11CL	14CL 15CL	
CNCNST	- 16CL	17CL	
CINDAT	- 18CL	19CL	
CINDEF	- 21CL	22CL 23CL 24CL	
CINPUT	- 26CL	27CL 28CL 29CL 30CL	
COSORT	- 78CO		
COSTHA	- 77CO		
COSTHB	- 77CO		
CPRINT	- 33CL		
CSKSI	- 18CO		
CSPRED	- 34CL		
CTAPE	- 35CL		
CTBLKP	- 36CL		
CXCNST	- 37CL		
DO	- 26CO		
DBYTH	- 27CO		
DCORN1	- 1		
DCORN2	- 58		
DCORN3	- 66		
DCORN4	- 71		
DCORN5	- 75		
DCORN6	- 90		
DEGRAD	- 14CO		
DELDEP	- 36CO		
DELIND	- 36CO		
DELT	- 18CO		
DELT2	- 28CO		
DOP	- 76CO	85ER	
DR	- 18CO		
END	- 22CO	54LG	
EXPS	- 19CO		
F0	- 43ER		
F1	- 11CO		
F10	- 11CO		
F180	- 15CO		
F1E3	- 14CO		
F1MIN	- 15CO		
F2	- 11CO		
F20	- 11CO		
F3	- 15CO		
F4	- 11CO		
F90	- 15CO		
FACTOR	- 36CO		
F03	- 19CO		
F0VS	- 18CO		
FCSGAR	- 72CO		
FGAR	- 5CO		
FILTER	- 22CO	54LG	
FLOG10	- 14CO		
FNBAND	- 2CO		
FPT5	- 11CO		
FZ2	- 19CO		
FZRO	- 28CO	46ER	
FZSO	- 19CO		
G0	- 22CO	54LG	
WBAND	- 16CO		

APPENDIX G

I N D E X

PROCEDURES FOR DOP

HEADS	-	17CO	45EQ		
MED	-	17CO			
NFRDP	-	16CO			
NOUPTY	-	3901	45EQ		
NSPRD	-	1600			
NSPRM	-	1600			
NTOT1	-	1700			
NTOT2	-	1700			
NTOT3	-	1700			
NUNIT	-	1600	45EQ		
IBLANK	-	45EQ			
IDATA	-	4001	46EQ		
IDATE	-	26CO			
IDC	-	26CO	46EQ		
IDV	-	26CO			
IFZRO	-	46EQ			
INFNT	-	14CO	52RL		
INPT	-	35CO			
IPEVRY	-	29CO			
IPLT	-	35CO			
IPRT	-	35CO			
ITABLE	-	36CO			
K0	-	37CO	43EQ		
K1	-	37CO	43EQ		
K10	-	37CO			
K2	-	37CO			
K3	-	37CO	43EQ		
K40	-	37CO			
K5	-	37CO			
K6	-	37CO			
K8	-	37CO			
KS1	-	27CO	52RL		
KS10	-	18CO	52RL		
KT	-	8CO			
KTSBND	-	22CO	54LG		
KTT	-	8CO			
LFLAGS	-	4101	48EQ	56LG	
LMBAND	-	2CO	91DA		
LMBND1	-	2CO	91DA		
LNKS	-	8CO	91DA		
LNKS2	-	8CO	91DA		
LNNT	-	43EQ			
LNRD	-	8CO	92DA		
LNSPRD	-	48EQ	92DA		
LNTIN	-	47EQ	92DA		
LNTRS	-	8CO	92DA		
LOG4PI	-	15CO	52RL		
LOGHV	-	27CO	52RL		
LOGHVI	-	19CO	52RL		
MBAND	-	2CO			
MNDND	-	2CO			
NAMCNT	-	21CO	47EQ	49EQ	50EQ
NAMDAT	-	21CO	47EQ	48EQ	
NBAND	-	2CO			
NBEAR	-	28CO			
NBOUND	-	3801	44EQ		
NBSPRD	-	49EQ			
NBYN	-	8CO			
NNAMES	-	21CO			
NOBTTH	-	22CO	54LG		
NOBRNT	-	22CO	54LG		
NOSURF	-	23CO	55LG		
NOTAPE	-	23CO	55LG		
NOVOLN	-	23CO	55LG		
NPAGE	-	33CO			
NPSTRY	-	33CO			
NSPR1	-	34CO			
NSPRH	-	34CO			
NSPRH1	-	34CO			
NSSPRD	-	49EQ			

I N D E X

PROCEDURES FOR DOP

NSURF	-	8C0	44E0
NTIME	-	47E0	
NTMAX	-	33C0	
NTMIN	-	33C0	
NVSPRD	-	50E0	
OMEGA	-	18C0	
OMEGAD	-	28C0	
OMT	-	78C0	
PAGE	-	33C0	531H
PI	-	14C0	
PI23	-	14C0	
PING	-	27C0	
PLOT	-	23C0	55L6
PULSE	-	29C0	
R	-	76C0	86E0
RBN	-	68C0	
RBNA	-	81C0	
RBND	-	82D1	86E0
RBT	-	68C0	
RDTA	-	81C0	
RDTD	-	82D1	86E0
RDTH	-	68C0	
RDTHA	-	81C0	
RDTWD	-	82D1	86E0
RDX	-	68C0	
RDXA	-	81C0	
RDXD	-	82D1	85E0
RECV	-	43E0	
RELDND	-	24C0	56L6
REVERD	-	61D1	64E0
RRFS	-	5C0	
RV	-	61D1	64E0
RVD	-	59C0	
RVS	-	59C0	64E0
RVT	-	59C0	
RVV	-	59C0	
S	-	27C0	
SHIFT	-	14C0	
SINOMY	-	78C0	
SNKSI	-	18C0	
SPREAD	-	23C0	55L6
SPRED	-	30C0	
T	-	76C0	86E0
TNA	-	76C0	
TND	-	76C0	86E0
TNTMAX	-	28C0	
TINCMP	-	23C0	55L6
TIRE	-	30C0	
TMIN	-	67C0	
TOTALS	-	23C0	55L6
TRS	-	11C0	
TRS2	-	11C0	
TRS3	-	11C0	
TVG	-	23C0	55L6
TMOPI	-	14C0	
VPTTRN	-	2C0	56L6
VS	-	28C0	
X	-	76C0	
XMIN	-	67C0	
XMIT	-	43E0	
YDRT	-	14C0	

APPENDIX G

I N D E X	PROGRAM DOP	PAGE 6
1	INCLUDE DCOM1	DOP 1
2	INCLUDE DCOM2	DOP 2
3	Z	DOP 3
4	C READ AND PROCESS INPUT, CARDS AND TAPE.	DOP 4
5	C	DOP 5
6	9000 CALL IDENT	DOP 6
7	IF (END) GO TO 20000	DOP 7
8	C	DOP 8
9	C SET UP BAND LIMITS.	DOP 9
10	C	DOP 10
11	CALL BCOMP	DOP 11
12	C	DOP 12
13	C EXTRACT SURFACE AND/OR BOTTOM DATA FROM INPUT TAPE, AND	DOP 13
14	C ARRANGE PROPERLY FOR DOP. WRITE ON TEMPORARY FILE.	DOP 14
15	C	DOP 15
16	CALL RBSORT	DOP 16
17	C	DOP 17
18	C PROCESS TABLE OF REVERBERATION TIMES AS NECESSARY.	DOP 18
19	C	DOP 19
20	CALL TCOMP	DOP 20
21	C	DOP 21
22	NTRAX = 0	DOP 22
23	C	DOP 23
24	C COMPUTE REVERBERATION FOR EACH TIME IN TABLE.	DOP 24
25	C	DOP 25
26	10000 NTRIN = NTRAX + K1	DOP 26
27	NTRAX = KINCL * NTRAX + LMNT, NTIME)	DOP 27
28	IF (SPREAD) NTRAX = NTRIN	DOP 28
29	C	DOP 29
30	C ZERO OUT REVERBERATION TABLE.	DOP 30
31	C	DOP 31
32	DO 10010 KT = 1, LRRB	DOP 32
33	REVERB(KT) = 0.	DOP 33
34	10010 CONTINUE	DOP 34
35	C	DOP 35
36	C COMPUTE A PAGE FULL--THREE TIMES OR ONE TIME WITH SPREADING.	DOP 36
37	C	DOP 37
38	DO 15000 KT = NTRIN, NTRAX	DOP 38
39	KTT = KT + K1 - NTRIN	DOP 39
40	C	DOP 40
41	C COMPUTE BOUNDARY AND VOLUME REVERB. AND SPREAD AS REQUIRED.	DOP 41
42	C COMPUTE TOTALS.	DOP 42
43	C	DOP 43
44	IF (.NOT. NOTAPE) CALL RBCOMP	DOP 44
45	IF (.NOT. NOVOLR) CALL RVCOMP	DOP 45
46	IF (SPREAD) CALL RVSPRD	DOP 46
47	CALL RTCOMP	DOP 47
48	15000 CONTINUE	DOP 48
49	C	DOP 49
50	C PRINT REVERBERATION DATA.	DOP 50
51	CALL RVPRNT	DOP 51
52	C	DOP 52
53	C	DOP 53
54	IF (NTRAX .LT. NTIME) GO TO 10000	DOP 54
55	GO TO 9000	DOP 55
56	C	DOP 56
57	C REWIND TAPES AS REQUIRED, AND EXIT.	DOP 57
58	C	DOP 58
59	20000 IF (NOTAPE) GO TO 20010	DOP 59
60	REWIND AR1	DOP 60
61	REWIND BR1	DOP 61
62	20010 IF (PLOT) REWIND IPLT	DOP 62
63	30000 STOP	DOP 63
64	END	DOP 64

I N D E X		PROGRAM DOP				
SYMBOL		REFERENCES				
9000	- 6*	55				
10000	- 26*	54				
10010	- 32	34*				
15000	- 38	48*				
20000	- 7	59*				
20010	- 59	62*				
30000	- 63*					
AR1	- 60					
BCOMP	- 11					
BR1	- 61					
DCOMN1	- 1					
DCOMN2	- 2					
END	- 7					
IDENT	- 6					
IPLT	- 62					
K1	- 26	39				
KT	- 32=	33	36=	39		
KTT	- 39=					
LMNT	- 27					
LMBB	- 32					
MIND	- 27					
NOTAPE	- 44	59				
NOVOLM	- 45					
NTIRE	- 27	54				
NTHAI	- 22=	26	27=	28=	38	54
NTHIN	- 26=	28	38	39		
PLOT	- 62					
RBCOMP	- 44					
RBSORT	- 16					
REVERB	- 33=					
RTCOMP	- 47					
RVCOMP	- 45					
RVPRT	- 51					
RVSPRD	- 46					
SPREAD	- 28	46				
STOP	- 63					
TCOMP	- 20					
TRAIN	- 0					

APPENDIX G

I N D E X	PAGE	8
1	SUBROUTINE IDENT	IDENT 1
2		IDENT 2
3	C	IDENT 3
4	INCLUDE DCONN1	IDENT 4
5	COMMON ID(12),I,J,K,L,M	IDENT 5
6	LOGICAL OUTFLG	IDENT 6
7	DATA INPFLG/O,OUTFLG/.TRUE./	IDENT 7
8	C	IDENT 8
9	WRITE HEADING ON INPUT DATA PAGE.	IDENT 9
10	C	IDENT 10
11	WRITE (IPRT,501) MED	IDENT 11
12	501 FORMAT (8A6,A4,16H-- INPUT DATA --/)	IDENT 12
13	C	IDENT 13
14	READ NEXT VARIABLE NAME AND RELATED DATA FROM DATA CARD(S).	IDENT 14
15	C	IDENT 15
16	600 CALL INPUT(NNAMES,IDC,INPFLG,OUTFLG)	IDENT 16
17	IF (GO) GO TO 700	IDENT 17
18	IF (END) GO TO 900	IDENT 18
19	IF (INPFLG .GT. 1) END = .TRUE.	IDENT 19
20	GO TO 600	IDENT 20
21	700 GO = .FALSE.	IDENT 21
22	IF (NOTAPE) GO TO 2000	IDENT 22
23	C	IDENT 23
24	READ FIRST HEADER RECORD FROM INPUT TAPE.	IDENT 24
25	C	IDENT 25
26	READ (AR1) (ID(I), I = 1, 6)	IDENT 26
27	IF (ID(6) .NE. 0) GO TO 1000	IDENT 27
28	C	IDENT 28
29	END = .TRUE.	IDENT 29
30	900 WRITE (IPRT,901)	IDENT 30
31	901 FORMAT (69X,18H*** END OF RUN ***)	IDENT 31
32	GO TO 30000	IDENT 32
33	C	IDENT 33
34	READ SECOND HEADER RECORD, PRESERVE ANY DATA FROM INPUT	IDENT 34
35	TAPE WHICH HAS NOT BEEN READ IN FROM CARDS.	IDENT 35
36	C	IDENT 36
37	1000 READ (AR1) (ID(I), I = 6, 12)	IDENT 37
38	DO 1500 I = 1, 12	IDENT 38
39	J = I	IDENT 39
40	IF (J .GT. K2) J = J - K1	IDENT 40
41	IF (NAMCNT(J) .EQ. 0) GO TO 1200	IDENT 41
42	IF (J .NE. 11) GO TO 1500	IDENT 42
43	KSI = KSI * DEGRAD	IDENT 43
44	GO TO 1500	IDENT 44
45	1200 IDATA(I) = ID(I)	IDENT 45
46	1500 CONTINUE	IDENT 46
47	C	IDENT 47
48	SCALE INPUT DATA AND PRECOMPUTE RELATED QUANTITIES.	IDENT 48
49	C	IDENT 49
50	2000 OMEGA = OMEGAD * DEGRAD	IDENT 50
51	DELT = DELT2/F2	IDENT 51
52	KSID = KSI/DEGRAD	IDENT 52
53	BWINT = BWIDTH	IDENT 53
54	IF (.NOT. KTSBND) BWINT = BWINT/F1E3	IDENT 54
55	LOGMYI = LOENH - LOG4PI	IDENT 55
56	CSKSI = COS(KSI)	IDENT 56
57	SKSI = SIN(KSI)	IDENT 57
58	BR = DELT2 * CD/F4	IDENT 58
59	COKT = CO * YDKT	IDENT 59
60	FCOVS = COKT/VS	IDENT 60
61	FCOS = CO**3 * TWOPI	IDENT 61
62	IF (FZRO .LE. 0.) FZRO = F1	IDENT 62
63	FZSQ = FZRO**2	IDENT 63
64	FZ2 = FZRO * F2	IDENT 64
65	EXPS = EXP(S/F10 + FLOG10)	IDENT 65
66	IF (THTMAX .EQ. 0.) THTMAX = F90	IDENT 66
67	IF (THTMAX .GT. F180) THTMAX = F180	IDENT 67
68	C	IDENT 68
69	NSPRN1 = K1	IDENT 69
70	SPREAD = SPREAD .OR. (NNSPRD.NE.0) .OR. (NBSPRD.NE.0) .OR. 1 (NVSPRD.NE.0)	IDENT 70

## APPENDIX G

INDEX	SUBROUTINE IDENT	PAGE
71	IF (.NOT. SPREAD) GO TO 5010	IDENT 71
72	C	IDENT 72
73	C GENERATE ANY REQUIRED MISSING SPREADING TABLES.	IDENT 73
74	C	IDENT 74
75	IF ((NSSPRD .EQ. 0) .OR. (NBSPRD .EQ. 0) .OR. (NVSPRD .EQ. 0))	IDENT 75
76	1 CALL SPRCMP	IDENT 76
77	NSPRM1 = MAX0(NSSPRD, NBSPRD, NVSPRD)	IDENT 77
78	C	IDENT 78
79	5010 NSPRM = NSPRM1 - K1	IDENT 79
80	NSPR1 = NSPRM + NSPRM1	IDENT 80
81	IF (NOPRNT) GO TO 7010	IDENT 81
82	C	IDENT 82
83	C SET UP APPROPRIATE PAGE HEADINGS.	IDENT 83
84	C	IDENT 84
85	K = 0	IDENT 85
86	J = K5	IDENT 86
87	IF (.NOT. SPREAD) GO TO 6020	IDENT 87
88	J = 0	IDENT 88
89	IF (TV6) K = K10	IDENT 89
90	IF (FILTER) K = K + K5	IDENT 90
91	6020 M = K1	IDENT 91
92	L = K1	IDENT 92
93	IF (KTSND) L = 0	IDENT 93
94	IF (.NOT. TOTALS) GO TO 6030	IDENT 94
95	NTOT3(1) = HEADS(L+36)	IDENT 95
96	L = K3	IDENT 96
97	M = K3	IDENT 97
98	C	IDENT 98
99	6030 L = L + K5	IDENT 99
100	DO 6040 I = K1, K5	IDENT 100
101	L = L + K1	IDENT 101
102	NBAND(I) = HEADS(L)	IDENT 102
103	J = J + K1	IDENT 103
104	HSPRD(I) = HEADS(J+10)	IDENT 104
105	K = K + K1	IDENT 105
106	NSPRM(I) = HEADS(K+15)	IDENT 106
107	6040 CONTINUE	IDENT 107
108	NFROM(1) = HEADS(M+37)	IDENT 108
109	NFROM(2) = HEADS(R+38)	IDENT 109
110	7010 IF (.NOT. NOTAPE) REWIND BR1	IDENT 110
111	30000 RETURN	IDENT 111
112	END	IDENT 112

## APPENDIX G

I N D E X		SUBROUTINE IDENT									
SYMBOL	=====	=====	=====	=====	=====	=====	=====	=====	=====	=====	=====
		REFERENCES									
501	-	10MR	11*								
600	-	15*	19								
700	-	16	20*								
900	-	17	29*								
901	-	29WR	30*								
1000	-	26	36*								
1200	-	40	44*								
1500	-	37	41	43		45*					
2000	-	21	49*								
5010	-	71	79*								
6020	-	87	91*								
6030	-	94	99*								
6040	-	100	107*								
7010	-	81	110*								
30000	-	31	111*								
AR1	-	25RD	36RD								
BR1	-	110									
BWIDTH	-	52									
BWINT	-	52=	53=								
CO	-	57	58	60							
COKT	-	58=	59								
COS	-	55									
CSKS1	-	55=									
DCORN1	-	3									
DEGRAD	-	42	49	51							
DELT	-	50=									
DELT2	-	50	57								
DR	-	57=									
END	-	17	18=	28=							
EXP	-	64									
EXPS	-	64=									
F1	-	61									
F10	-	64									
F180	-	66									
F1E3	-	53									
F2	-	50	63								
F4	-	57									
F90	-	65									
FC03	-	60=									
FC0VS	-	59=									
FILTER	-	90									
FLOG10	-	64									
FZ2	-	63=									
FZRO	-	61=	62	63							
FZSQ	-	62=									
G0	-	16	20=								
HBAND	-	102=									
HEADS	-	95	102	104	106	108	109				
HED	-	10MR									
HFROM	-	108=	109=								
HSPRD	-	104=									
HSPRW	-	106=									
HTOT3	-	95=									
I	-	4C0	25RD	36RD	37=	38	44	100=	102	104	106
ID	-	4C0	25RD	26	36RD	44					
IDATA	-	44=									
IDC	-	15AG									
IDENT	-	1									
INPFLG	-	6DA	15AG	18							
INPUT	-	15									
IPRT	-	10MR	29WR								
J	-	4C0	38=	39=	40	41	86=	88=	103=	104	
K	-	4C0	85=	89=	90=	105=	106				
K1	-	39	68	79	91	92	100	101	103	105	
K10	-	89									
K2	-	39									
K3	-	96	97								
K5	-	86	90	99	100						

APPENDIX G

I N D E X

SUBROUTINE IDENT

KSI	-	42=	31	55	56				
KSID	-	51=							
KTSBND	-	53	93						
L	-	400	92=	93=	95	96=	99=	101=	102
LOG4PI	-	54							
LOGNV	-	54							
LOGNVI	-	54=							
N	-	400	91=	97=	108	109			
NAXO	-	77							
NARCNT	-	40							
NDSPRD	-	69	75	77					
NNARES	-	15A6							
NOPRMT	-	81							
NOTAPE	-	21	110						
NSPR1	-	80=							
NSPRN	-	79=	80						
NSPRN1	-	68=	77=	79	80				
NSSPRD	-	69	75	77					
NVSPRD	-	70	75	77					
OMEGA	-	49=							
OMEGAD	-	49							
OUTFLG	-	5L6	69A	15A6					
RETURN	-	111							
S	-	64							
SIN	-	56							
SNKSI	-	56=							
SPRCMP	-	76							
SPREAD	-	69=	71	87					
TNTRAX	-	65=	66=						
TOTALS	-	94							
TVE	-	89							
TUOPI	-	60							
VS	-	59							
YDKT	-	58							



I N D E X

```

1      SUBROUTINE BCOMP                                BCOMP 1
2      C                                              BCOMP 2
3      INCLUDE DCOMH1                                BCOMP 3
4      COMMON B,DND(3),CNT(3),O,E,F,I,L,Q,          BCOMP 4
5      C                                              BCOMP 5
6      DND(3) = COS(THYMAX * DEGRAD) * VS          BCOMP 6
7      IF (THYMAX .EQ. F90) DND(3) = 0.           BCOMP 7
8      IF (THYMAX .EQ. F180) DND(3) = -VS         BCOMP 8
9      IF (KTSBND) GO TO 1000                       BCOMP 9
10     C                                              BCOMP 10
11     C      OUTPUT BAND LIMITS IN KILOHERZ.        BCOMP 11
12     C                                              BCOMP 12
13     O = (COKT + VS)/(COKT - VS)                  BCOMP 13
14     DND(1) = FZRO * O - FZRO                     BCOMP 14
15     D = FZRO                                       BCOMP 15
16     DND(2) = FZRO - FZRO/O                       BCOMP 16
17     D = FZRO                                       BCOMP 17
18     DND(3) = (COKT + DND(3))/(COKT - DND(3)) * FZRO - FZRO
19     GO TO 2000                                     BCOMP 18
20     C                                              BCOMP 19
21     C      OUTPUT BAND LIMITS IN KNOTS OF DOPPLER.
22     C                                              BCOMP 20
23     1000 DND(1) = VS                               BCOMP 21
24     D = 0.                                         BCOMP 22
25     DND(2) = VS                                   BCOMP 23
26     D = VS                                         BCOMP 24
27     C                                              BCOMP 25
28     2000 E = 0.                                    BCOMP 26
29     IF (CENTER) E = BWINT * FPT5                  BCOMP 27
30     D = D + E                                      BCOMP 28
31     IF (.NOT. RELBND) D = 0.                      BCOMP 29
32     C                                              BCOMP 30
33     C      COMPUTE NO. OF BANDS WITH POSITIVE AND NEGATIVE DOPPLER,
34     C      ALSO BAND LIMIT DUE TO THETA MAX.      BCOMP 31
35     C                                              BCOMP 32
36     DO 2500 I = 1, 3                               BCOMP 33
37     CNT(I) = ABS(AINT(DND(I)/BWINT))              BCOMP 34
38     IF (CNT(I) * BWINT + E .LT. ABS(DND(I))) CNT(I) = CNT(I) + F1
39     IF (CENTER) CNT(I) = CNT(I) + FPT5            BCOMP 35
40     2500 CONTINUE                                  BCOMP 36
41     CNT(3) = SIGN(CNT(3),DND(3))                  BCOMP 37
42     IF (DND(3) .GT. 0.) CNT(3) = CNT(3) - F1     BCOMP 38
43     C                                              BCOMP 39
44     C      NBAND = THEORETICAL NUMBER OF UNSPREAD BANDS.
45     C      NBAND - NSPRN = NO. OF UNSPREAD BANDS TO BE COMPUTED.
46     C      RNBAND = NO. OF BANDS TO BE OUTPUT, INCLUDING SPREADING.
47     C      NPSTRT = FIRST BAND TO BE PRINTED.    BCOMP 40
48     C                                              BCOMP 41
49     FNBAND = CNT(1) + CNT(2)                       BCOMP 42
50     RNBAND = FNBAND                               BCOMP 43
51     NBAND = MIN(LNBAND,RNBAND + NSPRN,IFIX(CNT(1) - CNT(3)) + NSPRN)
52     RNBAND = MIN(LNBAND, NBAND + NSPRN)           BCOMP 44
53     L = IFIX(CNT(1)) + NSPRN                      BCOMP 45
54     F = L                                          BCOMP 46
55     IF (.NOT. CENTER) L = L - K1                  BCOMP 47
56     NPSTRT = MOD(L, IPEVRY) + K1                  BCOMP 48
57     C                                              BCOMP 49
58     C      COMPUTE VALUES OF BAND LIMITS FOR COMPUTATION AND OUTPUT.
59     C                                              BCOMP 50
60     L = RNBAND + K1                                BCOMP 51
61     DO 3000 I = 1, L                               BCOMP 52
62     BAND(I) = BWINT * F + D                       BCOMP 53
63     BNDOUT(I) = BAND(I) - D                       BCOMP 54
64     IF (KTSBND) BAND(I) = FZRO + (COKT + BAND(I))/
65     1      (COKT - BAND(I))                       BCOMP 55
66     IF (FILTER) RRF(I-1) = RRF((BAND(I-1)+BAND(I))/FPT5)
67     F = F - F1                                     BCOMP 56
68     3000 CONTINUE                                  BCOMP 57
69     C                                              BCOMP 58
70     C      RESET FLAG FOR VOLUME REVERB. PATTERN COMP. (NON-TURNING).
    C                                              BCOMP 59
    C                                              BCOMP 60
    C                                              BCOMP 61
    C                                              BCOMP 62
    C                                              BCOMP 63
    C                                              BCOMP 64
    C                                              BCOMP 65
    C                                              BCOMP 66
    C                                              BCOMP 67
    C                                              BCOMP 68
    C                                              BCOMP 69
    C                                              BCOMP 70

```

I N D E X

SUBROUTINE BCOMP

PAGE 13

```

71 C
72   VPTRN = .FALSE.
73 C
74   RETURN
75   END

```

```

BCOMP 71
BCOMP 72
BCOMP 73
BCOMP 74
BCOMP 75

```

SYMBOL	REFERENCES										
1000	-	9	23*								
2000	-	19	28*								
2500	-	36	40*								
3000	-	61	68*								
ABS	-	37	38								
AINT	-	37									
B	-	4C0	15=	24=	30=	62					
BAND	-	62=	63	64=	65	66					
BCOMP	-	1									
BND	-	4C0	6=	7=	8=	14=	16=	18=	23=	25=	37
BNDOUT	-	38	41	42							
BWINT	-	63=									
CDRT	-	29	37	38	62						
CENYR	-	13	18	64	65						
CNT	-	29	39	55							
COS	-	4C0	37=	38=	39=	41=	42=	49	51	53	
D	-	6									
DCOM1	-	4C0	17=	26=	31=	63					
DEGRAD	-	3									
E	-	6									
F	-	4C0	28=	29=	30	38					
F1	-	4C0	54=	62	67=						
F180	-	38	42	67							
F90	-	8									
FILTER	-	7									
FNDAND	-	66									
FPTS	-	49=	50								
FZRO	-	29	39	66							
I	-	14	15	16	17	18	64				
IFIX	-	4C0	36=	37	38	39	61=	62	63	64	65
IPEVRY	-	66									
K1	-	51	53								
KTSBND	-	56									
L	-	55	56	60							
LDBAND	-	9	64								
LDAND	-	4C0	53=	54	55=	56	60=	61			
NDAND	-	51	52								
NIND	-	50=	51								
NNBND	-	51	52								
NOD	-	52=	60								
NBAND	-	56									
NPSTRY	-	51=	52								
NSPRN	-	56=									
O	-	51	52	53							
RELBND	-	4C0	13=	14	16						
RETURN	-	31									
RRF	-	74									
RRFS	-	66									
SIGN	-	66=									
TNTHAX	-	41									
VPYTRN	-	6	7	8							
VS	-	72=	8	13	23	25	26				
	-	6									

I N D E X

PAGE 15

1		SUBROUTINE RBSORT	RBSORT 1
2	C		RBSORT 2
3		INCLUDE DCOMN1	RBSORT 3
4		INCLUDE DCOMN3	RBSORT 4
5		COMMON I,J,K,L,M,N,NA,NB,NC,ND,A,D,TEST,WRFLG	RBSORT 5
6		LOGICAL WRFLG	RBSORT 6
7	C		RBSORT 7
8		NSURF = 0	RBSORT 8
9		NBTM = 0	RBSORT 9
10		IF (NOTAPE) GO TO 16	RBSORT10
11	C		RBSORT11
12		TEST = DBTM + SHIFT	RBSORT12
13		L = 0	RBSORT13
14	C		RBSORT14
15	C	READ DEPTH ID. RECORD AND TEST FOR SURFACE.	RBSORT15
16	C		RBSORT16
17		1 WRFLG = .FALSE.	RBSORT17
18		READ (A1) I, D, N	RBSORT18
19		IF (I .EQ. 0) GO TO 15	RBSORT19
20		IF (D .NE. 0.) GO TO 2	RBSORT20
21		IF (NOSURF) GO TO 7	RBSORT21
22		NSURF = N	RBSORT22
23		GO TO 5	RBSORT23
24	C		RBSORT24
25	C	TEST FOR BOTTOM DEPTH.	RBSORT25
26	C		RBSORT26
27		2 IF (ABS(D - DBTM) .GT. TEST) GO TO 7	RBSORT27
28		IF (NDBTM) GO TO 7	RBSORT28
29		NBTM = N	RBSORT29
30	C		RBSORT30
31	C	READ DATA FOR NEXT PATH. SKIP PATHS NOT AT (DESIRED) SURFACE	RBSORT31
32	C	OR BOTTOM.	RBSORT32
33	C		RBSORT33
34		5 WRFLG = .TRUE.	RBSORT34
35		7 DO 14 I = 1, M	RBSORT35
36		READ (A1) J, (RBTH(K), RBX(K), RBH(K), RBT(K), K = 1, J)	RBSORT36
37		IF (.NOT. WRFLG) GO TO 14	RBSORT37
38		DO 9 K = 1, J	RBSORT38
39		RBH(K) = RBH(K) - S	RBSORT39
40		9 CONTINUE	RBSORT40
41	C		RBSORT41
42	C	PUT DATA IN ASCENDING ORDER OF X, IF NECESSARY.	RBSORT42
43	C		RBSORT43
44		IF (RBX(2) .GT. RBX(1)) GO TO 12	RBSORT44
45		NA = J/2	RBSORT45
46		NB = -LMKS	RBSORT46
47		DO 11 K = 1, 4	RBSORT47
48		NB = NB + LMKS	RBSORT48
49		NC = NB + J	RBSORT49
50		DO 10 M = 1, NA	RBSORT50
51		ND = NB + M	RBSORT51
52		A = RBX(ND)	RBSORT52
53		RBX(ND) = RBX(NC)	RBSORT53
54		RBX(NC) = A	RBSORT54
55		NC = NC - 1	RBSORT55
56		10 CONTINUE	RBSORT56
57		11 CONTINUE	RBSORT57
58	C		RBSORT58
59	C	SAVE MINIMUM X AND T FOR EACH PATH, IF TIMCMP OPTION.	RBSORT59
60	C		RBSORT60
61		IF (.NOT. TIMCMP) GO TO 13	RBSORT61
62		12 L = L + 1	RBSORT62
63		XMIN(L) = RBX(1)	RBSORT63
64		TMIN(L) = RBT(1)	RBSORT64
65	C		RBSORT65
66	C	WRITE DATA ON INTERMEDIATE TAPE.	RBSORT66
67	C		RBSORT67
68		13 WRITE (B1) J, (RBX(K), RBT(K), RBTH(K), RBH(K), K = 1, J)	RBSORT68
69		14 CONTINUE	RBSORT69
70		GO TO 1	RBSORT70

APPENDIX G

I N D E X

SUBROUTINE RBSORT

PAGE 16

71 C  
72 15 REMIND DR1  
73 16 RETURN  
74 END

RBSORT71  
RBSORT72  
RBSORT73  
RBSORT74

I N D E X

SUBROUTINE RBSORT

SYMBOL	REFERENCES
1	17= 70
2	20 27*
5	23 34*
7	21 27 28 35*
9	38 40*
10	50 56*
11	47 57*
12	44 62*
13	61 68*
14	35 37 69*
15	19 72*
16	10 73*
A	50 52= 54
ABS	27
AR1	18RD 36RD
BR1	68MR 72
B	50 18RD 20 27
DBTTM	12 27
DCORN1	3
DCORN3	4
I	50 18RD 19 35=
J	50 36RD 38 45 49 68MR
K	50 36RD 38= 39 47= 68MR
L	50 13= 62= 63 64
LMS	46 48
M	50 50= 51
N	50 18RD 22 29 35
NA	50 45= 50
ND	50 46= 48= 49 51
NBTR	9= 29=
NC	50 49= 53 54 55=
ND	50 51= 52 53
NOBTTM	28
NOSURF	21
NOTAPE	10
NSURF	8= 22=
RDN	36RD 39= 68MR
RBSORT	1
RBT	36RD 64 68MR
RBTM	36RD 68MR
RDX	36RD 44 52 53= 54= 63 68MR
RETURN	73
S	39
SHIFT	12
TEST	50 12= 27
TINCMP	61
TRIN	64=
URFLG	50 6LG 17= 34= 37
XMIN	63=

I N D E X	PAGE	18
1	SUBROUTINE TCOMP	TCORP 1
2		TCORP 2
3	C INCLUDE DCOM1	TCORP 3
4	INCLUDE DCOM3	TCORP 4
5	COMMON I,J,K,M,IBOUND,NMIN,NMAX,NTBL	TCORP 5
6	C	TCORP 6
7	IF (.NOT. TINCRP) GO TO 10	TCORP 7
8	C	TCORP 8
9	C TIME COMPUTATION IS DESIRED. NOTE THAT CONSTANT CHECKING IS	TCORP 9
10	C DONE TO ENSURE THAT ALL ADDED TIMES LIE BETWEEN 1/2 DELTA T	TCORP 10
11	C AND PING INTERVAL. NO SUCH CHECK IS MADE ON INPUT TIMES.	TCORP 11
12	C ALSO LENGTH OF THE TIME ARRAY IS CHECKED TO AVOID OVER-FILLING.	TCORP 12
13	C	TCORP 13
14	IF (NTIME .EQ. LMTIM) GO TO 10	TCORP 14
15	NTIME = NTIME + K1	TCORP 15
16	IF (NTIME .EQ. LMTIM) GO TO 9	TCORP 16
17	TIME(NTIME) = DELT	TCORP 17
18	NTIME = NTIME + K1	TCORP 18
19	IF (NTIME .EQ. LMTIM) GO TO 9	TCORP 19
20	IF (NOTAPE) GO TO 6	TCORP 20
21	C	TCORP 21
22	C COMPUTE TIMES ASSOCIATED WITH WAVE-FRONT ARRIVAL OVER EACH	TCORP 22
23	C COMBINATION OF TWO-WAY PATHS.	TCORP 23
24	C	TCORP 24
25	NMAX = 0	TCORP 25
26	DO 4 IBOUND = K1, K2	TCORP 26
27	IF (NBOUND(IBOUND) .EQ. 0) GO TO 4	TCORP 27
28	NMIN = NMAX + K1	TCORP 28
29	NMAX = NMAX + NBOUND(IBOUND)	TCORP 29
30	DO 3 I = NMIN, NMAX	TCORP 30
31	READ (BR1) NTBL, (RBX(K), RBT(K), RBTH(K), RBM(K), K = 1, NTBL)	TCORP 31
32	C	TCORP 32
33	DO 2 J = 1, NMAX	TCORP 33
34	TIME(NTIME) = (TMIN(J) + TABLKP(XMIN(J), RBX, RBT, 1, NTBL)) + FPT5	TCORP 34
35	IF (ITABLE .EQ. 0) GO TO 2	TCORP 35
36	IF (TIME(NTIME) .GE. PING) GO TO 2	TCORP 36
37	M = NTIME	TCORP 37
38	IF (TIME(NTIME) .LE. DELT) GO TO 1	TCORP 38
39	NTIME = NTIME + K1	TCORP 39
40	IF (NTIME .EQ. LMTIM) GO TO 9	TCORP 40
41	TIME(NTIME) = TIME(M) - DELT	TCORP 41
42	IF (TIME(NTIME) .GT. DELT) NTIME = NTIME + K1	TCORP 42
43	IF (NTIME .EQ. LMTIM) GO TO 9	TCORP 43
44	1 TIME(NTIME) = TIME(M) + DELT	TCORP 44
45	IF (TIME(NTIME) .LT. PING) NTIME = NTIME + K1	TCORP 45
46	IF (NTIME .EQ. LMTIM) GO TO 9	TCORP 46
47	2 CONTINUE	TCORP 47
48	3 CONTINUE	TCORP 48
49	4 CONTINUE	TCORP 49
50	REWIND BR1	TCORP 50
51	C	TCORP 51
52	C ADD PRESET TABLE OF TIMES.	TCORP 52
53	C	TCORP 53
54	6 DO 7 I = K1, LNTRS	TCORP 54
55	IF (TRS(I) .GE. PING) GO TO 9	TCORP 55
56	TIME(NTIME) = TRS(I)	TCORP 56
57	IF (TIME(NTIME) .GT. DELT) NTIME = NTIME + K1	TCORP 57
58	IF (NTIME .EQ. LMTIM) GO TO 9	TCORP 58
59	7 CONTINUE	TCORP 59
60	C	TCORP 60
61	C CONTINUE WITH EVERY 1/2 SECOND TO PING. ADD PING INTERVAL.	TCORP 61
62	C	TCORP 62
63	8 TIME(NTIME) = TIME(NTIME-1) + FPT5	TCORP 63
64	IF (TIME(NTIME) .GE. PING) GO TO 9	TCORP 64
65	NTIME = NTIME + K1	TCORP 65
66	IF (NTIME .NE. LMTIM) GO TO 8	TCORP 66
67	C	TCORP 67
68	9 TIME(NTIME) = PING	TCORP 68
69	C	TCORP 69
70	C SORT TIME ARRAY INTO ASCENDING ORDER, ELIMINATING DUPLICATES.	TCORP 70

## APPENDIX G

I N D E X

SUBROUTINE TCOMP

PAGE 19

71	C		TCOMP 71
72		10 CALL SORT(TIME,NTIME)	TCOMP 72
73	C		TCOMP 73
74	C	INITIATE PAGE COUNTER AND COMPUTE TOTAL NUMBER OF PAGES OF	TCOMP 74
75	C	OUTPUT FOR THIS FILE OF INPUT DATA.	TCOMP 75
76	C		TCOMP 76
77		PAGE = 0	TCOMP 77
78		NMAX = (NTIME - K1)/K3 + K1	TCOMP 78
79		IF (SPREAD) NMAX = NTIME	TCOMP 79
80		NPAGE = ((NMBND - NPSTRT)/IPEVRY)/K40 + K1 + NMAX	TCOMP 80
81		IF (TOTALS) NPAGE = (NTIME - K1)/K40 + K1	TCOMP 81
82	C		TCOMP 82
83		RETURN	TCOMP 83
84		END	TCOMP 84

I N D E X		SUBROUTINE TCOMP										PAGE 20								
SYMBOL	=	=	=	=	=	=	=	=	=	=	=	REFERENCES	=	=	=	=	=	=	=	=
1	-	38	44*																	
2	-	33	35	36	47*															
3	-	30	48*																	
4	-	26	27	49*																
6	-	20	54*																	
7	-	54	59*																	
8	-	63*	66																	
9	-	16	19	40	43	46	55	58	64	68*										
10	-	7	14	72*																
BR1	-	31RD	50																	
DCOPN1	-	3																		
DCOPN3	-	4																		
DELT	-	17	38	41	42	44	57													
FPTS	-	34	63																	
I	-	50	30=	33	54=	55	56													
IBOUND	-	50	26=	27	29															
IPEVRY	-	80																		
ITABLE	-	35																		
J	-	50	33=	34																
K	-	50	31RD																	
K1	-	15	18	26	28	39	42	45	54	57	65									
		78	80	81																
K2	-	26																		
K3	-	78																		
K40	-	80	81																	
LMTIN	-	14	16	19	40	43	46	58	66											
LMTRS	-	54																		
M	-	50	37=	41	44															
MNBD	-	80																		
NBOUND	-	27	29																	
NMAX	-	50	25=	28	29=	30	33	78=	79=	80										
NMIN	-	50	28=	30																
NOTAPE	-	20																		
NPAGE	-	80=	81=																	
NPSTR	-	80																		
NTBL	-	50	31RD	34																
NTIRE	-	14	15=	16	17	18=	19	34	36	37	38									
		39=	40	41	42=	43	44	45=	46	56	57=									
		56	63	64	65=	66	68	72AG	78	79	81									
PAGE	-	77=																		
PING	-	36	45	55	64	68														
RPN	-	31RD																		
RET	-	31RD	34																	
RBTH	-	31RD																		
RBX	-	31RD	34																	
RETURN	-	83																		
SORT	-	72																		
SPREAD	-	79																		
TABLK	-	34																		
TCOMP	-	1																		
TIMCRP	-	7																		
TIRE	-	17=	34=	36	38	41=	42	44=	45	56=	57									
		63=	64	68=	72AG															
TWIN	-	34																		
TOTALS	-	81																		
TRS	-	55	56																	
XMIN	-	34																		

APPENDIX G

1		SUBROUTINE RBCOMP	RBCOMP 1
2	C		RBCOMP 2
3		INCLUDE DCOMN1	RBCOMP 3
4		INCLUDE DCOMN2	RBCOMP 4
5		INCLUDE DCOMN5	RBCOMP 5
6		COMMON DD(2),XD(2),TD(2),THAD(2),THBD(2),RB(2)	RBCOMP 6
7		COMMON CSHAD(2),CSHBD(2),OMTD(2),CSOMTD(2),SNOMTD(2)	RBCOMP 7
8		COMMON XTNU,OMTNU,CORTNU,SORTNU,CTHTNU(2)	RBCOMP 8
9		COMMON RT(2),THAT(2),THBT(2)	RBCOMP 9
10		COMMON ARG,FA,GA,GB,GC,GAB,GAC,GBG,GBBC,GAABC,GBABC	RBCOMP10
11		COMMON CSALFA,CSALFB,CSBETA,CSBETB,CSGANA,CSGAMB	RBCOMP11
12		COMMON CALFAP,CALFBP,CGARAP,CGARBP,CGSA,CGSB	RBCOMP12
13		COMMON PHI,PHMOT,DELRT,THMAX,THMIN,TTRAX,A,DOPSKP	RBCOMP13
14		COMMON X1(2),X2(2),X3(2),X4(2),Y1(2),Y2(2),Y3(2),Y4(2)	RBCOMP14
15		COMMON I,II,IJ,JA,JB,JBOUND,JC,JD,JDD,JDELT,JDRAJ,JDRIJ,JE	RBCOMP15
16		COMMON JMAX,JUMP,KBAND,KTIM,L,LEAP,LL,MLRU(2),MM,MN,MI,MA,MB,NEXT	RBCOMP16
17		EQUIVALENCE (MLRU(1),ML),(MLRU(2),MU),(DOP,IDOP),(MNRX,MN)	RBCOMP17
18		EQUIVALENCE (QCOS,QAABC),(QSIN,QBABC),(QCOSM,QAB)	RBCOMP18
19		DIMENSION IDOP(1),MNRX(2)	RBCOMP19
20		LOGICAL TTRAX,DOPSKP	RBCOMP20
21	C		RBCOMP21
22	C	BOUNDARY LOOP--	RBCOMP22
23	C	ONCE THROUGH EACH FOR SURFACE AND BOTTOM	RBCOMP23
24	C		RBCOMP24
25		DO 9C10 JBOUND = 1, 2	RBCOMP25
26		JMAX = NBOUND(JBOUND)	RBCOMP26
27		IF (JMAX .EQ. U) GO TO 9C10	RBCOMP27
28	C		RBCOMP28
29	C	PATH LOOP--	RBCOMP29
30	C	ONCE THROUGH FOR EACH SURFACE REFLECTED PATH AND EACH BOTTOM	RBCOMP30
31	C	REFLECTED PATH ON THE INTERMEDIATE TAPE. (PATH A)	RBCOMP31
32	C		RBCOMP32
33		DO 8010 JA = 1, JMAX	RBCOMP33
34	C		RBCOMP34
35	C	POSITION TAPE AT JA <sup>TH</sup> RECORD.	RBCOMP35
36	C		RBCOMP36
37		IF (JA .EQ. 1) GO TO 1020	RBCOMP37
38		DO 1010 I = JA, JMAX	RBCOMP38
39		BACKSPACE BR1	RBCOMP39
40		1010 CONTINUE	RBCOMP40
41	C		RBCOMP41
42		1020 READ (BR1) NA,(RBYA(I),RBYB(I),RBYC(I),RBYD(I), I = 1, NA)	RBCOMP42
43		BACKSPACE BR1	RBCOMP43
44	C		RBCOMP44
45	C	PATH COMBINATION LOOP--	RBCOMP45
46	C	ONCE THROUGH FOR EACH COMBINATION OF PATHS TO SURFACE	RBCOMP46
47	C	OR TO BOTTOM. (PATH B)	RBCOMP47
48	C		RBCOMP48
49		DO 7080 JB = JA, JMAX	RBCOMP49
50		READ (BR1) NB,(RBYB(I),RBYC(I),RBYD(I),RBYE(I), I = 1, NB)	RBCOMP50
51	C		RBCOMP51
52	C	DEFINE THE AREA COMMON TO THE TWO PATHS AND ALSO TO THE	RBCOMP52
53	C	CURRENT TIME INTERVAL, IF ANY SUCH AREA EXISTS.	RBCOMP53
54	C		RBCOMP54
55		TWMIN = AMAX1(TIME(KT)-DELRT,RBYA(1),RBYB(1))	RBCOMP55
56		TWMAX = AMIN1(TIME(KT)+DELRT,RBYA(NB),RBYB(NB))	RBCOMP56
57		IF (TWMAX .LE. TWMIN) GO TO 7080	RBCOMP57
58	C		RBCOMP58
59		DO 1030 JC = 1, NA	RBCOMP59
60		X(JC) = RBYA(JC)	RBCOMP60
61		1030 CONTINUE	RBCOMP61
62		JC = NA	RBCOMP62
63	C		RBCOMP63
64		DO 1040 I = 1, NA	RBCOMP64
65		JC = JC + K1	RBCOMP65
66		X(JC) = RBYB(I)	RBCOMP66
67		1040 CONTINUE	RBCOMP67
68		CALL SORT(X, JC)	RBCOMP68
69	C		RBCOMP69
70	C	EVALUATE TABLES FOR OVERLAPPED AREA.	RBCOMP70

```

71 C
72 JD = 0
73 II = K1
74 IJ = K1
75 DO 1050 I = 1, JC
76 T(JD+1) = TABLKP(X(I),RBXA,RBTA,II,NA)
77 IF (ITABLE .EQ. 0) GO TO 1050
78 II = ITABLE
79 T(JD+1) = (T(JD+1) + TABLKP(X(I),RBXB,RBTD,IJ,MB)) * FPT5
80 IF (ITABLE .EQ. 0) GO TO 1050
81 IJ = ITABLE
82 JD = JD + K1
83 X(JD) = X(I)
84 TND(JD) = AINTRP(RBTH) * DEGRAD
85 R(JD) = AINTRP(RBHB)
86 TMA(JD) = TABLKP(X(I),RBXA,RBTA,II,NA) * DEGRAD
87 R(JD) = EXP(FLOG10 * (AINTRP(RBHA) + R(JD)))/FZ0
88 COSTHA(JD) = COS(TMA(JD))
89 COSTNB(JD) = COS(TND(JD))
90 OMT(JD) = ANOD(OMEGA * T(JD), TNOPI)
91 IF (ABS(OMT(JD)) .GT. PI) OMT(JD) = OMT(JD) - SIGN(TNOPI, OMT(JD))
92 COSORT(JD) = COS(OMT(JD))
93 SINORT(JD) = SIGN(SORT(F1-COSORT(JD)**2),OMT(JD))
94
95 1050 CONTINUE
96 C
97 C TRANSMIT-RECEIVE LOOP--
98 C JC = 1, TRANSMIT PATH A, RECEIVE PATH B
99 C JC = 2, TRANSMIT PATH B, RECEIVE PATH A
100 C
101 DO 7070 JC = 1,2
102 C
103 C FORE - AFT LOOP--
104 C JE = 1, FORWARD HEMISPHERE, OR RECEIVE FREQUENCY GREATER
105 C THAN TRANSMIT FREQUENCY.
106 C JE = 2, AFTER HEMISPHERE, OR RECEIVE FREQ. LESS THAN XMIT FREQ.
107 C
108 DO 7050 JE = 1, 2
109 LL = (JC - K1) * LKX2
110 RM = LKX2 - LL
111 FA = K3 - JE * K2
112 QCOS = FA
113 QCOSM = FA
114 DO 2020 I = 1, JD
115 ML = LL + I
116 MU = RM + I
117 IF (OMEGA .EQ. F0) GO TO 2010
118 QA = COSTHA(MU) * COSORT(I) + COSTHA(ML)
119 QB = COSTHA(MU) * SINORT(I)
120 QC = QB * COSTHA(ML)/FCOVS
121 QAB = QA**2 + QB**2
122 QCOS = (QB * QC + FA * QA * SORT(QAB - QC**2))/QAB
123 QOSIN = (QB * QCOS - QC)/QA
124 QCOSM = (QCOS * COSORT(I) + QOSIN * SINORT(I))
125 2010 IDOP(I) = FZRO * ((COKT + VS * COSTHA(MU) * QCOSM)
126 1 /((COKT - VS * COSTHA(ML) * QCOS)
127 2020 CONTINUE
128 MN = K1
129 DOPSKP = .FALSE.
130 SONTRU = 0.
131 C
132 C LOOP TO PROCESS CONSECUTIVE STRINGS OF DATA WHICH ARE
133 C MONOTONIC IN "DOP"
134 C
135 3010 JDDEL = ISIGN(1, IDOP(MN) - IDOP(MN+1))
136 ML = K1 + (JDDEL + K1)/K2
137 MU = K3 - ML
138 IJ = JB - K1
139 DO 3020 I = MN, IJ
140 IF (JDDEL .NE. ISIGN(1, IDOP(I) - IDOP(I+1))) GO TO 3030
3020 CONTINUE
RBCOMP71
RBCOMP72
RBCOMP73
RBCOMP74
RBCOMP75
RBCOMP76
RBCOMP77
RBCOMP78
RBCOMP79
RBCOMP80
RBCOMP81
RBCOMP82
RBCOMP83
RBCOMP84
RBCOMP85
RBCOMP86
RBCOMP87
RBCOMP88
RBCOMP89
RBCOMP90
RBCOMP91
RBCOMP92
RBCOMP93
RBCOMP94
RBCOMP95
RBCOMP96
RBCOMP97
RBCOMP98
RBCOMP99
RBCOMP100
RBCOMP101
RBCOMP102
RBCOMP103
RBCOMP104
RBCOMP105
RBCOMP106
RBCOMP107
RBCOMP108
RBCOMP109
RBCOMP110
RBCOMP111
RBCOMP112
RBCOMP113
RBCOMP114
RBCOMP115
RBCOMP116
RBCOMP117
RBCOMP118
RBCOMP119
RBCOMP120
RBCOMP121
RBCOMP122
RBCOMP123
RBCOMP124
RBCOMP125
RBCOMP126
RBCOMP127
RBCOMP128
RBCOMP129
RBCOMP130
RBCOMP131
RBCOMP132
RBCOMP133
RBCOMP134
RBCOMP135
RBCOMP136
RBCOMP137
RBCOMP138
RBCOMP139
RBCOMP140

```

INDEX

SUBROUTINE RBCOMP

PAGE 23

141	I = JD	RBCOM141
142	C	RBCOM142
143	3030 MX = I	RBCOM143
144	JDMIN = MNMX(NL)	RBCOM144
145	JDMAX = MNMX(MU)	RBCOM145
146	C	RBCOM146
147	DD(1) = DOP(JDMAX)	RBCOM147
148	IF (JE .EQ. K2) DD(1) = FZRO	RBCOM148
149	JDD = JDMAX	RBCOM149
150	ASSIGN 3050 TO NEXT	RBCOM150
151	DO 3040 KBAND = NSPRM1, NBAND	RBCOM151
152	IF (DD(1) .GT. BAND(KBAND+1)) GO TO (3070, 3090), JE	RBCOM152
153	3040 CONTINUE	RBCOM153
154	GO TO 7030	RBCOM154
155	C	RBCOM155
156	C LOOP FOR ALL DESIRED BANDS AND FOR ALL DATA AT CONSTANT DOPPLER	RBCOM156
157	C WITHIN A BAND, IF BANDWIDTH IS GREATER THAN DATA SPACING.	RBCOM157
158	C IN THE FOLLOWING TABLES, THE SUBSCRIPTS 1 AND 2 REFER TO	RBCOM158
159	C DATA POINTS OF THE LOWEST AND HIGHEST FREQUENCY--SUBSCRIPTS	RBCOM159
160	C NL AND NU REFER TO POINTS OF THE LOWEST AND HIGHEST TIMES.	RBCOM160
161	C	RBCOM161
162	3050 ASSIGN 4020 TO NEXT	RBCOM162
163	C	RBCOM163
164	3060 DD(2) = DD(1)	RBCOM164
165	XD(2) = XD(1)	RBCOM165
166	TD(2) = TD(1)	RBCOM166
167	THAD(2) = THAD(1)	RBCOM167
168	THBD(2) = THBD(1)	RBCOM168
169	RD(2) = RD(1)	RBCOM169
170	CSTHAD(2) = CSTHAD(1)	RBCOM170
171	CSTHBD(2) = CSTHBD(1)	RBCOM171
172	OMTD(2) = OMTD(1)	RBCOM172
173	CSOMTD(2) = CSOMTD(1)	RBCOM173
174	SNOMTD(2) = SNOMTD(1)	RBCOM174
175	C	RBCOM175
176	JDD = JDD + JDDEL	RBCOM176
177	IF (DOP(JDD) .LT. BAND(KBAND+1)) GO TO 3080	RBCOM177
178	DD(1) = DOP(JDD)	RBCOM178
179	3070 XD(1) = X(JDD)	RBCOM179
180	TD(1) = T(JDD)	RBCOM180
181	THAD(1) = THA(JDD)	RBCOM181
182	THBD(1) = THB(JDD)	RBCOM182
183	RD(1) = R(JDD)	RBCOM183
184	CSTHAD(1) = COSTHA(JDD)	RBCOM184
185	CSTHBD(1) = COSTHB(JDD)	RBCOM185
186	OMTD(1) = OMT(JDD)	RBCOM186
187	CSOMTD(1) = COSONT(JDD)	RBCOM187
188	SNOMTD(1) = SINORT(JDD)	RBCOM188
189	GO TO 4010	RBCOM189
190	C	RBCOM190
191	3080 JDD = JDD - JDDEL	RBCOM191
192	DD(1) = BAND(KBAND+1)	RBCOM192
193	3090 XD(1) = TABLKP(DD(1),DOP,X,MN,MX)	RBCOM193
194	DOPSKP = ITABLE .EQ. 0	RBCOM194
195	IF (DOPSKP) GO TO NEXT	RBCOM195
196	TD(1) = AINTRP(T)	RBCOM196
197	THAD(1) = AINTRP(THA)	RBCOM197
198	THBD(1) = AINTRP(THB)	RBCOM198
199	RD(1) = AINTRP(R)	RBCOM199
200	CSTHAD(1) = AINTRP(COSTHA)	RBCOM200
201	CSTHBD(1) = AINTRP(COSTHB)	RBCOM201
202	OMTD(1) = AINTRP(OMT)	RBCOM202
203	CSOMTD(1) = AINTRP(COSONT)	RBCOM203
204	SNOMTD(1) = AINTRP(SINORT)	RBCOM204
205	C	RBCOM205
206	4010 GO TO NEXT	RBCOM206
207	C	RBCOM207
208	4020 ASSIGN 6010 TO LEAP	RBCOM208
209	KTIM = K1	RBCOM209
210	YTRAX = .FALSE.	RBCOM210

APPENDIX G

211	C		RBCOM211
212		IF (DOPSKP) GO TO 4040	RBCOM212
213		IF (RLMU(JE) .EQ. K1) GO TO 4030	RBCOM213
214		IF (TMIN .LT. TD(MU)) GO TO 4040	RBCOM214
215		GO TO 7020	RBCOM215
216	C		RBCOM216
217		4030 IF (TMAX .LT. TD(ML)) GO TO 7020	RBCOM217
218		IF (TMIN .LT. TD(ML)) GO TO 4080	RBCOM218
219		4040 ARG = TMIN	RBCOM219
220		GO TO 4120	RBCOM220
221	C		RBCOM221
222	C	LOOP FOR ALL TIMES AT CONSTANT DOPPLER	RBCOM222
223	C		RBCOM223
224		4050 IF (X(KTIM) .LE. XTNU) GO TO 7010	RBCOM224
225		RT(ML) = RT(MU)	RBCOM225
226		TNAT(ML) = TNAT(MU)	RBCOM226
227		TNBT(ML) = TNBT(MU)	RBCOM227
228	C		RBCOM228
229		ARG = AMIN(T(KTIM), TMAX)	RBCOM229
230		ASSIGN 4110 TO JUMP	RBCOM230
231		IF (ARG .LT. TMAX) ASSIGN 4100 TO JUMP	RBCOM231
232		IF (DOPSKP) GO TO JUMP	RBCOM232
233		IF (RLMU(JE) .EQ. K2) GO TO 4070	RBCOM233
234		IF (XTNU .GE. XD(MU)) GO TO JUMP	RBCOM234
235		4060 IF (ARG .LT. TD(MU)) GO TO JUMP	RBCOM235
236		MM = MU	RBCOM236
237		GO TO 4090	RBCOM237
238	C		RBCOM238
239		4070 IF (ARG .LT. TD(ML)) GO TO JUMP	RBCOM239
240		IF (XTNU .LT. XD(ML)) GO TO 4080	RBCOM240
241		IF (ARG .GE. TD(MU)) TMAX = .TRUE.	RBCOM241
242		GO TO 4060	RBCOM242
243		4080 MM = ML	RBCOM243
244	C		RBCOM244
245		4090 XTNU = XD(MM)	RBCOM245
246		RT(MU) = RB(MM)	RBCOM246
247		TNAT(MU) = TNAD(MM)	RBCOM247
248		TNBT(MU) = TNBD(MM)	RBCOM248
249		CTNTMU(1) = CSTHAD(MM)	RBCOM249
250		CTNTMU(2) = CSTHBD(MM)	RBCOM250
251		ONTTMU = ONTD(MM)	RBCOM251
252		CONTMU = CSOINT(MM)	RBCOM252
253		SONTMU = SNOINT(MM)	RBCOM253
254		KTIM = KTIM - K1	RBCOM254
255		GO TO 4130	RBCOM255
256	C		RBCOM256
257		4100 XTNU = X(KTIM)	RBCOM257
258		RT(MU) = R(KTIM)	RBCOM258
259		TNAT(MU) = TNAT(KTIM)	RBCOM259
260		TNBT(MU) = TNBT(KTIM)	RBCOM260
261		CTNTMU(1) = COSTNA(KTIM)	RBCOM261
262		CTNTMU(2) = COSTNB(KTIM)	RBCOM262
263		ONTTMU = ONT(KTIM)	RBCOM263
264		CONTMU = COSINT(KTIM)	RBCOM264
265		SONTMU = SINONT(KTIM)	RBCOM265
266		GO TO 4130	RBCOM266
267	C		RBCOM267
268		4110 TMAX = .TRUE.	RBCOM268
269		4120 XTNU = TABLKP(ARG,T,X,KTIM,JD)	RBCOM269
270		RT(MU) = AINTRP(R)	RBCOM270
271		TNAT(MU) = AINTRP(TNA)	RBCOM271
272		TNBT(MU) = AINTRP(TNB)	RBCOM272
273		CTNTMU(1) = AINTRP(COSTNA)	RBCOM273
274		CTNTMU(2) = AINTRP(COSTNB)	RBCOM274
275		ONTTMU = AINTRP(ONT)	RBCOM275
276		CONTMU = AINTRP(COSONT)	RBCOM276
277		SONTMU = AINTRP(SINONT)	RBCOM277
278	C		RBCOM278
279		4130 LL = K3 - JC	RBCOM279
280	C		RBCOM280

I N D E X

SUBROUTINE RBCOMP

```

281 C      LOOP FOR POINTS 3 AND 4--
282 C      I = 1, COMPUTE FOR POINTS 1 AND 3
283 C      I = 2, COMPUTE FOR POINTS 2 AND 4
284 C
285 C      DO 5020 I = 1, 2
286 C      L = K3 - I
287 C      FA = FZRO + CTHTRU(LL)
288 C      QA = DD(L) + CTHTRU(JC) + FA + COMTRU
289 C      QB = FA + SOMTRU
290 C      QC = FCOVS + (DD(L) - FZRO)
291 C      QAB = QA**2 + QB**2
292 C      QAC = QA * QC
293 C      QBC = QB * QC
294 C      QABC = SQRT(AMAX1(F0, QAB - QC**2))
295 C      QAABC = QA * QABC
296 C      QBABC = QB * QABC
297 C      II = K2 * (I - K1)
298 C
299 C      PORT - STARBOARD LOOP--
300 C      L = 1, AREA IN FIRST QUADRANT (OMEGA = 0)
301 C      L = 2, AREA IN FOURTH QUADRANT (OMEGA = 0)
302 C
303 C      DO 5010 L = 1, 2
304 C      IJ = L + II
305 C      A = K3 - L * K2
306 C      FA = XTMU/QAB
307 C
308 C      X1(IJ) = X3(IJ)
309 C      X3(IJ) = FA * (QAC - A * QBABC)
310 C      Y1(IJ) = Y3(IJ)
311 C      Y3(IJ) = FA * (QBC + A * QAABC)
312 C      5010 CONTINUE
313 C      5020 CONTINUE
314 C
315 C      GO TO LEAP
316 C      6010 ASSIGN 6020 TO LEAP
317 C      GO TO 7010
318 C
319 C      6020 CSGAMA = SIN((THAT(MU) + THAT(NL))/F2)
320 C      CSGAMB = SIN((THBT(MU) + THBT(NL))/F2)
321 C      COSA = SQRT(F1 - CSGAMA**2)
322 C      COSB = SQRT(F1 - CSGAMB**2)
323 C
324 C      PORT - STARBOARD LOOP--
325 C      L = 1, AREA IN FIRST QUADRANT (OMEGA = 0)
326 C      L = 2, AREA IN FOURTH QUADRANT (OMEGA = 0)
327 C
328 C      DO 6030 L = 1,2
329 C      A = ((X4(L)+Y2(L) + X3(L)+Y4(L) + X2(L)+Y1(L) + X1(L)+Y3(L)) -
330 C      1 (X2(L)+Y4(L) + X4(L)+Y3(L) + X1(L)+Y2(L) + X3(L)+Y1(L)))
331 C      A = ABS(A/(RT(MU) + RT(NL)))
332 C
333 C      PHI = ATAN2(Y1(L) + Y2(L) + Y3(L) + Y4(L),
334 C      1 X1(L) + X2(L) + X3(L) + X4(L))
335 C      PHMONT = PHI - ORTTMU
336 C
337 C      CSALFA = COSA * COS(PHI)
338 C      CSBETA = COSA * SIN(PHI)
339 C      CSALFB = COSB * COS(PHMONT)
340 C      CSBETB = COSB * SIN(PHMONT)
341 C
342 C      CALFAP = CSALFA + CSKSI + CSGAMA + SNKSI
343 C      CGAMAP = CSGAMA + CSKSI - CSALFA + SNKSI
344 C      CALFBP = CSALFB + CSKSI + CSGAMB + SNKSI
345 C      CGAMBP = CSGAMB + CSKSI - CSALFB + SNKSI
346 C
347 C      DELR = A * OXL(XMIT,CALFAP,CSBETA,CGAMAP) *
348 C      1 OXL(RECV,CALFBP,CSBETB,CGAMBP)
349 C
350 C      RV(KTT,KBAND,JBOUND) = RV(KTT,KBAND,JBOUND) + DELR

```

RBCOM281  
RBCOM282  
RBCOM283  
RBCOM284  
RBCOM285  
RBCOM286  
RBCOM287  
RBCOM288  
RBCOM289  
RBCOM290  
RBCOM291  
RBCOM292  
RBCOM293  
RBCOM294  
RBCOM295  
RBCOM296  
RBCOM297  
RBCOM298  
RBCOM299  
RBCOM300  
RBCOM301  
RBCOM302  
RBCOM303  
RBCOM304  
RBCOM305  
RBCOM306  
RBCOM307  
RBCOM308  
RBCOM309  
RBCOM310  
RBCOM311  
RBCOM312  
RBCOM313  
RBCOM314  
RBCOM315  
RBCOM316  
RBCOM317  
RBCOM318  
RBCOM319  
RBCOM320  
RBCOM321  
RBCOM322  
RBCOM323  
RBCOM324  
RBCOM325  
RBCOM326  
RBCOM327  
RBCOM328  
RBCOM329  
RBCOM330  
RBCOM331  
RBCOM332  
RBCOM333  
RBCOM334  
RBCOM335  
RBCOM336  
RBCOM337  
RBCOM338  
RBCOM339  
RBCOM340  
RBCOM341  
RBCOM342  
RBCOM343  
RBCOM344  
RBCOM345  
RBCOM346  
RBCOM347  
RBCOM348  
RBCOM349  
RBCOM350

APPENDIX G

351	4030 CONTINUE	RBCOM351
352	C	RBCOM352
353	7010 IF (TTMAX) GO TO 7020	RBCOM353
354	KTIM = KTIM + K1	RBCOM354
355	IF (KTIM .LE. JD) GO TO 4050	RBCOM355
356	7020 IF (DD(1) .LE. BAND(KBAND+1)) KRBAND = KBAND + K1	RBCOM356
357	IF (KRBAND .GT. NBAND) GO TO 7030	RBCOM357
358	IF (JDD .NE. JDMIN) GO TO 3060	RBCOM358
359	IF (DD(1) .LE. FZRO) GO TO 7030	RBCOM359
360	DOPSKP = .TRUE.	RBCOM360
361	DD(2) = DD(1)	RBCOM361
362	DD(1) = AMAX1(BAND(KBAND+1), FZRO)	RBCOM362
363	GO TO 4020	RBCOM363
364	C	RBCOM364
365	7030 IF (MX .EQ. JD) GO TO 7040	RBCOM365
366	MN = MX	RBCOM366
367	GO TO 3010	RBCOM367
368	C	RBCOM368
369	7040 MN = K1	RBCOM369
370	IF (TMTMAX .LE. F90) GO TO 7060	RBCOM370
371	7050 CONTINUE	RBCOM371
372	7060 IF (JA .EQ. JB) GO TO 7080	RBCOM372
373	7070 CONTINUE	RBCOM373
374	C	RBCOM374
375	7080 CONTINUE	RBCOM375
376	8C10 CONTINUE	RBCOM376
377	9010 CONTINUE	RBCOM377
378	C	RBCOM378
379	REWIND BR1	RBCOM379
380	RETURN	RBCOM380
381	END	RBCOM381

I N D E X

SUBROUTINE RDCOMP

SYMBOL	-----	REFERENCES	-----	-----	-----	-----	-----	-----	-----	-----
1010	- 38	40*								
1020	- 37	42*								
1030	- 59	61*								
1040	- 64	67*								
1050	- 75	77	80	94*						
2010	- 116	124*								
2020	- 113	126*								
3010	- 134*	367								
3020	- 138	140*								
3030	- 139	143*								
3040	- 151	153*								
3050	- 150	162*								
3060	- 164*	358								
3070	- 152	179*								
3080	- 177	191*								
3090	- 152	193*								
4010	- 189	206*								
4020	- 162	208*	363							
4030	- 213	217*								
4040	- 212	214	219*							
4050	- 224*	355								
4060	- 235*	242								
4070	- 233	239*								
4080	- 218	240	243*							
4090	- 237	245*								
4100	- 231	257*								
4110	- 230	268*								
4120	- 220	269*								
4130	- 255	266	279*							
5010	- 303	312*								
5020	- 285	313*								
6010	- 208	316*								
6020	- 316	319*								
6030	- 328	351*								
7010	- 224	317	353*							
7020	- 215	217	353	356*						
7030	- 154	357	359	365*						
7040	- 365	369*								
7050	- 107	371*								
7060	- 370	372*								
7070	- 100	373*								
7080	- 49	57	372	375*						
8010	- 33	376*								
9010	- 25	27	377*							
A	- 1300	305=	309	311	329=	331=	347			
ABS	- 91	331								
AINTRP	- 84	85	87	196	197	198	199	200	201	202
	- 203	204	270	271	272	273	274	275	276	277
AMAX1	- 55	294	362							
AMIN1	- 56	229								
AROD	- 90									
ARG	- 1000	219=	229=	231	235	239	241	269		
ATAN2	- 335									
BAND	- 152	177	192	356	362					
BR1	- 39	42RD	43	50RD	379					
COKT	- 124	125								
CALFAP	- 1200	342=	347							
CALFBP	- 1200	344=	348							
CGARAP	- 1200	343=	347							
CGARBP	- 1200	345=	348							
CORTNU	- 800	252=	264=	276=	288					
COS	- 88	89	92	337	339					
COSA	- 1200	321=	337	338						
COSB	- 1200	322=	339	340						
COSOMT	- 02=	93	117	123	187	203	264	276		
COSTNA	- 88=	117	118	119	124	125	184	200	261	273
COSTNB	- 89=	185	201	262	274					
CSALFA	- 1100	337=	342	343						

APPENDIX G





I N D E X

SUBROUTINE RBCOMP

THTMAX	-	370																		
TIME	-	55	56																	
TTMAX	-	1300	206	210=	241=	268=	353													
TWMAX	-	1300	56=	57	217	229	231													
TWRIN	-	1300	55=	57	214	218	219													
TWOPI	-	90	91																	
VS	-	124	125																	
X	-	60=	66=	68A6	76	79	83=	86	179	193	224									
	-	257	269																	
X1	-	1400	308=	329	330	334														
X2	-	1400	329	330	334															
X3	-	1400	308	309=	329	330	334													
X4	-	1400	329	330	334															
XD	-	600	165=	179=	193=	234	240	245												
XMIT	-	347																		
XTHU	-	800	224	234	240	245=	257=	269=	306											
Y1	-	1400	310=	329	330	333														
Y2	-	1400	329	330	333															
Y3	-	1400	310	311=	329	330	333													
Y4	-	1400	329	330	333															

INDEX

PAGE 31

1		SUBROUTINE RVCOMP	RVCOMP 1
2			RVCOMP 2
3	C	INCLUDE DCOMN1	RVCOMP 3
4		INCLUDE DCOMN2	RVCOMP 4
5		INCLUDE DCOMN4	RVCOMP 5
6		COMMON I,J,K,NN,OMT,CSORTF,SNORTF,FR,FRSQ,FXSQ,FX,CSA,SNA,PN,B,G	RVCOMP 6
7		COMMON SNPHI(2),CSPHI(2),X(2),Y(2),Z(2),D,DD,R,FRV	RVCOMP 7
8		COMMON T1,T2,A1,A2,VOL1,T3	RVCOMP 8
9			RVCOMP 9
10	C	COMPUTE ONE-WAY RANGE TO MIDPOINT OF TRANSMITTED PULSE.	RVCOMP10
11	C	PRE-COMPUTE RELATED VALUES FOR VOLUME AND FOR RANGE LOSSES.	RVCOMP11
12	C		RVCOMP12
13		R = TIME(KT) * CD * FPT5	RVCOMP13
14		FRV = EXP((LOGNVI - ALPNC + TIME(KT))/F10 * FLOG10)/R**4	RVCOMP14
15		IF (OMEGA .EQ. 0.) FRV = FRV *	RVCOMP15
16		((R + DR)**3 - ARAX1(R - DR, FO)**3) * P123	RVCOMP16
17		IF (VPTTRN) GO TO 9C00	RVCOMP17
18	C		RVCOMP18
19	C	PATTERN LOSSES MUST BE COMPUTED.	RVCOMP19
20	C		RVCOMP20
21		OMT = AMOD(OMEGA * TIME(KT), TWOPI)	RVCOMP21
22		IF (ABS(OMT) .GT. PI) OMT = OMT - SIGN(TWOPI, OMT)	RVCOMP22
23		CSORTF = COS(OMT)	RVCOMP23
24		SNORTF = SIGN(SORT(F1-CSORTF**2),OMT) * FZRO	RVCOMP24
25		CSORTF = CSORTF * FZ2	RVCOMP25
26		FCSGAM(NSPRH1) = 0.	RVCOMP26
27		IF (OMEGA .EQ. 0.) FCSGAM(NSPRH1) = F1	RVCOMP27
28		T1 = AMAX1(TIME(KT) - DELT, FO) * FPT5	RVCOMP28
29		T2 = ((TIME(KT) + DELT) * FPT5 - T1)/F10	RVCOMP29
30	C		RVCOMP30
31	C	COMPUTE AVERAGE PATTERN LOSSES FOR EACH BAND.	RVCOMP31
32	C		RVCOMP32
33		DO 8000 I = NSPRH1, NBAND	RVCOMP33
34		FGAM(I) = 0.	RVCOMP34
35		FR = (BAND(I) + BAND(I+1)) * FPT5	RVCOMP35
36		FRSQ = FR**2	RVCOMP36
37		FXSQ = FZSQ + FRSQ + FR * CSORTF	RVCOMP37
38		FX = SQRT(FXSQ)	RVCOMP38
39		A1 = FCOVS * (FR - FZRO)	RVCOMP39
40		CSA = A1/FX	RVCOMP40
41		IF (ABS(CSA) .GT. F1) CSA = SIGN(F1, CSA)	RVCOMP41
42		SNA = SQRT(F1 - CSA**2)	RVCOMP42
43		NN = MIN0(K2 + IFIX(FNBAND * SNA) + K1, 360)	RVCOMP43
44		PN = NN	RVCOMP44
45		DD = TWOPI/PN	RVCOMP45
46		D = 0.	RVCOMP46
47		SNPHI(1) = SNORTF/FX	RVCOMP47
48		SNPHI(2) = -SNPHI(1) * FR/FZRO	RVCOMP48
49		CSPHI(1) = SQRT(F1 - SNPHI(1)**2)	RVCOMP49
50		CSPHI(2) = SQRT(F1 - SNPHI(2)**2)	RVCOMP50
51		IF (ABS(FZSQ - FRSQ) .LE. FXSQ) GO TO 2000	RVCOMP51
52		CSPHI(1) = SIGN(CSPHI(1), CSA)	RVCOMP52
53		CSPHI(2) = -SIGN(CSPHI(1), CSA)	RVCOMP53
54		2000 DO 4000 J = 1,NN	RVCOMP54
55		D = D + DD	RVCOMP55
56		B = SNA * SIN(D)	RVCOMP56
57		G = SNA * COS(D)	RVCOMP57
58			RVCOMP58
59	C	DO 3000 K = 1, 2	RVCOMP59
60		X(K) = CSA * CSPHI(K) - B * SNPHI(K)	RVCOMP60
61		Y(K) = B * CSPHI(K) + CSA * SNPHI(K)	RVCOMP61
62		X(K) = X(K) * CSKSI + G * SNKSI	RVCOMP62
63		Z(K) = G * CSKSI - X(K) * SNKSI	RVCOMP63
64		3000 CONTINUE	RVCOMP64
65		FGAM(I) = FGAM(I) + OXL(XMIT,X(1),Y(1),Z(1))	RVCOMP65
66		1 * OXL(RECV,X(2),Y(2),Z(2))	RVCOMP66
67		4000 CONTINUE	RVCOMP67
68		FGAM(I) = FGAM(I)/PN * EXPS	RVCOMP68
69		IF (OMEGA .EQ. 0.) GO TO 8000	RVCOMP69
70		T3 = T1	RVCOMP70

## APPENDIX G

I N D E X

SUBROUTINE RVCOMP

PAGE 32

71	A2 = FZ2 * FR	RVCOMP71
72	A1 = A1/SQRT(A2)	RVCOMP72
73	A2 = (FRSQ + FZSQ)/A2	RVCOMP73
74	VOL1 = 0.	RVCOMP74
75	C	RVCOMP75
76	DO 5000 J = 1, 10	RVCOMP76
77	T3 = T3 + T2	RVCOMP77
78	VOL1 = VOL1 - T3**2 * ANAX1(F1 - A1/SQRT(A2 + COS(OMEGA * T3)),FC)	RVCOMP78
79	5000 CONTINUE	RVCOMP79
80	FCSGAM(I+1) = VOL1 * T2 * FC03	RVCOMP80
81	GOTO 7000	RVCOMP81
82	6000 FCSGAM(I+1) = FC0VS * (BAND(I+1) - FZRO)/(BAND(I+1) + FZRO)	RVCOMP82
83	7000 FGAM(I) = FGAM(I) * (FCSGAM(I) - FCSGAM(I+1))	RVCOMP83
84	RVV(KTT,I) = FRV * FGAM(I)	RVCOMP84
85	8000 CONTINUE	RVCOMP85
86	C	RVCOMP86
87	C FOR STRAIGHT-RUNNING CASE, PATTERN LOSSES FOR ANY BAND WILL	RVCOMP87
88	C BE THE SAME AT ALL TIMES.	RVCOMP88
89	C	RVCOMP89
90	IF (OMEGA .EQ. 0.) VPTRN = .TRUE.	RVCOMP90
91	GO TO 30000	RVCOMP91
92	9000 DO 10000 I = NSPRH1, NBAND	RVCOMP92
93	RVV(KTT,I) = FRV * FGAM(I)	RVCOMP93
94	10000 CONTINUE	RVCOMP94
95	30000 RETURN	RVCOMP95
96	END	RVCOMP96

APPENDIX G

SYMBOL	REFERENCES										
2000	-	51	54*								
3000	-	59	64*								
4000	-	54	67*								
5000	-	76	79*								
6000	-	69	82*								
7000	-	81	83*								
8000	-	33	85*								
9000	-	17	92*								
10000	-	92	94*								
30000	-	91	95*								
A1	-	8C0	39=	40	72=	78					
A2	-	8C0	71=	72	73=	78					
ABS	-	22	41	51							
ALPHC	-	14									
AMAX1	-	16	28	78							
AMOD	-	21									
B	-	6C0	56=	60	61						
BAND	-	35	82								
CO	-	13									
COS	-	23	57	78							
CSA	-	6C0	40=	41=	42	52	53	60	61		
CSKSI	-	62	63								
CSOMTF	-	6C0	23=	24	25=	37					
CSPHI	-	7C0	49=	50=	52=	53=	60	61			
D	-	7C0	46=	55=	56	57					
DCOMM1	-	3									
DCOMM2	-	4									
DCOMM4	-	5									
DB	-	7C0	45=	55							
DELT	-	28	29								
DR	-	16									
EXP	-	14									
EXPS	-	68									
FO	-	16	28	78							
F1	-	24	27	41	42	49	50	78			
F1C	-	14	29								
FCD3	-	80									
FCDVS	-	39	82								
FCSGAM	-	26=	27=	80=	82=	83					
FGAM	-	34=	65=	68=	83=	84	93				
FLOG10	-	14									
FNBAND	-	43									
FPTS	-	13	28	29	35						
FR	-	6C0	35=	36	37	39	48	71			
FRSQ	-	6C0	36=	37	51	73					
FRV	-	7C0	14=	15=	84	93					
FX	-	6C0	38=	40	47						
FXSQ	-	6C0	37=	38	51						
FZ2	-	25	71								
FZRO	-	24	39	48	82						
FZSQ	-	37	51	73							
G	-	6C0	57=	62	63						
I	-	6C0	33=	34	35	65	68	80	82	83	84
	-	92=	93								
IFIX	-	43									
J	-	6C0	54=	76=							
K	-	6C0	59=	60	61	62	63				
K1	-	43									
K2	-	43									
KT	-	13	14	21	28	29					
KTT	-	84	93								
LOGNVI	-	14									
MINO	-	43									
NBAND	-	33	92								
NN	-	6C0	43=	44	54						
NSPRH1	-	26	27	33	92						
OMEGA	-	15	21	27	69	78	90				
ORT	-	6C0	21=	22=	23	24					

APPENDIX G

I N D E X

SUBROUTINE RVCOMP

ORL	-	65	66				
PI	-	22					
PI23	-	16					
PN	-	6C0	44=	45	68		
R	-	7C0	13=	14	16		
RECV	-	66					
RETURN	-	95					
RVCOMP	-	1					
RVV	-	84=	93=				
SIGN	-	22	24	41	52	53	
SIN	-	56					
SNA	-	6C0	42=	43	56	57	
SNKSI	-	62	63				
SNORTF	-	6C0	24=	47			
SNPHI	-	7C0	47=	48=	49	50	60
SBRT	-	24	30	42	49	50	72
T1	-	8C0	28=	29	70		
T2	-	8C0	29=	77	80		
T3	-	8C0	70=	77=	78		
TINE	-	13	14	21	28	29	
TNOPI	-	21	22	45			
VOL1	-	8C0	74=	78=	80		
VPTRN	-	17	90=				
X	-	7C0	60=	62=	63	65	66
XMIT	-	65					
Y	-	7C0	61=	65	66		
Z	-	7C0	63=	65	66		

## INDEX

PAGE 35

1		SUBROUTINE RVSPRD	RVSPRD 1
2	C		RVSPRD 2
3		INCLUDE DCORN1	RVSPRD 3
4		INCLUDE DCORN2	RVSPRD 4
5		COMMON INAR,I,II,J,K,KK	RVSPRD 5
6	C		RVSPRD 6
7		DO 13 J = K1, K3	RVSPRD 7
8		DO 11 I = NSPRN1, NBAND	RVSPRD 8
9		II = I-NSPRN	RVSPRD 9
10		DO 10 K = K1, NSPR1	RVSPRD10
11		KK = ABS(K-NSPRN1) + K1	RVSPRD11
12		RV(2,II,J) = RV(2,II,J) + RV(1,I,J) + SPRED(KK,J)	RVSPRD12
13		II = II + 1	RVSPRD13
14		IF (II .GT. LNBAND) GO TO 11	RVSPRD14
15		10 CONTINUE	RVSPRD15
16		11 CONTINUE	RVSPRD16
17		13 CONTINUE	RVSPRD17
18		RETURN	RVSPRD18
19		END	RVSPRD19

## APPENDIX G

I N D E X		SUBROUTINE RVSPRD			
SYMBOL		REFERENCES			
10	-	10	15*		
11	-	8	14	16*	
13	-	7	17*		
ABS	-	11			
OCORN1	-	3			
OCORN2	-	4			
I	-	5C0	8=	9	12
II	-	5C0	9=	12	13= 14
IMAX	-	5C0			
J	-	5C0	7=	12	
K	-	5C0	10=	11	
K1	-	7	10	11	
K3	-	7			
KK	-	5C0	11=	12	
LMBAND	-	14			
MBAND	-	8			
NSPR1	-	10			
NSPRH	-	9			
NSPRH1	-	8	11		
RETURN	-	18			
RV	-	12=			
RVSPRD	-	1			
SPRED	-	12			

I N D E X

PAGE 37

1		SUBROUTINE RTCOMP	RTCOMP 1
2	C		RTCOMP 2
3		INCLUDE DCONN1	RTCOMP 3
4		INCLUDE DCONN2	RTCOMP 4
5		COMMON IRAX,I,J,T,TR	RTCOMP 5
6	C		RTCOMP 6
7		IRAX = KTT	RTCOMP 7
8		IF (.NOT. SPREAD) GO TO 2	RTCOMP 8
9		IRAX = K2	RTCOMP 9
10		IF (.NOT. (FILTER .OR. TVG)) GO TO 2	RTCOMP10
11		IRAX = K3	RTCOMP11
12		T = F1	RTCOMP12
13		IF (TVG) T = TVGF(TIRE(KT))	RTCOMP13
14		DO 1 I = 1, NMBND	RTCOMP14
15		TR = T	RTCOMP15
16		IF (FILTER) TR = T * RRFS(I)	RTCOMP16
17		RVS(3,I) = RVS(2,I) * TR	RTCOMP17
18		RVB(3,I) = RVB(2,I) * TR	RTCOMP18
19		RVV(3,I) = RVV(2,I) * TR	RTCOMP19
20		1 CONTINUE	RTCOMP20
21	C		RTCOMP21
22		2 DO 5 I = KTT, IRAX	RTCOMP22
23		J = 0	RTCOMP23
24	C		RTCOMP24
25		3 J = J + K1	RTCOMP25
26		RVS(I,LMBND1) = RVS(I,LMBND1) + RVS(I,J)	RTCOMP26
27		RVB(I,LMBND1) = RVB(I,LMBND1) + RVB(I,J)	RTCOMP27
28		RVV(I,LMBND1) = RVV(I,LMBND1) + RVV(I,J)	RTCOMP28
29	C		RTCOMP29
30		4 RVT(I,J) = RVS(I,J) + RVB(I,J) + RVV(I,J)	RTCOMP30
31		IF (RVS(I,J) .NE. 0.) RVS(I,J) = F10 * ALOG10(RVS(I,J))	RTCOMP31
32		IF (RVB(I,J) .NE. 0.) RVB(I,J) = F10 * ALOG10(RVB(I,J))	RTCOMP32
33		IF (RVV(I,J) .NE. 0.) RVV(I,J) = F10 * ALOG10(RVV(I,J))	RTCOMP33
34		IF (RVT(I,J) .NE. 0.) RVT(I,J) = F10 * ALOG10(RVT(I,J))	RTCOMP34
35	C		RTCOMP35
36		IF (J .LT. NMBND) GO TO 3	RTCOMP36
37		IF (J .EQ. LMBND1) GO TO 5	RTCOMP37
38		J = LMBND1	RTCOMP38
39		GO TO 4	RTCOMP39
40	C		RTCOMP40
41		5 CONTINUE	RTCOMP41
42		RETURN	RTCOMP42
43		END	RTCOMP43

APPENDIX G

G-41

I N D E X		SUBROUTINE RTCOMP									
SYMBOL	REFERENCES	REFERENCES	REFERENCES	REFERENCES	REFERENCES	REFERENCES	REFERENCES	REFERENCES	REFERENCES	REFERENCES	REFERENCES
1	- 14	20*									
2	- 8	10	22*								
3	- 25*	36									
4	- 30*	39									
5	- 22	37	41*								
ALOG10	- 31	32	33	34							
DCOM1	- 3										
DCOM2	- 4										
F1	- 12										
F10	- 31	32	33	34							
FILTER	- 10	16									
I	- 5C0	14=	16	17	18	19	22=	26	27	28	
		30	31	32	33	34					
INAX	- 5C0	7=	9=	11=	22						
J	- 5C0	23=	25=	26	27	28	30	31	32	33	
		34	36	37	38=						
K1	- 25										
K2	- 9										
K3	- 11										
KT	- 13										
KTT	- 7	22									
LMBND1	- 26	27	28	37	38						
MNBND	- 14	36									
RETURN	- 42										
RRFS	- 16										
RTCOMP	- 1										
RVB	- 16=	27=	30	32=							
RVS	- 17=	26=	30	31=							
RVT	- 30=	34=									
RVV	- 19=	28=	30	33=							
SPREAD	- 8										
T	- 5C0	12=	13=	15	16						
TIME	- 13										
TR	- 5C0	15=	16=	17	18	19					
TV6	- 10	13									
TV6F	- 13										

I N D E X

PAGE 39

```

1      SUBROUTINE RVPRNT                                RVPRNT 1
2      C                                                RVPRNT 2
3      INCLUDE DCOMN1                                  RVPRNT 3
4      INCLUDE DCOMN2                                  RVPRNT 4
5      COMMON I,J,K,L,II                               RVPRNT 5
6      DIMENSION HRVB(6)                               RVPRNT 6
7      DATA NTIME/6MTIME =/, (HRVB(I), I = 1,6)       RVPRNT 7
8      1 /6H SUR, 6MFACE , 6MBOTTOM, 6H VOL, 6HUME , 6H TOTAL/ RVPRNT 8
9      DATA ITOTAL/1/                                  RVPRNT 9
10     C                                                RVPRNT10
11     IF (PLOT) WRITE (IPLT) TIME(NTMIN),MNBND,(BNDOUT(K),BNDOUT(K+1), RVPRNT11
12     1 RVS(2,K),RVB(2,K),RVV(2,K),RVT(2,K), K = 1, MNBND) RVPRNT12
13     IF (NOPRNT) GO TO 30000                          RVPRNT13
14     IF (TOTALS) GO TO 2000                          RVPRNT14
15     J = NPSTRT                                       RVPRNT15
16     1 PAGE = PAGE + K1                                RVPRNT16
17     WRITE (IPRT,10) MED, IDC, IDV, IDATE, PAGE, NPAGE, RVPRNT17
18     1 VS, CO, FZRO, DC, S, KSID, OMEGAD, PING, DELT2, DBTTM RVPRNT18
19     IF (TOTALS) GO TO 2020                          RVPRNT19
20     C                                                RVPRNT20
21     IF (SPREAD) GO TO 5                              RVPRNT21
22     WRITE (IPRT,11) MBAND, (MTIME, TIME(K), K = NTMIN, NTHAX) RVPRNT22
23     GO TO 6                                          RVPRNT23
24     C                                                RVPRNT24
25     5 WRITE (IPRT,11) MBAND, (MTIME, TIME(NTMIN), K = 1, 1) RVPRNT25
26     C                                                RVPRNT26
27     6 WRITE (IPRT,12) MOUTPT, (HRVB, K = 1, 1)      RVPRNT27
28     IF (TOTALS) GO TO 2100                          RVPRNT28
29     DO 3 K = K1, K8                                  RVPRNT29
30     WRITE (IPRT,20)                                  RVPRNT30
31     C                                                RVPRNT31
32     DO 2 L = K1, K5                                  RVPRNT32
33     WRITE (IPRT, 20) BNDOUT(J), BNDOUT(J+1),        RVPRNT33
34     1 (RVS(II,J), RVP(II,J), RVV(II,J), RVT(II,J), II = 1, 1) RVPRNT34
35     J = J + IPEVRT                                   RVPRNT35
36     IF (J .GT. MNBND) GO TO 4                      RVPRNT36
37     C                                                RVPRNT37
38     2 CONTINUE                                       RVPRNT38
39     3 CONTINUE                                       RVPRNT39
40     GO TO 1                                          RVPRNT40
41     C                                                RVPRNT41
42     4 WRITE (IPRT,30) HTOT1, (RVS(II,LMBND1),RVB(II,LMBND1), RVPRNT42
43     1 RVV(II,LMBND1),RVT(II,LMBND1), II = 1, 1) RVPRNT43
44     GO TO 30000                                      RVPRNT44
45     C                                                RVPRNT45
46     2000 IF (.NOT. SPREAD) I = K1                   RVPRNT46
47     J = K1                                           RVPRNT47
48     II = NTMIN                                       RVPRNT48
49     2010 ITOTAL = ITOTAL - K1                       RVPRNT49
50     IF (ITOTAL .NE. 0) GO TO 2100                  RVPRNT50
51     ITOTAL = K40                                     RVPRNT51
52     GO TO 1                                          RVPRNT52
53     C                                                RVPRNT53
54     2020 WRITE (IPRT,13) HTOT1,MNBND,HTOT2,BMIDTH,HTOT3 RVPRNT54
55     GO TO 6                                          RVPRNT55
56     C                                                RVPRNT56
57     2100 IF (MOD(ITOTAL,K5) .EQ. 0) WRITE (IPRT,20) RVPRNT57
58     WRITE (IPRT,21) TIME(II), (RVS(K,LMBND1),RVB(K,LMBND1), RVPRNT58
59     1 RVV(K,LMBND1),RVT(K,LMBND1), K = J, 1) RVPRNT59
60     J = J + K1                                       RVPRNT60
61     J = J + K1                                       RVPRNT61
62     II = II + K1                                       RVPRNT62
63     IF (II .LE. NTHAX) GO TO 2010                 RVPRNT63
64     C                                                RVPRNT64
65     30000 RETURN                                     RVPRNT65
66     C                                                RVPRNT66
67     10 FORMAT (8A6,A4,9H IDC ,A6,6X,6HIDV , A6,7X,4HDATE,2A6,7X, RVPRNT67
68     1 4MPAGE,15,3M OF,15/                          RVPRNT68
69     2132MGV.S, KTS. C.C, YDS./SEC. F.O, KHZ. D.O, FT. S, DR. RVPRNT69
70     3XI, DEG. OMEGA, DEG./SEC. P.I., SEC. DEL. T, SEC. D. BTM.,RVPRNT70

```

APPENDIX G

G-43

I N D E X

SUBROUTINE RVPRNT

PAGE 40

71		4 FT./ F8.2,F15.2,F15.4,F13.4,F9.2,F10.3,F15.3,F16.4,F13.4,F17.4)	RVPRNT71
72	C		RVPRNT72
73		11 FORMAT (1H0, 2A6, A4, 3(13X,A6,F12.8,7X))	RVPRNT73
74	C		RVPRNT74
75		12 FORMAT (5X,2A6,17X,2A6,23X,3A6,13X,5A6/3X,2A6,3X,3(2X,6A6))	RVPRNT75
76	C		RVPRNT76
77		13 FORMAT (1H0,30X,4A6,14,2A6,A3,F6.3,3A6)	RVPRNT77
78	C		RVPRNT78
79		20 FORMAT (1X,F8.4,F9.4,3(2X,4F9.2))	RVPRNT79
80	C		RVPRNT80
81		21 FORMAT (F17.8,1X,3(2X,4F9.2))	RVPRNT81
82	C		RVPRNT82
83		30 FORMAT (1H0,3A6,A1,4F9.2,2(2X,4F9.2))	RVPRNT83
84		END	RVPRNT84

APPENDIX G

I N D E X

SUBROUTINE RVPRT

SYMBOL	-----	REFERENCES	-----	-----	-----	-----	-----	-----	-----	-----
1	-	16*	40	52						
2	-	32	38*							
3	-	29	39*							
4	-	36	42*							
5	-	21	25*							
6	-	23	27*	55						
10	-	17WR	67*							
11	-	22WR	25WR	73*						
12	-	27WR	75*							
13	-	54WR	77*							
20	-	30WR	33WR	57WR	79*					
21	-	58WR	81*							
30	-	42WR	83*							
2000	-	14	46*							
2010	-	49*	63							
2020	-	19	54*							
2100	-	28	50	57*						
30000	-	13	44	65*						
BNDOUT	-	11WR	33WR							
BWIDTH	-	54WR								
CO	-	18WR								
DO	-	18WR								
DDTTM	-	18WR								
DCORR1	-	3								
DCORR2	-	4								
DELT2	-	18WR								
FZRO	-	18WR								
MBAND	-	22WR	25WR							
NEB	-	17WR								
NOUPT	-	27WR								
NRVD	-	6DI	7DA	27WR						
NTIME	-	7DA	22WR	25WR						
NTOT1	-	42WR	54WR							
NTOT2	-	54WR								
NTOT3	-	54WR								
I	-	5CO	7DA	25WR	27WR	34WR	43WR	46*	59WR	60*
IDATE	-	17WR								
IDC	-	17WR								
IDV	-	17WR								
II	-	5CO	34WR	42WR	43WR	48*	58WR	62*	63	
IPEVRY	-	35								
IPLT	-	11WR								
IPRT	-	17WR	22WR	25WR	27WR	30WR	33WR	42WR	54WR	57WR
ITOTAL	-	9DA	49*	50	51*	57				58WR
J	-	5CO	15*	33WR	34WR	35*	36	47*	59WR	61*
K	-	5CO	11WR	12WR	22WR	25WR	27WR	29*	58WR	59WR
K1	-	16	29	32	46	47	49	60	61	62
K40	-	51								
K5	-	32	57							
K8	-	29								
KSID	-	18WR								
L	-	5CO	32*							
LMBND1	-	42WR	43WR	58WR	59WR					
MNBND	-	11WR	12WR	36	54WR					
MOD	-	57								
NOPRNT	-	13								
NPAGE	-	17WR								
NPSTR	-	15								
NTRAX	-	22WR	63							
NTRIN	-	11WR	22WR	25WR	48					
OREGAD	-	18WR								
PAGE	-	16*	17WR							
PING	-	18WR								
PLOT	-	11								
RETURN	-	65								
RVD	-	12WR	34WR	42WR	58WR					
RVPRT	-	1								
RVS	-	12WR	34WR	42WR	58WR					

APPENDIX G

I N D E X

SUBROUTINE RVPRT

RVT	-	12WR	34WR	43WR	59WR
RVV	-	12WR	34WR	43WR	59WR
S	-	18WR			
SPREAD	-	21	46		
TIME	-	11WR	22WR	25WR	58WR
TOTALS	-	14	19	28	
VS	-	18WR			

INDEX

BLOCK DATA FOR DOP

PAGE 43

1		BLOCK DATA	BLOCK 1
2	C	INCLUDE DCONM1	BLOCK 2
3		INCLUDE DCONM6	BLOCK 3
4			BLOCK 4
5	C		BLOCK 5
6		DATA K0/0/,K1/1/,K2/2/,K3/3/,K5/5/,K6/6/,K8/8/,K10/10/,K40/40/	BLOCK 6
7		DATA (TR8(I), I = 1,4)/.01,.05,.1,.2,.3,.4/,FPT5/.5/,	BLOCK 7
8		1 (TR82(I), I = 1,4)/.6,.7,.8,.9/,F1/1./,	BLOCK 8
9		2 (TR83(I), I = 1,4)/1.2,1.4,1.6,1.8/,F2/2./,F4/4./,F10/10./,	BLOCK 9
10		3 F20/20./,FLOG10/2-30258509/,INFMT/1.E38/	BLOCK 10
11		4 PI23/2.09439510/,PI/3.14159265/,TWOPI/6.28318531/,	BLOCK 11
12		5 DEGRAD/.0174532925/,SHIFT/0150400000000/,YDKT/1.77625736/,	BLOCK 12
13		6 F1E3/1000./,L064P1/10.9920986/,F1MIN/020077777777/,F3/3./,	BLOCK 13
14		7 F90/90./,F180/180./	BLOCK 14
15		DATA AR1/22/,DR1/28/,INPT/5/,IPRT/6/,IPLT/15/	BLOCK 15
16		DATA NEB/52N1PROGRAM 800003 -- DOPPLER CONTENT OF REVERBERATION /	BLOCK 16
17		DATA (HEADS(I), I = 1, 4)/30N DOPPLER BAND, KNOTS ,	BLOCK 17
18	1	30N FREQUENCY BAND, KILOHERTZ ,	BLOCK 18
19	2	30N PURE TONE AFTER SPREADING ,	BLOCK 19
20	3	30N ,	BLOCK 20
21	4	30N SPREAD WITH FILTER ,	BLOCK 21
22	5	30N SPREAD WITH TVG ,	BLOCK 22
23	6	30N SPREAD WITH FILTER AND TVG ,	BLOCK 23
24	7	36N KNOTS HERTZFROM- TO- TIME /	BLOCK 24
25		DATA (HTOT1(I), I = 1, 4)/24HTOTAL REVERBERATION FROM/	BLOCK 25
26		DATA (HTOT2(I), I = 1, 3)/18N BANDS, EACH OF /	BLOCK 26
27		DATA (HTOT3(I), I = 1, 3)/18N BANDWIDTH /	BLOCK 27
28		DATA ITABMN/1/,IPEVRV/1/	BLOCK 28
29	C		BLOCK 29
30		DATA NNAMES/40/,NANCHT/24 * 0/,LFLAGS/16 * .FALSE./	BLOCK 30
31		DATA ((NANDAT(I,J), J = 1, 3), I = 1, 40)/	BLOCK 31
32	A	6NIDC , 0, 4,6NDATE , 1, 2,6NIDV , 3, 1,BLOCK 32	
33	B	6NID , 4, 1,6NCO , 5, 1,6NHALPHC , 6, 1,BLOCK 33	
34	C	6NPING , 7, 1,6NDBYTH , 8, 1,6NLOGRV , 9, 1,BLOCK 34	
35	D	6NS , 10, 1,6NXI , 11, 1,6NVS , 12, 1,BLOCK 35	
36	E	6NBWIDTH, 13, 1,6NDELT , 14, 1,6NFO , 15, 1,BLOCK 36	
37	F	6NDBEAR , 16, 1,6NOMEGA , 17, 1,6NTNTRAX, 18, 1,BLOCK 37	
38	G	6NPULSE , 19, 1,6NPRINTE, 20, 1, BLOCK 38	
39	H	6NTIME ,21,400,6NSSPREB,421,150,6NBSPREB,571,150,BLOCK 39	
40	I	6NVS PREB,721,150, BLOCK 40	
41	J	6NCENTER, 0, 1,6NCO , 0, 1,6NEND , 0,1,BLOCK 41	
42	K	6NFILTER, 0, 1,6NKNOTS , 0, 1,6NNOBOTT, 0,1,BLOCK 42	
43	L	6NNOPRIN, 0, 1,6NNOSURF, 0, 1,6NNOTAPE, 0,1,BLOCK 43	
44	M	6NNOVOLU, 0, 1,6NPLOT , 0, 1,6NSPREAD, 0,1,BLOCK 44	
45	N	6NTIRECO, 0, 1,6NTOTALS, 0, 1,6NTVG , 0,1,BLOCK 45	
46	O	6NRELATI, 0, 1/ BLOCK 46	
47		END	BLOCK 47

SYMBOL	REFERENCES
AR1	150A
BR1	150A
DCOMM1	3
DCOMM6	4
DEGRAD	120A
F1	80A
F10	90A
F180	140A
FTE3	130A
FININ	130A
F2	90A
F20	100A
F3	130A
F4	90A
F90	140A
FLOG10	100A
FPT5	70A
HEADS	170A
HED	160A
HTOT1	250A
HTOT2	260A
HTOT3	270A
I	70A 80A 90A 170A 250A 260A 270A 310A
INFNT	100A
INPT	150A
IPEVRY	280A
IPLT	150A
IPRT	150A
ITABRN	280A
J	310A
K0	60A
K1	60A
K10	60A
K2	60A
K3	60A
K40	60A
K5	60A
K6	60A
K8	60A
LFLAGS	300A
LOG4PI	130A
NAMCNT	300A
NAMDAT	310A
NNAMES	300A
PI	110A
PI23	110A
SHIFT	120A
TRS	70A
TRS2	80A
TRS3	90A
TUOP1	110A
YDKT	120A
10LCK	1

## INDEX

PAGE 45

1		FUNCTION FCNS(ARG)	FCNS 1
2	C		FCNS 2
3		ENTRY OXL (IFLAG,COSA,COSB,COSC)	FCNS 3
4	C		FCNS 4
5	C	NBEAM = 0 FOR NARROW BEAM	FCNS 5
6	C	= 1 FOR BROAD BEAM	FCNS 6
7	C	IFLAG = 0 FOR RECEIVE	FCNS 7
8	C	= 1 FOR TRANSMIT	FCNS 8
9	C		FCNS 9
10		COMMON /CINPUT/ X(16), NBEAM	FCNS 10
11	C		FCNS 11
12		A = ACOS(COSA)	FCNS 12
13		FCNS = 10**(-2.*A)	FCNS 13
14		IF (IFLAG .EQ. 0) GO TO 1	FCNS 14
15		FCNS = FCNS * COS(A*2.0)**2	FCNS 15
16		IF (NBEAM .NE. 0) RETURN	FCNS 16
17		FCNS = FCNS * ABS(COSA)	FCNS 17
18		1 FCNS = FCNS * COS(A*4.0)**2	FCNS 18
19		RETURN	FCNS 19
20	C		FCNS 20
21		ENTRY RRF(FREQ)	FCNS 21
22	C		FCNS 22
23		FCNS = 1. - (FREQ/31.4159)**4	FCNS 23
24		RETURN	FCNS 24
25	C		FCNS 25
26		ENTRY TVGF(TIME)	FCNS 26
27	C		FCNS 27
28		FCNS = 0.1 + .9 * TIME/2.	FCNS 28
29		RETURN	FCNS 29
30		END	FCNS 30

I N D E X		FUNCTION FCNS(ARG)			
SYMBOL	-----	REFERENCES -----			
1	- 14	18*			
A	- 12*	13	15	18	
ABS	- 17				
ACOS	- 12				
ARG	- 1AG				
CINPUT	- 10CL				
CCS	- 15	18			
COSA	- 3	12	17		
COSB	- 3				
COSC	- 3				
FCNS	- 13*	15*	17*	18*	
FCNS	- 1	23*	28*		
FREQ	- 21	23			
IFLAG	- 3	14			
NDIAR	- 10CO	16			
OXL	- 3				
RETURN	- 16	19	24	29	
RRF	- 21				
TIME	- 26	28			
TVGF	- 26				
X	- 10CO				

APPENDIX G

I N D E X	PAGE 47	
1	SUBROUTINE SORT(ARRAY,LENGTH)	SORT 1
2	DIMENSION ARRAY(1)	SORT 2
3	C	SORT 3
4	SORT IN ASCENDING ORDER (SIMPLE REPLACEMENT SORT)	SORT 4
5	C	SORT 5
6	IF (LENGTH .LE.1) GO TO 4	SORT 6
7	DO 2 J = 2,LENGTH	SORT 7
8	IF (ARRAY(J) .GE. ARRAY(J-1)) GO TO 2	SORT 8
9	TEMP = ARRAY(J)	SORT 9
10	I = J	SORT 10
11	C	SORT 11
12	1 ARRAY(I) = ARRAY(I-1)	SORT 12
13	I = I - 1	SORT 13
14	IF ((I .GT. 1) .AND. (TEMP .LT. ARRAY(I-1))) GO TO 1	SORT 14
15	ARRAY(I) = TEMP	SORT 15
16	2 CONTINUE	SORT 16
17	C	SORT 17
18	REMOVE DUPLICATE ENTRIES	SORT 18
19	C	SORT 19
20	DO 3 I = 2, LENGTH	SORT 20
21	IF (ARRAY(I) .EQ. ARRAY(I-1)) GO TO 5	SORT 21
22	3 CONTINUE	SORT 22
23	4 RETURN	SORT 23
24	C	SORT 24
25	5 J = LENGTH	SORT 25
26	LENGTH = I - 1	SORT 26
27	6 IF (I .GE. J) GO TO 4	SORT 27
28	I = I + 1	SORT 28
29	IF (ARRAY(I) .EQ. ARRAY(I-1)) GO TO 6	SORT 29
30	LENGTH = LENGTH + 1	SORT 30
31	ARRAY(LENGTH) = ARRAY(I)	SORT 31
32	GO TO 6	SORT 32
33	C	SORT 33
34	END	SORT 34

## APPENDIX G

I N D E X		SUBROUTINE SORT(ARRAY,LENGTH)									
SYMBOL		REFERENCES									
1	-	12*	14								
2	-	7	8	16*							
3	-	20	22*								
4	-	6	23*	27							
5	-	21	25*								
6	-	27*	29	32							
ARRAY	-	1AG	2DI	8	9	12*	14	15*	21	29	31*
I	-	10*	12	13*	14	15	20*	21	26	27	28*
		29	31								
J	-	7*	8	9	10	25*	27				
LENGTH	-	1AG	6	7	20	25	26*	30*	31		
RETURN	-	23									
SORT	-	1									
TEMP	-	9*	14	15							

## I N D E X

PAGE 49

1		FUNCTION TABLKP(ARG,INDEP,DEPND,ITABMN,ITABMX)	TABLKP 1
2	C		TABLKP 2
3		COMMON /CTBLKP/ DELIND,DELDEP,FACTOR,ITABLE	TABLKP 3
4		DIMENSION INDEP(1),DEPND(1)	TABLKP 4
5		REAL INDEP	TABLKP 5
6	C		TABLKP 6
7		DELIND = INDEP(2) - INDEP (1)	TABLKP 7
8		DO 3 ITABLE = ITABMN, ITABMX	TABLKP 8
9		FACTOR = ARG - INDEP(ITABLE)	TABLKP 9
10		IF (FACTOR * DELIND) 5, 6, 3	TABLKP10
11	3	CONTINUE	TABLKP11
12	4	ITABLE = 0	TABLKP12
13		GO TO 7	TABLKP13
14	C		TABLKP14
15	5	IF (ITABLE .EQ. 1) GO TO 4	TABLKP15
16		DELIND = INDEP(ITABLE) - INDEP(ITABLE-1)	TABLKP16
17		FACTOR = FACTOR/DELIND	TABLKP17
18	C		TABLKP18
19	6	TABLKP = AINTRP(DEPND)	TABLKP19
20	7	RETURN	TABLKP20
21		END	TABLKP21

## APPENDIX G

I N D E X

FUNCTION TABLEP(ARG,INDEP,DEPND,ITADRN,ITABRX)

SYMBOL	REFERENCES				
3	8	10	11*		
4	12*	15			
5	10	15*			
6	10	19*			
7	13	20*			
AINTRP	19				
ARG	1AG	9			
CTBLKP	3CL				
DELDEP	3CO				
DELIND	3CO	7=	10	16=	17
DEPND	1AG	4DI	19		
FACTOR	3CO	9=	10	17=	
INDEP	1AG	4DI	5RL	7	9
ITABLE	3CO	8=	9	12=	15
ITADRN	1AG	8			16
ITABRX	1AG	8			16
RETURN	20				
TABLEP	1	19=			

## INDEX

PAGE 51

1		FUNCTION AINTRP(DEPND)	AINTRP 1
2	C		AINTRP 2
3		COMMON /CTBLKP/ DELIND,DELDEP,FACTOR,ITABLE	AINTRP 3
4		DIMENSION DEPND(1)	AINTRP 4
5	C		AINTRP 5
6		IF (FACTOR .NE. 0.) GO TO 1	AINTRP 6
7		AINTRP = DEPND(ITABLE)	AINTRP 7
8		GO TO 2	AINTRP 8
9	C		AINTRP 9
10		1 DELDEP = DEPND(ITABLE) - DEPND(ITABLE-1)	AINTRP10
11		AINTRP = DEPND(ITABLE) + DELDEP * FACTOR	AINTRP11
12		2 RETURN	AINTRP12
13		END	AINTRP13

APPENDIX G

G-55

PAGE 52

I N D E X	FUNCTION AINTRP(DEPND)				
SYMBOL	REFERENCES				
1	-	6	10*		
2	-	8	12*		
AINTRP	-	1	7*	11*	
CTBLEP	-	3CL			
DELDEP	-	3CO	10*	11	
DELIND	-	3CO			
DEPND	-	1AG	401	7	10 11
FACTOR	-	3CO	6	11	
ITABLE	-	3CO	7	10	11
RETURN	-	12			

APPENDIX G

## INDEX

PAGE 53

1		SUBROUTINE INPUT(NARTAB,DATA,INPFLG,OUTFLG)	INPUT 1
2	C		INPUT 2
3		COMMON /CINCOB/ INAP,IIMAGE,IMAGE(80),IBLANK,NUMBER(21)	INPUT 3
4		EQUIVALENCE (IQUOTE,NUMBER(17)),(ICOMMA,NUMBER(20))	INPUT 4
5		EQUIVALENCE (IEQUAL,NUMBER(21))	INPUT 5
6		COMMON /CMACHN/ NWORD,NCHAR,MAXCOL	INPUT 6
7	C		INPUT 7
8		LOGICAL BCDFLG,DECPY,EXPNT,CXDOTM,OUTFLG,LVALUE,LTRUE	INPUT 8
9		DOUBLE PRECISION VALUE,D10	INPUT 9
10		DIMENSION NARTAB(1),DATA(1),AVALUE(1)	INPUT 10
11		EQUIVALENCE (VALUE,AVALUE,IVALUE,LVALUE,NAME),(I,IIMAGE),	INPUT 11
12	1	(NTRUE,LTRUE)	INPUT 12
13	1	DATA ITYPE/0/,J/3/,ITRUE/5/NTRUE./,D10/1.D1/,FRMAT1/6H(80A1)/,	INPUT 13
14	1	LTRUE/.TRUE./	INPUT 14
15	C		INPUT 15
16	C	ITYPE = 1, INTEGER (NO DECIMAL POINT)	INPUT 16
17	C	ITYPE = 2, REAL (WITH OR WITHOUT EXPONENT)	INPUT 17
18	C	ITYPE = 3, DOUBLE PRECISION (D-TYPE EXPONENT)	INPUT 18
19	C	ITYPE = 4, COMPLEX (TWO REAL NUMBERS IN PARENTHESES)	INPUT 19
20	C	ITYPE = 5, LOGICAL (.TRUE. OR .FALSE. ONLY)	INPUT 20
21	C	ITYPE = 6, ALPHAMERIC (ENCLOSED IN APOSTROPHES, THUS 'ABC')	INPUT 21
22	C		INPUT 22
23		GO TO (1260, 1600, 1030, 2000), J	INPUT 23
24	1030	READ FRMAT1, IMAGE	INPUT 24
25		IF (OUTFLG) PRINT 2001, IMAGE	INPUT 25
26		I = 0	INPUT 26
27		GO TO 1600	INPUT 27
28	1100	I = I + 1	INPUT 28
29		IF (ITYPE .EQ. 6) GO TO 1160	INPUT 29
30		IF (IMAGE(I) .EQ. IBLANK) GO TO 1900	INPUT 30
31		IF (IMAGE(I) .NE. ICOMMA) GO TO (1130, 1110), J	INPUT 31
32	1105	GO TO (1200, 1400), J	INPUT 32
33	1110	DO 1120 K = 1, 19	INPUT 33
34		IF (IMAGE(I) .NE. NUMBER(K)) GO TO 1120	INPUT 34
35		IF (K .LT. 18) GO TO 1300	INPUT 35
36		IF (DECPY) GO TO 1300	INPUT 36
37	1120	CONTINUE	INPUT 37
38		IF (L + NAME .NE. 0) GO TO 1995	INPUT 38
39		J = 1	INPUT 39
40		IF (DECPY) ITYPE = 5	INPUT 40
41	1130	IF (IMAGE(I) .EQ. IEQUAL) GO TO 1200	INPUT 41
42	1140	IF (L .LT. NWORD) GO TO 1150	INPUT 42
43		IF (ITYPE .NE. 6) GO TO (1900, 1210), J	INPUT 43
44		IF (BCDFLG) I = I - 1	INPUT 44
45		GO TO (1500, 1210), J	INPUT 45
46	1150	FLD(L,NCHAR,NAME) = FLD(0,NCHAR,IMAGE(I))	INPUT 46
47		L = L + NCHAR	INPUT 47
48		GO TO (1900, 1140), J	INPUT 48
49	1160	IF (BCDFLG) GO TO 1170	INPUT 49
50		IF (IMAGE(I) .EQ. ICOMMA) GO TO 1200	INPUT 50
51		GO TO 1900	INPUT 51
52	1170	IF (IMAGE(I) .NE. IQUOTE) GO TO 1140	INPUT 52
53		NQT = 1 - NQT	INPUT 53
54		IF (NQT .EQ. 0) GO TO 1140	INPUT 54
55		IF (IMAGE(I+1) .NE. IQUOTE) BCDFLG = .FALSE.	INPUT 55
56		GO TO 1900	INPUT 56
57	1200	J = 2	INPUT 57
58		K = I	INPUT 58
59		I = 81	INPUT 59
60		GO TO 1140	INPUT 60
61	1210	I = K	INPUT 61
62		IF (ITYPE .GE. 5) GO TO 1500	INPUT 62
63		NNAMES = NARTAB(1)	INPUT 63
64		INPFLG = 0	INPUT 64
65		NANSV = NAME	INPUT 65
66		DO 1220 K = 1, NNAMES	INPUT 66
67		IF (NAME .NE. NARTAB(K+1)) GO TO 1220	INPUT 67
68		IF (ITYPE .EQ. 0) GO TO 1260	INPUT 68
69		J = 1	INPUT 69
70		GO TO 1999	INPUT 70

## APPENDIX G

71	1220	CONTINUE	INPUT 71
72		GO TO 1996	INPUT 72
73	1260	NL = NNARES + K + 1	INPUT 73
74		NM = NNARES + NL	INPUT 74
75		NC = NNARES + NM	INPUT 75
76		NARTAB(NC) = 0	INPUT 76
77		IF (IPAGE(1) .EQ. IEQUAL) GO TO 1600	INPUT 77
78		J = 2	INPUT 78
79		NARTAB(NC) = NTRUE	INPUT 79
80		GO TO 1998	INPUT 80
81	1300	IF (K .GT. 10) GO TO 1320	INPUT 81
82		IF (.NOT. EXPNT) GO TO 1310	INPUT 82
83		IEXP = IEXP + 10 + SIGN(K - 1, IESIGN)	INPUT 83
84		GO TO 1900	INPUT 84
85	1310	IF (DECPY) L = L + 1	INPUT 85
86		VALUE = VALUE + DTG * DBLE(FLOAT(SIGN(K - 1, IVSIGN)))	INPUT 86
87		GO TO 1900	INPUT 87
88	1320	K = K - 10	INPUT 88
89		GO TO (1330, 1330, 1350, 1360, 1380, 1900, 1390, 1325, 1335),K	INPUT 89
90	1325	ITYPE = 3	INPUT 90
91	1330	IF (.NOT. DECPY) GO TO 1340	INPUT 91
92		IF (K .EQ. 2) IESIGN = - 1	INPUT 92
93	1335	EXPNT = .TRUE.	INPUT 93
94		GO TO 1900	INPUT 94
95	1340	IF (K .EQ. 2) IVSIGN = - 1	INPUT 95
96		GO TO 1900	INPUT 96
97	1350	DECPY = .TRUE.	INPUT 97
98		ITYPE = 2	INPUT 98
99		GO TO 1900	INPUT 99
100	1360	IREPT = VALUE	INPUT100
101		GO TO 1620	INPUT101
102	1380	ITYPE = 4	INPUT102
103		GO TO 1900	INPUT103
104	1390	ITYPE = 6	INPUT104
105		BCDFLG = .TRUE.	INPUT105
106		J = 1	INPUT106
107		NOT = 0	INPUT107
108		GO TO 1900	INPUT108
109	1400	IF (INPFLG .NE. 0) GO TO 1600	INPUT109
110		L = IEXP - L	INPUT110
111		IEXP = ABS(L)	INPUT111
112		DO 1430 K = 1, IEXP	INPUT112
113		IF (L) 1410, 1440, 1420	INPUT113
114	1410	VALUE = VALUE/DTG	INPUT114
115		GO TO 1430	INPUT115
116	1420	VALUE = VALUE * DTG	INPUT116
117	1430	CONTINUE	INPUT117
118	1440	IF (ITYPE .NE. 4) GO TO 1500	INPUT118
119		IF (CXBOTH) GO TO 1500	INPUT119
120		CXVAL = VALUE	INPUT120
121		CXBOTH = .TRUE.	INPUT121
122		GO TO 1610	INPUT122
123	1500	IF (INPFLG .NE. 0) GO TO 1600	INPUT123
124		DO 1590 K = 1, IREPT	INPUT124
125	1505	INDEX = NARTAB(NC) + 1	INPUT125
126		IF (INDEX .GT. NARTAB(NM)) GO TO 1997	INPUT126
127		NARTAB(NC) = INDEX	INPUT127
128		INDEX = INDEX + NARTAB(NL)	INPUT128
129		GO TO (1520, 1530, 1540, 1540, 1560, 1580, 1570), ITYPE	INPUT129
130	1520	IVALUE = VALUE	INPUT130
131	1525	DATA(INDEX) = AVALUE(1)	INPUT131
132		GO TO 1590	INPUT132
133	1530	DATA(INDEX) = VALUE	INPUT133
134		GO TO 1590	INPUT134
135	1540	INDEX = INDEX + NARTAB(NC) - 1	INPUT135
136		IF (ITYPE .EQ. 4) GO TO 1550	INPUT136
137		DATA(INDEX+1) = AVALUE(2)	INPUT137
138		GO TO 1525	INPUT138
139	1550	DATA(INDEX) = CXVAL	INPUT139
140		DATA(INDEX+1) = VALUE	INPUT140

I N D E X

SUBROUTINE INPUT(NAMTAB,DATA,INPFLG,OUTFLG)

PAGE 55

141	GO TO 1590	INPUT141
142	1560 LVALUE = .FALSE.	INPUT142
143	IF (NAME .EQ. ITRUE) LVALUE = .TRUE.	INPUT143
144	GO TO 1525	INPUT144
145	1570 M = INDEX - IEXP	INPUT145
146	DATA(INDEX) = DATA(M)	INPUT146
147	IF (M .EQ. L) GO TO 1585	INPUT147
148	GO TO 1505	INPUT148
149	1580 DATA(INDEX) = AVALUE(1)	INPUT149
150	IEXP = IEXP + 1	INPUT150
151	IF (BCDFLG) GO TO 1610	INPUT151
152	ITYPE = 7	INPUT152
153	1585 L = INDEX	INPUT153
154	1590 CONTINUE	INPUT154
155	1600 CXBOTH = .FALSE.	INPUT155
156	IREPT = 1	INPUT156
157	J = 2	INPUT157
158	K = 0	INPUT158
159	ITYPE = 1	INPUT159
160	1610 L = 0	INPUT160
161	IEXP = 0	INPUT161
162	IESIGN = 0	INPUT162
163	IVSIGN = 0	INPUT163
164	DEPT = .FALSE.	INPUT164
165	EXPNT = .FALSE.	INPUT165
166	1620 VALUE = 0.	INPUT166
167	1900 IF (I .LT. MAXCOL) GO TO 1100	INPUT167
168	IF (K .NE. 0) GO TO 1105	INPUT168
169	GO TO 1030	INPUT169
170	1995 IF (INPFLG .NE. 0) GO TO 1900	INPUT170
171	INPFLG = 1	INPUT171
172	1996 INPFLG = 1 + INPFLG	INPUT172
173	1997 INPFLG = 1 + INPFLG	INPUT173
174	J = 4	INPUT174
175	1998 ITYPE = 0	INPUT175
176	1999 RETURN	INPUT176
177	2000 IF (INPFLG .EQ. 0) GO TO 1600	INPUT177
178	IF (.NOT. OUTFLG) PRINT 2001, IMAGE	INPUT178
179	2001 FORMAT (20X,20A1)	INPUT179
180	DO 2010 J = 1, 50	INPUT180
181	IMAGE(J) = IBLANK	INPUT181
182	2010 CONTINUE	INPUT182
183	IMAGE(IIMAGE) = NUMBER(14)	INPUT183
184	PRINT 2001, IMAGE	INPUT184
185	J = 2	INPUT185
186	GO TO (2020, 2030, 2040), INPFLG	INPUT186
187	2020 PRINT 2021, NAMSAV	INPUT187
188	2021 FORMAT (20X, 17H100 MUCH DATA IN , A67)	INPUT188
189	GO TO 1999	INPUT189
190	2030 PRINT 2031, NAMSAV	INPUT190
191	2031 FORMAT (20X, A6, 17H NOT IN NAME LIST//)	INPUT191
192	GO TO 1999	INPUT192
193	2040 PRINT 2041	INPUT193
194	2041 FORMAT (20X, 33HSYNTAX ERROR OR ILLEGAL CHARACTER//)	INPUT194
195	GO TO 1999	INPUT195
196	END	INPUT196

APPENDIX G

I N D E X

SUBROUTINE INPUT(NAMTAB,DATA,INPFLG,OUTFLG)

SYMBOL	-----	REFERENCES	-----	-----	-----	-----	-----	-----	-----	-----
103C	- 23	24*	169							
1100	- 28*	167								
1105	- 32*	168								
1110	- 31	33*								
1120	- 33	34	37*							
1130	- 31	41*								
114C	- 42*	48	52	54	60					
1150	- 42	46*								
116C	- 29	49*								
117C	- 49	52*								
1200	- 32	41	50	57*						
1210	- 43	45	61*							
1220	- 66	67	71*							
1260	- 23	68	73*							
1300	- 35	36	81*							
1310	- 82	85*								
1320	- 81	88*								
1325	- 89	90*								
1330	- 89	91*								
1335	- 89	93*								
1340	- 91	95*								
1350	- 89	97*								
1360	- 89	100*								
1380	- 89	102*								
1390	- 89	104*								
1400	- 32	109*								
1410	- 113	114*								
1420	- 113	116*								
1430	- 112	115	117*							
1440	- 113	118*								
1500	- 45	62	118	119	123*					
1505	- 125*	146								
1520	- 129	130*								
1525	- 131*	138	144							
1530	- 129	133*								
1540	- 129	135*								
1550	- 136	139*								
1560	- 129	142*								
1570	- 129	145*								
1580	- 129	149*								
1585	- 147	153*								
1590	- 124	132	134	141	154*					
1600	- 23	27	77	109	123	155*	177			
1610	- 122	151	160*							
1620	- 101	166*								
1900	- 30	43	48	51	56	84	87	89	94	96
	99	103	108	167*	170					
1995	- 38	170*								
1996	- 72	172*								
1997	- 126	173*								
1998	- 80	175*								
1999	- 70	176*	189	192	195					
2000	- 23	177*								
2001	- 25PR	178PR	179*	184PR						
2010	- 180	182*								
2020	- 186	187*								
2021	- 187PR	188*								
2030	- 186	190*								
2031	- 190PR	191*								
2040	- 186	193*								
2041	- 193PR	194*								
ABS	- 111									
AVALUE	- 1001	11E0	131	137	149					
BCDFLG	- 8L6	44	49	55*	105*	151				
CJNCDD	- 3CL									
CMACMN	- 6CL									
CXBOTh	- 8L6	119	121*	155*						
CXVAL	- 120*	139								

APPENDIX G

I N D E X		SUBROUTINE INPUT(NARTAB,DATA,INPFLG,OUTFLG)										PAGE 57										
D10	-	9DB	13DA	86	114	116																
DATA	-	1AG	10DI	131=	133=	137=	139=	140=	146=	149=												
DPLE	-	86																				
DEPRT	-	8LG	36	4G	85	91	97=	164=														
EXPNT	-	8LG	82	93=	165=																	
FLD	-	46=																				
FLOAT	-	86																				
FRMAT1	-	13DA	24RD																			
I	-	11EQ	26=	28=	30	31	34	41	44=	50	52											
		55	58	59=	61=	77	167															
IBLANK	-	3CO	30	181																		
ICORNA	-	4EQ	31	50																		
IEQUAL	-	5EQ	41	77																		
IESIGN	-	83	92=	162=																		
IEAP	-	83=	11C	111=	112	145	150=	161=														
IIMAGE	-	3CO	11EQ	183																		
IMAGE	-	3CO	24RD	25PR	30	31	34	41	50	52	55											
		77	178PR	181=	183=	184PR																
INAM	-	3CO																				
INDEX	-	125=	126	127	128=	131	133	135=	137	139	140											
		145	146	149	153																	
INPFLG	-	1AG	64=	109	123	170	171=	172=	173=	177	186											
INPUT	-	1																				
IQUOTE	-	4EQ	52	55																		
IREFP	-	10J=	124	156=																		
ITRUE	-	13DA	143																			
ITYPE	-	13DA	29	40=	43	62	68	90=	98=	102=	104=											
		118	129	136	152=	159=	175=															
IVALUE	-	11EQ	130=																			
IVSIGN	-	86	95=	163=																		
J	-	13DA	23	31	32	39=	43	45	48	57=	69=											
		7J=	106=	157=	174=	180=	181	185=														
K	-	33=	34	35	58=	61	66=	67	73	81	83											
		86	88=	89	92	95	112=	124=	158=	168												
L	-	38	42	46	47=	85=	110=	111	112	147	153=											
		160=																				
LTRUE	-	8LG	12EQ	14DA																		
LVALUE	-	3LG	11EQ	142=	143=																	
M	-	145=	146	147																		
MAXCOL	-	6CO	167																			
NAME	-	11EQ	38	46	65	67	143															
NARSAV	-	65=	187PR	190PR																		
NARTAB	-	1AG	10DI	63	67	76=	79=	125	126	127=	128											
		135																				
NC	-	75=	76	79	125	127	135															
NCHAR	-	6CO	46	47																		
NL	-	73=	74	128																		
NM	-	74=	75	126																		
NNAMES	-	63=	66	73	74	75																
NOT	-	53=	54	107=																		
NTRUE	-	12EQ	79																			
NUMBER	-	3CO	4EQ	5EQ	34	183																
WORD	-	6CO	42																			
OUTFLG	-	1AG	8LG	25	178																	
RETURN	-	176																				
SIGN	-	93	86																			
VALUE	-	9DB	11EQ	86=	100	114=	116=	120	130	133	140											
		166=																				

APPENDIX G

I N D E X

BLOCK DATA FOR INPUT SUBROUTINE

PAGE 58

1	BLOCK DATA	BLOCK 1
2	COMMON /CINCO/ INAM,IIMAGE,IMAGE(80),IBLANK,NUMBER(21)	BLOCK 2
3	DATA IBLANK/1H /	BLOCK 3
4	DATA (NUMBER(I),I=1,21)/1H0,1H1,1H2,1H3,1H4,1H5,1H6,1H7,1H8,1H9,	BLOCK 4
5	1H0,1H-,1H.,1H=,1H(,1H),1H",1H\$,1H%,1H^,1H#	BLOCK 5
6		BLOCK 6
7	C NOTE THAT THE FOLLOWING DATA IS MACHINE DEPENDENT.	BLOCK 7
8	C NWORD = NO.OF BITS IN MACHINE WORD.	BLOCK 8
9	C NCHAR = NO.OF BITS IN ALPHA-NUMERIC CHARACTER.	BLOCK 9
10	C MAXCOL = NO.OF COLUMNS TO BE READ FROM CARDS.	BLOCK 10
11		BLOCK 11
12	COMMON /CRACHN/ NWORD,NCHAR,MAXCOL	BLOCK 12
13	DATA NWORD/36/,NCHAR/6/,MAXCOL/80/	BLOCK 13
14	END	BLOCK 14

APPENDIX G

I N D E X

BLOCK DATA FOR INPUT SUBROUTINE

SYMBOL	REFERENCES
CINCOB -	2CL
CPACHN -	12CL
I -	4DA
IBLANK -	2CO 3BA
IIMAGE -	2CO
IPAGE -	2CO
INAM -	2CO
PARCOL -	12CO 13BA
NCHAR -	12CO 13BA
NUMBR -	2CO 4DA
NWORD -	12CO 13BA
TBLCR0 -	1

SYMBOL	ROUTINES IN WHICH THE SYMBOL IS USED						
A	- FNCNS	RBCOMP	RBSORT				
A1	- RVCORP						
A2	- RVCORP						
ABS	- BCOMP	FNCNS	INPUT	RBCOMP	RBSORT	RVCORP	RVSPRD
ACOS	- FNCNS						
AINT	- BCOMP						
AINTRP	- RBCOMP	TABLKP					
ALOG10	- RTCOMP						
ALPHC	- DCONN1	RVCORP					
AMAX1	- RBCOMP	RVCORP					
AMIN1	- RBCOMP						
AMOD	- RBCOMP	RVCORP					
AR1	- DCONN1	IDENT	RBSORT	1BLCK	1MAIN		
ARG	- FNCNS	RBCOMP	TABLKP				
ARRAY	- SORT						
ATAN2	- RBCOMP						
AVALUE	- INPUT						
B	- BCOMP	RVCORP					
BAND	- BCOMP	DCONN1	RBCOMP	RVCORP			
BCBFLG	- INPUT						
BCORP	- 1MAIN						
BND	- BCOMP						
BNDOUT	- BCOMP	DCONN1	RVPRT				
BR1	- DCONN1	IDENT	RBCOMP	RBSORT	TCOMP	1BLCK	1MAIN
BW10TH	- DCONN1	IDENT	RVPRT				
BWINT	- BCOMP	DCONN1	IDENT				
CD	- DCONN1	IDENT	RVCORP	RVPRT			
CDRT	- BCOMP	DCONN1	IDENT	RBCOMP			
CALFAP	- RBCOMP						
CALFBP	- RBCOMP						
CBAND	- DCONN1						
CCOUNT	- DCONN1						
CENTER	- BCOMP	DCONN1					
CFNST	- DCONN1						
CGAPAP	- RBCOMP						
CGARBP	- RBCOMP						
CNCNST	- DCONN1						
CINCOB	- INPUT	1BLCKD					
CINDAT	- DCONN1						
CINDEF	- DCONN1						
CINPUT	- DCONN1	FNCNS					
CMACHN	- INPUT	1BLCKD					
CNT	- BCOMP						
CONTRU	- RBCOMP						
COS	- BCOMP	FNCNS	IDENT	RBCOMP	RVCORP		
COSA	- FNCNS	RBCOMP					
COSB	- FNCNS	RBCOMP					
COSC	- FNCNS						
COSORT	- DCONN5	RBCOMP					
COSTHA	- DCONN5	RBCOMP					
COSTNB	- DCONN5	RBCOMP					
CPRINT	- DCONN1						
CSA	- RVCORP						
CSALFA	- RBCOMP						
CSALFB	- RBCOMP						
CSBETA	- RBCOMP						
CSBETB	- RBCOMP						
CSGANA	- RBCOMP						
CSGAMB	- RBCOMP						
CSKSI	- DCONN1	IDENT	RBCOMP	RVCORP			
CSOPTB	- RBCOMP						
CSORTF	- RVCORP						
CSPI1	- RVCORP						
CSPREB	- DCONN1						
CSTNAB	- RBCOMP						
CSTNDB	- RBCOMP						
CTAPE	- DCONN1						
CTBLKP	- AINTRP	DCONN1	TABLKP				

I N D E X

\*\*\*\*\* SUPER INDEX \*\*\*\*\*

CTHTR1	-	RBCOMP						
CR00TH	-	INPUT						
CRNST	-	DCOMN1						
CRVAL	-	INPUT						
D	-	RBCOMP	RESORT	RVCOMP				
DD	-	DCOMN1	FLFRNT					
DIG	-	INPUT						
DATA	-	INPUT						
DPLE	-	INPUT						
DBTTP	-	DCOMN1	RESORT	RVPRNT				
DCOMN1	-	RBCOMP	IDENT	RBCOMP	RESORT	RTCOMP	RVCOMP	RVPRAT
		TCOMP	1BLCK	1MAIN				RVSPRD
DCOMN2	-	RBCOMP	RTCOMP	RVCOMP				
DCOMN3	-	RBSORT	TCOMP					
DCOMN4	-	RVCOMP						
DCOMN5	-	RBCOMP						
DCOMN6	-	1ELCK						
DD	-	RBCOMP	RVCOMP					
DECPY	-	INPUT						
DEGRAD	-	RBCOMP	DCOMN1	IDENT	RBCOMP	1BLCK		
DELDEP	-	AINTRP	DCOMN1					
DELIND	-	DCOMN1	TARLKP					
DELR	-	RBCOMP						
DELT	-	DCOMN1	IDENT	RBCOMP	RVCOMP	TCOMP		
DELT2	-	DCOMN1	IDENT	RVPRNT				
DEPND	-	AINTRP	TARLKP					
DOP	-	DCOMN5	RBCOMP					
DOPSKP	-	RBCOMP						
DR	-	DCOMN1	IDENT	RVCOMP				
E	-	RBCOMP						
END	-	DCOMN1	IDENT	1MAIN				
EXP	-	IDENT	RBCOMP	RVCOMP				
EXPNT	-	INPUT						
EXPS	-	DCOMN1	IDENT	RVCOMP				
F	-	RBCOMP						
FC	-	DCOMN1	RBCOMP	RVCOMP				
F1	-	RBCOMP	DCOMN1	IDENT	RBCOMP	RTCOMP	RVCOMP	1BLCK
F10	-	DCOMN1	IDENT	RTCOMP	1BLCK			
F100	-	RBCOMP	DCOMN1	IDENT	1BLCK			
F1E3	-	DCOMN1	IDENT	1BLCK				
F1RIN	-	DCOMN1	1BLCK					
F2	-	DCOMN1	IDENT	RBCOMP	1BLCK			
F20	-	DCOMN1	RBCOMP	1BLCK				
F3	-	DCOMN1	1BLCK					
F4	-	DCOMN1	IDENT	1ELCK				
F90	-	RBCOMP	DCOMN1	IDENT	RBCOMP	1BLCK		
FA	-	RBCOMP						
FACTOR	-	AINTRP	DCOMN1	TARLKP				
FCC3	-	DCOMN1	IDENT	RVCOMP				
FCCVS	-	DCOMN1	IDENT	RBCOMP	RVCOMP			
FCNS	-	FCNS						
FCSGM	-	DCOMN4	RVCOMP					
FGAP	-	DCOMN1	RVCOMP					
FILTER	-	RBCOMP	DCOMN1	IDENT	RTCOMP			
FLD	-	INPUT						
FLOAT	-	INPUT						
FLOG10	-	DCOMN1	IDENT	RBCOMP	RVCOMP	1BLCK		
FNAND	-	RBCOMP	DCOMN1	RVCOMP				
FPT5	-	RBCOMP	DCOMN1	RBCOMP	RVCOMP	TCOMP	1BLCK	
FR	-	RVCOMP						
FREQ	-	FCNS						
FRMAT1	-	INPUT						
FRSQ	-	RVCOMP						
FRV	-	RVCOMP						
FX	-	RVCOMP						
FXSQ	-	RVCOMP						
FZ2	-	DCOMN1	IDENT	RVCOMP				
FZRO	-	RBCOMP	DCOMN1	IDENT	RBCOMP	RVCOMP	RVPRNT	
FZSQ	-	DCOMN1	IDENT	RVCOMP				
G	-	RVCOMP						

I N D E X

\*\*\*\*\* SUPER INDEX \*\*\*\*\*

GO	-	DCOMN1	IDENT							
NBAND	-	DCOMN1	IDENT	RVPRNT						
HEADS	-	DCOMN1	IDENT	1BLCK						
HEB	-	DCOMN1	IDENT	RVPRNT	1BLCK					
HFROM	-	DCOMN1	IDENT							
HOUTPT	-	DCOMN1	RVPRNT							
HRYB	-	RVPRNT								
HSPRD	-	DCOMN1	IDENT							
HSPRV	-	DCOMN1	IDENT							
HTIME	-	RVPRNT								
HTOT1	-	DCOMN1	RVPRNT	1BLCK						
HTOT2	-	DCOMN1	RVPRNT	1BLCK						
HTOT3	-	DCOMN1	IDENT	RVPRNT	1BLCK					
HUNIT	-	DCOMN1								
I	-	BCOMP	IDENT	INPUT	RBSORT	RTCOMP	RVCOMP	RVPRNT		
		RVSPRD	SORT	TCOMP	1BLCKO					
IPLANK	-	DCOMN1	INPUT	1BLCKO						
IBOUND	-	TCOMP								
ICOMMA	-	INPUT								
ID	-	IDENT								
IDATA	-	DCOMN1	IDENT							
IDATE	-	DCOMN1	RVPRNT							
IDC	-	DCOMN1	IDENT	RVPRNT						
IDENT	-	1MAIN								
IDOP	-	RBCOMP								
IDV	-	DCOMN1	RVPRNT							
IEQUAL	-	INPUT								
IESIGN	-	INPUT								
IEXP	-	INPUT								
IFIX	-	BCOMP	RVCOMP							
IFLAG	-	FNENS								
IFZRO	-	DCOMN1								
II	-	RBCOMP	RVPRNT	RVSPRD						
IIMAGE	-	INPUT								
IJ	-	RBCOMP								
IMAGE	-	INPUT								
IMAX	-	RTCOMP								
INDEP	-	TABLKP								
INDEX	-	INPUT								
INFMT	-	DCOMN1	1BLCK							
INPFLG	-	IDENT	INPUT							
INPT	-	DCOMN1	1BLCK							
INPUT	-	IDENT								
IPEVRY	-	BCOMP	DCOMN1	RVPRNT	TCOMP	1BLCK				
IPLT	-	DCOMN1	RVPRNT	1BLCK	1MAIN					
IPRT	-	DCOMN1	IDENT	RVPRNT	1BLCK					
IQUOTE	-	INPUT								
IREPT	-	INPUT								
ISIGN	-	RBCOMP								
ITABLE	-	AINTRP	DCOMN1	RBCOMP	TABLKP	TCOMP				
ITABMN	-	TABLKP	1BLCK							
ITABMX	-	TABLKP								
ITOTAL	-	RVPRNT								
ITRUE	-	INPUT								
ITYPE	-	INPUT								
IVALUE	-	INPUT								
IVSIGN	-	INPUT								
J	-	IDENT	INPUT	RBSORT	RTCOMP	RVCOMP	RUPRNT	RVSPRD	SORT	
		TCOMP	1BLCK							
JA	-	RBCOMP								
JB	-	RBCOMP								
JBOUND	-	RBCOMP								
JC	-	RBCOMP								
JD	-	RBCOMP								
JDD	-	RBCOMP								
JBELT	-	RBCOMP								
JDMAX	-	RBCOMP								
JDMIN	-	RBCOMP								
JE	-	RBCOMP								
JMAX	-	RBCOMP								

I N D E X

\*\*\*\*\* SUPER INDEX \*\*\*\*\*

JUMP	-	RBCOMP						
K	-	IDENT	INPUT	RBSORT	RVCOMP	RVPRNT	RVSPRD	TCOMP
K0	-	DCOMN1	1BLCK					
K1	-	BCOMP	DCOMN1	IDENT	RBCOMP	RTCOMP	RVCOMP	RVPRNT
		TCOMP	1BLCK	1MAIN				RVSPRD
K10	-	DCOMN1	IDENT	1BLCK				
K2	-	DCOMN1	IDENT	RBCOMP	RTCOMP	RVCOMP	TCOMP	1BLCK
K3	-	DCOMN1	IDENT	RBCOMP	RTCOMP	RVSPRD	TCOMP	1BLCK
K40	-	DCOMN1	RVPRNT	TCOMP	1BLCK			
K5	-	DCOMN1	IDENT	RVPRNT	1BLCK			
K6	-	DCOMN1	1BLCK					
K8	-	DCOMN1	RVPRNT	1BLCK				
KBAND	-	RBCOMP						
KK	-	RVSPRD						
KS1	-	DCOMN1	IDENT					
KSID	-	DCOMN1	IDENT	RVPRNT				
KT	-	DCOMN1	RBCOMP	RTCOMP	RVCOMP	1MAIN		
KTJM	-	RBCOMP						
KTSBND	-	BCOMP	DCOMN1	IDENT				
KTT	-	DCOMN1	RBCOMP	RTCOMP	RVCOMP	1MAIN		
L	-	BCOMP	IDENT	INPUT	RBCOMP	RBSORT	RVPRNT	
LEAP	-	RBCOMP						
LENGTH	-	SORT						
LFLAGS	-	DCOMN1	1BLCK					
LL	-	RBCOMP						
LPBAND	-	BCOMP	DCOMN1	DCOMN6	RVSPRD			
LPBND1	-	DCOMN1	DCOMN6	RTCOMP	RVPRNT			
LRKS	-	DCOMN1	DCOMN6	RBSORT				
LRKS2	-	DCOMN1	DCOMN6	RBCOMP				
LRNT	-	DCOMN1	1MAIN					
LRRB	-	DCOMN1	DCOMN6	1MAIN				
LRSPRD	-	DCOMN1	DCOMN6					
LRTJM	-	DCOMN1	DCOMN6	TCOMP				
LRTRS	-	DCOMN1	DCOMN6	TCOMP				
LOG4P1	-	DCOMN1	IDENT	1BLCK				
LOGRV	-	DCOMN1	IDENT					
LOGRVI	-	DCOMN1	IDENT	RVCOMP				
LTRUE	-	INPUT						
LVALUE	-	INPUT						
M	-	IDENT	INPUT	RBSORT	TCOMP			
MAXC	-	IDENT						
MAXCOL	-	INPUT	1BLCK0					
MBAND	-	BCOMP	DCOMN1					
MINC	-	BCOMP	RVCOMP	1MAIN				
ML	-	RBCOMP						
MLRU	-	RBCOMP						
MM	-	RBCOMP						
MN	-	RBCOMP						
MNBND	-	BCOMP	DCOMN1	RTCOMP	RVPRNT	TCOMP		
MNRX	-	RBCOMP						
MOD	-	BCOMP	RVPRNT					
MU	-	RBCOMP						
MX	-	RBCOMP						
N	-	RBSORT						
NA	-	RBCOMP	RBSORT					
NAMCNT	-	DCOMN1	IDENT	1BLCK				
NAMDAT	-	DCOMN1	1BLCK					
NAME	-	INPUT						
NANSV	-	INPUT						
NARTAB	-	INPUT						
NB	-	RBCOMP	RBSORT					
NBAND	-	BCOMP	DCOMN1	RBCOMP	RVCOMP	RVSPRD		
NBEAR	-	DCOMN1	FNCS					
NBOUND	-	DCOMN1	RBCOMP	TCOMP				
NBSPRD	-	DCOMN1	IDENT					
NBTR	-	DCOMN1	RBSORT					
NC	-	INPUT	RBSORT					
NCHAR	-	INPUT	1BLCK0					
ND	-	RBSORT						
NEXT	-	RBCOMP						

APPENDIX G

I N D E X

\*\*\*\*\* SUPER INDEX \*\*\*\*\*

NL	-	INPUT				
NR	-	INPUT				
NMAX	-	TCOMP				
NRIN	-	TCOMP				
NN	-	RVCOMP				
NNAMES	-	DCOMN1	IDENT	INPUT	1BLCK	
NOBTM	-	DCOMN1	RBSORT			
NOPRNT	-	DCOMN1	IDENT	RVPRNT		
NOSURF	-	DCOMN1	RBSORT			
NOTAPE	-	DCOMN1	IDENT	RBSORT	TCOMP	1MAIN
NOVOLM	-	DCOMN1	1MAIN			
NPAGE	-	DCOMN1	RVPRNT	TCOMP		
NPSTR	-	BCOMP	DCOMN1	RVPRNT	TCOMP	
NQT	-	INPUT				
NSPR1	-	DCOMN1	IDENT	RVSPRD		
NSPRN	-	BCOMP	DCOMN1	IDENT	RVSPRD	
NSPRN1	-	DCOMN1	IDENT	RBCOMP	RVCOMP	RVSPRD
NSSPRD	-	DCOMN1	IDENT			
NSURF	-	DCOMN1	RBSORT			
NTBL	-	TCOMP				
NTIME	-	DCOMN1	TCOMP	1MAIN		
NTMAX	-	DCOMN1	RVPRNT	1MAIN		
NTMIN	-	DCOMN1	RVPRNT	1MAIN		
NTRUE	-	INPUT				
NUMBER	-	INPUT	1BLCKD			
NVSPRD	-	DCOMN1	IDENT			
NWORD	-	INPUT	1BLCKD			
OMEGA	-	DCOMN1	IDENT	RBCOMP	RVCOMP	
OMEGAD	-	DCOMN1	IDENT	RVPRNT		
OMT	-	DCOMN5	RBCOMP	RVCOMP		
OPTD	-	RBCOMP				
OMTTRU	-	RBCOMP				
OUTFLG	-	IDENT	INPUT			
DXL	-	FNCHS	RBCOMP	RVCOMP		
PAGE	-	DCOMN1	RVPRNT	TCOMP		
PHI	-	RBCOMP				
PHMONT	-	RBCOMP				
PI	-	DCOMN1	RBCOMP	RVCOMP	1BLCK	
PI23	-	DCOMN1	RVCOMP	1BLCK		
PING	-	DCOMN1	RVPRNT	TCOMP		
PLOT	-	DCOMN1	RVPRNT	1MAIN		
PN	-	RVCOMP				
PULSE	-	DCOMN1				
Q	-	BCOMP				
QA	-	RBCOMP				
QAADC	-	RBCOMP				
QAB	-	RBCOMP				
QAPC	-	RBCOMP				
QAC	-	RBCOMP				
QB	-	RBCOMP				
QBABC	-	RBCOMP				
QBC	-	RBCOMP				
QC	-	RBCOMP				
QCOS	-	RBCOMP				
QCOSH	-	RBCOMP				
Q SIN	-	RBCOMP				
R	-	DCOMN5	RBCOMP	RVCOMP		
RBCOMP	-	1MAIN				
RBN	-	DCOMN3	RBSORT	TCOMP		
RBNH	-	DCOMN5	RBCOMP			
RBNB	-	DCOMN5	RBCOMP			
RBSORT	-	1MAIN				
RBT	-	DCOMN3	RBSORT	TCOMP		
RBTB	-	DCOMN5	RBCOMP			
RBTB	-	DCOMN5	RBCOMP			
RBTB	-	DCOMN3	RBSORT	TCOMP		
RPTNA	-	DCOMN5	RBCOMP			
RBTNB	-	DCOMN5	RBCOMP			
RBE	-	DCOMN3	RBSORT	TCOMP		
RBNH	-	DCOMN5	RBCOMP			



I N D E X

\*\*\*\*\* SUPER INDEX \*\*\*\*\*

WRFLG	-	RBSORT		
X	-	DCOM5	RBCORP	RVCOMP
X1	-	RBCOMP		
X2	-	RBCOMP		
X3	-	RBCOMP		
X4	-	RBCOMP		
XD	-	RBCOMP		
XMIN	-	DCOM3	RBSORT	TCOMP
XMIT	-	DCOM1	RBCORP	RVCOMP
XTHU	-	RBCOMP		
Y	-	RVCOMP		
Y1	-	RBCOMP		
Y2	-	RBCOMP		
Y3	-	RBCOMP		
Y4	-	RBCOMP		
YDKT	-	DCOM1	IDENT	1DLCK
Z	-	RVCOMP		

.....

I N D E X  
 END OF COMPUTATION,  
 6 APRIL 1976 VERSION.  
 (PROGRAM INDEX COPYRIGHT 1966, HARRY N. MURPHY, JR.)  
 (AS MODIFIED AT NUC BY P. MARSH, R. ALLIES, M. PINNEY, ET AL)